

JOURNAL OF

# CHROMATOGRAPHY

INCLUDING ELECTROPHORESIS AND OTHER SEPARATION METHODS

### EDITORS

- R. W. Giese (Boston, MA)
- J. K. Haken (Kensington, N.S.W.)
- K. Macek (Prague)
- L. R. Snyder (Orinda, CA)

EDITORS, SYMPOSIUM VOLUMES,  
E. Heftmann (Orinda, CA), Z. Deyl (Prague)

### EDITORIAL BOARD

- D. W. Armstrong (Rolla, MO)
- W. A. Aue (Halifax)
- P. Bocek (Brno)
- A. A. Boulton (Saskatoon)
- P. W. Carr (Minneapolis, MN)
- N. H. C. Cooke (San Ramon, CA)
- V. A. Davankov (Moscow)
- Z. Deyl (Prague)
- S. Dilli (Kensington, N.S.W.)
- H. Engelhardt (Saarbrücken)
- F. Erni (Basle)
- M. B. Evans (Hatfield)
- J. L. Glajch (N. Billerica, MA)
- G. A. Guiochon (Knoxville, TN)
- P. R. Haddad (Kensington, N.S.W.)
- I. M. Hais (Hradec Králové)
- W. S. Hancock (San Francisco, CA)
- S. Hjertén (Uppsala)
- Cs. Horváth (New Haven, CT)
- J. F. K. Huber (Vienna)
- K.-P. Hupe (Waldbronn)
- T. W. Hutchens (Houston, TX)
- J. Janák (Brno)
- P. Jandera (Pardubice)
- B. L. Karger (Boston, MA)
- E. sz. Kováts (Lausanne)
- A. J. P. Martin (Cambridge)
- L. W. McLaughlin (Chestnut Hill, MA)
- E. D. Morgan (Keele)
- J. D. Pearson (Kalamazoo, MI)
- H. Poppe (Amsterdam)
- F. E. Regnier (West Lafayette, IN)
- P. G. Righetti (Milan)
- P. Schoenmakers (Eindhoven)
- G. Schomburg (Mülheim/Ruhr)
- R. Schwarzenbach (Dübendorf)
- R. E. Shoup (West Lafayette, IN)
- A. M. Siouffi (Marseille)
- D. J. Strydom (Boston, MA)
- K. K. Unger (Mainz)
- R. Verpoorte (Leiden)
- Gy. Vigh (College Station, TX)
- J. T. Watson (East Lansing, MI)
- B. D. Westerlund (Uppsala)

### EDITORS, BIBLIOGRAPHY SECTION

- Z. Deyl (Prague), J. Janák (Brno), V. Schwarz (Prague), K. Macek (Prague)

ELSEVIER

**Scope.** The *Journal of Chromatography* publishes papers on all aspects of chromatography, electrophoresis and related methods. Contributions consist mainly of research papers dealing with chromatographic theory, instrumental development and their applications. The section *Biomedical Applications*, which is under separate editorship, deals with the following aspects: developments in and applications of chromatographic and electrophoretic techniques related to clinical diagnosis or alterations during medical treatment; screening and profiling of body fluids or tissues with special reference to metabolic disorders; results from basic medical research with direct consequences in clinical practice; drug level monitoring and pharmacokinetic studies; clinical toxicology; analytical studies in occupational medicine.

**Submission of Papers.** Manuscripts (in English; *four* copies are required) should be submitted to: Editorial Office of *Journal of Chromatography*, P.O. Box 681, 1000 AR Amsterdam, The Netherlands, Telefax (+31-20) 5862 304, or to: The Editor of *Journal of Chromatography, Biomedical Applications*, P.O. Box 681, 1000 AR Amsterdam, The Netherlands. Review articles are invited or proposed by letter to the Editors. An outline of the proposed review should first be forwarded to the Editors for preliminary discussion prior to preparation. Submission of an article is understood to imply that the article is original and unpublished and is not being considered for publication elsewhere. For copyright regulations, see below.

**Publication.** The *Journal of Chromatography* (incl. *Biomedical Applications*) has 38 volumes in 1991. The subscription prices for 1991 are:

*J. Chromatogr.* (incl. *Cum. Indexes, Vols. 501-550*) + *Biomed. Appl.* (Vols. 535-572):  
Dfl. 7220.00 plus Dfl. 1140.00 (p.p.h.) (total ca. US\$ 4519.00)

*J. Chromatogr.* (incl. *Cum. Indexes, Vols. 501-550*) only (Vols. 535-561):  
Dfl. 5859.00 plus Dfl. 810.00 (p.p.h.) (total ca. US\$ 3604.75)

*Biomed. Appl.* only (Vols. 562-572):  
Dfl. 2387.00 plus Dfl. 330.00 (p.p.h.) (total ca. US\$ 1468.75).

**Subscription Orders.** The Dutch guilder price is definitive. The US\$ price is subject to exchange-rate fluctuations and is given as a guide. Subscriptions are accepted on a prepaid basis only, unless different terms have been previously agreed upon. Subscriptions orders can be entered only by calendar year (Jan.-Dec.) and should be sent to Elsevier Science Publishers, Journal Department, P.O. Box 211, 1000 AE Amsterdam, The Netherlands, Tel. (+31-20) 5803 642, Telefax (+31-20) 5803 598, or to your usual subscription agent. Postage and handling charges include surface delivery except to the following countries where air delivery via SAL (Surface Air Lift) mail is ensured: Argentina, Australia, Brazil, Canada, Hong Kong, India, Israel, Japan\*, Malaysia, Mexico, New Zealand, Pakistan, PR China, Singapore, South Africa, South Korea, Taiwan, Thailand, USA. \* For Japan air delivery (SAL) requires 50% additional charge of the normal postage and handling charge. For all other countries airmail rates are available upon request. Claims for missing issues must be made within three months of our publication (mailing) date, otherwise such claims cannot be honoured free of charge. Back volumes of the *Journal of Chromatography* (Vols. 1-534) are available at Dfl. 208.00 (plus postage). Customers in the USA and Canada wishing information on this and other Elsevier journals, please contact Journal Information Center, Elsevier Science Publishing Co. Inc., 655 Avenue of the Americas, New York, NY 10010, USA, Tel. (+1-212) 633 3750, Telefax (+1-212) 633 3990.

**Abstracts/Contents Lists** published in Analytical Abstracts, Biochemical Abstracts, Biological Abstracts, Chemical Abstracts, Chemical Titles, Chromatography Abstracts, Clinical Chemistry Lookout, Current Contents/Life Sciences, Current Contents/Physical, Chemical & Earth Sciences, Deep-Sea Research/Part B: Oceanographic Literature Review, Excerpta Medica, Index Medicus, Mass Spectrometry Bulletin, PASCAL-CNRS, Pharmaceutical Abstracts, Referativnyi Zhurnal, Research Alert, Science Citation Index and Trends in Biotechnology.

**See inside back cover** for Publication Schedule, Information for Authors and information on Advertisements.

All rights reserved. No part of this publication may be reproduced, stored in a retrieval system or transmitted in any form or by any means, electronic, mechanical, photocopying, recording or otherwise, without the prior written permission of the publisher, Elsevier Science Publishers B.V., P.O. Box 330, 1000 AH Amsterdam, The Netherlands.

Upon acceptance of an article by the journal, the author(s) will be asked to transfer copyright of the article to the publisher. The transfer will ensure the widest possible dissemination of information.

Submission of an article for publication entails the authors' irrevocable and exclusive authorization of the publisher to collect any sums or considerations for copying or reproduction payable by third parties (as mentioned in article 17 paragraph 2 of the Dutch Copyright Act of 1912 and the Royal Decree of June 20, 1974 (S. 351) pursuant to article 16 b of the Dutch Copyright Act of 1912) and/or to act in or out of Court in connection therewith.

**Special regulations for readers in the USA.** This journal has been registered with the Copyright Clearance Center, Inc. Consent is given for copying of articles for personal or internal use, or for the personal use of specific clients. This consent is given on the condition that the copier pays through the Center the per-copy fee stated in the code on the first page of each article for copying beyond that permitted by Sections 107 or 108 of the US Copyright Law. The appropriate fee should be forwarded with a copy of the first page of the article to the Copyright Clearance Center, Inc., 27 Congress Street, Salem, MA 01970, USA. If no code appears in an article, the author has not given broad consent to copy and permission to copy must be obtained directly from the author. All articles published prior to 1980 may be copied for a per-copy fee of US\$ 2.25, also payable through the Center. This consent does not extend to other kinds of copying, such as for general distribution, resale, advertising and promotion purposes, or for creating new collective works. Special written permission must be obtained from the publisher for such copying.

No responsibility is assumed by the Publisher for any injury and/or damage to persons or property as a matter of products liability, negligence or otherwise, or from any use or operation of any methods, products, instructions or ideas contained in the materials herein. Because of rapid advances in the medical sciences, the Publisher recommends that independent verification of diagnoses and drug dosages should be made.

Although all advertising material is expected to conform to ethical (medical) standards, inclusion in this publication does not constitute a guarantee or endorsement of the quality or value of such product or of the claims made of it by its manufacturer.

This issue is printed on acid-free paper.

## CONTENTS

(Abstracts/Contents Lists published in *Analytical Abstracts, Biochemical Abstracts, Biological Abstracts, Chemical Abstracts, Chemical Titles, Chromatography Abstracts, Current Contents/Life Sciences, Current Contents/Physical, Chemical & Earth Sciences, Deep-Sea Research/Part B: Oceanographic Literature Review, Excerpta Medica, Index Medicus, Mass Spectrometry Bulletin, PASCAL-CNRS, Referativnyi Zhurnal, Research Alert and Science Citation Index*)

## REGULAR PAPERS

*Column Liquid Chromatography*

- Use of the LeVan-Vermeulen isotherm model for the calculation of elution band profiles in non-linear chromatography  
by S. Golshan-Shirazi and G. Guiochon (Oak Ridge, TN, USA) (Received February 5th, 1991) . . . . . 1
- Optimisation of frontal chromatography by partial loading  
by P. Dantigny, Y. Wang, J. Hubble and J. A. Howell (Bath, UK) (Received February 15th, 1991) . . . . . 27
- Comparison of a new ovomucoid and a second-generation  $\alpha_1$ -acid glycoprotein-based chiral column for the direct high-performance liquid chromatography resolution of drug enantiomers  
by K. M. Kirkland, K. L. Neilson and D. A. McCombs (Wilmington, DE, USA) (Received March 6th, 1991) . . . . . 43
- Effect of organic modifier concentration on retention in reversed-phase ion-pair liquid chromatography  
by H. Zou, Y. Zhang and P. Lu (Dalian, China) (Received December 31st, 1990) . . . . . 59
- Quantification of methyl farnesoate levels in hemolymph by high-performance liquid chromatography  
by D. W. Borst and B. Tsukimura (Normal, IL, USA) (Received February 26th, 1991) . . . . . 71
- Separation and purification of oligonucleotides using a new bonded-phase packing material  
by P. A. D. Edwardson, I. J. Collins, M. D. Scawen and T. Atkinson (Wiltshire, UK) and G. B. Cox, S. Sivakoff and R. W. Stout (Wilmington, DE, USA) (Received February 12th, 1991) . . . . . 79
- Optimized high-performance liquid chromatographic procedure for the separation and determination of the main folacin and some derivatives. II. Extraction method and application to rat liver  
by A. Hahn, K. H. Flaig and G. Rehner (Giessen, Germany) (Received January 10th, 1991) . . . . . 91
- Optimization of chromatographic selectivity of twelve sulphonamides in reversed-phase high-performance liquid chromatography using mixture designs and multi-criteria decision making  
by J. Wieling, J. Schepers, J. Hempenius, C. K. Mensink and J. H. G. Jonkman (Assen, The Netherlands) (Received January 22nd, 1991) . . . . . 101
- Separation and estimation of small amounts of the enantiomers of carbidopa and methyl dopa on a chiral stationary phase with L-phenylalanine as selector in ligand-exchange chromatography  
by B. Lausecker (Berlin, Germany) and F.-M. Albert (Zwickau, Germany) (Received January 4th, 1991) . . . . . 115
- Anomalous bandspreading of ethylenediaminetetraacetato-chromium(III) ion in reversed-phase high-performance liquid chromatography. An example of slow equilibrium kinetics  
by J. H. Knox and M. Shibukawa (Edinburgh, UK) (Received January 30th, 1991) . . . . . 123

(Continued overleaf)

Contents (continued)

Supercritical Fluid Chromatography

- Generalized treatment of spatial and temporal column parameters, applicable to gas, liquid and supercritical fluid chromatography. II. Application to supercritical CO<sub>2</sub>  
by D. E. Martire and R. L. Riester (Washington, DC, USA), T. J. Bruno (Boulder, CO, USA)  
and A. Hussam and D. P. Poe (Washington, DC, USA) (Received February 5th, 1991) . . . 135
- Factors governing the analytical supercritical fluid extraction and supercritical fluid chromatographic retention of polycyclic aromatic hydrocarbons  
by J. Rein, C. M. Cork and K. G. Furton (Miami, FL, USA) (Received February 19th, 1991) . . . 149

Planar Chromatography

- Chromatographic behaviour of diastereoisomers. X. Thin-layer chromatographic retentions on silica of some (*E*- and (*Z*)-oxazolones and related cinnamates as a function of mobile phase effects or Hammett constants  
by M. D. Palamareva, B. J. Kurtev and I. Kavrakova (Sofia, Bulgaria) (Received January 24th, 1991) . . . 161
- Resolution and concentration detection limit in capillary gel electrophoresis  
by J. Macek, U. R. Tjaden and J. van der Greef (Leiden, The Netherlands) (Received January 2nd, 1991) . . . 177

SHORT COMMUNICATIONS

Column Liquid Chromatography

- Peptide separation by gel filtration high-performance liquid chromatography using a gradient elution system  
by T. Araki, M. Kuramoto and T. Torikata (Kumamoto, Japan) (Received January 11th, 1991) . . . 183
- Use of chromatofocusing for separation of  $\beta$ -lactamases. IX. Analytical chromatofocusing for the separation of a chromosomal cephalosporinase from *Proteus vulgaris* 1028  
by S. Gál, A. Tar, B. L. Toth-Martinez and F. J. Hernadi (Debrecen, Hungary) (Received October 30th, 1990) . . . 189
- Separation of ribosomal subunits on Trisacryl GF 2000  
by D. Bhoolia and K. L. Manchester (Johannesburg, South Africa) (Received December 6th, 1990) . . . 196
- Determination of vitamin D<sub>2</sub> in shiitake mushroom (*Lentinus edodes*) by high-performance liquid chromatography  
by K. Takamura, H. Hoshino, T. Sugahara and H. Amano (Tokyo, Japan) (Received February 13th, 1991) . . . 201
- High-performance liquid chromatography of rubber antidegradants with diode-array detection  
by E. Brandšteterová (Bratislava, Czechoslovakia), M. Štubňa (Púchov, Czechoslovakia) and J. Lehotay and D. Derneschová (Bratislava, Czechoslovakia) (Received December 28th, 1990) . . . 205

Planar Chromatography

- Multiple-development high-performance thin-layer chromatography of organochlorine pesticides  
by G. Lodi and A. Betti (Ferrara, Italy) and Y. D. Kahie and A. M. Mahamed (Mogadishu, Somalia) (Received December 4th, 1990) . . . 214

BOOK REVIEWS

Chromatographic analysis of pharmaceuticals (edited by J. A. Adamovics), reviewed by K. Macek 219

Chromatographic analysis of alkaloids (by M. Popl, J. Fährlich and V. Tatar), reviewed by R. Verpoorte . . . . . 221

\*\*\*\*\*  
\*  
\* In articles with more than one author, the name of the author to whom correspondence should be addressed is indicated in the  
\* article heading by a 6-pointed asterisk (\*)  
\*  
\*\*\*\*\*

# International Journal of Mass Spectrometry and Ion Processes

## EDITORS:

**M.T. Bowers**, *Santa Barbara, CA, USA*; **H. Schwarz**, *Berlin, FRG*;  
**J.F.J. Todd**, *Canterbury, UK*

The journal contains papers dealing with fundamental aspects of mass spectrometry and ion processes, and the study of the application of mass spectrometric techniques to specific problems in chemistry and physics. The following topics, amongst others, can be found in the journal:

- Theoretical and experimental studies of ion formation (i.e. by electrons, laser or other forms of radiation, heavy ions, high-energy particles, etc.), ion separation and ion detection processes.
- The design and performance of instruments (or their parts) and accessories.
- Measurements of natural isotopic abundances, precise isotopic masses, ionization, appearance and excitation energies, ionization cross-sections.
- Development of techniques related to determining molecular structures, geological age determination, studies of thermodynamic properties, chemical kinetics, surface phenomena, radiation

chemistry, and chemical analyses.

- Theory of mass spectra, application of computer techniques to mass spectral data.
- Chemistry and physics of cluster ions.
- Spectroscopy of gaseous ions including studies related to interstellar chemistry.
- Mechanistic studies of unimolecular processes and ion/molecule reactions in the gas phase including computational aspects.
- Physical organic chemistry of isolated ions.

## Abstracted/Indexed in:

Chemical Abstracts, Current Contents: Physical, Chemical & Earth Sciences, Excerpta Medica, INSPEC, Mass Spectrometry Bulletin, PAS-CAL/CNRS

## Subscription Information

1991: Vols. 100-107 (24 issues)

US\$ 1405.50 / Dfl. 2600.00

incl. postage

ISSN 0168-1176



*For a Free Sample Copy Write to:*

**ELSEVIER SCIENCE PUBLISHERS**

P.O. Box 330, 1000 AH Amsterdam, The Netherlands

P.O. Box 882, Madison Square Station, New York, NY 10159, USA

JOURNAL OF CHROMATOGRAPHY

VOL. 545 (1991)





# JOURNAL of CHROMATOGRAPHY

INCLUDING ELECTROPHORESIS AND OTHER SEPARATION METHODS

## EDITORS

R. W. GIESE (Boston, MA), J. K. HAKEN (Kensington, N.S.W.), K. MACEK (Prague),  
L. R. SNYDER (Orinda, CA)

## EDITORS, SYMPOSIUM VOLUMES

E. HEFTMANN (Orinda, CA), Z. DEYL (Prague)

## EDITORIAL BOARD

D. W. Armstrong (Rolla, MO), W. A. Aue (Halifax), P. Boček (Brno), A. A. Boulton (Saskatoon), P. W. Carr (Minneapolis, MN), N. H. C. Cooke (San Ramon, CA), V. A. Davankov (Moscow), Z. Deyl (Prague), S. Dilli (Kensington, N.S.W.), H. Engelhardt (Saarbrücken), F. Erni (Basle), M. B. Evans (Hatfield), J. L. Glajch (N. Billerica, MA), G. A. Guiochon (Knoxville, TN), P. R. Haddad (Kensington, N.S.W.), I. M. Hais (Hradec Králové), W. S. Hancock (San Francisco, CA), S. Hjertén (Uppsala), Cs. Horváth (New Haven, CT), J. F. K. Huber (Vienna), K.-P. Hupe (Waldbronn), T. W. Hutchens (Houston, TX), J. Janák (Brno), P. Jandera (Pardubice), B. L. Karger (Boston, MA), E. sz. Kováts (Lausanne), A. J. P. Martin (Cambridge), L. W. McLaughlin (Chestnut Hill, MA), E. D. Morgan (Keele), J. D. Pearson (Kalamazoo, MI), H. Poppe (Amsterdam), F. E. Regnier (West Lafayette, IN), P. G. Righetti (Milan), P. Schoenmakers (Eindhoven), G. Schomburg (Mülheim/Ruhr), R. Schwarzenbach (Dübendorf), R. E. Shoup (West Lafayette, IN), A. M. Siouffi (Marseille), D. J. Strydom (Boston, MA), K. K. Unger (Mainz), R. Verpoorte (Leiden), Gy. Vigh (College Station, TX), J. T. Watson (East Lansing, MI), B. D. Westerlund (Uppsala)

## EDITORS, BIBLIOGRAPHY SECTION

Z. Deyl (Prague), J. Janák (Brno), V. Schwarz (Prague), K. Macek (Prague)



ELSEVIER  
AMSTERDAM — OXFORD — NEW YORK — TOKYO

---

*J. Chromatogr.*, Vol. 545 (1991)

All rights reserved. No part of this publication may be reproduced, stored in a retrieval system or transmitted in any form or by any means, electronic, mechanical, photocopying, recording or otherwise, without the prior written permission of the publisher, Elsevier Science Publishers B.V., P.O. Box 330, 1000 AH Amsterdam, The Netherlands.

Upon acceptance of an article by the journal, the author(s) will be asked to transfer copyright of the article to the publisher. The transfer will ensure the widest possible dissemination of information.

Submission of an article for publication entails the authors' irrevocable and exclusive authorization of the publisher to collect any sums or considerations for copying or reproduction payable by third parties (as mentioned in article 17 paragraph 2 of the Dutch Copyright Act of 1912 and the Royal Decree of June 20, 1974 (S. 351) pursuant to article 16 b of the Dutch Copyright Act of 1912) and/or to act in or out of Court in connection therewith.

**Special regulations for readers in the USA.** This journal has been registered with the Copyright Clearance Center, Inc. Consent is given for copying of articles for personal or internal use, or for the personal use of specific clients. This consent is given on the condition that the copier pays through the Center the per-copy fee stated in the code on the first page of each article for copying beyond that permitted by Sections 107 or 108 of the US Copyright Law. The appropriate fee should be forwarded with a copy of the first page of the article to the Copyright Clearance Center, Inc., 27 Congress Street, Salem, MA 01970, USA. If no code appears in an article, the author has not given broad consent to copy and permission to copy must be obtained directly from the author. All articles published prior to 1980 may be copied for a per-copy fee of US\$ 2.25, also payable through the Center. This consent does not extend to other kinds of copying, such as for general distribution, resale, advertising and promotion purposes, or for creating new collective works. Special written permission must be obtained from the publisher for such copying.

No responsibility is assumed by the Publisher for any injury and/or damage to persons or property as a matter of products liability, negligence or otherwise, or from any use or operation of any methods, products, instructions or ideas contained in the materials herein. Because of rapid advances in the medical sciences, the Publisher recommends that independent verification of diagnoses and drug dosages should be made. Although all advertising material is expected to conform to ethical (medical) standards, inclusion in this publication does not constitute a guarantee or endorsement of the quality or value of such product or of the claims made of it by its manufacturer.

This issue is printed on acid-free paper.

## Use of the LeVan–Vermeulen isotherm model for the calculation of elution band profiles in non-linear chromatography

SADRODDIN GOLSHAN-SHIRAZI and GEORGES GUIOCHON\*

*\*Department of Chemistry, University of Tennessee, Knoxville, TN 37996-1600 and Division of Analytical Chemistry, Oak Ridge National Laboratory, Oak Ridge, TN 37831-6120 (USA)*

(First received October 26th, 1990; revised manuscript received February 5th, 1991)

---

### ABSTRACT

The two-term LeVan–Vermeulen isotherm is the simplest competitive isotherm based on the ideal adsorbed solution model. It applies when both components follow individually the single-component Langmuir isotherm model. It takes into account the influence of the difference in the column saturation capacity for these two components. Individual band profiles calculated with this isotherm are in qualitative agreement with experimental results. They exhibit a stronger displacement effect, a weaker tag-along effect and a higher degree of band separation than predicted by the Langmuir competitive isotherm when the column saturation capacity is larger for the second component than for the first. Conversely, when the column saturation capacity is larger for the first component than for the second, the displacement effect is less intense and the tag-along effect is stronger than with the competitive Langmuir isotherm and the separation deteriorates. When the sample size is increased, a reversal of the elution order is observed.

---

### INTRODUCTION

As we have previously reported, there is excellent agreement between the band profiles measured experimentally and those calculated in the case of single-component or binary mixture samples when the equilibrium isotherms of the compounds involved can be accounted for exactly [1–6]. With most single-component samples, adsorption data in normal- and reversed-phase chromatography are well accounted for by a Langmuir [1,2] or a bi-Langmuir isotherm [4]. This is in agreement with results reported by others [7,8]. On the other hand, with binary mixtures, the adsorption data could be fitted correctly on a bi-Langmuir isotherm only for enantiomers [4]. In other instances [3,5], no Langmuir-type competitive isotherm could account accurately for the data, although the single-component Langmuir isotherm accounted well for the data corresponding to the two single-component samples.

These results are in agreement with the assumptions of the Langmuir model, essentially that the solution and the adsorbed phase behave ideally and that there are no molecular interactions. With enantiomers, the chiral selective sites which have the highest interaction energy and a low saturation capacity are filled first and their

saturation is reached at low concentrations in the mobile phase, so deviations from ideal behavior in the solution are small [4,6]. As the density of chiral selective sites on the surface of the stationary phase is low, molecular interactions between adsorbate molecules are insignificant and deviations from ideal behavior in the adsorbed phase remain small. Finally, the column saturation capacities for the two enantiomers are nearly equal [4,6]. All these favorable circumstances are absent in the other instances, where isomers or less closely related compounds were studied [3,5].

Another fundamental assumption made in the competitive Langmuir model is that the column saturation capacity is the same for the components involved. Otherwise, the Langmuir competitive isotherm does not satisfy the Gibbs adsorption isotherm equation and, consequently, is thermodynamically inconsistent [9]. This restriction is of great practical importance because in most instances the more retained component of a pair has the larger molecule, which interacts more strongly with the stationary phase but also which occupies the larger surface area on the adsorbent surface, and hence has the lower saturation capacity. In such a case, the single-component isotherms intersect. In the converse case, when the column saturation capacity for the more strongly retained component is larger than that of the less retained component, the single-component isotherms diverge. In both instances, however, the Langmuir competitive isotherm predicts that the selectivity,  $(q_2/C_2)/(q_1/C_1)$  (where  $q_i$  and  $C_i$  are the concentrations of component  $i$  in the stationary and mobile phase, respectively), remains constant and equal to the relative retention under linear (*i.e.*, analytical) conditions,  $\alpha = k'_{0,2}/k'_{0,1}$ . This is a basic characteristic of the competitive Langmuir isotherm model that the selectivity is constant, independent of the concentrations of the two compounds. Its consequences are important.

We have shown that in overloaded elution chromatography, if the Langmuir competitive isotherm model is valid, the ideal model predicts that the intensity of the displacement effect is increased and at the same time the separation deteriorates if the column saturation capacity of the second component is decreased (and isotherm intersection takes place) at a constant column saturation capacity for the first component and constant sample size [10]. This is explained by the resulting increase in the loading factor for the second component ( $L_{r,2} = n_2/W_2$ , where  $n_2$  is the amount of component 2 and  $W_2$  is the column saturation capacity). If the sample size is reduced to keep constant the loading factor for the second component at the same time as the column saturation capacity for the second component is reduced, the displacement effect is increased and the separation is improved. Conversely, if the column saturation capacity of the second component is increased at constant column saturation capacity for the first component and constant sample size (and isotherm divergence takes place), the intensity of the tag-along effect increases and the intensity of the displacement effect decreases, but at the same time the separation is improved because the loading factor corresponding to a given sample size is decreased [10]. Restoring the initial value of the loading factor by increasing also the sample size gives a chromatogram in which the displacement effect is less intense, the tag-along effect more intense and the degree of separation degraded.

These results are confirmed by the chromatograms calculated using the semi-ideal model and competitive Langmuir isotherms with various ratios of the column saturation capacities for the two components [11]. Calculations also show that the formation of an isotachic train is not affected by the intersection of the single-

component isotherms of the two components of a binary mixture, as long as the competitive Langmuir model is valid. The conditions under which the isotachic train forms depend essentially on the value of the loading factors and on the column efficiency [12]. The only consequence of the isotherm intersection is that the height of the concentration plateau of the second band is lower than that of the concentration plateau of the first band.

These theoretical consequences of the Langmuir competitive isotherm model are in direct contradiction with many experimental observations. Cox and Snyder [13] reported that when the more retained component of a binary mixture has the lower column saturation capacity, the intensity of the displacement effect of the first component by the second is minimal, the broadening of the second component band is important, extensive band overlap takes place and poor separation is achieved. Conversely, when the two single-component isotherms diverge, the intensity of the displacement effect is enhanced, the tailing of the first component band behind the front of the second band is reduced and the separation is improved. Similarly, Horváth [14] and Subramanian and Cramer [15] reported that it is impossible (or at least very difficult) to obtain an isotachic train in displacement chromatography when the single-component isotherms of the mixture components intersect. Displacement can be achieved only by changing the mobile phase composition [14], which alters the isotherms.

This contradiction between experimental and theoretical results suggests that the competitive Langmuir model is not satisfactory, at least when the column saturation capacities of the two components are significantly different. This conclusion also agrees with our experimental results [1–6]. It is also supported by theoretical considerations. As mentioned above, the competitive Langmuir isotherm is not consistent with the Gibbs adsorption isotherm equation unless the column saturation capacities of the mixture components are equal, at least when the adsorption of the solvent is ignored [9]. In fact, the Langmuir competitive isotherm is justified only on the basis of very simple kinetic considerations [16]. Its popularity stems from the convenience with which the parameters of the competitive isotherms are derived from the single-component isotherms. More sophisticated isotherms, however, enjoy also this property. The models derived from the ideal adsorbed solution (IAS) theory belong to this group.

The IAS theory was developed by Myers and Prausnitz [17], precisely to allow the prediction of multi-component isotherms using data obtained from single-component measurements. The IAS theory is essentially a procedure permitting the derivation of a competitive isotherm consistent with a given set of single-component isotherms (*e.g.*, Langmuir or Freundlich isotherms) and consistent with the basic thermodynamic requirements (*i.e.*, the Gibbs adsorption isotherm equation). The IAS theory is based on the same assumptions as the Langmuir isotherm, an ideal adsorbed solution for both the stationary and the mobile phases. However, as the IAS theory based its interpretation of the deviation of the adsorption behavior from the Langmuir competitive model on the Gibbs adsorption isotherm, the IAS isotherm obtained is always consistent with thermodynamics, regardless of the relative values of the column saturation capacities.

Henson and Kabel [18] showed that the IAS theory predicts competitive gas–solid adsorption isotherms of gases which are accurate at low surface coverages but

deviate systematically from experimental data at high coverages. Later, the IAS theory was extended to competitive liquid–solid adsorption in the case of dilute solutions [19]. It was also used in combination with a trial-and-error procedure for the prediction of competitive binary gas–solid isotherms for species obeying the single-component Langmuir isotherm [20] or the Freundlich isotherm [21].

Using the IAS theory, LeVan and Vermeulen [22] derived gas–solid competitive binary isotherms in the form of a rapidly converging series expansion, provided that the single-component isotherms are either Langmuir or Freundlich isotherms. The competitive isotherm reduces to the single-component isotherm when the concentration of the other component approaches zero. The LeVan–Vermeulen isotherm, based on single-component Langmuir isotherms, reduces to the classical competitive Langmuir isotherm when the specific saturation capacities of the two components are equal. When these capacities are unequal, the isotherms satisfy the Gibbs adsorption isotherm equation and hence they are thermodynamically consistent. Extension of these IAS isotherms to liquid–solid isotherms is straightforward, provided that we assume that the solution is dilute and the adsorption of the solvent can be neglected.

The aim of this paper is to examine the implications of using the LeVan–Vermeulen isotherm in preparative chromatography and the influence of the ratio of the column saturation capacities on the intensity of the displacement and the tag-along effects.

## THEORY

A most important problem in the thermodynamics of phase equilibria is whether we can predict the competitive equilibrium behavior of two components knowing only their single-component isotherms. In principle, this should not be possible since it is tantamount to neglecting the difference  $E_{1,2} - (E_{1,1} + E_{2,2})/2$  between the molecular interaction energy of the unsymmetrical pair,  $E_{1,2}$  and the average of the molecular interaction energies of the symmetrical pairs of molecules,  $E_{1,1}$  and  $E_{2,2}$ . In many applications in the separation sciences, however, we are interested in pairs of closely related compounds which have similar properties. In such cases, deviations from this assumption may be expected to be small, so the problem can be rephrased as follows. Can we predict the competitive isotherms of a binary mixture from the single-component isotherms with an accuracy compatible with the accuracy we require for the prediction of the individual band profiles in chromatography and the need for a reasonably accurate calculation of the influence of experimental parameters on the production rate and recovery yield.

We assume in the following that the single-component equilibrium isotherms of the two components of the mixture follow the Langmuir isotherm model:

$$q_i = \frac{b_i q_{s,i} C_i}{1 + b_i C_i} \quad (1)$$

where  $q_i$  and  $C_i$  are the stationary and mobile phase concentrations of component  $i$  at equilibrium,  $a_i$  and  $b_i$  are numerical coefficients characteristic of the component  $i$  and  $q_{s,i}$  is the specific column saturation capacity, reported as the amount of component  $i$  needed to form a monolayer per unit volume of packing material. Eqn. 1 is equivalent to the conventional Langmuir isotherm, with  $a_i = b_i q_{s,i}$ .

Based on the IAS theory, LeVan and Vermeulen [22] derived an isotherm for mixtures of gases and vapors which follow the single-component Langmuir model. Extended to the case of solutions, this isotherm can be written as

$$q_i = \frac{b_i q_s C_i}{1 + b_1 C_1 + b_2 C_2} + C_i \cdot \frac{\partial q_s}{\partial C_i} \ln (1 + b_1 C_1 + b_2 C_2) \quad (2)$$

In eqn. 2,  $q_s$  can be considered as a weighted average monolayer capacity. Depending on the number of terms which are considered in the Taylor series expansion giving  $q_s$ , a family of isotherms can be derived. We consider here the first three members of this family.

Formally, the classical competitive Langmuir isotherm could be obtained by writing that  $q_s = q'_s = (q_{s,1} + q_{s,2})/2$ . We obtain

$$q_i = \frac{q'_s b_i C_i}{1 + b_1 C_1 + b_2 C_2} \quad (3a)$$

Eqn. 3a is a correct competitive Langmuir isotherm only if  $q_{s,1} = q_{s,2}$ . Then, it is the first-term expansion of the LeVan–Vermeulen isotherm. The classical competitive Langmuir isotherm, where  $q'_s$  in eqn. 3a is replaced with  $q_{s,i}$ :

$$q_i = \frac{q_{s,i} b_i C_i}{1 + b_1 C_1 + b_2 C_2} \quad (3b)$$

is not an IAS isotherm if  $q_{s,1} \neq q_{s,2}$ .

For the two-term expansion of the LeVan–Vermeulen isotherm, the value of  $q_s$  is given by

$$q_s = \frac{q_{s,1} b_1 C_1 + q_{s,2} b_2 C_2}{b_1 C_1 + b_2 C_2} \quad (4)$$

Hence the two-term expansion of the LeVan–Vermeulen isotherm is obtained by combining eqns. 2 and 4:

$$q_1 = \frac{q_s b_1 C_1}{1 + b_1 C_1 + b_2 C_2} + \Delta_{1,2} \quad (5)$$

and

$$q_2 = \frac{q_s b_2 C_2}{1 + b_1 C_1 + b_2 C_2} - \Delta_{1,2} \quad (6)$$

with

$$\Delta_{1,2} = (q_{s,1} - q_{s,2}) \frac{b_1 b_2 C_1 C_2}{(b_1 C_1 + b_2 C_2)^2} \ln (1 + b_1 C_1 + b_2 C_2) \quad (7)$$

For the three-term expansion of the LeVan–Vermeulen isotherm, the value of  $q_s$ , denoted  $q_s^*$  for the sake of clarity, is written as

$$q_s^* = \frac{q_{s,1}b_1C_1 + q_{s,2}b_2C_2}{b_1C_1 + b_2C_2} + 2 \frac{(q_{s,1} - q_{s,2})^2}{(q_{s,1} + q_{s,2})} \cdot \frac{b_1b_2C_1C_2}{(b_1C_1 + b_2C_2)^2} \cdot \left[ \left( \frac{1}{b_1C_1 + b_2C_2} + 1/2 \right) \ln(1 + b_1C_1 + b_2C_2) - 1 \right] \quad (8)$$

Hence the three-term expansion of the LeVan–Vermeulen isotherm becomes

$$q_1 = \frac{q_s^*b_1C_1}{1 + b_1C_1 + b_2C_2} + \Delta_{1,2}(1 + \Delta_{1,3}) \quad (9)$$

and

$$q_2 = \frac{q_s^*b_2C_2}{1 + b_1C_1 + b_2C_2} - \Delta_{1,2}(1 + \Delta_{2,3}) \quad (10)$$

In eqns. 9 and 10,  $\Delta_{1,2}$  is given by eqn. 7 and

$$\Delta_{1,3} = \frac{q_{s,1} - q_{s,2}}{q_{s,1} + q_{s,2}} \cdot \frac{1}{b_1C_1 + b_2C_2} \left[ \frac{(b_2C_2)^2 + 2b_2C_2 - 4b_1C_1 - (b_1C_1)^2}{b_1C_1 + b_2C_2} \cdot \ln(1 + b_1C_1 + b_2C_2) + \frac{3(b_1C_1)^2 + 4b_1C_1 + b_1b_2C_1C_2 - 2b_2C_2 - 2(b_2C_2)^2}{1 + b_1C_1 + b_2C_2} \right] \quad (11)$$

$$\Delta_{2,3} = \frac{q_{s,2} - q_{s,1}}{q_{s,1} + q_{s,2}} \cdot \frac{1}{b_1C_1 + b_2C_2} \left[ \frac{(b_1C_1)^2 + 2b_1C_1 - 4b_2C_2 - (b_2C_2)^2}{b_1C_1 + b_2C_2} \cdot \ln(1 + b_1C_1 + b_2C_2) + \frac{3(b_2C_2)^2 + 4b_2C_2 + b_1b_2C_1C_2 - 2b_1C_1 - 2(b_1C_1)^2}{1 + b_1C_1 + b_2C_2} \right] \quad (12)$$

Although complex, these isotherm equations depend on only four parameters, the two specific column saturation capacities,  $q_{s,i}$  and the two coefficients  $b_i$  which are respectively equal to the ratios  $a_i/q_{s,i} = k'_{i,0}/Fq_{s,i}$ , where  $F$  is the phase ratio of the column and  $k'_{i,0}$  is the retention factor under linear (*i.e.*, analytical) conditions. These four parameters can be derived simply from the single-component isotherms, provided that these isotherms are accounted for by a simple Langmuir isotherm.

Examination of these equations shows that when the column saturation capacity for the first-eluted component is smaller than that for the second component (diverging isotherms), the amount of first component adsorbed at equilibrium is lower than that predicted by the simple Langmuir competitive model and the amount of the second component adsorbed at equilibrium is larger than that predicted by this model. The converse is true when the column saturation capacity for the first component is the larger (isotherm intersection). When the two column saturation capacities are equal



( $q_{s,1} = q_{s,2} = q_s$ ), eqns. 5 and 6 or 9 and 10 are reduced to the classical Langmuir competitive isotherm, eqn. 3b.

We have used the three series of equations, eqns. 3b, 5 and 6, and 9 and 10, for simulation purposes, using the semi-ideal model of chromatography described previously [23–25]. The results are reported and compared in the next section.

## RESULTS AND DISCUSSION

We have studied the influence of the ratio of the column saturation capacities for the two components and the influence of the composition ratio of the feed.

### *Influence of the ratio of the column saturation capacities*

Figs. 1–5 were calculated for the same mixture composition (concentration ratio

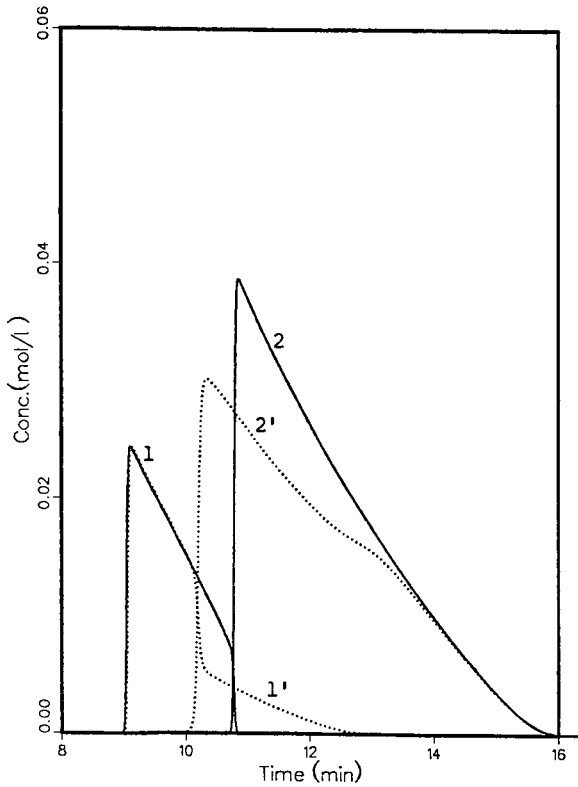


Fig. 1. Overloaded elution of a binary mixture. Comparison between the band profiles calculated using the two-term expansion of the LeVan-Vermeulen isotherm (eqns. 4–7, solid lines) and the conventional Langmuir competitive isotherm (eqn. 3b, dotted lines). Experimental conditions: (I) column, phase ratio  $F = 0.25$ ; flow velocity,  $0.125$  cm/s; column length,  $25$  cm; column efficiency,  $N = 5000$ ; (II) isotherm, limiting retention factor of the first component,  $k'_{0,1} = 3$ ; relative retention,  $\alpha = k'_{0,2}/k'_{0,1} = 1.2$ ;  $b_i = a_i/q_{s,i} = k_{ij}Fq_{s,i}$ ; specific column saturation capacities,  $q_{s,2} = 2$  mmol/ml,  $q_{s,1} = 1$  mmol/ml; (III) sample, feed composition, 1:3; sample size,  $n_1 + n_2 = 0.166$  mmol; injection time,  $t_p = 10$  s; concentrations in the feed,  $C_1^0 = 0.25$  M,  $C_2^0 = 0.75$  M; loading factor for the first component,  $L_{f,1} = 0.05$ , and for the second component,  $L_{f,2} = 0.075$ .

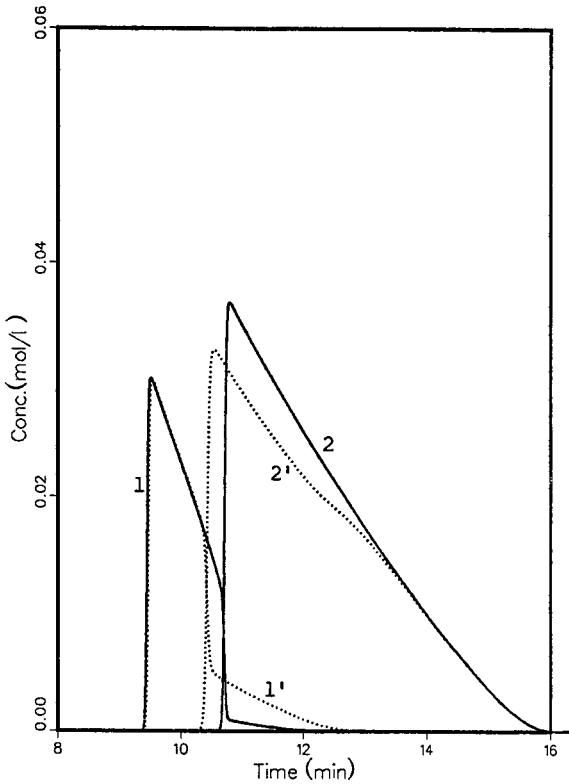


Fig. 2. Overloaded elution of a binary mixture. Comparison between the band profiles calculated using the two-term expansion of the LeVan-Vermeulen isotherm (eqns. 4-7, solid lines) and the conventional Langmuir competitive isotherm (eqn. 3b, dotted lines). Experimental conditions as in Fig. 1, except  $q_{s,1} = 1.5$  mmol/ml and  $L_{f,1} = 0.033$ .

of the first and second components = 1:3), the same sample size and the same column saturation capacity for the second component ( $q_{s,2} = 2$ ), and hence for the same loading factor for the second component ( $L_{f,2} = 7.5\%$ ). The specific column saturation capacity for the second component increases from 1 (Fig. 1) to 1.5 (Fig. 2), 2 (Fig. 3), 3 (Fig. 4) and 4 (Fig. 5). The loading factor for the first component decreases in proportion to the reverse of the column saturation capacity. In each figure, the profiles calculated with the Langmuir competitive isotherm (dotted lines) and with the two-term expansion of the LeVan-Vermeulen isotherm (solid lines) are superimposed.

As expected, when the column saturation capacities for the two components are the same (Fig. 3), the LeVan-Vermeulen isotherm reduces to the Langmuir competitive isotherm and the band profiles calculated with the two isotherms are identical. When the column saturation capacity of the first component is lower than that of the second component (Figs. 1 and 2), the LeVan-Vermeulen isotherm predicts a better separation of the two components, a much narrower mixed zone, a weak tag-along effect and a very strong displacement effect. This is especially noticeable in Fig. 1, where the separation predicted by the LeVan-Vermeulen isotherm is nearly total, which is far from the case for the separation predicted by the Langmuir

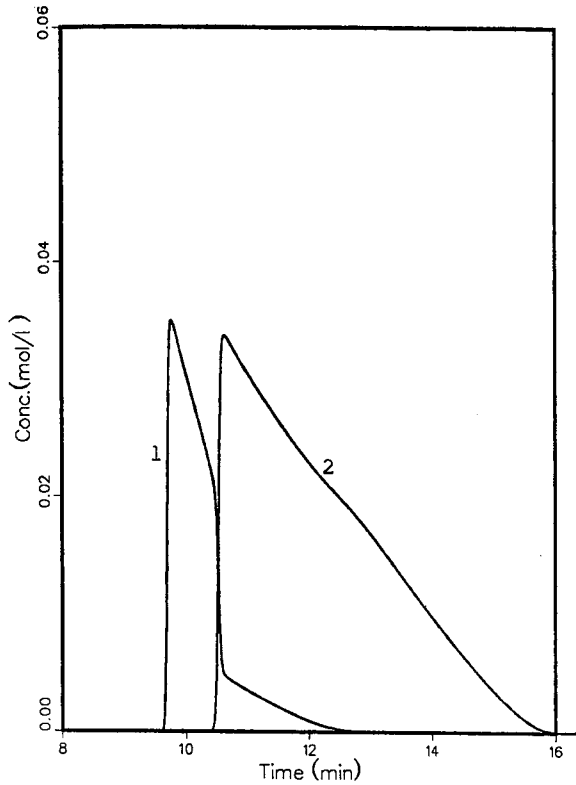


Fig. 3. Overloaded elution of a binary mixture. Comparison between the band profiles calculated using the two-term expansion of the LeVan-Vermeulen isotherm (eqns. 4-7, solid lines) and the conventional Langmuir competitive isotherm (eqn. 3b, dotted lines). In this case, solid and dotted lines are superimposed and cannot be distinguished. Experimental conditions as in Fig. 1, except  $q_{s,1} = 2$  mmol/ml and  $L_{r,1} = 0.025$ .

competitive isotherm. In this case (Fig. 1), the band profile for the second component is nearly identical whether the component is injected pure or in a mixture with the first component. This result is in agreement with experimental observations reported previously [13,26]. Its consequence is a production rate that is higher than that predicted with the competitive Langmuir isotherm.

In contrast, when the column saturation capacity of the first component is larger than that of the second (Figs. 4 and 5), the chromatograms calculated with the LeVan-Vermeulen isotherms exhibit an enhanced tag-along effect and a weak (Fig. 4) or very reduced (Fig. 5) displacement effect. In the latter instance, the mixed zone is very important. With the sample load used ( $L_{r,2} = 7.5\%$ ), a negligible amount of the first component can be recovered pure and the production rate for the second component is abnormally low. This means that a smaller sample size should be used for preparative applications and the production rate is much decreased compared with the prediction based on calculations carried out with the competitive Langmuir isotherm model.

In summary, in agreement with the experimental results and in contrast with the

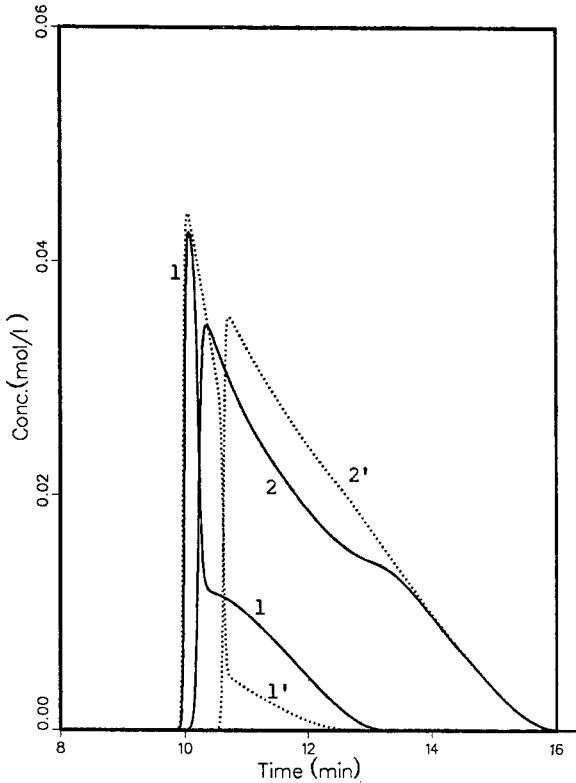


Fig. 4. Overloaded elution of a binary mixture. Comparison between the band profiles calculated using the two-term expansion of the LeVan-Vermeulen isotherm (eqns. 4-7, solid lines) and the conventional Langmuir competitive isotherm (eqn. 3b, dotted lines). Experimental conditions as in Fig. 1, except  $q_{s,1} = 3$  mmol/ml and  $L_{r,1} = 0.0166$ .

Langmuir competitive isotherm, the LeVan-Vermeulen isotherm predicts that the displacement effect is enhanced and the tag-along effect depressed when the column saturation capacity ratio,  $q_{s,1}/q_{s,2}$ , is smaller than unity and the maximum production rate is larger, while the opposite is true when the ratio  $q_{s,1}/q_{s,2}$  is larger than unity.

#### *Influence of the feed composition on band interference*

*Ratio of the column saturation capacities,  $q_{s,1}/q_{s,2}$ , smaller than unity.* In this case, we assume that the specific saturation capacities for the first and second components are 1 and 2, respectively ( $q_{s,1}/q_{s,2} = 0.5$ ). Figs. 6-8 compare the two-term expansion (solid lines) and the three-term expansion (dotted lines) of the LeVan-Vermeulen isotherm with the competitive Langmuir isotherm (dashed lines), as plots of the stationary phase concentrations,  $q_1$  and  $q_2$ , versus the sum  $C = C_1 + C_2$  for three relative compositions,  $C_1/C_2$ , equal to 1:9, 1:1 and 9:1. These figures represent the three intersections of the isotherm surface by the vertical planes through the origin having slopes of 1/9, 1 and 9.

In none of the three cases is there any significant difference between the solid and

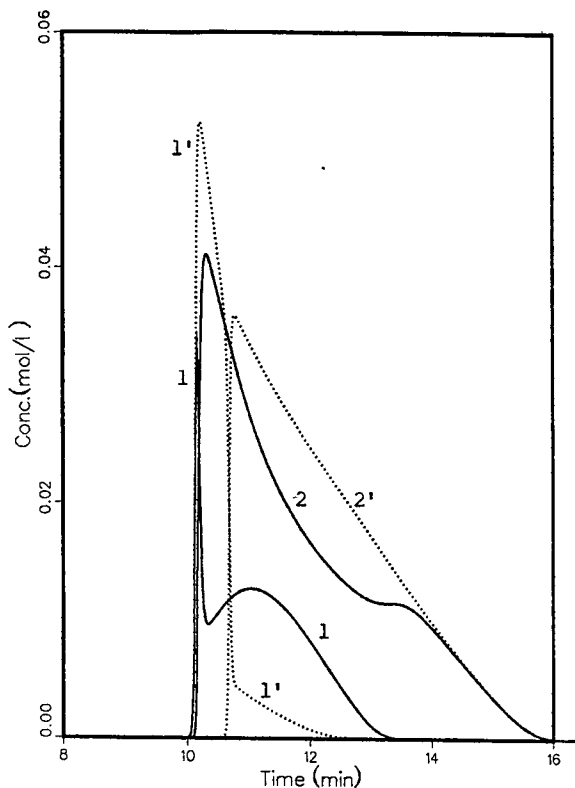


Fig. 5. Overloaded elution of a binary mixture. Comparison between the band profiles calculated using the two-term expansion of the LeVan-Vermeulen isotherm (eqns. 4-7, solid lines) and the conventional Langmuir competitive isotherm (eqn. 3b, dotted lines). Experimental conditions as in Fig. 1, except  $q_{s,1} = 4$  mmol/ml and  $L_{f,1} = 0.0125$ .

the dotted lines. This shows that in the concentration range investigated here the correction introduced by the third term of the expansion in eqns. 9 and 10 is negligible. This concentration range (0-200 mM) includes those typically used in preparative liquid chromatography. This result is important because the third-term correction is needed as a matter of principle to give physical sense to the isotherm and avoid the existence of a maximum of the stationary phase concentration for some intermediate mobile phase concentration. On the other hand, significant differences are observed between the predictions of the LeVan-Vermeulen and the Langmuir competitive isotherms, especially in the intermediate range of relative concentrations (see Fig. 7).

One of the characteristic features of the Langmuir isotherm is that the separation factor,  $(q_2/C_2)/(q_1/C_1) = a_2/a_1 = \alpha$ , is independent of the concentrations  $C_1$  and  $C_2$ . This result is obtained directly from the isotherm eqn. 3b. Thus, the ratio  $r_q = q_2/q_1$  is constant for the Langmuir competitive isotherms in each of Figs. 6-8, and equal to  $\alpha C_2/C_1$ . This ratio  $r_q$  is equal to  $9\alpha$  in Fig. 6, to  $\alpha$  in Fig. 7 and to  $\alpha/9$  in Fig. 8. We observe in these figures that the LeVan-Vermeulen isotherms of the two components are further apart than predicted by the Langmuir competitive model. With the

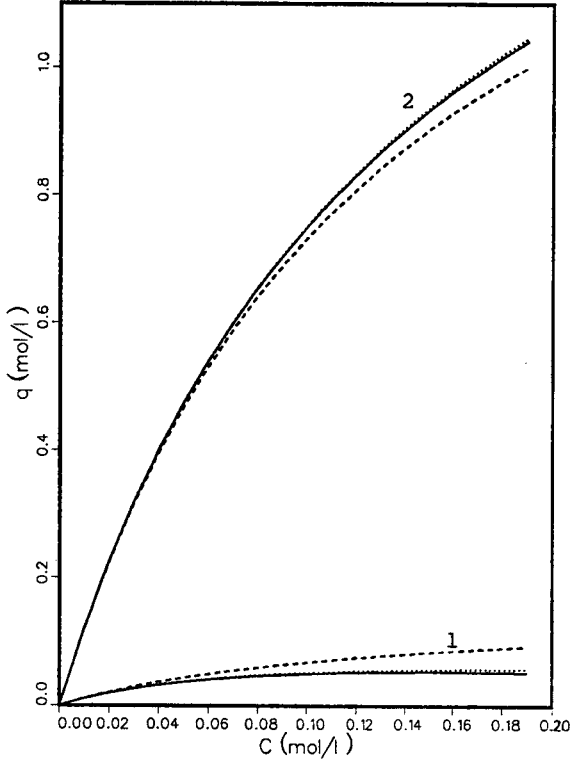


Fig. 6. Equilibrium isotherms. Comparison between the two-term (solid lines) and the three-term (dotted lines) expansions of the LeVan-Vermeulen isotherm and the Langmuir (dashed lines) competitive isotherm. Plots of (1)  $q_1$  and (2)  $q_2$  versus the total mobile phase concentration,  $C = C_1 + C_2$ . Experimental conditions: (I) column, column phase ratio  $F = 0.25$ ; (II) isotherm, specific column saturation capacity  $q_{s,1} = 1$  mmol/ml;  $q_{s,2} = 2$  mmol/ml;  $k'_{0,1} = 3$ ;  $\alpha = k'_{0,2}/k'_{0,1} = 1.2$ ;  $b_i = a_i/q_{s,i} = k_i/Fq_{s,i}$ ; (III) sample, feed composition, 1:9.

LeVan-Vermeulen model, the separation factor is not constant. It increases with increasing total concentration when the column saturation capacity of the first component is smaller than that of the second component. This can be seen in eqn. 9, where the correction term  $\Delta_{1,2}$  is negative in this instance. Accordingly, the stationary phase concentration of the first component at equilibrium,  $q_1$ , is smaller with the LeVan-Vermeulen isotherm than with the Langmuir competitive isotherm and, conversely,  $q_2$  calculated with the LeVan-Vermeulen isotherm is greater than that derived from the Langmuir competitive isotherm. The difference between the values predicted by the two isotherm equations increase with increasing mobile phase concentration.

Figs. 9–12 illustrate the influence of the composition of the feed on the individual elution band profiles of the two components at constant total sample size ( $n_1 + n_2 = 0.166$  mmol) and with values of the specific saturation capacities of 1 and 2 mmol/ml for the first and second components, respectively. Because the column saturation

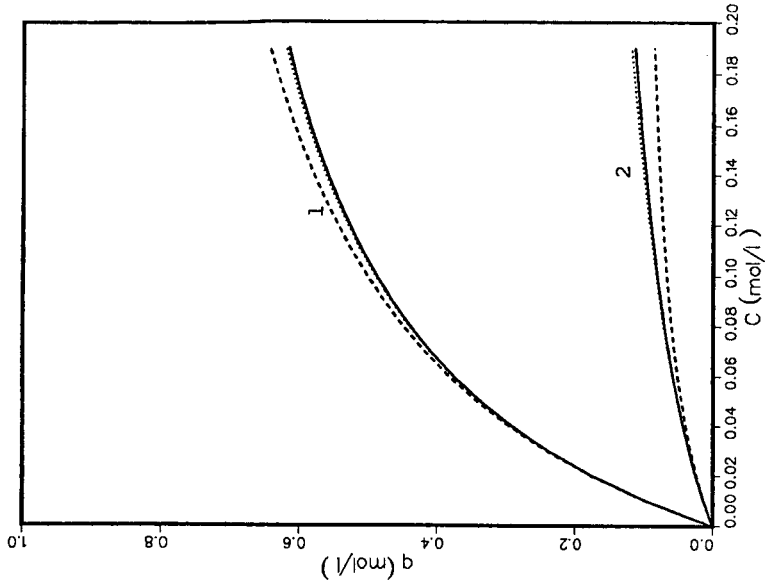


Fig. 7. Equilibrium isotherms. Same as Fig. 6, except feed composition = 1:1.

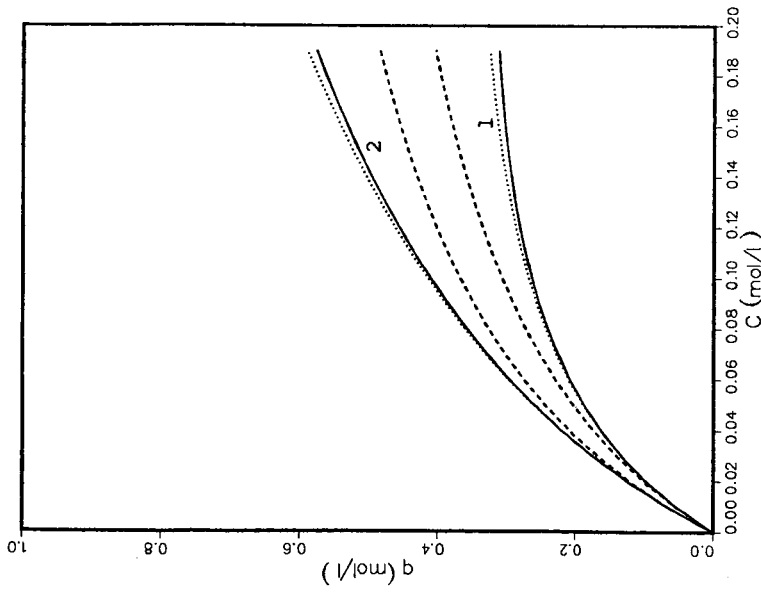


Fig. 8. Equilibrium isotherms. Same as Fig. 6, except feed composition = 9:1.

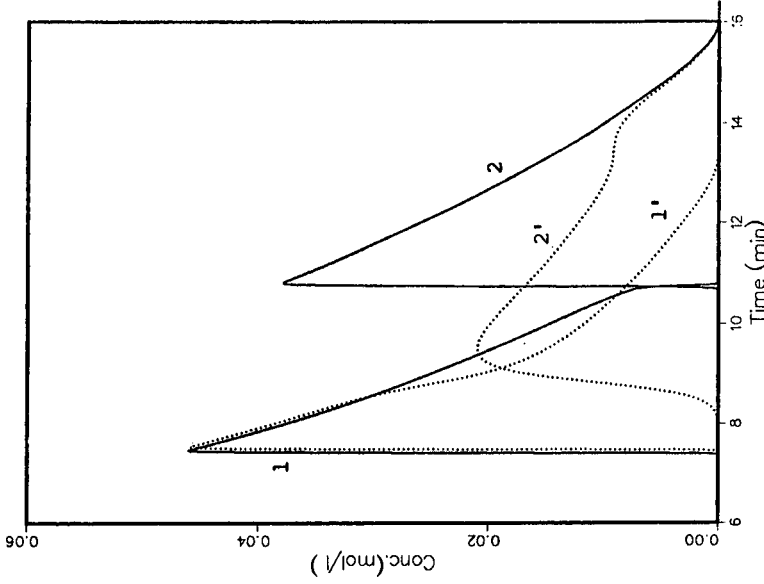


Fig. 9. Overloaded elution of a binary mixture. Influence of feed composition on the band profiles calculated using the two-term expansion of the LeVan-Vermeulen isotherm (eqns. 4-7, solid lines) and the conventional Langmuir competitive isotherm (eqn. 3b, dotted lines). Experimental conditions as in Fig. 1, except feed composition = 1:9.

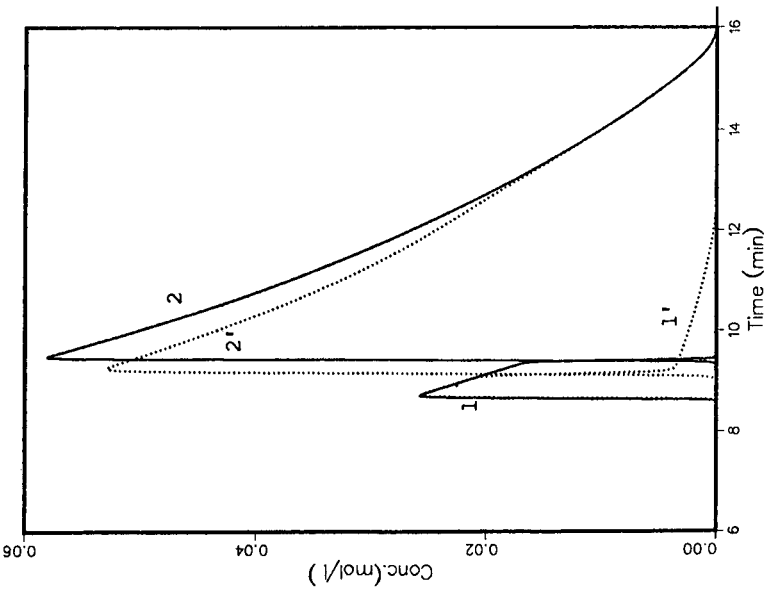


Fig. 10. Overloaded elution of a binary mixture. Influence of feed composition on the band profiles calculated using the two-term expansion of the LeVan-Vermeulen isotherm (eqns. 4-7, solid lines) and the conventional Langmuir competitive isotherm (eqn. 3b, dotted lines). Experimental conditions as in Fig. 1, except feed composition = 1:1.



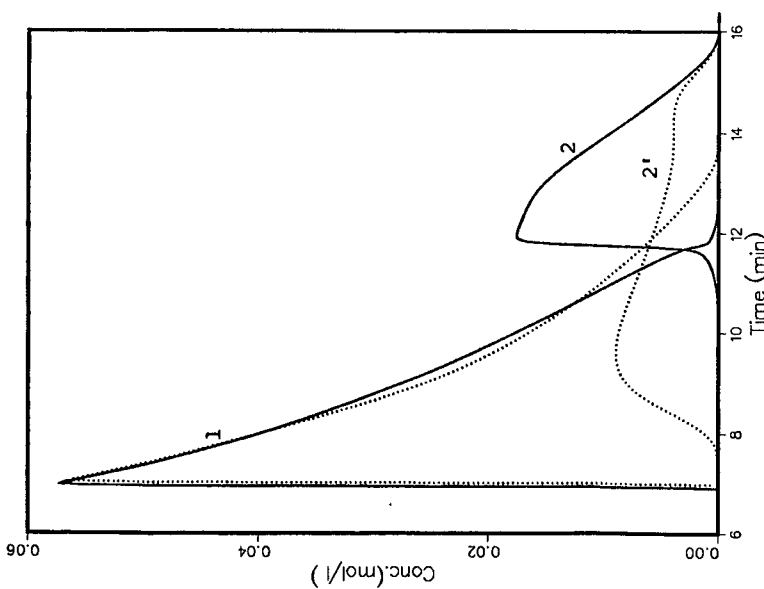
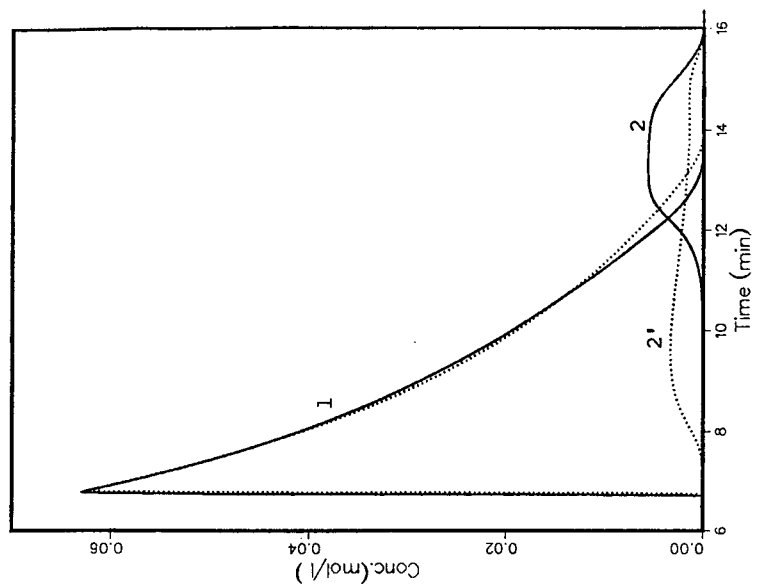


Fig. 11. Overloaded elution of a binary mixture. Influence of feed composition on the band profiles calculated using the two-term expansion of the Le Van-Vermeulen isotherm (eqns. 4-7, solid lines) and the conventional Langmuir competitive isotherm (eqn. 3b, dotted lines). Experimental conditions as in Fig. 1, except feed composition = 3:1.

Fig. 12. Overloaded elution of a binary mixture. Influence of feed composition on the band profiles calculated using the two-term expansion of the Le Van-Vermeulen isotherm (eqns. 4-7, solid lines) and the conventional Langmuir competitive isotherm (eqn. 3b, dotted lines). Experimental conditions as in Fig. 1, except feed composition = 9:1.

capacities for the two components are different, however, the total loading factor is not constant. As above (Figs. 1–5), the solid lines give the profiles calculated with the LeVan–Vermeulen isotherm and the dotted lines those calculated with the Langmuir competitive isotherm. The differences are profound, much larger than the relatively modest differences between the isotherms (Figs. 6–8) would lead one to expect. The chromatogram in Fig. 9 (feed composition = 1:9) is similar to that in Fig. 1 (feed composition = 1:3). The displacement effect is much enhanced compared with the prediction of the Langmuir competitive isotherm; the band profile of the second component is nearly identical with the profile obtained for the same amount of pure component; the separation is nearly total. A similar result is also obtained for the chromatogram in Fig. 10 (feed composition = 1:1). Again, the displacement effect is very strong and the separation is nearly total. The tag-along effect predicted on the basis of the use of the Langmuir competitive isotherm is absent.

As with the Langmuir isotherm, a further decrease in the feed concentration of the second component reduces the intensity of the displacement effect (Fig. 11, feed composition = 3:1) and eventually makes it vanish (Fig. 12, feed composition = 9:1). In contrast to what takes place with the Langmuir competitive isotherm, the separation calculated with the LeVan–Vermeulen isotherm remains satisfactory for a 3:1 mixture, in spite of the large sample size used, and even for a 9:1 mixture the recovery yields in preparative chromatography remain large. This is due to a reduced tailing of the first band and to a considerably depressed tag-along effect. Only a weak tag-along effect is seen in Fig. 11 for the profiles calculated with the LeVan–Vermeulen isotherm. The top of the second component band is flattened whereas its profile becomes wider and shorter than would be observed for the same amount of pure second component. Nevertheless, no concentration plateau is recorded at this feed composition. Even for a 9:1 feed composition (Fig. 12), the concentration plateau of the second component band (solid line) is narrow. The band is much taller and narrower than predicted by the Langmuir competitive isotherm, and it interferes to a much lesser degree with the first component band.

In summary, when the ratio of the column saturation capacities,  $q_{s,1}/q_{s,2}$ , is smaller than unity, the displacement effect is enhanced at all feed compositions, the tag-along effect is depressed and the separation between the two bands is markedly improved, allowing a large increase in the production rate, especially under recovery yield constraints.

*Ratio of the column saturation capacities,  $q_{s,1}/q_{s,2}$ , greater than unity.* In this case we have assumed  $q_{s,1} = 4$  and  $q_{s,2} = 2$ . Figs. 13–15 show the competitive isotherms calculated using the two-term expansion (solid lines) and the three-term expansion (dotted lines) of the LeVan–Vermeulen isotherm and the Langmuir competitive model (dashed lines). In all instances, the equilibrium concentrations in the stationary phase are plotted *versus* the total mobile phase concentration, as in Figs. 6–8. As in the previous instance, there is little difference between the two- and the three-term expansions of the LeVan–Vermeulen isotherm, even for the 1:1 mixture (Fig. 14) for which the isotherms of the two components intersect.

In contrast, there are marked differences between the LeVan–Vermeulen and the Langmuir competitive isotherms. As in this instance  $\Delta_{1,2}$  is positive, the LeVan–Vermeulen isotherm predicts values of  $q_1$  which are larger and values of  $q_2$  which are smaller than those calculated by the Langmuir competitive isotherm. The first

component appears to be more retained and the second component less retained with the LeVan–Vermeulen model than with the Langmuir model. In the three figures, the ratio  $q_2/q_1$  remains constant for the Langmuir competitive isotherms, as was observed in the previous instance (Figs. 6–8,  $q_{s,1}/q_{s,2} < 1$ ). The separation factor is constant with the Langmuir competitive model, whereas it is not with the LeVan–Vermeulen model; the separation factor may even become smaller than unity and the competitive isotherms intersect (Fig. 14). As a consequence of these effects, the calculated band profiles are very different, depending on which isotherm model is used.

Figs. 16–20 illustrate the influence of the feed composition on the individual band profiles. The five chromatograms have been calculated for the same total sample size ( $n_1 + n_2 = 0.05$  mmol, 0.3 times the amount used for Figs. 9–12). The feed composition is changed from 1:9 (Fig. 16) to 9:1 (Fig. 20). When the relative concentration of the second component decreases, we always observe a progressive decrease in the intensity of the displacement effect and a correlative increase in the intensity of the tag-along effect. This was already noted with the Langmuir competitive isotherm [10]. This was also observed in the previous section (Figs. 9–12). This is seen again in Figs. 16–20. However, the displacement effect was extremely strong when  $q_{s,1}/q_{s,2} = 0.5$  and disappeared only at very low values of  $C_2/C_1$ , whereas the tag-along effect was weak in the best cases. The situation is reversed in the present case.

The displacement effect is already weak for the 1:9 mixture (Fig. 16). It becomes negligible as soon as the concentration of the first component exceeds that of the second (Figs. 19 and 20). In all chromatograms, the first component band tails severely beyond the front of the second component band. In contrast, the tag-along effect is important for all values of the relative feed composition. It appears noticeable in Fig. 16 (feed composition = 1:9), whereas it is not seen on the profiles calculated with the Langmuir competitive isotherm in Figs. 16–18. The chromatograms derived from the Langmuir competitive model in Figs. 16–20 correspond to nearly touching bands. In contrast, the band interference is important for the chromatograms calculated with the LeVan–Vermeulen isotherm. In Figs. 18–20 the profile of the second component calculated with the LeVan–Vermeulen isotherm exhibits two maxima, especially noticeable in Fig. 19 (feed composition = 3:1).

Figs. 21–24 show the band profiles calculated for a larger sample size ( $n_1 + n_2 = 0.166$  mmol, the same amount as for Figs. 1–5 and 9–12). The values used for the feed composition are 1:9 (Fig. 21), 1:1 (Fig. 22), 3:1 (Fig. 23) and 9:1 (Fig. 24). The chromatogram for a feed composition of 1:3 was shown in Fig. 5. The effects of the sample size and of the nature of the isotherm used for the calculations are striking. With the Langmuir competitive isotherm, increasing the sample size from 0.05 to 0.166 mmol changes the chromatogram from a touching bands to an overlapping bands case. The intensity of both the displacement and tag-along effects increases with increasing sample size, whereas the resolution between the two bands decreases [10].

With the LeVan–Vermeulen isotherms, the influence of the sample size on the chromatograms is more important. For all feed compositions, the two band fronts are eluted simultaneously. The band profile of the first component exhibits two maxima. The first is very sharp and is eluted at the common front, coincidental with the first band front as calculated with the Langmuir competitive isotherm. The second maximum of the first band is eluted well after the maximum of the second component band. The rear profile of the second band is depressed by the presence of the first band

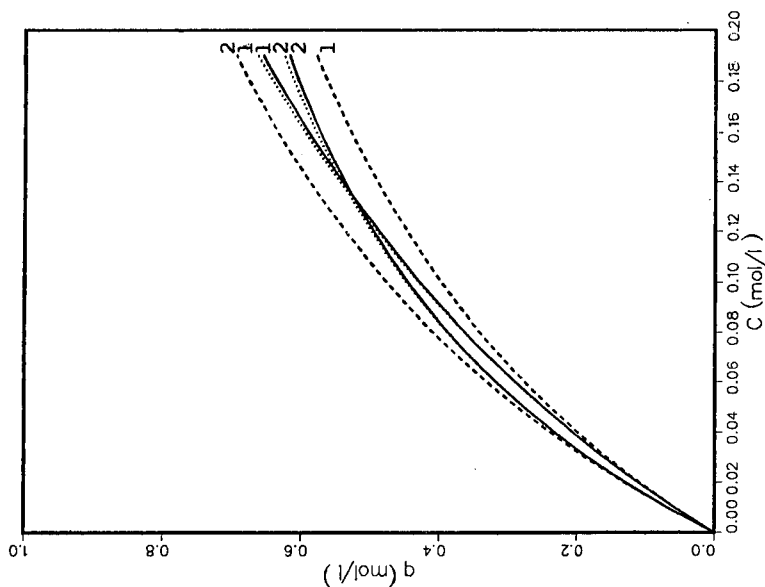


Fig. 13. Equilibrium isotherms. Comparison between the two-term (solid lines) and the three-term (dotted lines) expansion of the LeVan-Vermeulen isotherm and the Langmuir (dashed lines) competitive isotherm. Plots of (1)  $q_1$  and (2)  $q_2$  versus the total mobile phase concentration,  $C = C_1 + C_2$ . Experimental conditions as in Fig. 6, except  $q_{s,1} = 4$  mmol/ml.

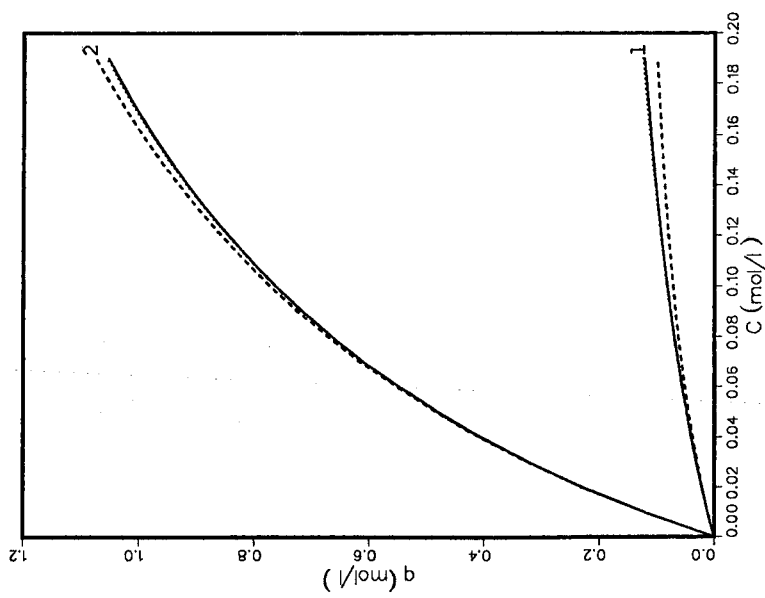


Fig. 14. Equilibrium isotherms. Same as Figs. 6 and 13. Experimental conditions as in Fig. 6, except  $q_{s,1} = 4$  mmol/ml and feed composition = 1:1.

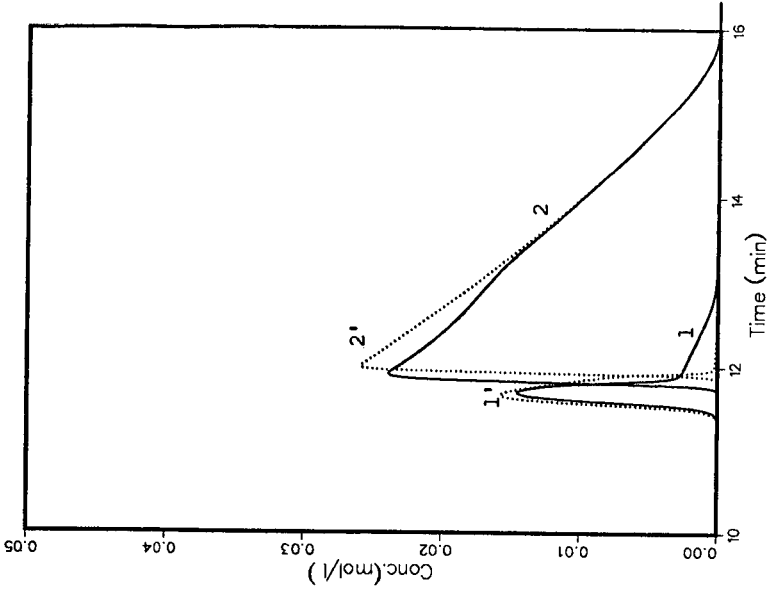


Fig. 15. Equilibrium isotherms. Same as Figs. 6 and 13. Experimental conditions as in Fig. 6, except  $q_{s,1} = 4$  mmol/ml and feed composition = 9:1.

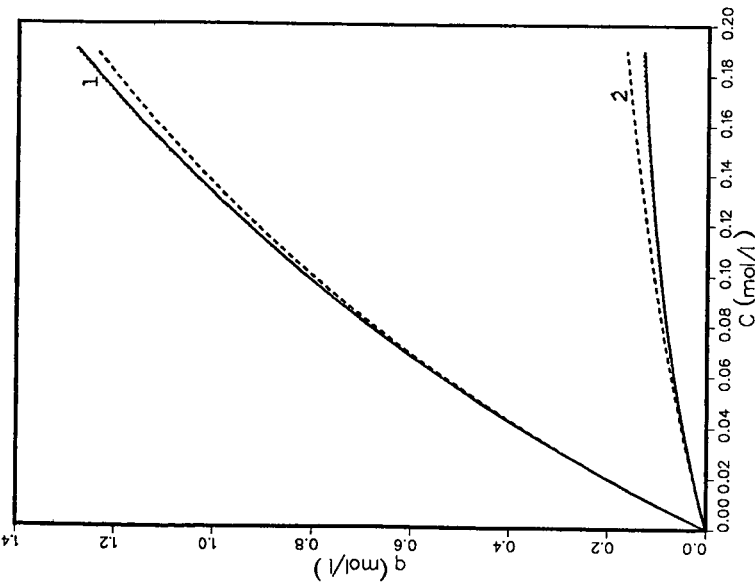


Fig. 16. Overloaded elution of a binary mixture. Influence of feed composition on the band profiles calculated using the two-term expansion of the LeVan-Vermeulen isotherm (eqns. 4-7, solid lines) and the conventional Langmuir competitive isotherm (eqn. 3b, dotted lines). Experimental conditions as in Fig. 1, except  $q_{s,1} = 4$  mmol/ml, sample size = 0.05 mmol and feed composition = 1:9.

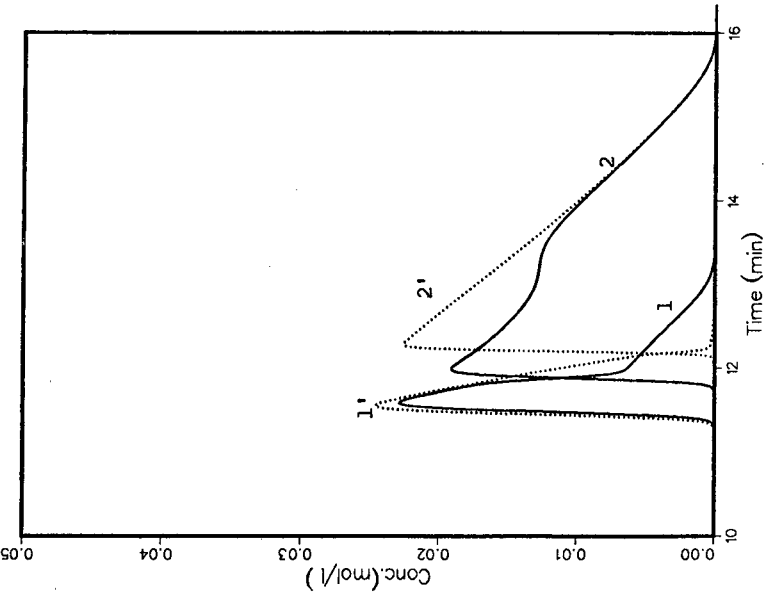
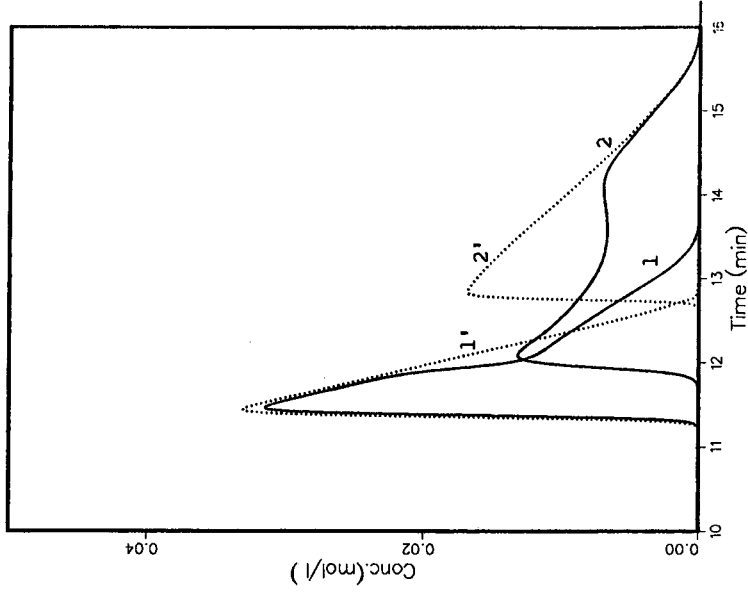


Fig. 17. Overloaded elution of a binary mixture. Influence of feed composition on the band profiles calculated using the two-term expansion of the LeVan-Vermeulen isotherm (eqns. 4-7, solid lines) and the conventional Langmuir competitive isotherm (eqn. 3b, dotted lines). Experimental conditions as in Fig. 16, except feed composition = 1:3.

Fig. 18. Overloaded elution of a binary mixture. Influence of feed composition on the band profiles calculated using the two-term expansion of the LeVan-Vermeulen isotherm (eqns. 4-7, solid lines) and the conventional Langmuir competitive isotherm (eqn. 3b, dotted lines). Experimental conditions as in Fig. 16, except feed composition = 1:1.

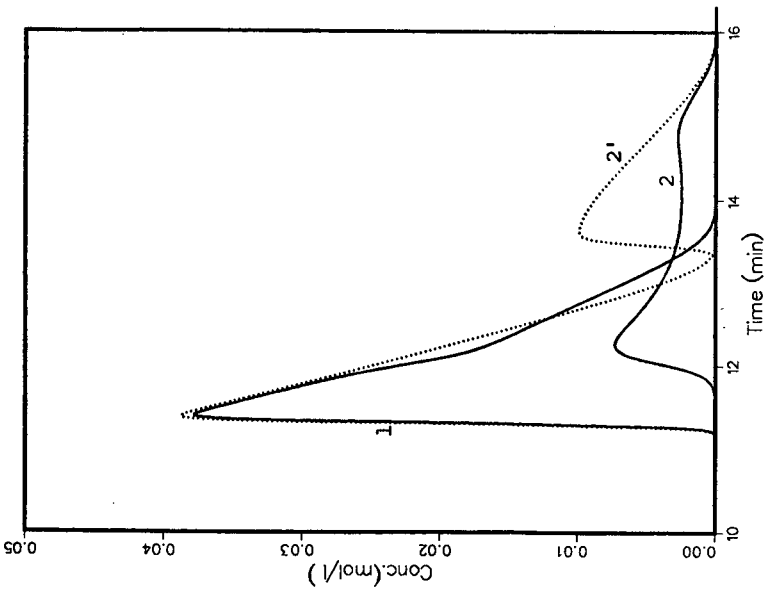
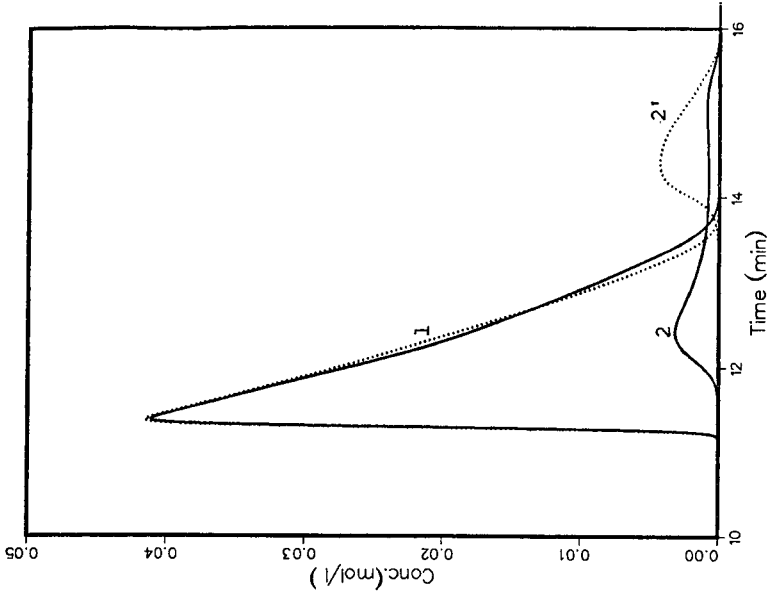


Fig. 19. Overloaded elution of a binary mixture. Influence of feed composition on the band profiles calculated using the two-term expansion of the LeVan-Vermeulen isotherm (eqns. 4-7, solid lines) and the conventional Langmuir competitive isotherm (eqn. 3b, dotted lines). Experimental conditions as in Fig. 16, except feed composition = 3:1.

Fig. 20. Overloaded elution of a binary mixture. Influence of feed composition on the band profiles calculated using the two-term expansion of the LeVan-Vermeulen isotherm (eqns. 4-7, solid lines) and the conventional Langmuir competitive isotherm (eqn. 3b, dotted lines). Experimental conditions as in Fig. 16, except feed composition = 9:1.

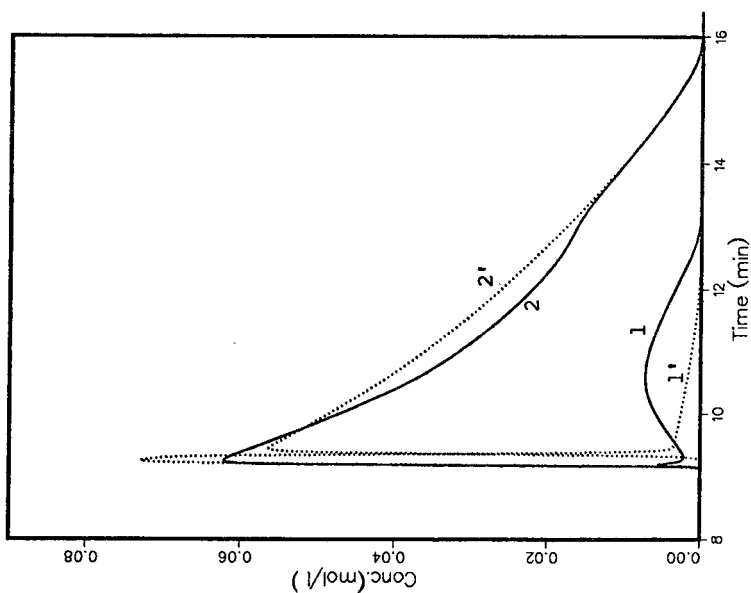
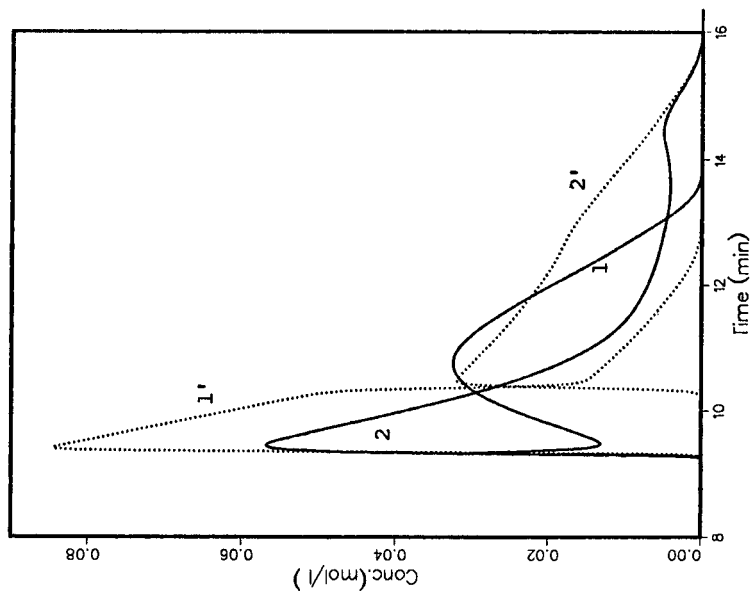


Fig. 21. Overloaded elution of a binary mixture. Influence of feed composition on the band profiles calculated using the two-term expansion of the LeVan-Vermeulen isotherm (eqns. 4-7, solid lines) and the conventional Langmuir competitive isotherm (eqn. 3b, dotted lines). Experimental conditions as in Fig. 16, except sample size = 0.166 mmol.

Fig. 22. Overloaded elution of a binary mixture. Influence of feed composition on the band profiles calculated using the two-term expansion of the LeVan-Vermeulen isotherm (eqns. 4-7, solid lines) and the conventional Langmuir competitive isotherm (eqn. 3b, dotted lines). Experimental conditions as in Fig. 21, except feed composition = 1:1.



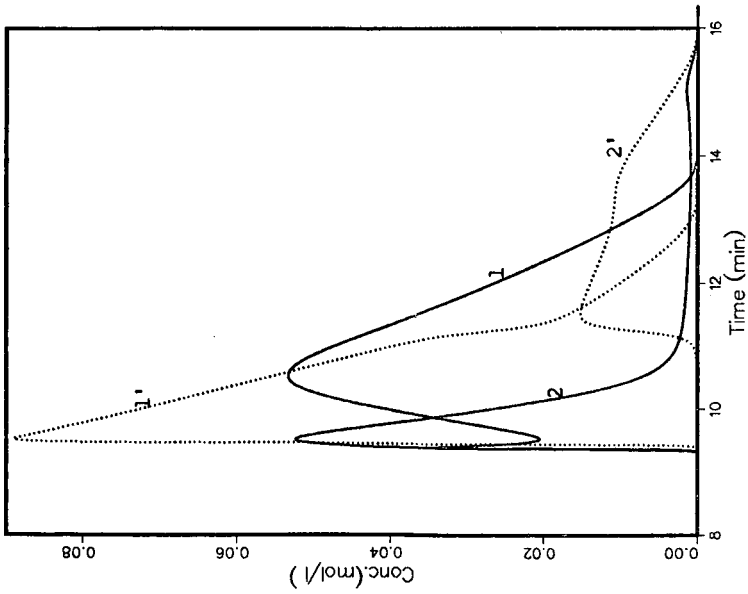
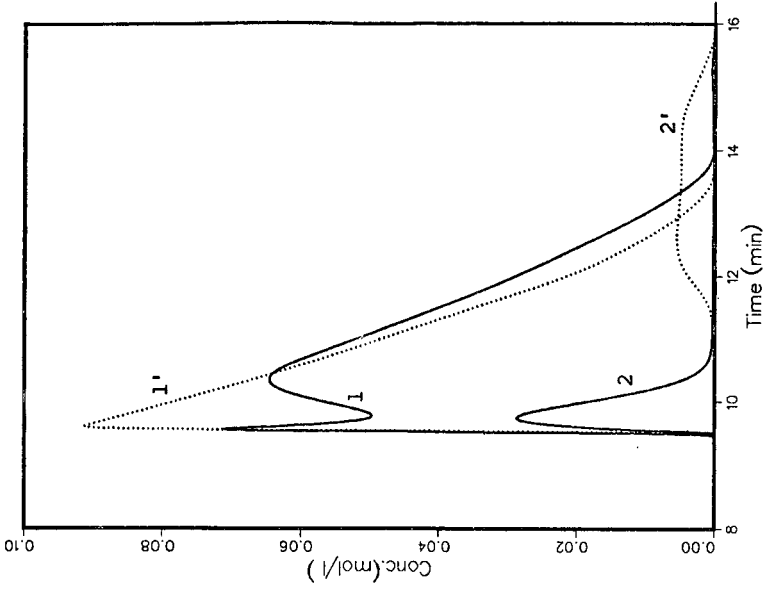


Fig. 23. Overloaded elution of a binary mixture. Influence of feed composition on the band profiles calculated using the two-term expansion of the LeVan-Vermeulen isotherm (eqns. 4-7, solid lines) and the conventional Langmuir competitive isotherm (eqn. 3b, dotted lines). Experimental conditions as in Fig. 21, except feed composition = 3:1.

Fig. 24. Overloaded elution of a binary mixture. Influence of feed composition on the band profiles calculated using the two-term expansion of the LeVan-Vermeulen isotherm (eqns. 4-7, solid lines) and the conventional Langmuir competitive isotherm (eqn. 3b, dotted lines). Experimental conditions as in Fig. 21, except feed composition = 9:1.

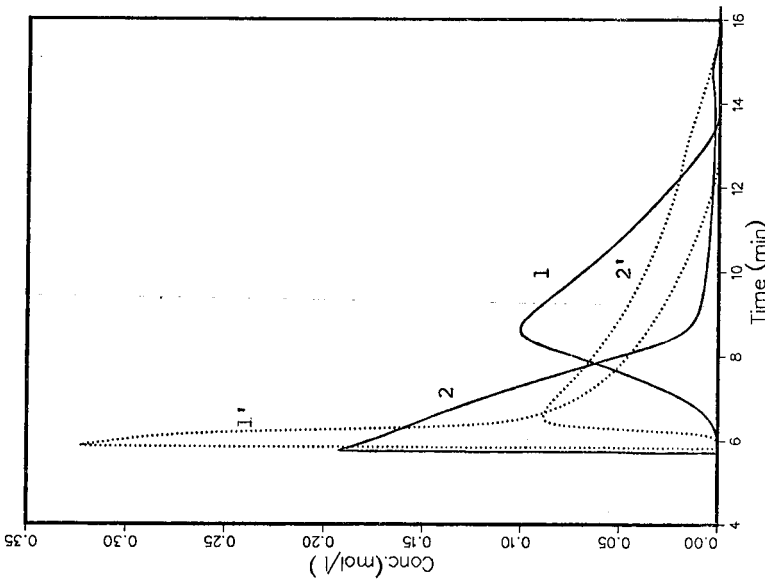
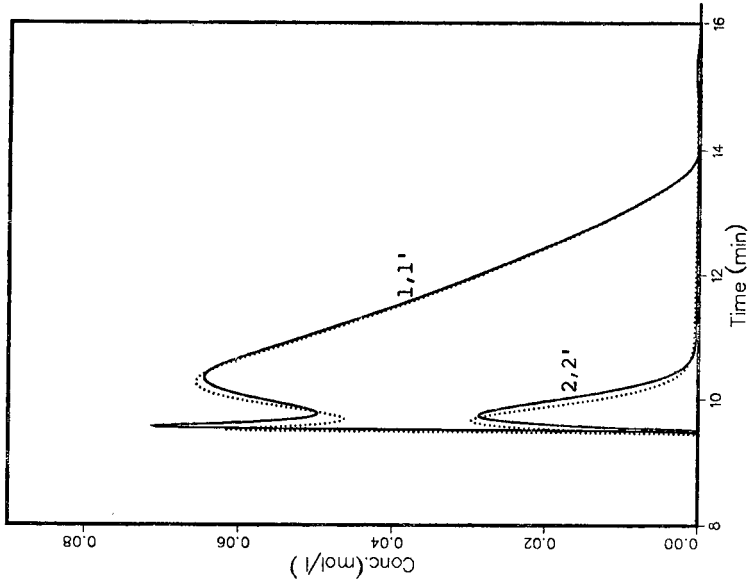


Fig. 25. Overloaded elution of a binary mixture. Influence of feed composition on the band profiles calculated using the two-term expansion of the LeVan-Vermeulen isotherm (eqns. 4-7, solid lines) and the conventional Langmuir competitive isotherm (eqn. 3b, dotted lines). Experimental conditions as in Fig. 1, except  $q_{s,1} = 4$  mmol/ml, sample size = 0.664 mmol and feed composition = 1:1 (also, same conditions as in Fig. 18, except sample size). The Langmuir isotherm elution order is the reverse of the order predicted by the LeVan-Vermeulen isotherm.

Fig. 26. Overloaded elution of a binary mixture. Comparison between the band profiles calculated using the two-term expansion (eqns. 4-7, solid lines) and the three-term expansion of the LeVan-Vermeulen isotherm (eqns. 8-12, dotted lines). Experimental conditions as in Fig. 24.

(see Figs. 5, 21 and 22) and ends in a long tail (Figs. 22 and 23). This same tail exists in the second-component profile in the chromatogram in Fig. 24, but is barely visible.

Compared with the chromatograms in Figs. 16–20, those in Figs. 5 and 21–24 are intermediates in the reversal of the elution order which takes place when the sample size increases. This is illustrated by Fig. 25, which shows the individual profiles calculated for a sample size of 0.664 mmol (feed composition = 1:1). Even in this instance, however, the second-component band exhibits a long, low tail which ends only at the limiting retention time of the second-component under linear conditions. In all instances, the LeVan–Vermeulen isotherm predicts a separation between the two bands which is much worse than that predicted by the Langmuir competitive isotherm. It is not possible to recover any pure fraction of the first-component under any of the conditions simulated in Figs. 5 and 21–25. The amounts of 98% pure first- or second-component which can be recovered with these chromatograms is very low, much lower than with the chromatograms obtained with the Langmuir competitive isotherms.

Fig. 25 demonstrates that the LeVan–Vermeulen isotherm predicts the inversion of the elution order of the components of a binary mixture at large sample sizes when their equilibrium isotherms intersect. A similar result has been described previously in displacement chromatography [27]. The elution order of the two-component bands in the isotachic train depends on the displacer concentration. The Langmuir competitive isotherm model is unable to explain this effect.

Finally, Fig. 26 compares the chromatograms calculated with the two-term (solid lines) and the three-term (dotted lines) expansions of the LeVan–Vermeulen isotherm. Although the sample size is large (0.166 mmol), the differences between these chromatograms are hardly significant. This demonstrates that the LeVan–Vermeulen series converges very rapidly.

## CONCLUSIONS

The LeVan–Vermeulen isotherm offers several practical advantages over the Langmuir competitive isotherm, in addition to the theoretical advantage of being consistent with the Gibbs adsorption isotherm equation. In agreement with experimental results, it predicts an enhanced displacement effect, a decreased tag-along effect, a better separation and a higher production rate when the column saturation capacity of the first-component is smaller than that of the second. Conversely, it also predicts a reduced displacement effect, a larger tag-along effect and a degraded separation, with considerable band interference, in the opposite case, when the column saturation capacity is larger for the first-component than for the second.

The reversal of the elution order of *cis*- and *trans*-androsterone with increasing sample size has been previously observed [28]. It has remained unexplained so far and is in contradiction with the Langmuir competitive model. It is accounted for by the LeVan–Vermeulen isotherm. By the same token, it would also explain the unexpected difficulties reported in the separation of some mixtures by preparative chromatography, where the recovery of pure fractions was impossible. This phenomenon is the elution equivalent of the difficulties encountered in the development of separations by displacement chromatography in the case of compounds exhibiting the isotherm intersection effect [27].

In spite of these advantages, the LeVan–Vermeulen isotherm is still unable to permit the quantitative prediction of the individual band profiles for multi-component samples in chromatography. Like the Langmuir isotherm, this model assumed ideal behavior of the mobile and stationary phases. These assumptions restrict the validity of the model to cases where the mobile phase concentrations of the compounds studied are low, of the order of a few millimolar.

#### ACKNOWLEDGEMENTS

This work was supported in part by Grant CHE-8901382 of the National Science Foundation and by the cooperative agreement between the University of Tennessee and the Oak Ridge National Laboratory. We acknowledge the support of our computational effort by the University of Tennessee Computing Center.

#### REFERENCES

- 1 S. Golshan-Shirazi, S. Ghodbane and G. Guiochon, *Anal. Chem.*, 60 (1988) 2630.
- 2 S. Golshan-Shirazi and G. Guiochon, *Anal. Chem.*, 60 (1988) 2634.
- 3 A. M. Katti and G. Guiochon, *J. Chromatogr.*, 499 (1990) 5.
- 4 S. Jacobson, S. Golshan-Shirazi and G. Guiochon, *J. Am. Chem. Soc.*, 112 (1990) 6492.
- 5 M. Z. El Fallah and G. Guiochon, *J. Chromatogr.*, 522 (1990) 1.
- 6 S. Jacobson, S. Golshan-Shirazi and G. Guiochon, *J. Chromatogr.*, 522 (1990) 23.
- 7 J. Jacobson, J. Frenz and Cs. Horváth, *J. Chromatogr.*, 316 (1984) 53.
- 8 Gy. Vigh, G. Quintero and Gy. Farkas, *J. Chromatogr.*, 484 (1989) 237.
- 9 C. Kemball, E. K. Rideal and E. A. Guggenheim, *Trans. Faraday Soc.*, 44 (1948) 948.
- 10 S. Golshan-Shirazi and G. Guiochon, *Anal. Chem.*, 62 (1990) 217.
- 11 M. Z. El Fallah, S. Golshan-Shirazi and G. Guiochon, *J. Chromatogr.*, 511 (1990) 1.
- 12 S. Golshan-Shirazi, M. Z. El Fallah and G. Guiochon, *J. Chromatogr.*, 541 (1991) 195.
- 13 G. B. Cox and L. R. Snyder, *J. Chromatogr.*, 483 (1989) 95.
- 14 Cs. Horváth, presented at the 6th International Symposium on Preparative Chromatography, PREP'89, Washington, DC, May 1989.
- 15 G. Subramanian and S. Cramer, *Biotechnol. Prog.*, 5, No. 3 (1989) 92.
- 16 J. A. V. Butler and C. Ockrent, *J. Phys. Chem.*, 34 (1930) 2841.
- 17 A. L. Myers and J. M. Prausnitz, *AIChE J.*, 11 (1965) 121.
- 18 T. L. Henson and R. L. Kabel, *Chem. Eng. Prog., Symp. Ser. No. 74*, 63 (1967) 36.
- 19 C. J. Radke and J. M. Prausnitz, *AIChE J.*, 18 (1972) 761.
- 20 A. L. Myers and F. Moser, *Chem. Eng. Sci.*, 32 (1977) 529.
- 21 W. Fritz and E. U. Schlaender, *Chem. Eng. Sci.*, 36 (1981) 721.
- 22 M. D. LeVan and T. Vermeulen, *J. Phys. Chem.*, 85 (1981) 3247.
- 23 G. Guiochon, S. Golshan-Shirazi and A. Jaulmes, *Anal. Chem.*, 60 (1988) 1856.
- 24 M. Czok and G. Guiochon, *Anal. Chem.*, 62 (1990) 189.
- 25 S. Golshan-Shirazi and G. Guiochon, *J. Chromatogr.*, 506 (1990) 495.
- 26 J. Newburger and G. Guiochon, *J. Chromatogr.*, 484 (1989) 153.
- 27 Cs. Horváth, presented at the 7th International Symposium on Preparative Chromatography, PREP'90, Ghent, April 1990.
- 28 M. J. Gonzalez, A. Jaulmes, P. Valentin and C. Vidal-Madjar, *J. Chromatogr.*, 386 (1986) 333.

## Optimisation of frontal chromatography by partial loading

PHILIPPE DANTIGNY, YUYAN WANG, JOHN HUBBLE and JOHN A. HOWELL\*

*School of Chemical Engineering, University of Bath, Claverton Down, Bath BA2 7AY (UK)*

(First received February 15th, 1990; revised manuscript received February 15th, 1991)

---

### ABSTRACT

Quantitative assessment of adsorbate losses during washing is used to provide the basis for a new approach to optimising the performance of packed-bed adsorption chromatography. This paper presents this new approach, and shows, through simulating the performance of the adsorption and washing processes how it can be used with a variety of performance criteria. These include: maximum use of column capacity, minimum product loss and maximum process throughput. The results show that for product loss to be minimised, it is advantageous to stop adsorption before column breakthrough is detected, in order to leave unused capacity capable of scavenging unadsorbed material and product eluted during the washing process. The effect of changes in axial dispersion, length of column loading, inherent adsorbent capacity and adsorption rate or mass transfer are analysed and discussed with respect to optimising the point at which washing is started. It is shown that the application of the new approach can improve column performance significantly and minimise waste without any serious consequence on column capacity utilisation and process throughput.

---

### INTRODUCTION

In any of the current methods of adsorption chromatography used in biotechnology, including ion-exchange, reversed-phase and affinity interactions, it is the typical operating procedure to load a bed until close to breakthrough. This is defined as the first detectable quantity of product in the column effluent. The column is then washed to remove impurities from the bed beyond the minimum point of the column monitor. If the contaminant does not adsorb to the affinity packing but simply diffuse into the pores, Arnold *et al.* [1] indicate that a maximum of three bed volumes of washing solution can be required. In other cases, Arve and Liapis [2] indicate that up to eight bed volumes can be required. It is recognised [3-5] that the washing procedure may cause valuable products to be lost, but as yet there is no quantitative method for assessing wastage continuously. As a consequence, alternative operating protocols for minimising product loss have yet to be developed.

Before optimisation is considered, it is necessary to define the objectives of the adsorption operation so that a rational operating procedure can be defined. Chase [5], in suggesting that the first objective in these processes is the achievement of maximum product purity, discussed the first and second stages of the process as adsorption followed by washing to reduce the level of contaminants in the bed to a predetermined level. There are other possible objectives which may be achievable simultaneously with

the first [*i.e.*, (1) maximisation of product bound; (2) minimisation of product loss; (3) minimisation of process time; and (4) maximisation of process productivity]. The weight of these objectives will depend on the relative costs of the raw materials, column operation and the product value. The controllable variable is the flow-rate which Lowe and Dean [6] suggested should be kept slow to ensure the attainment of equilibrium in the bed. So far most research has focused on the objectives of improving product purity and maximising bed capacity during the adsorption phase.

This paper focuses on the sources of product loss and shows a new approach by which this can be minimised whilst maintaining a high column utilisation efficiency. The approach requires the determination of the position of the saturation front within the bed, defined as the leading edge of the adsorbate-saturated region within the column. As this cannot easily be experimentally determined at present, the current work uses simulation to determine the best strategy assuming the saturation point can be localised or predicted. It is shown that the benefits of operating in the new fashion are considerable and thus it is highly desirable to find ways of experimentally locating the saturation front. A possible method which has been assumed to be applicable is the detection of the thermal changes due to the liberation of the enthalpy of adsorption [7,8]. It is suggested that this might be detected as saturation is nearly complete (say >95% complete).

It turns out that it is necessary to stop adsorption when the saturation front remains well within the column. The exact position depends on several process parameters which also must be determined.

This work presents the results of simulations of bed performance showing the effects of different operating protocols on product loss, overall productivity, process time and utilisation of bed capacity.

## METHODS

### *Model*

Modern methods of adsorption operations include the use of fluidised beds [9–11], where axial dispersion may be higher than is usual in fixed-bed operation. Accordingly, the effect of axial dispersion is included specifically in the formulation and evaluated as one of the parameters influencing the process.

The equations are [12–14]

$$D_L \frac{\partial^2 c}{\partial x^2} - u \frac{\partial c}{\partial x} - \frac{\partial c}{\partial t} - \left( \frac{1 - \varepsilon}{\varepsilon} \right) \frac{\partial q}{\partial t} = 0 \quad (1)$$

$$\frac{\partial q}{\partial t} = k_1 c (q_m - q) - k_2 q \quad (2)$$

The boundary conditions are

$$uc - D_L \frac{\partial c}{\partial x} = c_0 u A(t) \Big|_{x=0} \quad (3)$$

$$\frac{\partial c}{\partial x} = 0 \Big|_{x=1} \quad (4)$$

where

$$A(t) = 1 \text{ if } 0 \leq t < t_{ws} \quad (5)$$

$$A(t) = 0 \text{ if } t \geq t_{ws}$$

Using the following dimensionless groups

$$C = \frac{c}{c_0}; Q = \frac{q}{q_m}; \theta = \frac{ut}{l}; z = \frac{x}{l}$$

$$Pe = \frac{ul}{D_L}; B = \left( \frac{1 - \varepsilon}{\varepsilon} \right) \frac{q_m}{c_0}; k_A = \frac{k_1 c_0 l}{u}; k_B = \frac{k_2 l}{u}$$

Eqns. 1-4 become

$$\frac{1}{Pe} \frac{\partial^2 C}{\partial z^2} - \frac{\partial C}{\partial z} - \frac{\partial C}{\partial \theta} - B \frac{\partial Q}{\partial \theta} = 0 \quad (6)$$

$$\frac{dQ}{d\theta} = k_A C(1 - Q) - k_B Q \quad (7)$$

with the boundary conditions

$$\frac{dc}{dz} = Pe[C - A(\theta)] \Big|_{z=0} \quad (8)$$

$$\frac{dC}{dz} = 0 \Big|_{z=1} \quad (9)$$

The two-dimensional block pulse function (BPF) method has been used to transform eqns. 6-9 into non-linear algebraic recursive equations (see Appendix). A Fortran program has been coded on a PC apricot XEN-i 286/45 in order to solve the latter equations. The bed was divided into twenty identical sections, therefore simulation results were available every 0.05 step.

#### *Comparison of operational protocols*

The traditional operating procedure is to load the bed before the concentration of adsorbate in the effluent reaches 1, 5 or 10% of its value in the feed [14-17]. For the simulations of the traditional procedure, the washing starts when  $C = 0.05$  at the outlet (Fig. 1).

The partial-loading approach requires the position of the breakthrough front to be determined within the bed. It is assumed that the adsorption wave can be thermally detected with certainty when  $C = 0.95$  (Fig. 1). This approach allows the column feed to be controlled such that different levels of bed utilisation are achieved. For example,  $Z^* = 0.5$  means that the washing starts when the adsorption front reaches the middle of the column (say  $C = 0.95$  at  $z = 0.5$ ).

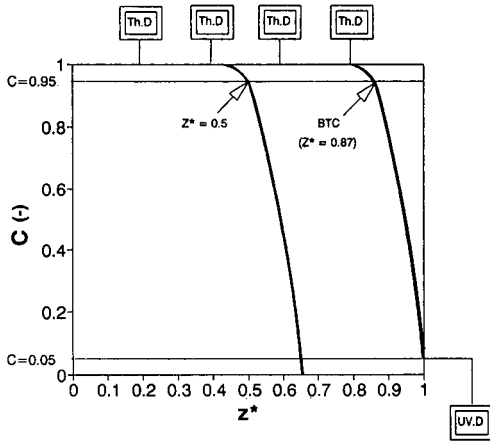


Fig. 1. Adsorption waves within the bed at the end of loading, without axial dispersion, exhibiting the differences between the partial loading approach ( $Z^* = 0.5$ ) and the traditional procedure [Breakthrough curve (BTC)]. Th. D. = Thermal detector; UV. D. = UV detector.

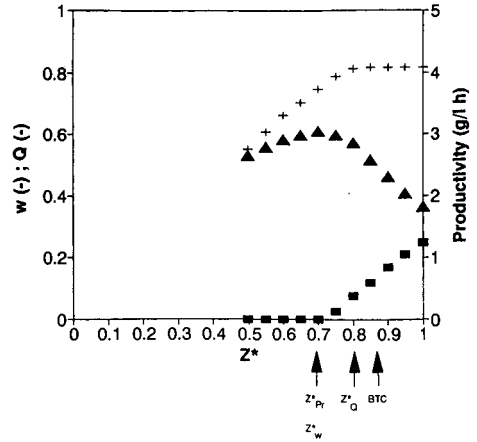


Fig. 2. Product loss ( $w$ ), use of the column ( $Q$ ) and productivity ( $Pr$ ) after washing vs. position of the saturation front at the beginning of washing ( $Z^*$ ) for no axial mixing:  $1/Pe = 0$ ;  $B = 16.64$ ;  $k_A = 9.38$ ;  $k_B = 0.232$ ; (+)  $Q$ , (■)  $w$ , (▲)  $Pr$ .

In practical systems washing continues beyond the minimum detection point of the column monitor, but for simulations the washing volume has been chosen equal to ten bed volumes to ensure high purity of the product. The influence of the washing volume is not considered here.

The model applies to a single-component system, but it will also be possible to extend the analysis to non-interacting multicomponent systems by introducing different parameters for each component.

### Simulation plan

The effect of axial dispersion, the capacity of the column and the kinetic constants ( $k_1$  and  $k_2$ ) on the results obtained with the different techniques was studied by varying the dimensionless groups in which each of these parameters appears (*i.e.*, varying the Peclet number,  $B$ ,  $k_A$  and  $k_B$  shows the variation of each of the first four parameters).

A set of matrix parameters for lysozyme on Blue Sepharose as used for affinity adsorption [18,19] has been taken:  $c_0 = 10^{-3}$  g/cm<sup>3</sup>;  $q_m = 1.2 \cdot 10^{-2}$  g/cm<sup>3</sup>;  $k_1 = 20.2$  cm<sup>3</sup>/gs;  $k_2 = 5 \cdot 10^{-4}$  s<sup>-1</sup>;  $l = 10.4$  cm;  $u = 224$   $\mu$ m/s.

Other physical parameters have been taken from Onwuasoanya [20] to describe a matrix with particularly high axial dispersion:  $D_L = 0.0233$ . The voidage was  $\varepsilon = 0.589$ .

As the model includes mass transport limitations in the adsorption and desorption rate terms, the identification of the parameters of the model is easy. The experimental procedure to determine the parameters  $q_m$ ,  $k_1$  and  $k_2$  was described previously by Chase [14]. Nevertheless, further work is now proceeding using a distributed parameter model to isolate the mass transport effects, in order to assess specifically the influence of the flow-rate on productivity.



The values of the dimensionless groups from the above parameters are:  $1/Pe = 0.1$ ;  $B = 16.6$ ;  $k_A = 9.38$ ;  $k_B = 0.232$ .

## RESULTS

Each of the Figs. 2–6 shows three variables ( $w$ ,  $Q$  and  $Pr$ ) obtained at the end of the washing stage. The curves show the evolution of each of the variables as a function of  $Z^*$ .

### *Basic case*

Firstly, axial dispersion is assumed negligible. The shape of adsorption waves within the bed, at the beginning of washing, is shown in Fig. 1. When breakthrough is detected, it is shown in Fig. 1 that  $C = 0.95$  at  $Z^* = 0.87$ . Hence,  $Z^* = 0.87$  refers to the traditional procedure (BTC) (Fig. 2).

A considerable fraction of the product loaded is lost ( $w = 0.16$ ) by applying the traditional protocol in this case. The loss of product arises from both unadsorbed product and bound product. Because the elution phenomena also occur during the washing stage, only 81% of the maximum capacity of the column can be attained at the end of washing (Fig. 2).

If the goal of the process is the maximisation of the product bound, the traditional method is convenient, but it is also possible to use the partial loading approach. By loading the bed until  $Z^* = 0.8$ , the same amount of product is bound at the end of the washing, whereas the amount of product loaded is less. In that case, the loading time is shorter, thus reducing the overall time of the process and minimising the loss of product to  $w = 0.08$ . The time which can be saved by partially loading the column may be valuable if the loading time represents a significant fraction of the overall processing time. In any case, it is pointless to continue loading beyond the time at which the front reaches  $Z_Q^*$ .

Assuming a constant linear velocity with no axial dispersion, the product bound at the end of washing should be proportional to the fraction of the column loaded until product is lost at the outlet ( $Z^* = 0.70$ ). In fact, the relation between  $Q$  and  $Z^*$  is not rigorously proportional (Fig. 2) due to the remaining product in solution at the end of washing. The average concentration of the product in solution after the washing is negligible compared to the concentration of product bound, but varies in a range 0.06–0.10 for  $Z^*$  from 0.50 to 0.70. For  $Z^*$  greater than 0.70,  $C = 0.10$ .

If the goal of the process is the minimisation of product losses, the partial loading approach is valuable compared to the traditional one. The loss is reduced from 16 to 0% by loading the bed until  $Z^* = 0.70$  (Table I).

Productivity is the main criterion chosen to evaluate the relative worth of different operating conditions as it is the one most nearly related to the value of the process. The above two other criteria are noted because they have been used by laboratory workers, or by manufacturers, as prime measures of process worth. It may well be desirable to have higher column utilisation by developing more effective packing. However, for a given packing, it is not the fractional utilisation of the column which counts, but the productivity per unit time. Without a detailed cost analysis an optimum productivity cannot be totally defined. The expression for productivity (see nomenclature) has been arbitrarily constructed and includes elements for the costs of

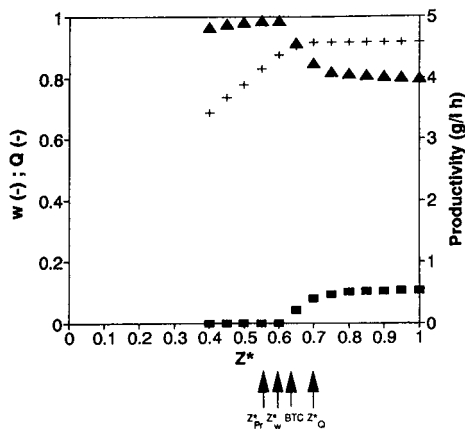
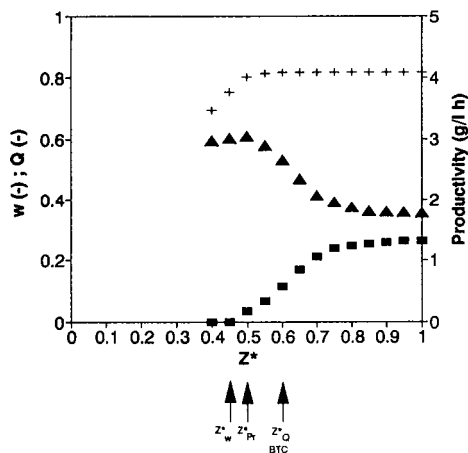


Fig. 3. Product loss ( $w$ ), use of the column ( $Q$ ) and productivity ( $Pr$ ) after washing vs. position of the saturation front at the beginning of washing ( $Z^*$ ) for the basic case:  $1/Pe = 0.1$ ;  $B = 16.64$ ;  $k_A = 9.38$ ;  $k_B = 0.232$ ; (+)  $Q$ , (■)  $w$ , (▲)  $Pr$ .

Fig. 4. Product loss ( $w$ ), use of the column ( $Q$ ) and productivity ( $Pr$ ) after washing vs. position of the saturation front at the beginning of washing ( $Z^*$ ) for the case of high column capacity:  $1/Pe = 0.1$ ;  $B = 83.2$ ;  $k_A = 9.38$ ;  $k_B = 0.232$ ; (+)  $Q$ , (■)  $w$ , (▲)  $Pr$ .

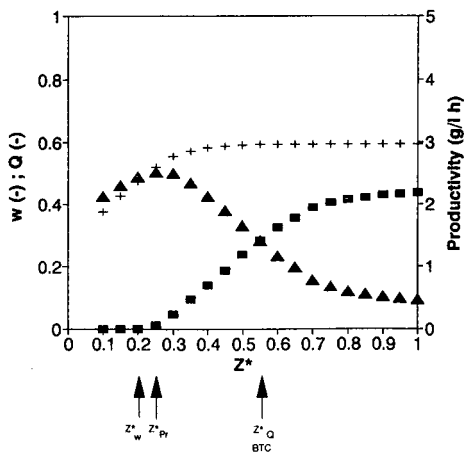
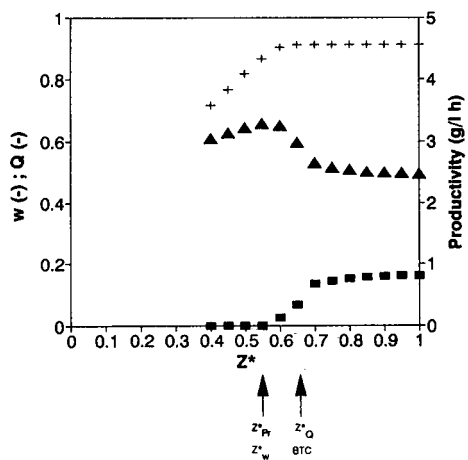


Fig. 5. Product loss ( $w$ ), use of the column ( $Q$ ) and productivity ( $Pr$ ) after washing vs. position of the saturation front at the beginning of washing ( $Z^*$ ) for the case of fast adsorption:  $1/Pe = 0.1$ ;  $B = 16.64$ ;  $k_A = 46.9$ ;  $k_B = 0.232$ ; (+)  $Q$ , (■)  $w$ , (▲)  $Pr$ .

Fig. 6. Product loss ( $w$ ), use of the column ( $Q$ ) and productivity ( $Pr$ ) after washing vs. position of the saturation front at the beginning of washing ( $Z^*$ ) for the case of fast desorption:  $1/Pe = 0.1$ ;  $B = 16.64$ ;  $k_A = 9.38$ ;  $k_B = 1.16$ ; (+)  $Q$ , (■)  $w$ , (▲)  $Pr$ .

TABLE I

INFLUENCE OF THE DIMENSIONLESS GROUPS ( $Pe$ ,  $B$ ,  $k_A$  AND  $k_B$ ) ON THE PRODUCT LOSS ( $w$ ), THE TOTAL PROCESS TIME ( $\theta_{tot}$ ), THE USE OF THE CAPACITY OF THE COLUMN ( $Q$ ) AND THE OVERALL PRODUCTIVITY ( $Pr$ ) OBTAINED BY THE PARTIAL LOADING APPROACH ( $Z_w^*$ ,  $Z_{Pr}^*$  AND  $Z_Q^*$ ) AND BY TRADITIONAL PROCEDURE (BTC)

Parameters of the model				Simulation results				
$1/Pe$	$B$	$k_A$	$k_B$	$Z^*$	$w$	$\theta_{tot}$	$Q$	$Pr$
0	16.64	9.38	0.232	$Z_w^* = 0.70$	0	22.7	0.74	3.03
				$Z_{Pr}^* = 0.70$	0	22.7	0.74	3.03
				$Z_Q^* = 0.80$	0.08	24.5	0.81	2.83
				(BTC) 0.87	0.16	26	0.81	2.45
0.1	16.64	9.38	0.232	$Z_w^* = 0.45$	0	22.6	0.75	2.99
				$Z_{Pr}^* = 0.50$	0.03	23.5	0.79	3.03
				$Z_Q^* = 0.60$	0.11	25	0.81	2.63
				(BTC) 0.60	0.11	25	0.81	2.63
0.1	83.2	9.38	0.232	$Z_{Pr}^* = 0.58$	0	80.2	0.85	4.95
				$Z_w^* = 0.60$	0	82	0.87	4.92
				(BTC) 0.62	0.02	84	0.88	4.72
				$Z_Q^* = 0.70$	0.10	91	0.91	4.24
0.1	16.64	46.9	0.232	$Z_w^* = 0.57$	0	24.9	0.88	3.24
				$Z_{Pr}^* = 0.57$	0	24.9	0.88	3.24
				$Z_Q^* = 0.62$	0.05	25.8	0.91	2.88
				(BTC) 0.62	0.05	25.8	0.91	2.88
0.1	16.64	9.38	1.16	$Z_w^* = 0.20$	0	18	0.47	2.43
				$Z_{Pr}^* = 0.25$	0.02	18.8	0.51	2.48
				$Z_Q^* = 0.55$	0.30	25.5	0.59	1.42
				(BTC) 0.55	0.30	25.5	0.59	1.42

the resin, of the product and of the equipment. This can be modified if different relative costs need to be used. It does allow the concept that the true optimum will differ from that chosen either on grounds of wastage of product or of resin cost alone. By loading the column until  $Z^* = 0.70$ , this criterion is increased by 24% when compared to the traditional protocol (Table I).

#### *Influence of the Peclet number*

$$1/Pe = 0.1 + \text{reference for } B, k_A, k_B$$

To increase the accuracy of the model, axial dispersion is now accounted for, using a Peclet number of 10 ( $1/Pe = 0.1$ ). The adsorption wave broadens and the breaktime is now equal to fifteen compared to sixteen when axial dispersion was assumed negligible (Table I). The decrease of the breaktime with decreasing Peclet number has been also reported by Raghaven and Ruthven [21]. The detection of the breakthrough at the outlet might correspond to a detection of the adsorption front at  $Z^* = 0.60$ .

The traditional method maximises the bound product. It is shown in Table I that axial dispersion has no influence on the maximum amount of product which can be

bound. Due to early breakthrough, unused capacity has been left in the lower area of the column. During the washing, the desorbed material of the upper region has been trapped in the lower, thus reducing the product loss to  $w = 0.11$ .

Due to axial dispersion, the product bound at the end of washing is not proportional to  $Z^*$  (Fig. 3). A great decrease of the product bound is observed with decreasing  $Z^*$  from  $Z^* = 0.50$ . It is shown that the maximum productivity can be achieved by loading the column until  $Z_{pr}^* = 0.50$ ; in that case little product is lost ( $w = 0.03$ ). The productivity obtained loading until  $Z_w^*$  is nearly the same as until  $Z_{pr}^*$ , suggesting that, unless the product is very expensive, there is little benefit in loading until  $Z_w^*$  or  $Z_{pr}^*$ .

It is shown in Table I that the productivity can be maintained at 3.03 g/lh by using a partial-loading approach. Contrarily, productivity is greatly dependent on the Peclet number when using the traditional protocol. The productivity is increased only by 15% with the partial-loading approach, compared to 24% in the previous case. This result indicates that partial-loading is more valuable when axial dispersion is negligible, for example when high flow-rates can be used.

For small Peclet numbers (less than 50), the fraction of the column loaded must be evaluated from the loading time instead of  $Z^*$ . For example, a great decrease of  $Z_w^*$  is shown in Table I with decreasing the Peclet number, whereas the loading time remains nearly constant. This result shows that the amount of product which must be loaded for optimising the process is in fact slightly dependent on the Peclet number.

#### *Influence of the capacity of the column*

$$B = 83.2 + \text{reference for } 1/Pe, k_A, k_B$$

To show the influence of an increase in the capacity of the column, the effect of a five-fold increase in  $q_m$  has been studied. The results show that maximum working capacity of the column is higher ( $Q = 0.91$ ) than previously ( $Q = 0.81$ ). The average concentration of the product in solution after washing is higher than the previous example (0.14–0.28 compared to 0.06–0.10), thus allowing a greater fraction of the capacity of the column to be used.

The maximum working capacity is obtained by loading the column until  $Z^* = 0.70$ . This occurs when 50% of the inlet concentration of adsorbate is detected at the outlet. Hence, the maximum working capacity is not obtained by using the traditional protocol, which is described by a lower value of  $Z^*$  (Table I). Surprisingly enough, the partial-loading approach should allow a larger loading time than the traditional procedure if the goal is the maximisation of the product bound. However, the productivity obtained loading until  $Z_Q^*$  can be improved because 10% of the product loaded is lost during the washing.

This can be achieved for example by using the traditional technique. However, a very low concentration of the product in the effluent must be detected in order to stop the loading period. Otherwise, the productivity may decrease significantly as indicated by the shape of the curve productivity vs.  $Z^*$  shown in Fig. 4. Generally, it is seen that the productivity obtained with the traditional technique is located in the region of steep decrease of the curve as mentioned above.

Increasing  $B$  (e.g., by having better adsorbent capacity), increases operation time

of the column. The optimal productivity is marginally higher (+5%) with the new approach because overall productivity becomes less sensitive to the exact value of  $Z^*$ . Maximum productivity is only about 60% more with a column capacity increased by 500% (Table I).

The productivity decreases slightly from  $Z^* = 0.50$  with decreasing  $Z^*$ . Because adsorption time dominates processing time, the decrease of the product bound is balanced by the reduction of the processing time. In that case, it is possible to stop adsorption earlier than  $Z_{pr}^*$  without significant loss of productivity. This facility may be useful when the exact position of the adsorption front cannot be accurately determined. It should be possible to load the bed until  $Z_{pr}^* (\pm 0.05 Z^* \text{ units})$  without any significant effect on productivity.

#### *Influence of kinetic constants*

“On” constant:  $k_1$ .

$$k_A = 46.9 + \text{reference for } 1/Pe, B, k_B$$

To show the influence of an increase in the value of  $k_1$ ,  $k_A$  has increased five fold. Because the value of the velocity has been kept constant, an increase in  $k_1$  means an improvement in the strength of the interaction between the product and the binding site. The average concentration of the product in solution after washing is less than  $C = 0.10$ . The useful capacity of the column has a greater value ( $Q = 0.91$ ) than for  $k_A = 9.38$  ( $Q = 0.81$ ) due to a more favourable shape of the adsorption isotherm.

Less product can be eluted during washing, and the product loss falls to only 5% when the traditional technique is used (Table I). It is shown in Fig. 5 that the product loss rapidly increases up to  $w = 0.14$  with increasing  $Z^*$  from 0.57 to 0.70. The new approach increases the productivity by 13%, at the same time no product is lost by loading the bed until  $Z^* = 0.57$ .

“Off” constant:  $k_2$ .

$$k_B = 1.16 + \text{reference for } 1/Pe, B, k_A$$

To show the influence of an increase in  $k_2$ ,  $k_B$  has increased five fold. An increase of  $k_2$  means a decrease of the strength of the interaction. Hence, the amount of product eluted during washing is large; under these conditions, the concentration of the product in solution after washing can reach  $C = 0.20$ . Only 60% of the theoretical capacity of the column can be utilised by using the traditional procedure, highlighting the influence of  $k_B$  on the process throughput.

Product loss appears during washing for loading over  $Z^* = 0.20$  (Fig. 6). During washing, 30% of the product loaded is wasted by using the traditional technique. Sufficient capacity in the lower region of the column must be left in order to adsorb the material which desorbs in the upper area. By loading the columns until  $Z^* = 0.25$ , the productivity is maximised and the product lost is reduced to only 2% (Table I).

When  $k_B$  is increased by 500%, the maximum productivity decreases by 18% and the productivity obtained using the traditional method decreases by 46%. In repetitive operation, one of the major effects of an increased number of cycles is an increased

non-specific adsorption and thus a decrease in the maximum capacity of the column. It may also result in a lower affinity of the remaining active sites for the adsorbate [5,22], described here as a decrease of  $k_2$ . The above effects result in a decrease of productivity. Thus, if the adsorbent needs to be replaced when the productivity falls below a critical value, this will take longer with the new approach. Therefore, the new approach permits larger number of cycles in repetitive operation, further increasing productivity.

## CONCLUSIONS

A partial-loading approach has been studied with a model of adsorption chromatography, the central concept being to stop the adsorption before the breakthrough is detected at the outlet. The Peclet number, the maximum capacity of the column, and the kinetic constants have all been assessed with respect to: product loss, the use of column capacity and productivity. A systematic investigation of the effects of these parameters has been made using four dimensionless groups:  $Pe$ ,  $B$ ,  $k_A$  and  $k_B$ . Compared to the traditional procedure, the new approach allows product losses to be reduced without important decrease in bound material, hence increasing the process throughput. By stopping adsorption before all capacity is saturated, unbound product and also material removed in the upper region of the column during washing can be re-adsorbed in the lower regions of the column. The benefits of the partial-loading approach is most clearly demonstrated when the capacity of the column is low or when the interaction between the product and the binding site is weak. Under these conditions the productivity of the process can be increased by 75% using the partial-loading approach.

## SYMBOLS

$a_{ij}$	Element of matrix $\alpha$	
$A$	Heaviside function of eqn. 5	
$B$	Dimensionless group of eqn. 5	
$c$	Concentration of product in solution	g/cm <sup>3</sup>
$c_0$	Initial concentration of product	g/cm <sup>3</sup>
$C$	Dimensionless concentration of product in solution; $C = c/c_0$	
$C(\theta)$	Vector of liquid-phase dimensionless concentration at time $\theta$ , $i$ th element of which refers to the concentration at $i$ th stage of the column	
$D_L$	Axial diffusivity	cm <sup>2</sup> /s
$E$	Constant matrix defined in eqn. A18	
$F$	BPF parameter matrix defined in eqn. A3	
$G$	Function defined by eqn. A13 or A30	
$h_{ij}$	Two-dimensional block pulse function defined in eqn. A1	
$H_m$	One-dimensional BPF vector for time $\theta$	
$H_n$	One-dimensional BPF vector for distance $z$	
$I$	Unit matrix with order $n$	
$J$	Function defined in eqn. A29	
$k_A$	Dimensionless group of eqn. 6	
$k_B$	Dimensionless group of eqn. 6	

$k_1$	Forward rate constant	$\text{cm}^3/\text{gs}$
$k_2$	Backward rate constant	$\text{s}^{-1}$
$l$	Length of the column	cm
$m$	Integer step of $\theta$	
$n$	Integer step of $z$	
$P_m$	Operational matrix for variable $\theta$ defined in eqn. A9	
$P_n$	Operational matrix for variable $z$ defined in eqn. A10	
$Pe$	Peclet number	
$Pr$	Productivity of the process; $Pr = 3.6 \cdot 10^6 \left[ q - c_0(\theta_{\text{tot}} - 10)w \frac{1 - \varepsilon}{\varepsilon} \right] \frac{1}{t}$	$\text{g/lh}$
$q$	Solid-phase concentration of product	$\text{g/cm}^3$
$q_m$	Maximum capacity of the column	$\text{g/cm}^3$
$Q$	Dimensionless solid-phase concentration of product; $Q = q/q_m$	
$Q(\theta)$	Vector of solid-phase dimensionless concentration at time $\theta$ , $i$ th element of which refers to the concentration at $i$ th stage of the column	
$t$	Time	s
$T$	Largest value of $t$	s
$t_{\text{ws}}$	Washing start time	s
$u$	Velocity	cm/s
$w$	Product lost/product loaded	
$x$	Axial position along the column	cm
$z$	Dimensionless distance	
$Z$	Largest value of $z$	
$Z^*$	Distance reached by the adsorption front at the beginning of washing	
$Z_{Pr}^*$	Value of $Z^*$ which maximises $Pr$	
$Z_Q^*$	Smallest value of $Z^*$ which maximises $Q$	
$Z_w^*$	Highest value of $Z^*$ with $w = 0$	
$\alpha$	Matrix defined in eqn. A28	
$\varepsilon$	Voidage	
$\theta$	Dimensionless time	
$\theta_{\text{tot}}$	Dimensionless process time	
$\theta_{\text{ws}}$	Dimensionless washing start time	

## ACKNOWLEDGEMENTS

Financial support from the following sources is gratefully acknowledged. P.D.: European Community; Y.W.: State Education Commission of the Peoples Republic of China.

## APPENDIX

A two-dimensional block pulse function (BPF) is defined below

$$h_{ij}(z,t) = \left\{ \begin{array}{l} 1, \frac{(j-1)Z}{n} < z \leq \frac{jZ}{n}; \frac{(i-1)T}{m} < t \leq \frac{iT}{m} \\ 0, \text{ else} \end{array} \right\} \quad (\text{A1})$$

A function  $f(z,t)$  absolutely integrable in the region  $t \in (0,T)$  and  $z \in (0,Z)$  can be approximated as

$$f(z,t) = \sum_{i=1}^m \sum_{j=1}^n f_{ij} h_{ij}(z,t) = H_m^T(t) F H_n(z) \quad (\text{A2})$$

where

$$F = [f_{ij}]_{m \times n} \quad (\text{A3})$$

$$f_{ij} = \frac{m}{T} \frac{n}{Z} \int_{\frac{(j-1)Z}{n}}^{\frac{jZ}{n}} \int_{\frac{(i-1)T}{m}}^{\frac{iT}{m}} f(z,t) dt dz \quad (\text{A4})$$

$$H_m(t) = \begin{bmatrix} h_1(t) \\ \dots \\ h_m(t) \end{bmatrix} \quad (\text{A5})$$

$$H_n(z) = \begin{bmatrix} h_1(z) \\ \dots \\ h_n(z) \end{bmatrix} \quad (\text{A6})$$

Applying the integration theorem [15] to eqn. A2

$$\int_0^z \int_0^t f(z,t) dt dz = H_m^T(t) P_m^T F P_n H_n(z) \quad (\text{A7})$$

$$\int_z^1 \int_0^t f(z,t) = H_m^T(t) P_m^T F P_n^T H_n(z) \quad (\text{A8})$$

where

$$P_m = \frac{T}{m} \begin{bmatrix} \frac{1}{2} & 1 & \dots & \dots & 1 \\ 0 & \frac{1}{2} & 1 & \dots & 1 \\ \dots & \dots & \dots & \dots & \dots \\ 0 & \dots & \dots & \dots & \frac{1}{2} \end{bmatrix}_{m \times m} ; \quad P_n = \frac{Z}{n} \begin{bmatrix} \frac{1}{2} & 1 & \dots & \dots & \dots \\ 0 & \frac{1}{2} & 1 & \dots & 1 \\ \dots & \dots & \dots & \dots & \dots \\ 0 & \dots & \dots & 0 & \frac{1}{2} \end{bmatrix}_{n \times n} \quad (\text{A9})$$

(A10)

By integrating eqn. 6 with respect to  $z$ , we have

$$\int_0^z \frac{\partial C}{\partial \theta} dz = \frac{1}{Pe} \frac{\partial C(z,\theta)}{\partial z} - C(z,\theta) - \int_0^z G(z,\theta) dz - \frac{1}{Pe} \frac{\partial C(0,\theta)}{\partial z} + C(0,\theta) \quad (\text{A11})$$



$$\int_z^1 \int_0^z \frac{\partial C}{\partial \theta} dz dz = \frac{1}{Pe} [C(1, \theta) - C(z, \theta)] - \int_z^1 C(z, \theta) dz - \int_z^1 \int_0^z G(z, \theta) dz dz + \int_z^1 \left[ -\frac{1}{Pe} \frac{\partial C(0, \theta)}{\partial z} + C(0, \theta) \right] dz \quad (A12)$$

where

$$G = B[k_A C(1 - Q) - k_B Q] \quad (A13)$$

From the boundary conditions, eqn. 8, we obtain

$$-\frac{1}{Pe} \frac{\partial C(0, \theta)}{\partial z} + C(0, \theta) = A(\theta) \quad (A14)$$

Substituting eqns. A14 and 9 into eqn. A11

$$C(1, \theta) = A(\theta) - \int_0^1 \left[ G(z, \theta) + \frac{\partial C}{\partial \theta} \right] dz \quad (A15)$$

Substituting eqn. A14 and eqn. A15 into eqn. A12

$$\int_z^1 \int_0^z \frac{\partial C}{\partial \theta} dz dz = \frac{1}{Pe} \left\{ A(\theta) - \int_0^1 \left[ G(z, \theta) + \frac{\partial C}{\partial \theta} \right] dz - C(z, \theta) \right\} - \int_z^1 C(z, \theta) dz - \int_z^1 \int_0^z G(z, \theta) dz dz + \int_z^1 A(\theta) dz \quad (A16)$$

Applying the integration theorem to eqn. A16 we obtain

$$\begin{aligned} \frac{d\vec{C}(\theta)}{d\theta} P_n P_n^T H_n(z) &= \frac{A(\theta)}{Pe} E^T H_n(z) - \frac{1}{Pe} \vec{C}(\theta) H_n(z) - \\ \left[ \vec{G}(\theta) + \frac{d\vec{C}(\theta)}{d\theta} \right] \frac{1}{nPe} EE^T H_n(z) &- \vec{C}(\theta) P_n^T H_n(z) - \\ &\vec{G}(\theta) P_n P_n^T H_n(z) + A(\theta) E^T P_n^T H_n(z) \end{aligned} \quad (A17)$$

where

$$E = \begin{bmatrix} 1 \\ 1 \\ \dots \\ 1 \end{bmatrix} \quad (A18)$$

Equating the coefficients  $h_i(z)$ , eqn. A17 gives

$$\begin{aligned} \frac{d\vec{C}(\theta)}{d\theta} P_n P_n^T &= \frac{A(\theta)}{Pe} E^T - \frac{1}{Pe} \vec{C}(\theta) - \frac{1}{Pe} \left[ \vec{G}(\theta) + \frac{d\vec{C}(\theta)}{d\theta} \right] \frac{1}{n} EE^T H_n(z) - \\ &\quad \vec{C}(\theta) P_n^T - \vec{G}(\theta) P_n P_n^T + A(\theta) E^T P_n^T \end{aligned} \quad (\text{A19})$$

Eventually, after some manipulations, eqn. A19 becomes

$$\frac{d\vec{C}}{d\theta} = (A(\theta) E^T - \vec{C}) \left( \frac{1}{Pe} + P_n^T \right) \left[ P_n P_n^T + \frac{1}{nPe} EE^T \right]^{-1} - \vec{G} \quad (\text{A20})$$

Applying the product theorem [16] to eqn. 7, we have on the other hand

$$\frac{d\vec{Q}(\theta)}{d\theta} H_n(z) = k_A [\vec{C}(\theta) H_n(z) - C\vec{Q}(\theta) H_n(z)] - k_B \vec{Q}(\theta) H_n(z) \quad (\text{A21})$$

where

$$C\vec{Q}(\theta) = \begin{bmatrix} c_1(\theta) \times q_1(\theta) \\ \dots \\ c_n(\theta) \times q_n(\theta) \end{bmatrix} \quad (\text{A22})$$

Equating the coefficients  $h_i(z)$ , eqn. A21 gives

$$\frac{d\vec{Q}(\theta)}{d\theta} = k_A [\vec{C}(\theta) - C\vec{Q}(\theta)] - k_B \vec{Q}(\theta) \quad (\text{A23})$$

From initial conditions we have

$$\vec{C}(\theta) = \vec{Q}(\theta) = 0 \Big|_{\theta=0} \quad (\text{A24})$$

Eqns. A20, A23 and A24 can be rewritten as

$$\frac{dc_i(\theta)}{d\theta} = \sum_{j=1}^n [c_j(\theta) - A(\theta)] a_{ij} - G[c_i(\theta), q_i(\theta)] \quad (\text{A25})$$

$$\frac{dq_i(\theta)}{d\theta} = J[c_i(\theta), q_i(\theta)] \quad (\text{A26})$$

$$c_i(0) = q_i(0) = 0, \quad i = 1, \dots, n \quad (\text{A27})$$

where

$$\alpha = (a_{ij}) = - \left[ P_n P_n^T + \frac{1}{nPe} EE^T \right]^{-1} \left[ P_n^T + \frac{I_{(n \times n)}}{Pe} \right] \quad (\text{A28})$$

$$J(C, Q) = k_A C [1 - Q] - k_B Q \quad (\text{A29})$$

$$G(C, Q) = F(C, Q) B \quad (\text{A30})$$

$$c_i(\theta) = \frac{n}{Z} \int_{(i-1)Z/n}^{iZ/n} C(z, \theta) dz \quad (\text{A31})$$

$$q_i(\theta) = \frac{n}{Z} \int_{(i-1)Z/n}^{iZ/n} Q(z, \theta) dz \quad (\text{A32})$$

If we are noting

$$c_{ij} = \frac{m}{\theta_{\text{tot}}} \int_{(j-1)\theta_{\text{tot}}/m}^{j\theta_{\text{tot}}/m} c_i(\theta) d\theta \quad (\text{A33})$$

$$q_{i,j} = \frac{m}{\theta_{\text{tot}}} \int_{(j-1)\theta_{\text{tot}}/m}^{j\theta_{\text{tot}}/m} q_i(\theta) d\theta \quad (\text{A34})$$

$$\vec{C}_j = \begin{bmatrix} c_{1j} \\ \dots \\ c_{nj} \end{bmatrix}, \quad \vec{Q}_j = \begin{bmatrix} q_{1j} \\ \dots \\ q_{nj} \end{bmatrix} \quad (\text{A35}), (\text{A36})$$

Applying the forward recursive formula [15] to eqns. A25–A27, we eventually find algebraic recursive relations

$$\vec{C}_{j+1} = \left( \mathbf{I} - \frac{\theta_{\text{tot}}}{2m} \alpha \right)^{-1} \left\{ \left( \mathbf{I} + \frac{\theta_{\text{tot}}}{2m} \alpha \right) \vec{C}_j - \frac{\theta_{\text{tot}}}{2m} \left[ \Gamma(j) A(\theta) \alpha E + G(\vec{C}_j, \vec{Q}_j) + G(\vec{C}_{j+1}, \vec{Q}_{j+1}) \right] \right\} \quad (\text{A37})$$

$$\vec{Q}_{j+1} = \vec{Q}_j + \frac{\theta_{\text{tot}}}{2m} \left[ J(\vec{C}_j, Q_j) + J(\vec{C}_{j+1}, \vec{Q}_{j+1}) \right] \quad (\text{A38})$$

for  $j = 0, 1, \dots, m - 1$

$$\vec{C}_0 = \vec{Q}_0 = 0 \quad (\text{A39})$$

$$\Gamma(j) = \begin{cases} 1, j = 0 \\ 2, j > 0 \end{cases} \quad (\text{A40})$$

## REFERENCES

- 1 F. H. Arnold, H. W. Blanch and C. R. Wilke, *Chem. Eng. J.*, 30 (1985) B9.
- 2 B. H. Arve and I. A. Liapis, *AIChE J.*, 33 (1987) 179.
- 3 D. J. Graves and Y.-T. Wu, *Adv. Biochem. Eng.*, 12 (1979) 219.
- 4 P. C. Wankat, *Anal. Chem.*, 46 (1974) 1400.
- 5 H. A. Chase, *Chem. Eng. Sci.*, 39 (1984) 1099.
- 6 C. R. Lowe and P. D. G. Dean, *Affinity Chromatography*, Wiley, London, 1974.
- 7 S. Kagueli, Q. Yu and N. Wakao, *Chem. Eng. Sci.*, 40 (1985) 1069.
- 8 M. J. Matz and K. S. Knaebel, *Ind. Eng. Chem. Res.*, 26 (1987) 1638.
- 9 M. Yoshikawa, K. Katushi, S. Goto and H. Teshima, *J. Chem. Eng. Jpn.*, 14(6) (1981) 444.
- 10 A. Illanes and Y. Gorgillon, *Enz. Microb. Technol.*, 8 (1986) 81.
- 11 M. Wells, A. Lyddiatt and K. Patel, in M. S. Verrall and M. J. Hudson (Editors), *Separations for Biotechnology*, Ellis Horwood, Chichester, 1987, p. 217.
- 12 H. C. Thomas, *J. Am. Chem. Soc.*, 66 (1944) 1664.
- 13 C.-M. Yang and G. T. Tsao, *Adv. Biochem. Eng.*, 25 (1982) 1.
- 14 H. A. Chase, *J. Chromatogr.*, 297 (1984) 179.
- 15 J. M. Zhu and Y. Z. Lu, *Int. J. Control*, 46 (1987) 441.
- 16 N. S. Hsu and B. Chen, *Int. J. Control*, 36 (1982) 281.
- 17 B. H. Arve and A. I. Liapis, *Biotechnol. Bioeng.*, 32 (1988) 616.
- 18 G. H. Cowan, I. S. Gosling, J. F. Laws and W. P. Sweetenham, *J. Chromatogr.*, 363 (1986) 37.
- 19 J. Hubble, *Biotechnol. Tech.*, 3 (1989) 113.
- 20 D. Onwuasoanya, *Ph.D. Thesis*, University of Bath, Bath, 1987.
- 21 N. S. Raghaven and D. M. Ruthven, *AIChE J.*, 29 (1983) 922.
- 22 P. A. Tice, I. Mazsaroff, N. T. Lin and F. E. Regnier, *J. Chromatogr.*, 410 (1987) 43.

CHROM. 23 264

## **Comparison of a new ovomucoid and a second-generation $\alpha_1$ -acid glycoprotein-based chiral column for the direct high-performance liquid chromatography resolution of drug enantiomers**

K. M. KIRKLAND\*, K. L. NEILSON and D. A. McCOMBS

*ICI Pharmaceuticals Group, Concord Pike and Murphy Rd., Wilmington, DE 19897 (USA)*

(First received January 31st, 1991; revised manuscript received March 6th, 1991)

---

### ABSTRACT

A new commercially-available glycoprotein chiral stationary phase (CSP) based on immobilized ovomucoid protein has been evaluated. This column has been quantitatively compared to the second-generation  $\alpha_1$ -acid glycoprotein CSP for the direct resolution of enantiomers of sixteen commercially-available racemic drugs and eight proprietary drug candidates. The experimental protocol utilized simple aqueous-organic mobile phases with optimization schemes varying only in phosphate buffer concentration, pH and organic solvent modifier type and concentration. Cationic and anionic modifiers were not used to achieve separations due to concerns for consistent column performance. Column stability was monitored by comparing separation factors, resolution, and column efficiency following 200 sample injections during method development. The ovomucoid column showed generally higher resolution, greater flexibility in operating parameters, and better long-term stability than the acid glycoprotein column.

---

### INTRODUCTION

At present there are several choices of chiral stationary phase (CSP) high-performance liquid chromatographic (HPLC) columns that can directly separate enantiomers. These phases include the Pirkle type, inclusion complex formation such as with the cyclodextrin and cellulosic materials, ligand exchange and immobilized protein supports. A number of publications have classified the various chromatographic approaches and defined the bases of CSP-solute interactions [1–4]. Increased regulatory pressures on the pharmaceutical/agricultural industries, coupled with interest in stereoselective bioprocesses [5,6], have resulted in chiral separations of racemic drugs and metabolites being an important issue.

Based on our interest in the chiral recognition of drugs and metabolites in biological systems, we have focused our attention on the protein-based columns, primarily because of the stereoselective network of enzymes, receptors, and cell membranes that exist *in vivo*. Protein-based chiral stationary phases have become popular for the direct separation of drug enantiomers because of their broad applicability, and the use of aqueous buffered mobile phases that are compatible with many biological

samples [3]. The initial immobilized protein HPLC columns for chiral recognition were based on bovine serum albumin (BSA) and  $\alpha$ -acid glycoprotein (orosomuroid), as a result of the pioneering work of Allenmark [7] and Hermansson and Eriksson [8], respectively. Recently, columns based on immobilized human serum albumin [9] and the glycoprotein, fungal cellulase [10], have been used to resolve enantiomers.

We have extensively evaluated another column with a different immobilized glycoprotein: ovomucoid. This stationary phase was reported by Miwa and co-workers [11,12] to have excellent chiral recognition properties. The advantages of this ovomucoid protein for chiral HPLC separations include good stability to changes in temperature, pH, organic solvent composition and antitrypsin activity [13]. To prepare a HPLC column, ovomucoid is isolated and purified from chicken eggwhite, then chemically bound to aminopropyl silica [11]. A column with this ovomucoid protein (OVM) has been recently commercialized and preliminary studies reported [14-16].

Distinguishing features of the various chiral columns with immobilized protein stationary phases are shown in Table I. The second generation  $\alpha_1$ -acid glycoprotein (AGP) column primarily has been used to resolve basic or cationic enantiomers [17,18], however, applications for some acidic drugs also have been reported [8]. Most compounds resolved on the BSA column have been acids [17,18]. The major differences between the ovomucoid and orosomuroid proteins, aside from molecular weight, is in their isoelectric points. This is a direct consequence of the higher sialic acid residue content of orosomuroid. In addition, the larger number of disulfide bridges imparts a more rigid structure to the ovomucoid, which may account for the exceptional stability of the ovomucoid protein [13]. Table I shows that the physical characteristics of ovomucoid are intermediate between orosomuroid and BSA. This suggests that the ovomucoid protein might permit the separation of both acidic and basic enantiomers.

## EXPERIMENTAL

### *Apparatus*

Ovomucoid-based analytical and guard HPLC columns (Ultron ES-OVM, 15

TABLE I  
CHARACTERISTICS OF SOME PROTEINS USED AS STATIONARY PHASES FOR CHIRAL HPLC COLUMNS

Property	Orosomuroid [19]	Ovomucoid [13]	Bovine serum albumin [7]
Molecular weight	41 000	28 800	66 000
Isoelectric point	2.7	3.9-4.5	4.7
Sialic acid residues	14	0.3	
Disulfide bridges	2	8	17
% Carbohydrate	45	30	

$\times 0.46$  cm I.D., and  $1.0 \times 0.4$  cm I.D., respectively) and the achiral column (Zorbax Rx-C<sub>8</sub>,  $25 \times 0.46$  cm I.D.) were obtained from Mac-Mod Analytical (Chadds Ford, PA, USA). Chiral AGP columns ( $10 \times 0.4$  cm I.D.) were acquired from ChromTech AB (Uppsala, Sweden). The HPLC system consisted of two pumps (Model 400, ABI Analytical, Ramsey, NJ, USA), a Model 7125 loop injector (Rheodyne, Cotati, CA, USA), and a variable-wavelength UV detector (ABI, Model 783G). The chromatographic data was acquired and analyzed using the Multichrom data system (Version 1.8, VG Laboratory Systems, Manchester, UK). The detector output was also monitored using a strip-chart recorder (Model BD-41, Kipp and Zonen, Delft, the Netherlands).

### *Chemicals*

The seven proprietary racemic drug candidates (ICI-1–7), a proprietary mixture of diastereomers (ICI-8), lorglumide, and Tröger's base all were synthesized by ICI Pharmaceuticals (Wilmington, DE, USA). Halofantrine hydrochloride was kindly provided by Dr. I. W. Wainer of McGill University (Montreal, Canada). The remaining compounds were obtained from either Research Biochemicals (Natick, MA, USA) or Sigma (St. Louis, MO, USA): 8-OH-DPAT, SKF-38393, SCH-83566, ( $\pm$ )-vesamicol, SCH-23390, SCH-23388, normethyl SCH-23390, normethyl SCH-23388, 2,3-dichloro- $\alpha$ -methylbenzylamine, verapamil, warfarin, lorazepam, atenolol, propranolol and pindolol. Structures for the commercially-available compounds are given in Fig. 1. Reagent-grade potassium dihydrogen phosphate, potassium hydroxide, HPLC-grade water, methanol and acetonitrile were obtained from J. T. Baker (Phillipsburg, NJ, USA). Absolute ethanol was from Quantum Chemicals (Cincinnati, OH, USA).

### *Chromatographic conditions*

Phosphate buffers of pH 5–7 were 10 mM, or as described in the text or in figure captions. Organic modifiers were acetonitrile and ethanol of various concentrations. All separations were performed at ambient temperature (20–25°C). Mobile phase flow-rates were 1.0 ml/min, or as shown. Separation times were within 15 min with capacity factors:  $k'_{\text{OVM}} < 10$ ,  $k'_{\text{AGP}} < 15$ .

Buffers were prepared from 1.25, 2.5, 5.0, 10, 20 or 25 nM solutions adjusted to the desired pH with 1.0 M potassium hydroxide. Stock solutions of 1 mg/ml in methanol were prepared for all test compounds. SCH-23390 and SCH-23388 and the normethyl derivatives of these compounds were obtained as single enantiomers. Chiral separations were performed using solutions of the racemic drugs prepared by mixing equal volumes of each enantiomer.

### *Chromatography procedures*

Separations of sixteen commercially-available racemates and eight ICI proprietary racemic compounds were attempted on both the AGP and OVM protein columns. The commercial test compounds include  $\beta$ -blockers, dopamine agonists and antagonists, and various other pharmacological agents. Both sets of the commercial and ICI compounds contained basic or acidic (carboxylic) functionalities.

Our experiments used only the OVM and the AGP columns for comparison, because previous studies suggested that these two columns might have the desired

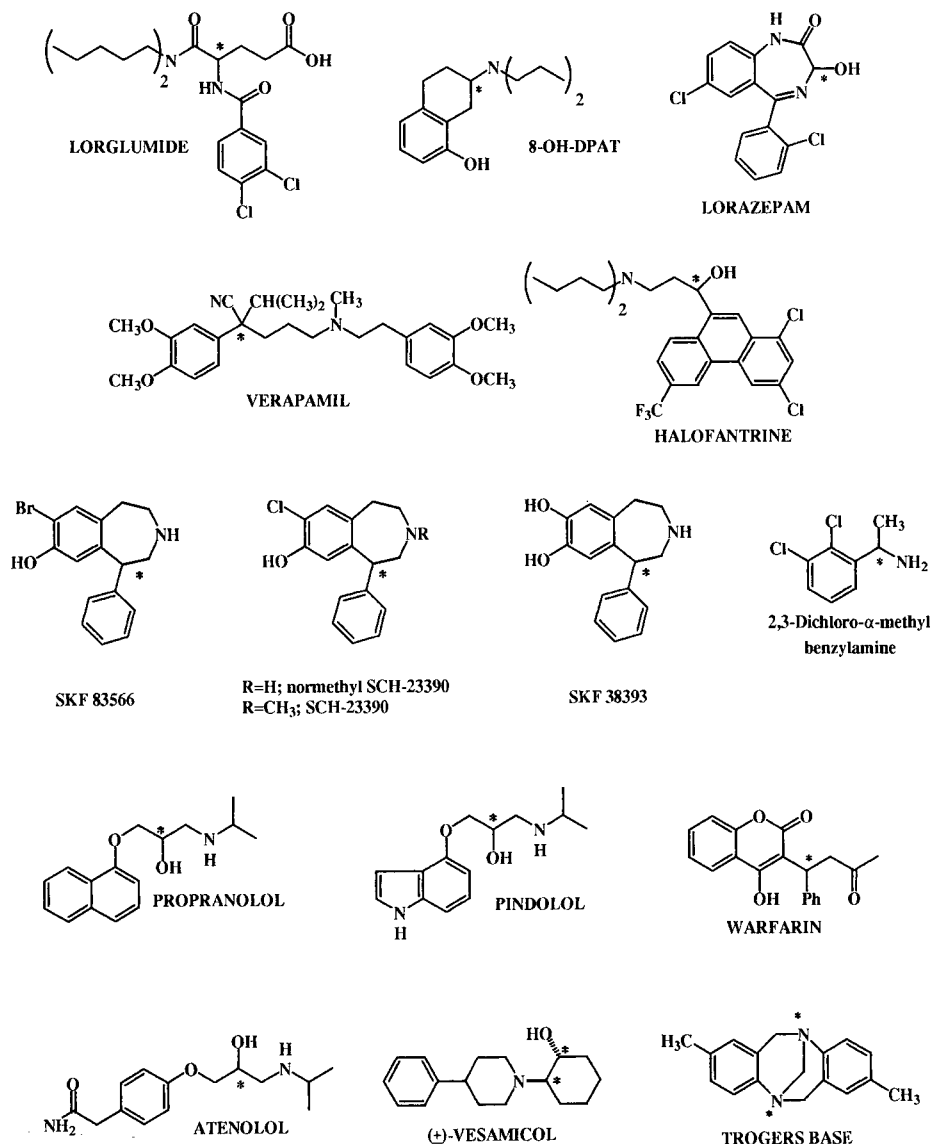


Fig. 1. Structures of commercially-available racemic compounds studied.

range of applicability [8,11,19]. HPLC separations were performed at ambient temperature using a mobile phase flow-rate of 1.0 ml/min. The UV detector was adjusted to the maximum-absorption wavelength for each drug. Injection volumes were 20  $\mu$ l, corresponding to 0.5–1  $\mu$ g of racemate. Separations were achieved with simple mobile phases consisting of only phosphate buffers and organic solvents. Dimethyloctylamine has been reported [19] to be a useful charged additive for separations with the



AGP column. However, in our work with the OVM column, this modifier was not required.

Buffers used were in the pH 5–7 range; initial buffer concentration was 10 mM. The effect of buffer concentration on resolution was studied using verapamil, halofantrine and lorglumide over the 1.25–25 mM range. (The chromatographic behavior of verapamil on the OVM column also has previously been reported by Miwa *et al.* [12].) Similarly, the effect of pH on resolution and selectivity was investigated for the same three compounds. The influence of organic modifier type and concentration was determined in detail only for verapamil.

Resolution of enantiomers for the 24 racemic drugs was optimized by varying pH and the organic modifier, usually ethanol or acetonitrile. The primary objective was to obtain baseline separations in less than 15 min. This corresponds to  $k'$  values of about 10 and 15 on the OVM and AGP columns, respectively.

Stability of both the OVM and AGP columns was studied by evaluating column performance after initial column installation and after 200 injections made during various method development studies. Separations of the test racemic drug probes, SKF-83566 and ICI-1 were performed at various times during these method development studies.

Column-to-column performance of the OVM column was examined using halofantrine as the probe. Separation of halofantrine enantiomers was established on two independent HPLC systems equipped with different OVM columns using identical mobile phases. One OVM column had a history of 90 injections before this test. The other OVM column had separated 400 method development samples prior to the test injection.

The effect of structure on retention and separation resolution for different nitrogen substitution was studied for both the OVM and AGP column using SKF-38393, the racemate prepared from SCH-23390 and SCH-23388 and its *o*-methyl analogues.

Column loading capacity was determined for the OVM column by injecting increasing amounts of the basic drug, halofantrine, and the acidic compound, lorglumide. A 15% decrease in resolution was the arbitrary criterion used to establish column capacity.

Two applications of the OVM column were explored. First, column suitability for diastereomer separations was examined using the experimental protocol for ICI-8. Second, Sequential coupling of an achiral separation of Zorbax Rx-C<sub>8</sub>, followed by a chiral separation on the OVM column, was performed with ICI-2 isolated from human plasma. For the chiral study, standard calibration curves were prepared in 0.5 ml of control human plasma, corresponding to the concentration range of 10–1000 ng/ml of each enantiomer. Plasma samples were adjusted with ammonia to pH 9 and extracted with five equal volumes of ethyl acetate. Following phase separation by centrifugation, the organic layer was removed and evaporated to dryness under nitrogen. The residue was reconstituted in 100  $\mu$ l of the achiral mobile phase [methanol–water (50:50)] and 90  $\mu$ l of this solution was injected into the HPLC system. Achiral reversed-phase separations were performed on a Zorbax Rx-C<sub>8</sub> column at 1.3 ml/min with the UV detector set at 270 nm. The HPLC peak at 5.5 min corresponding to ICI-2 elution was collected in polypropylene tubes, taken to dryness under nitrogen, and reconstituted in 50  $\mu$ l of chiral mobile phase [acetonitrile–0.01 M KH<sub>2</sub>PO<sub>4</sub>

(15:85), pH 6.0]. Approximately 45  $\mu$ l of this solution was injected on the OVM column. Peak areas for both enantiomers were determined with the VG Multichrom data system.

#### Chromatographic calculations

Capacity factor ( $k'$ ) values, selectivity factors ( $\alpha$ ), plate numbers ( $N$ ), plate heights ( $H$ ) and resolution values ( $R_S$ ) were measured using the relationships given in ref. 20.

#### RESULTS AND DISCUSSION

Table II is a summary of data obtained on the 23 test compounds with the OVM and AGP columns. Optimum  $\alpha$  values determined for 23 compounds are depicted for the OVM and AGP columns in Fig. 2 (ICI-8 was not included since it was a diastereomer). To determine the conditions for the best separations for all of these compounds, optimum pH and organic modifier type and composition were deter-

TABLE II  
SUMMARY OF CHIRAL WORK ON AGP AND OVM COLUMNS

Compound	$k'^a$		$N^a$		HETP ( $\cdot 10^{-3}$ ) <sup>a</sup>		$\alpha$		Resolution	
	AGP	OVM	AGP	OVM	AGP	OVM	AGP	OVM	AGP	OVM
8-OH-DPAT	6.3	0.9	1813	4169	5.5	3.6	1.2	1.4	1.7	2.8
SKF-38393	—	1.6	—	3191	—	4.7	1.0	1.3	—	1.9
SKF-83566	9.3	3.5	1484	2270	6.7	6.6	1.2	1.3	1.4	2.1
Vesamicol-HCl	10.2	1.9	—	2548	—	5.9	1.1	1.3	0.8	1.8
Methyl-SCH	8.7	2.6	1956	2242	5.4	6.7	1.2	1.2	1.6	1.3
Normethyl-SCH	—	1.6	—	2458	—	6.1	1.0	1.3	—	1.8
2,3-Dichloro- $\alpha$ -methylbenzylamide	6.8	2.7	2067	2720	4.8	5.5	1.3	1.2	2.4	1.2
Verapamil-HCl	6.8	4.0	1216	1625	8.2	9.3	1.3	1.4	1.7	2.5
Tröger's Base	6.6	3.9	361	1648	27.7	9.1	1.6	1.2	2.3	1.2
Warfarin	4.6	2.2	—	1338	—	11.2	1.3	1.3	0.6	1.7
Lorazepam	5.9	2.7	114	859	87.5	17.5	1.4	1.3	1.0	1.8
Atenolol	6.9	—	550	—	18.2	—	1.2	1.0	1.2	—
Propranolol	29.2	3.9	1639	—	6.1	—	1.1	1.1	1.1	0.8
Pindolol	6.1	2.5	3005	992	3.3	15.1	1.2	1.6	1.9	2.3
Halofantrine	—	0.8	—	913	—	16.4	1.0	2.6	—	4.2
Lorglumide	—	1.5	—	1510	—	9.9	1.0	2.6	—	5.2
ICI-1	5.9	8.7	1734	2221	5.8	6.8	1.4	1.2	2.8	1.6
ICI-2	3.5	0.8	333	4928	30.0	3.0	1.6	1.4	1.7	2.6
ICI-3	7.6	3.7	369	2935	27.1	5.1	1.1	1.4	1.0	3.3
ICI-4	10.6	1.2	—	2325	—	6.5	1.1	1.2	0.7	1.3
ICI-5	4.6	1.7	152	2202	65.8	6.8	1.4	3.3	1.3	7.3
ICI-6	—	1.2	—	1415	—	10.6	1.0	1.3	—	1.8
ICI-7	—	4.2	—	1727	—	8.7	1.0	1.4	—	3.4

<sup>a</sup> Calculations for first-eluting enantiomer.

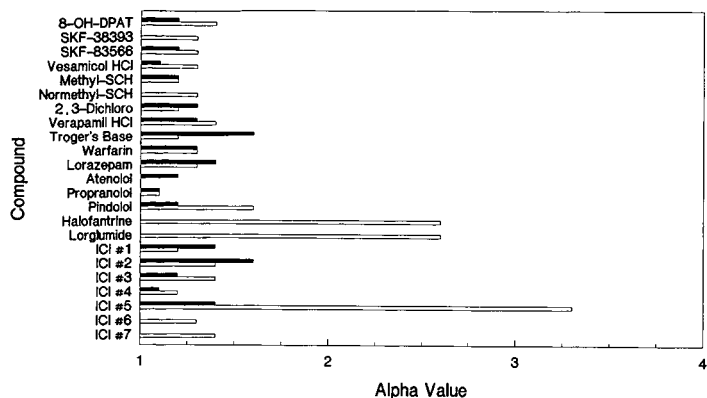


Fig. 2. Separation selectivity factors ( $\alpha$  values) for the chiral separation of racemates. Columns: ■ = Chiral AGP,  $10 \times 0.40$  cm I.D.; □ = Ultron ES-OVM,  $15 \times 0.46$  cm I.D.; mobile phase: optimized as discussed in text; flow-rate: 1.0 ml/min; temperature: ambient; sample:  $20 \mu\text{l}$  of 0.025 mg/ml; UV detector: 270 nm.

mined by experimentation. No separation of enantiomers was obtained for four of the commercial and two of the proprietary compounds on the AGP column. Atenolol was the only compound not separated on the OVM column. Note the very large  $\alpha$  values (*ca.* 3) for halofantrine, lorglumide and drug ICI-5 on the OVM column.  $\alpha$  Values were similar for the remaining compounds on both columns.

Resolution of most enantiomers was higher on the OVM column, as shown in Fig. 3. Atenolol and propranolol were better resolved on the AGP column. However, a very long retention time ( $k' > 20$ ) was required to produce a resolution of 1.1 with an  $\alpha$  value of 1.1 for propranolol. The acidic compounds, lorglumide and ICI-3, are better resolved on the OVM column. Typically,  $k'$  values (and retention times) required to produce the resolution values shown in Fig. 3 were 3 to 8 times larger on the AGP column compared to the OVM column.

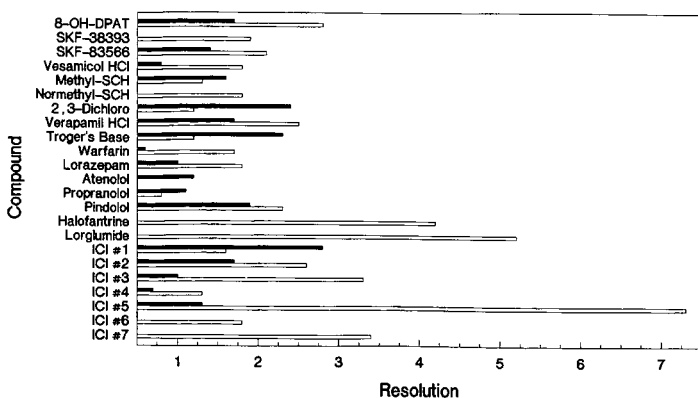


Fig. 3. Resolution values ( $R_s$ ) for the chiral separation of racemates. Conditions as in Fig. 2.

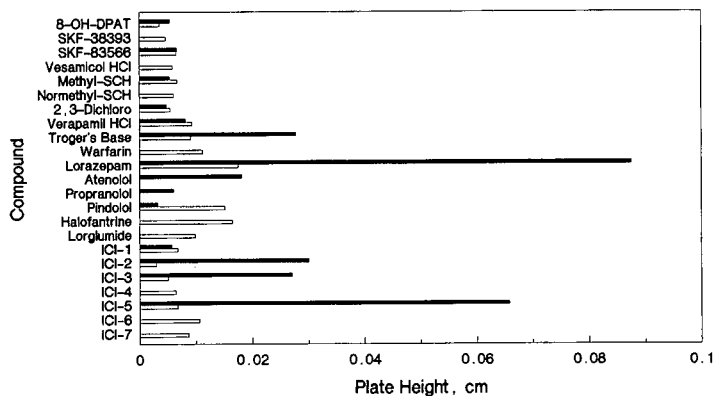


Fig. 4. Plate heights of columns used for the chiral separation of racemates. Conditions as in Fig. 2.

The greater resolution observed for the OVM column relative to the AGP column is a direct result of better column efficiency, as expressed by the plate height values summarized in Fig. 4. Plate heights could not be calculated for nine of the racemates on the AGP column and two racemates on the OVM column, because of poor resolution of the enantiomers.

The direct enantiomeric separation of halofantrine, verapamil and lorglumide on the OVM column was studied as a function of pH and buffer concentration. The effect of organic modifier concentration on chiral selectivity was investigated for verapamil. These particular compounds were selected as models since halofantrine and verapamil are basic compounds, while lorglumide is a carboxylic acid. We found that the  $\alpha$  values for these particular compounds were relatively insensitive to pH changes in the mobile phase buffer, as shown in Fig. 5.

In contrast, as shown in Fig. 6, the enantiomeric resolution of these three

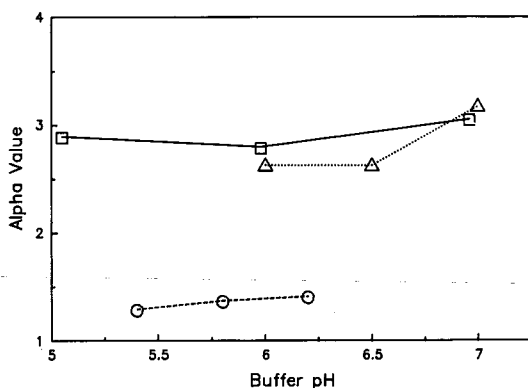


Fig. 5. Effect of buffer pH on enantiomer separation factors for OVM column. Column: Ultron ES-OVM,  $15 \times 0.46$  cm I.D.; mobile phase: organic modifier as follows with  $0.01$  M phosphate buffer; compounds: ○ = verapamil, 17.5% ethanol; □ = halofantrine, 45% acetonitrile; △ = lorglumide, 26% acetonitrile; rest of conditions as in Fig. 2.

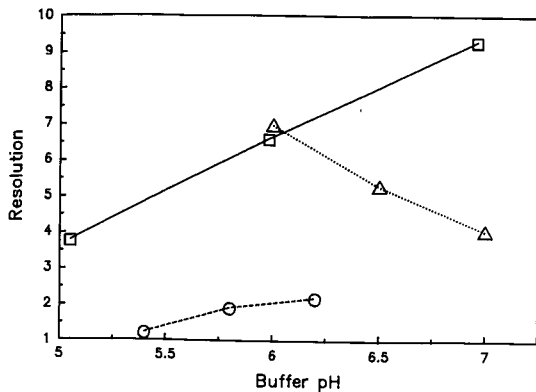


Fig. 6. Effect of buffer pH on enantiomer resolution values for OVM Column. Conditions and symbols as in Fig. 5.

compounds was significantly affected by buffer pH. This trend is the same as reported by Hermansson [19] for acidic and basic solutes on the AGP column. The resolution for the basic drugs increased with increasing pH. The acidic drug, lorglumide, showed increasing resolution with decreasing pH. These effects may be attributed to changes in the surface charge of the immobilized protein which affects coulombic interactions with cationic or anionic drugs. Since the  $\alpha$  values for these enantiomers are not significantly altered by mobile phase pH, the change in resolution is a function of column efficiency. The large variation in column efficiency may result from mass transfer effects occurring from the pH alteration of the charge density on the protein substrate. Dependence of resolution on mobile phase pH may be related to the  $pK_a$  of the drug.

The effect of mobile phase velocity on the plate heights of the three test drugs is shown in Fig. 7. These data were determined using conditions that produced opti-

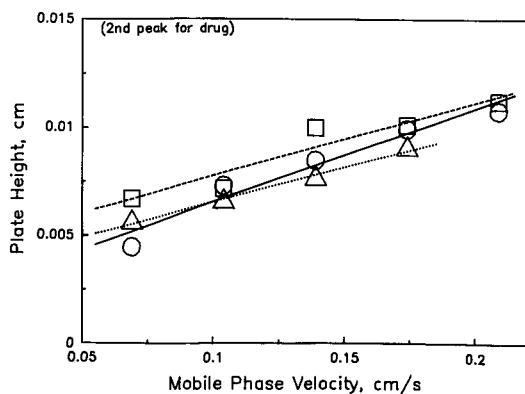


Fig. 7. Mobile phase velocity vs. plate heights for drug enantiomers on OVM column. Compounds and mobile phases (in 13 mM phosphate buffer):  $\circ$  = halofantrine, 45% acetonitrile, pH 6;  $\square$  = lorglumide, 26% acetonitrile, pH 6.3;  $\triangle$  = verapamil, 18% ethanol, pH 6.2. Conditions as in Fig. 5.

imum resolution of the enantiomeric pairs. For these systems, plate heights were similar for the three test compounds. The slightly lower plate heights for halofantrine at lower mobile phase velocities may be due to the lower viscosity associated with the mobile phase containing a high concentration of acetonitrile.

The influence of organic mobile phase modifiers was investigated with verapamil as an arbitrary test compound. Similar results were obtained on other drug compounds. Large decreases in  $\alpha$  (and  $k'$ ) values were observed with increasing amounts of acetonitrile, ethanol, and methanol, as also reported by Miwa *et al.* [11,12]. The separation of verapamil enantiomers was not improved by using methanol as the organic modifier.

The  $\alpha$  values for the three drugs, halofantrine, verapamil and lorglumide, were unaffected by buffer concentration in the range of 1.25 to 25 mM. Fig. 8 shows that resolution also is essentially independent of buffer concentration within the range studied. The exception was halofantrine which showed a slight decrease in resolution at the highest buffer concentration tested. The optimized separations that were achieved using the OVM column for lorglumide, halofantrine and verapamil are shown in Fig. 9. Most noteworthy is the mobile phase concentration of acetonitrile (45%) that was found best for the OVM column in separating the enantiomers of halofantrine. No significant changes in retention and resolution were seen for the OVM column during the method development period (*ca.* one week) with this 45%-acetonitrile mobile phase. This observation compares with the 15–20% limitation in organic solvent composition experienced in this laboratory and by others [21] for the second-generation AGP column.

The ability of a chiral column to resolve particular enantiomers is important. However, equally important is the question of column stability or robustness. The stability of both the OVM and AGP columns was studied using SKF-83566 and ICI-1 as probes. Approximately 200 injections were made during similar method development schemes, and the separations found for the probes was examined during the stability test. During these tests, the initial AGP column had to be replaced after demonstrating significant loss in resolution after only 80 injections. The results ob-

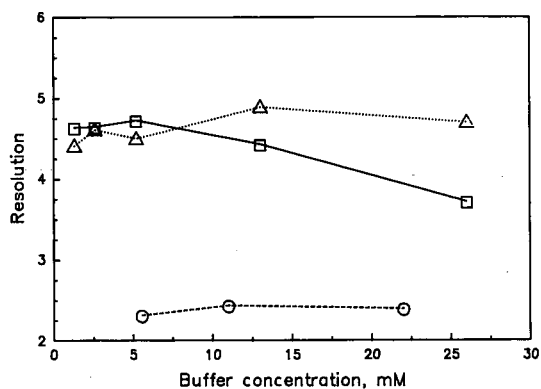


Fig. 8. Effect of buffer concentration on the resolution of enantiomers with OVM column. Compounds and organic modifier:  $\circ$  = verapamil, 17.5% ethanol; pH 6.2;  $\square$  = halofantrine, 45% acetonitrile, pH 5.5;  $\triangle$  = lorglumide, 26% acetonitrile, pH 6.5. Conditions as in Fig. 5.

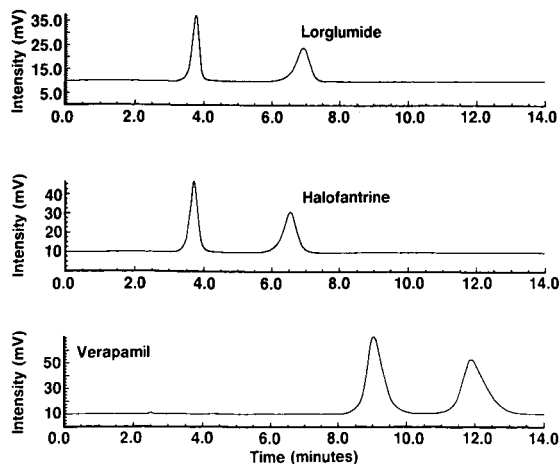


Fig. 9. Optimized separation of enantiomers with OVM column. Conditions as in Fig. 5, except mobile phases: lorglumide, 26% acetonitrile–74% 0.01 *M* phosphate buffer, pH 6.5; halofantrine, 45% acetonitrile–55% 0.01 *M* phosphate, pH 5.5; verapamil, 18% ethanol–82% 0.01 *M* phosphate buffer, pH 6.2.

tained for SKF-83566 on a fresh OVM column and the same column after 200 method development samples is shown in Fig. 10. Fig. 11 shows the same probe compound on an AGP column using a similar stability test protocol. In this test the OVM column exhibited significantly greater stability than the AGP column. This result was found to be typical in several tests. For example, similar results were obtained for the proprietary ICI-1 probe compound. Note that the separations in Fig. 10 with the OVM column used a guard column, whereas a guard column was not available for the AGP column. Proper use of the recently commercially-available guard column for the AGP column should increase its lifetime. Some investigators have reported that the AGP column has acceptable stability when the column is dedicated to a specific analysis without the organic mobile phase composition and pH changes that are often required in method development studies [19,21].

The data in Fig. 10 indicate excellent stability for the OVM column when used properly. Preliminary data on column-to-column reproducibility was also obtained, as illustrated in Fig. 12. We found that  $\alpha$  values, resolution and column efficiency were unchanged on two different OVM column with up to 400 sample injections. For this test, halofantrine was used as the test compound with 45% acetonitrile in the mobile phase.

It has been reported that steric bulk around the basic nitrogen of some drugs can affect enantioselectivity on the AGP column [19,22]. As shown in Fig. 13, a selective dopamine antagonist containing a methyl substituent is well resolved on both the OVM and AGP columns. Removal of the methyl substituent results in a total loss of resolution of the AGP column, but not on the OVM column, as illustrated in Fig. 14. Similarly, we found that the desmethylated benzazepin, SKF-38393, was baseline resolved on the OVM column in less than 7 min, while only a single tailing peak was observed on an AGP column. It is possible that certain mobile phase additives (*e.g.*, dimethyloctylamine [19]) may improve the AGP column performance for these drugs; however, our experimental protocol did not provide for the use of

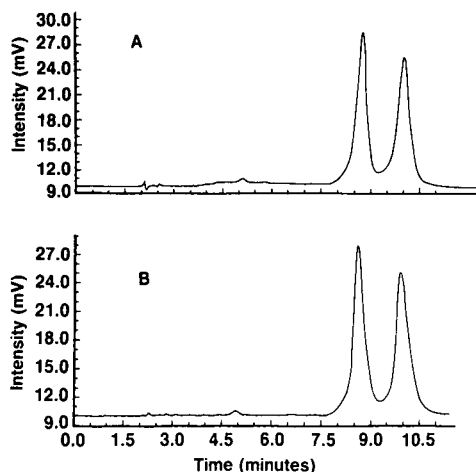


Fig. 10. Stability of OVM column for enantiomeric separation of SKF-83566. (A) Fresh column; (B) same column after 200 sample injections. Conditions: same as for Fig. 5, except mobile phase, 18% acetonitrile–82% 0.01 *M* phosphate buffer, pH 6.0.

such additives. These data suggest that the OVM column may be especially useful for stereoselective metabolism studies involving *N*-dealkylated products.

The effect of sample loading on the resolution of drug enantiomers of halofantrine and lorglumide for the OVM column is shown in Fig. 15.  $\alpha$  Values (solid points) are independent of sample loading for both of these acidic and basic drugs throughout the limited range studied. However, compared to the basic halofantrine, about

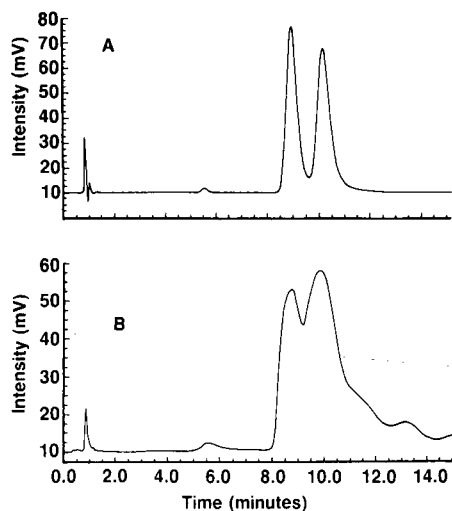


Fig. 11. Stability of AGP column for enantiomeric separation of SKF-83566. (A) Fresh column; (B) same column after 200 sample injections. Column: Chiral AGP, 10  $\times$  0.40 cm I.D.; mobile phase: 12% acetonitrile–88% 0.01 *M* phosphate buffer, pH 6.0; flow-rate: 1.0 ml/min; other conditions as in Fig. 2.



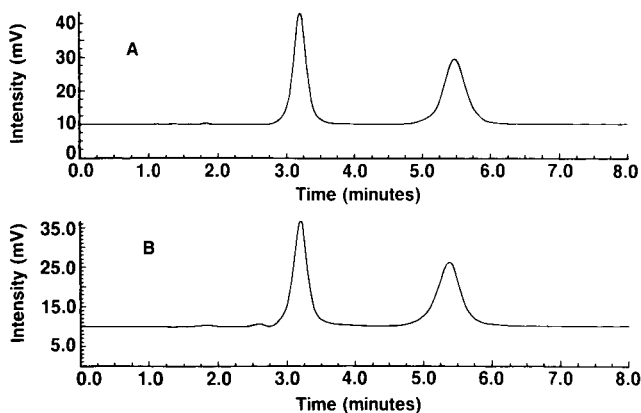


Fig. 12. Column-to-column stability of OVM with high concentration of organic modifier. (A) Column after 90 sample injections; (B) another column of the same type after 400 sample injections. Column: Ultron ES-OVM,  $15 \times 0.46$  cm I.D.; conditions as in Fig. 9 for halofantrine.

twice the amount of the acidic lorglumide can be injected before a 15% decrease in resolution is observed. The low sample loading limit of 1.5–3 nmol/g (about 2.5–5  $\mu$ g of these two drugs) for a 15% decrease in resolution confirms the relatively poor loading capacity of protein-based CSPs [19].

Preliminary experiments on applying the OVM column to enantiomers and diastereomers in biological systems have been quite encouraging [14–16]. For example, sequential coupling of an achiral reversed-phase separation with a chiral separation using the OVM column was performed to analyze for ICI-2 in human plasma. Fig. 16 indicates the fraction collected during the achiral separation of a plasma extract, and the resulting chiral separation of the enantiomers at a concentration of 10 ng/ml of each enantiomer. With appropriate validation, a method with this sensi-

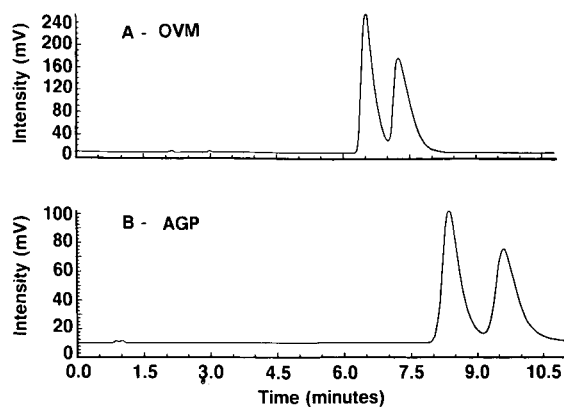


Fig. 13. Enantiomeric separation of SCH-23390 with methylated nitrogen SCH-23390 enantiomers. (A) OVM column; mobile phase, 15% acetonitrile–85% 0.01 *M* phosphate buffer, pH 6.0. (B) AGP column; mobile phase, 10% acetonitrile–90% 0.01 *M* phosphate buffer, pH 6.0. Rest of conditions as in Fig. 2.

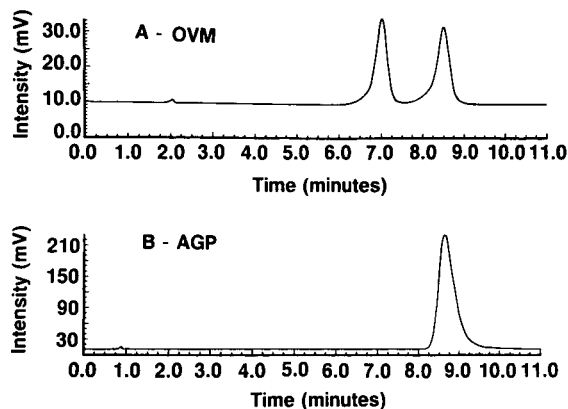


Fig. 14. Enantiomeric separation of SCH-23390 normethyl analogue. Conditions as in Fig. 13, except mobile phase for OVM column was 20% acetonitrile–80% phosphate buffer, pH 6.0.

tivity appears suitable for the pharmacokinetic monitoring of each enantiomer.

The OVM column also has demonstrated utility in resolving four diastereomers from drugs containing two chiral centers, as shown for ICI-8 in Fig. 17A. Fig. 17B shows that two of the diastereomers coeluted on an AGP column.

## CONCLUSIONS

The new immobilized-ovomuroid OVM column represents a valuable addition to the family of protein-based columns for enantiomer separations by HPLC. The OVM column exhibits excellent stability during method development where pH and mobile phase composition must be frequently manipulated. Compared to the AGP column, the OVM column has demonstrated superior resolution and efficiency in our laboratory. These advantages permit rapid and simple method development. The

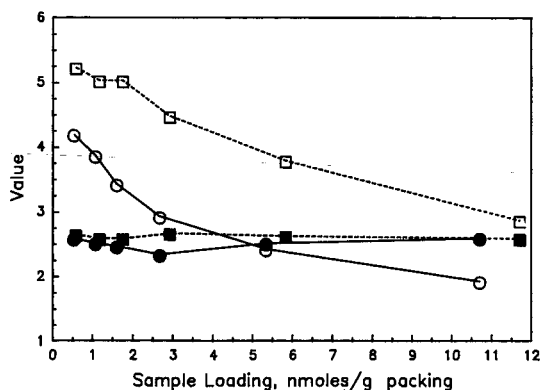


Fig. 15. Effect of sample loading on separation of enantiomers with OVM column.  $\circ = R_S$  and  $\bullet = \alpha$  values of halofantrine;  $\square = R_S$  and  $\blacksquare = \alpha$  values of lorglumide. Conditions same as in Fig. 9.

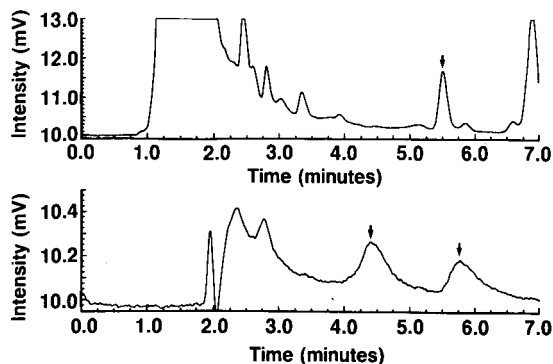


Fig. 16. Achiral/chiral trace analysis in spiked human plasma. Top: isolation of 20 ng of ICI-2 with achiral Zorbax Rx-C<sub>8</sub> column, 25 × 0.46 cm I.D.; mobile phase, 50% acetonitrile–50% water; flow-rate, 1.3 ml/min. Bottom: chiral separation of isolate with OVM column; mobile phase, 15% acetonitrile–85% 0.01 *M* phosphate buffer pH 6.0; flow-rate, 1.0 ml/min; enantiomers shown by arrows.

OVM column appears to be broadly applicable to both acidic and basic drugs without requiring special mobile-phase modifiers. The column is suited for trace analysis, with particular applicability to studies involving stereoselective pharmacokinetics and metabolism. The OVM column also appears useful for monitoring process intermediates during bulk synthesis, and for formulation studies to measure the rate of possible drug racemization.

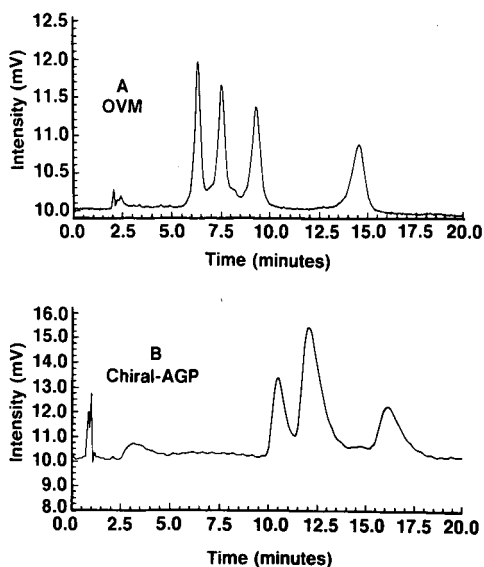


Fig. 17. Enantiomeric separation of diastereomers: ICI-8. (A) OVM column; mobile phase, 22% acetonitrile–78% 0.01 *M* phosphate buffer, pH 6.0. (B) AGP column; mobile phase, 15% acetonitrile–85% 0.01 *M* phosphate buffer, pH 6.5.

## ACKNOWLEDGEMENT

We thank Dr. R. T. Jacobs for his helpful technical discussions.

## REFERENCES

- 1 W. J. Lough and I. W. Wainer, in W. J. Lough (Editor), *Chiral Liquid Chromatography*, Chapman & Hall, New York, 1989, p. 139.
- 2 I. W. Wainer, *A Practical Guide to the Selection and Use of HPLC Chiral Stationary Phases*, J. T. Baker, Phillipsburg, NJ, 1988.
- 3 I. W. Wainer and M. Alembik, in M. Zief and L. J. Crane (Editors), *Chromatographic Chiral Separations*, Marcel Dekker, New York, 1988, p. 357.
- 4 A. C. Mehta, *J. Chromatogr.*, 426 (1988) 1.
- 5 E. Ariens, E. Wuis and E. Veringa, *Biochem. Pharmacol.*, 37 (1988) 9.
- 6 B. Testa, *Chirality*, 1 (1989) 7.
- 7 S. Allenmark, *J. Chromatogr.*, 264 (1983) 63.
- 8 J. Hermansson and M. Eriksson, *J. Liq. Chromatogr.*, 9 (1986) 621.
- 9 T. A. Noctor, G. Felix and I. W. Wainer, *Chromatographia*, in press.
- 10 P. Erlandsson, I. Marle, L. Hansson, R. Isaksson, G. Pettersson and C. Pettersson, *J. Am. Chem. Soc.*, 112 (1990) 4573.
- 11 T. Miwa, T. Miyakawa and M. Kayano, *Chem. Pharm. Bull.*, 35 (1987) 682.
- 12 T. Miwa, T. Miyakawa and M. Kayano, *J. Chromatogr.*, 408 (1987) 316.
- 13 M. D. Melamed, in A. Gottschalk (Editor), *Glycoproteins*, Elsevier, New York, 1966, p. 317.
- 14 G. Tamai, M. Edani and H. Imai, *Biomed. Chromatogr.*, 4 (1990) 157.
- 15 M. Okamoto and H. Nakazawa, *J. Chromatogr.*, 508 (1990) 217.
- 16 J. Haginaka, J. Wakai, K. Takahashi, H. Yasuda and T. Katagi, *Chromatographia*, 29 (1990) 587.
- 17 A. Pryde, in W. J. Lough (Editor), *Chiral Liquid Chromatography*, Chapman & Hall, New York, 1989, p. 23.
- 18 I. W. Wainer, in W. J. Lough (Editor), *Chiral Liquid Chromatography*, Chapman & Hall, New York, 1989, p. 129.
- 19 J. Hermansson, *Trends Anal. Chem.*, 8 (1989) 251.
- 20 L. R. Snyder and J. J. Kirkland, *Introduction to Modern Liquid Chromatography*, Wiley, New York, 1979, Ch. 5.
- 21 A. Krstulovic and J. Vende, *Chirality*, 1 (1989) 243.
- 22 J. Hermansson and K. Strom, *Chromatographia*, 24 (1978) 520.

## Effect of organic modifier concentration on retention in reversed-phase ion-pair liquid chromatography

HANFA ZOU\*, YUKUI ZHANG and PEICHANG LU

*Dalian Chromatographic R & D Centre of China, Dalian Institute of Chemical Physics, Academia Sinica, Dalian 116011 (China)*

(First received August 1st, 1990; revised manuscript received December 31st, 1990)

---

### ABSTRACT

The concentration of organic modifier in the eluent is one of the most important factors that affect the retention of ionized solutes in reversed-phase ion-pair liquid chromatography (RP-IPC). Linear regression analysis of  $\ln k'_{ip}$  vs. methanol concentration ( $C_b$ ) according to the equation  $\ln k'_{ip} = \ln k_{ip}^w + c_{ip} C_b$  was carried out;  $\ln k_{ip}^w$  and  $c_{ip}$  are constants for a given solute with a given column system, where  $\ln k_{ip}^w$  is determined mainly by the electrostatic and non-electrostatic free-energy change of retention at  $C_b = 0$ , and  $c_{ip}$  is mainly determined by the interaction behaviour between the ion-pair reagent, the ionized solute and the mobile phase. This equation has been confirmed experimentally. The absolute values of  $\ln k_{ip}^w$  and  $c_{ip}$  in RP-IPC are much larger than those in RP high-performance liquid chromatography (HPLC), which means that there is a much stronger effect of methanol concentration on retention in RP-IPC than in RP-HPLC. On the other hand, ionized compounds with the same kind and number of charges show almost the same value of electrostatic free-energy change, and  $\ln k'_{ip}$  and  $\ln k_{ip}^w$  in RP-IPC can be well correlated with  $\ln k'_{ip}$  and  $\ln k_{ip}^w$  in RP-HPLC.

---

### INTRODUCTION

Reversed-phase ion-pair liquid chromatography (RP-IPC) is widely used in separations of ionized organic compounds and inorganic ions [1–3]. The retention can be regulated by the properties and concentrations of the organic modifier and counter ion and also by a competing ion with the same charge as the analyte. Many models of the so-called “mechanism” of RP-IPC have been published [4–10].

Most of the proposed models, including the ion-pair model [4] and the dynamic ion-exchange model [4,8,9] are stoichiometric, *i.e.*, they construct a reaction scheme and the corresponding equilibrium constants express the interaction between the oppositely charged ion-pair reagent and analyte ions in the system. By combining these constants with the Langmuir isotherm, equations are obtained for the capacity factor as a function of different variables. Recently, the Gouy–Chapman theory in combination with a modified Langmuir isotherm [11,12] and statistical thermodynamic method [13] in combination with the Freundlich isotherm were applied to ion-pair liquid chromatography. These treatments are complicated. Jandera *et al.* [14] used the equation  $\ln k'_{ip} = \ln k_{ip}^w - c_{ip} C_b$ , where  $\ln k_{ip}^w$  and  $c_{ip}$  are constants for a given solute with a given column system and  $C_b$  is the concentration of organic modifier, to

correlate  $\ln k'$  with organic modifier concentration in RP-IPC. In this paper, linear regression analysis of  $\ln k'_{ip}$  vs. methanol concentration ( $C_b$ ) according to this equation was carried out, and it was observed that the absolute value of  $\ln k'_{ip}$  and  $c_{ip}$  in RP-IPC are much larger than those in RP high-performance liquid chromatography (HPLC). For compounds with the same kind and number of charges,  $\ln k'_{ip}$  and  $\ln k'_{ip}$  in RP-IPC can be quantitatively correlated with  $\ln k'_{Rp}$  and  $\ln k'_{Rp}$  in RP-HPLC. These results showed that both the hydrophobic and the electrostatic interaction play an important role in the retention of solutes in RP-IPC.

#### RETENTION EQUATION TO DESCRIBE THE EFFECT OF ORGANIC MODIFIER CONCENTRATION ON CAPACITY FACTORS IN RP-IPC

Jandera *et al.* [14] used the following equation to describe the effect of organic modifier concentration on capacity factor in RP-IPC:

$$\log k' = A - Bc \quad (1)$$

where  $A$  and  $B$  are constants for a given solute with a given column system and  $c$  is the concentration of organic modifier. We used a thermodynamic method in combination with an empirical relationship to derive the retention equation in RP-IPC as follows:

$$\ln k'_{ip} = \ln k''_{ip} + c_{ip}C_b \quad (2)$$

where  $\ln k''_{ip}$  is the extrapolated logarithm of the capacity factor at  $C_b = 0$  and  $c_{ip}$  is mainly determined by the interaction behaviour between the ion-pair reagent, ionized solute and the mobile phase,  $C_b$  is the concentration of organic modifier (expressed as methanol to buffer ratio, v/v),  $\ln k''_{ip}$  and  $c_{ip}$  are the constants at a given column system and can be expressed as

$$\ln k''_{ip} = \ln \Phi - (\Delta G_R^\circ + \Delta G_e^\circ)/RT \quad (3)$$

$$c_{ip} = -(\gamma x_2 ZF + x_1)/RT \quad (4)$$

$$\Delta G_e^\circ = (\beta + \gamma \ln N_s^\circ)ZF \quad (5)$$

where  $R$  and  $T$  are the gas constant and absolute temperature, respectively,  $\Delta G_R^\circ$  and  $\Delta G_e^\circ$  are the non-electrostatic and electrostatic free-energy change of retention at  $C_b = 0$ ,  $x_1$  and  $x_2$  are mainly determined by the interaction behaviour between the solute, the ion-pair reagent and the mobile phase and are constants for a given column system,  $Z$  and  $F$  are the charge number of the solute and Faraday constant, respectively,  $\gamma$  and  $\beta$  are empirical constants and  $N_s^\circ$  is amount of the ion-pair reagent adsorbed on the surface at  $C_b = 0$  (these were given by Deelder and Van den Berg [15]) and  $\Phi$  is the phase ratio.

#### EXPERIMENTAL

##### *Materials*

The compounds analysed (listed in Table I) were obtained from the Dyestuff Laboratory, Chemical Engineering Department, Dalian University of Science and

Technology. Standard solutions were prepared in water. Doubly distilled water was used throughout. Tetrabutylammonium iodide (Beijing Chemical Reagent Factory, Beijing, China), methanol,  $\text{NaH}_2\text{PO}_4$ ,  $\text{NaOH}$  and  $\text{HCl}$  were of analytical-reagent grade. The capacity factors were calculated using the equation  $k' = (t_r - t_0)/t_0$ , where  $t_r$  is the retention time of the solute and  $t_0$  is the dead time of the column, which was measured as retention time of the methanol peak at a detection wavelength 220 nm in RP-HPLC.

#### Apparatus

HPLC was carried out at room temperature ( $23 \pm 1^\circ\text{C}$ ) regulated by a room cooling system and using a stainless-steel column ( $200 \times 4.0$  mm I.D.) that contained a Spherisorb  $\text{C}_{18}$  reversed-phase packing material with  $5\text{-}\mu\text{m}$  particle diameter (Phase Separations, Deeside, U.K.), which was packed at the Dalian Chromatographic R & D Centre of China. The mobile phase was delivered by two Waters Model 510 pumps. The ratio of methanol to phosphate buffer in eluents A and B was 0.95:0.05 and 0.60:0.40 (v/v), respectively, and the concentration of the ion-pair reagent tetrabutylammonium iodide, the  $\text{NaH}_2\text{PO}_4$  concentration and pH in both eluents were 4 mmol/l, 10 mmol/l and 7.15, respectively. The organic modifier concentration in the eluent was controlled and regulated by a NEC APCIV computer with a Waters System Interface Module (Waters Assoc., Milford, MA, U.S.A.) by changing the ratio of eluent A to eluent B. The eluates were detected by a Waters Model 490 programmable multi-wavelength detector set at 254 nm. Samples were loaded with a U6K syringe loading sample injector. The flow-rate of eluent was 1.0 ml/min. The eluent pH was measured with an SA-720 pH meter (Orion Research, Chicago, IL, U.S.A.). All experimental data were processed on an NEC APCIV personal computer.

#### RESULTS AND DISCUSSION

RP-IPC is often used to separate ionized organic compounds. Figs. 1 and 2 show the separation of some phenylamine- and naphthylaminesulphonic acids by RP-IPC. Table I lists the capacity factors of sixteen of these compounds at different organic modifier concentrations (methanol to buffer ratios). We obtained a linear regression according to eqn. 2 for the experimental data shown in Table I.  $\ln k'_{\text{ip}}$  and  $c_{\text{ip}}$  values and the regression coefficient  $r$  are listed in Table II. It can be seen that the regression coefficient for all solutes is larger than 0.99, which strongly supports the relationship shown in eqn. 2.

Table III shows the capacity factors of seven phenylamine- and naphthylamine-sulphonic acids at different methanol concentrations in RP-HPLC, which were taken from a previous paper [16]. It has been generally accepted that the effect of the organic modifier concentration ( $C_b$ ) on the logarithm of the capacity factor ( $k'$ ) in RP-HPLC can be described by

$$\ln k'_{\text{Rp}} = \ln k_{\text{Rp}}^{\text{w}} + c_{\text{Rp}} C_b \quad (6)$$

where  $k_{\text{Rp}}^{\text{w}}$  is the capacity factor measured when pure water (or buffer) is used as the mobile phase and  $c_{\text{Rp}}$  is mainly determined by the molecular interaction between the solute and the mobile phase. Table IV lists  $\ln k_{\text{Rp}}^{\text{w}}$ ,  $c_{\text{Rp}}$  calculated from the data in Table

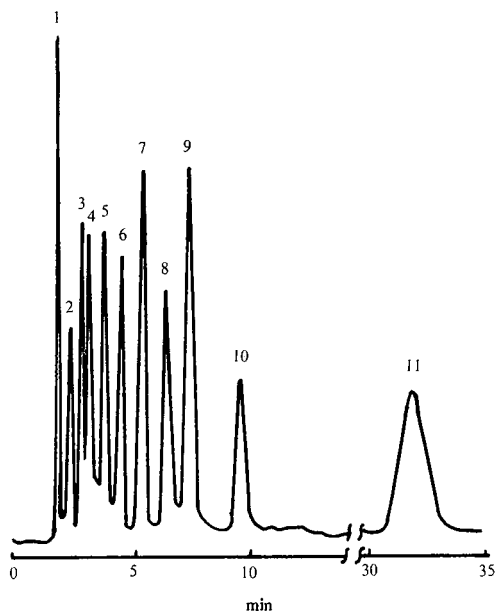


Fig. 1. Chromatogram of a mixture of eleven phenylamine- and naphthylaminesulphonic acids. Mobile phase, methanol-phosphate buffer (0.281:0.719) containing 10 mmol/l  $\text{NaH}_2\text{PO}_4$ , ion-pair reagent 4 mmol/l tetrabutylammonium iodide (pH 7.15). Peaks: 1 = phenylamine-4-sulphonic acid; 2 = phenylamine-3-sulphonic acid; 3 = phenylamine-2,5-disulphonic acid; 4 = phenylamine-2-sulphonic acid; 5 = 4-methylphenylamine-3-sulphonic acid; 6 = 2-aminonaphthalene-3-sulphonic acid; 7 = 2-aminonaphthalene-3,6-disulphonic acid; 8 = 2-aminonaphthalene-6-sulphonic acid; 9 = 4-nitrophenylamine-2-sulphonic acid; 10 = 2-aminonaphthalene-1-sulphonic acid; 11 = naphthylamine-8-sulphonic acid.

III and the values of  $\Delta c = c_{ip} - c_{Rp}$  and  $\Delta \ln k = \ln k_{ip}^w - \ln k_{Rp}^w$  for seven phenylamine- and naphthylaminesulphonic acids. It can be seen that the absolute values of  $\ln k_{ip}^w$  and  $c_{ip}$  in RP-IPC are much larger than those in RP-HPLC, which is as expected. The values of  $\Delta \ln k$  taken from Jandera *et al.* [14] are listed in Table V. It can also be seen that  $\ln k_{ip}^w$  in RP-IPC was much larger than those in RP-HPLC when both  $C_{18}$  and  $C_8$  are used as packing materials.  $\ln k_{ip}^w$  in RP-IPC tends to increase with increasing charge number of the solutes, which agrees with our results for the thermodynamic treatment. It is necessary to investigate the effect of the charge number of the solute on  $\ln k_{ip}^w$  and  $c_{ip}$ .  $\ln k_{ip}^w$  and  $c_{ip}$  in RP-IPC and  $\ln k_{Rp}^w$  and  $c_{Rp}$  in RP-HPLC calculated from the experimental data of Bartha and Vigh [17] are listed in Table VI. It can also be seen that  $\ln k_{ip}^w$  and  $c_{ip}$  in RP-IPC are larger than those in RP-HPLC.

The larger value of  $\ln k_{ip}^w$  means that there is a much larger free-energy change of retention at  $C_b = 0$  in RP-IPC than in RP-HPLC. It is known that in addition to the contribution of non-electrostatic free-energy change to  $\ln k_{ip}^w$  in RP-IPC, similarly to that in RP-HPLC,  $\ln k_{ip}^w$  also has a contribution from the electrostatic free-energy change of retention. The values of  $\Delta c$  in Table IV are almost constant, which is mainly due to the interaction behaviour between the ion-pair reagent and the mobile phase, and should not change substantially for different solutes. Although this phenomenon cannot be seen from the data of Jandera *et al.* [14], it may be implied from the high concentration of salt used in RP-HPLC. The parameter  $c_{ip}$  is always negative, which



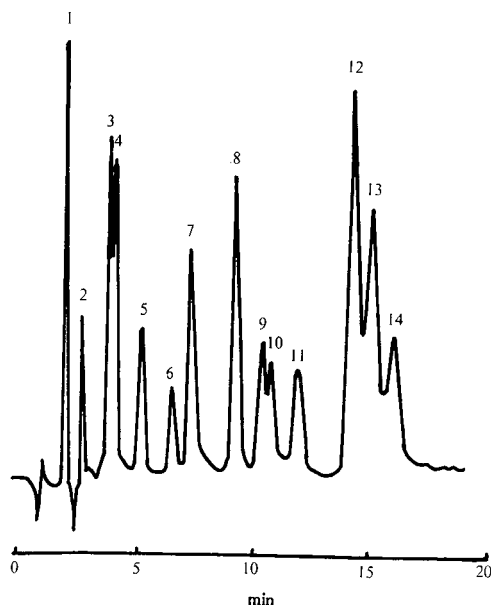


Fig. 2. Chromatogram of a mixture of fourteen phenylamine- and naphthylaminesulphonic acids. Mobile phase, methanol-phosphate buffer (0.239:0.761) containing 10 mmol/l  $\text{NaH}_2\text{PO}_4$ , ion-pair reagent 4 mmol/l tetrabutylammonium iodide (pH 7.15). Peaks: 1 = phenylamine-4-sulphonic acid; 2 = phenylamine-3-sulphonic acid; 3 = phenylamine-2,5-disulphonic acid; 4 = phenylamine-2-sulphonic acid; 5 = 4-methylphenylamine-3-sulphonic acid; 6 = naphthylamine-5-sulphonic acid; 7 = 2-aminonaphthalene-5-sulphonic acid; 8 = 2-aminonaphthalene-3,6-disulphonic acid; 9 = 2-aminonaphthalene-6-sulphonic acid; 10 = 4-nitrophenylamine-2-sulphonic acid; 11 = 4-methylphenylamine-2-sulphonic acid; 12 = 2-aminonaphthalene-4,6,8-trisulphonic acid; 13 = 2-aminonaphthalene-3,6,8-trisulphonic acid; 14 = 2-aminonaphthalene-1-sulphonic acid.

TABLE I

## CAPACITY FACTORS OF 16 PHENYLAMINE- AND NAPHTHYLAMINESULPHONIC ACIDS AT DIFFERENT ORGANIC MODIFIER CONCENTRATION IN RP-IPC

For experimental conditions, see Experimental.

Solute	Methanol to buffer ratio (v/v)			
	0.325	0.281	0.239	0.198
Phenylamine-2-sulphonic acid	0.461	1.00	1.60	3.04
Phenylamine-3-sulphonic acid	0.255	0.53	0.84	1.34
Phenylamine-4-sulphonic acid	0.152	0.301	0.489	1.01
4-Methylphenylamine-2-sulphonic acid	1.54	3.27	5.69	9.86
4-Methylphenylamine-3-sulphonic acid	0.70	1.45	2.35	4.09
4-Methoxyphenylamine-2-sulphonic acid	0.751	1.56	2.46	4.97
4-Methoxyphenylamine-3-sulphonic acid	0.189	0.339	0.554	1.15
4-Nitrophenylamine-2-sulphonic acid	1.41	3.23	5.38	10.25
6-Chlorophenylamine-3-sulphonic acid	1.45	3.15	5.29	9.65
4-Chlorophenylamine-3-sulphonic acid	0.498	0.985	1.62	3.07
1,3-Diaminophenyl-4-sulphonic acid	0.142	0.283	0.433	0.948
Naphthylamine-5-sulphonic acid	0.620	1.28	2.22	4.21
2-Aminonaphthalene-1-sulphonic acid	—	4.53	8.04	18.34
Naphthylamine-8-sulphonic acid	8.67	17.41	—	—
2-Aminonaphthalene-5-sulphonic acid	0.779	1.63	2.94	5.75
2-Aminonaphthalene-6-sulphonic acid	1.23	2.80	5.01	9.85

TABLE II

LN  $k_{ip}^w$  AND  $c_{ip}$  REGRESSED BY EXPERIMENTAL DATA SHOWN IN TABLE I

Solute	Ln $k_{ip}^w$	$c_{ip}$	$r$
Phenylamine-2-sulphonic acid	3.982	-14.50	0.9967
Phenylamine-3-sulphonic acid	2.887	-12.88	0.9946
Phenylamine-4-sulphonic acid	2.853	-14.57	0.9972
4-Methylphenylamine-2-sulphonic acid	5.190	-14.49	0.9979
4-Methylphenylamine-3-sulphonic acid	4.135	-13.67	0.9973
4-Methoxyphenylamine-2-sulphonic acid	4.441	-14.48	0.9967
4-Methoxyphenylamine-3-sulphonic acid	2.839	-13.95	0.9960
4-Nitrophenylamine-2-sulphonic acid	5.351	-15.25	0.9963
6-Chlorophenylamine-3-sulphonic acid	5.206	-14.72	0.9976
4-Chlorophenylamine-4-sulphonic acid	3.894	-14.08	0.9986
1,3-Diaminophenyl-4-sulphonic acid	2.745	-14.46	0.9939
Naphthylamine-5-sulphonic acid	4.384	-14.89	0.9963
2-Aminonaphthalene-1-sulphonic acid	6.197	-16.83	0.9939
2-Aminonaphthalene-6-sulphonic acid	4.828	-15.57	0.9994
2-Aminonaphthalene-5-sulphonic acid	5.493	-16.14	0.9984
Naphthylamine-8-sulphonic acid	7.309	-15.84	1.0000

TABLE III

CAPACITY FACTORS OF SEVEN PHENYLAMINE- AND NAPHTHYLAMINESULPHONIC ACIDS MEASURED AT DIFFERENT METHANOL TO BUFFER RATIOS WITH 10 mmol/l  $\text{NaH}_2\text{PO}_4$  (pH 6.8) AS THE MOBILE PHASEStainless-steel column (200 × 4.0 mm I.D.) packed with Polygosile- $\text{C}_{18}$  with particle diameter 5  $\mu\text{m}$  obtained from Macherey, Nagel & Co. (Düren, Germany).

Solute	Methanol to buffer ratio (v/v)					
	0	0.05	0.1	0.15	0.2	0.25
Phenylamine-3-sulphonic acid	1.03	0.59	0.44	0.33	0.26	0.21
4-Methylphenylamine-3-sulphonic acid	2.97	1.05	0.77	0.57	0.42	0.32
4-Methoxyphenylamine-2-sulphonic acid	6.62	2.93	1.86	1.25	0.93	0.74
4-Nitrophenylamine-2-sulphonic acid	9.51	4.54	2.95	1.97	1.60	1.11
2-Aminonaphthalene-6-sulphonic acid	12.02	4.84	2.72	1.66	1.28	0.86
2-Aminonaphthalene-1-sulphonic acid	15.95	6.32	3.63	2.35	1.74	1.13
Naphthylamine-8-sulphonic acid	30.00	14.03	8.72	6.01	4.71	3.64

TABLE IV

LN  $k_{Rp}^w$  AND  $c_{Rp}$  CALCULATED FROM THE DATA IN TABLE III AND THE VALUES OF  $\Delta \ln k$  AND  $\Delta c$  FOR SEVEN PHENYLAMINE- AND NAPHTHYLAMINESULPHONIC ACIDS

Solute	Ln $k_{Rp}^w$	$\Delta \ln k$	$c_{Rp}$	$\Delta c$
Phenylamine-3-sulphonic acid	-0.295	3.182	-5.184	-7.70
4-Methylphenylamine-3-sulphonic acid	0.388	3.793	-5.966	-7.70
4-Methoxyphenylamine-2-sulphonic acid	1.343	3.098	-6.891	-7.59
4-Nitrophenylamine-2-sulphonic acid	1.802	3.549	-6.934	-8.32
2-Aminonaphthalene-6-sulphonic acid	1.899	2.929	-8.418	-7.72
2-Aminonaphthalene-1-sulphonic acid	2.187	4.010	-8.357	-8.47
Naphthylamine-8-sulphonic acid	2.882	4.427	-6.626	-9.21

TABLE V

VALUES OF  $\Delta \ln k$  FOR AROMATIC SULPHONIC ACIDS ON OCTADECYLSILICA (C<sub>18</sub>) AND OCTYLSILICA (C<sub>8</sub>) COLUMNS $\Delta \ln k$  was calculated using  $\Delta \ln k = 2.30(A_{ip} - A_{Rp})$ . All experimental data were taken from Jandera *et al.* [14].

Acid	$\Delta \ln k$	
	C <sub>18</sub> column	C <sub>8</sub> column
2-Naphthalenesulphonic	2.22	3.12
1,5-Naphthalenedisulphonic	6.71	7.19
1,6-Naphthalenedisulphonic	5.18	5.69
2,6-Naphthalenedisulphonic	5.83	5.66
2,7-Naphthalenedisulphonic	5.19	5.42
1-Naphthylamine-4-sulphonic	2.57	2.54
1-Naphthylamine-5-sulphonic	2.53	2.57
1-Naphthylamine-6-sulphonic	1.80	2.05
1-Naphthylamine-7-sulphonic	2.24	2.64
2-Naphthylamine-6-sulphonic	2.71	—
1-Naphthylamine-8-sulphonic	4.84	5.96
2-Naphthol-1-sulphonic	—	4.43
1-Naphthol-4-sulphonic	3.08	3.38
2-Naphthol-6-sulphonic	2.69	2.70
R-acid	5.80	6.48
G-acid	5.48	6.08
2-Amino-5-naphthol-7-sulphonic	2.34	—
1-Amino-8-naphthol-3,6-disulphonic	2.56	—
2-Amino-5-naphthol-1,7-disulphonic	5.72	—
1-Anthraquinonesulphonic	1.44	—
1,5-Anthraquinonedisulphonic	5.10	6.07
2,6-Anthraquinonedisulphonic	4.110	5.05
1,8-Anthraquinonedisulphonic	3.88	4.66

TABLE VI

LN  $k_{ip}^w$  AND  $c_{ip}$  IN RP-IPC WITH 2 mmol/l TETRABUTYLAMMONIUM BROMIDE AS MOBILE PHASE AND LN  $k_{Rp}^w$  AND  $c_{Rp}$  IN RP-HPLC CALCULATED FROM THE EXPERIMENTAL DATA OF BARTHA AND VIGH (17)The effect of mobile phase pH on  $k'$  was neglected in regression analysis. The range of  $C_b$  (methanol to buffer ratio) for DCSA is 0–0.6, for PTSA 0–0.5, for BuSO<sub>3</sub> 0–0.6, for HexSO<sub>3</sub> 0.375–0.6 and for HepSO<sub>3</sub> 0.375–0.7 in RP-IPC and RP-HPLC. The ranges of  $C_b$  for PeSO<sub>3</sub> in RP-IPC and RP-HPLC are 0.1–0.375 and 0.1–0.25, respectively.

Solute <sup>a</sup>	Ln $k_{Rp}^w$	$c_{Rp}$	$r$	Ln $k_{ip}^w$	$c_{ip}$	$r$
DCSA	2.223	-6.901	0.9918	3.152	-8.390	0.9980
PTSA	2.973	-7.373	0.9983	3.342	-7.870	0.9984
BuSO <sub>3</sub>	1.080	-5.326	0.9897	1.533	-5.866	0.9998
PeSO <sub>3</sub>	2.42	-6.460	1.0000	3.063	-7.374	0.9993
HexSO <sub>3</sub>	3.688	-6.888	0.9989	4.205	-7.702	0.9990
HepSO <sub>3</sub>	5.172	-8.163	0.9990	5.533	-8.653	0.9989

<sup>a</sup> DCSA = *d,l*-10-camphorsulphonic acid; PTSA = *p*-toluenesulphonic acid; BuSO<sub>3</sub> = sodium butylsulphonate; PeSO<sub>3</sub> = sodium pentanesulphonate; HexSO<sub>3</sub> = sodium hexanesulphonate; HepSO<sub>3</sub> = sodium heptanesulphonate.

means that the capacity factor of a solute decreases with increasing organic modifier concentration; the larger absolute value of  $c_{ip}$  in RP-IPC means that there is a much stronger effect of organic modifier concentration on the retention of a solute in RP-IPC than in RP-HPLC.

It has been observed that the capacity factor of phenylamine- and naphthylaminesulphonic acids increases with increasing salt concentration in the mobile phase in RP-HPLC, which may be caused by the salting-out effect [14] or changes in mobile phase surface tension [18]. In RP-IPC, the mobile phase containing an ion-pair reagent will increase the capacity factors of phenylamine- and naphthylaminesulphonic acids by the salting-out effect. However, in general, the salting-out effect of an ion-pair reagent makes only a minor contribution to the retention owing to the lower concentration of the ion-pair reagent in RP-IPC. We consider that the main contribution of the ion-pair reagent to retention is from the electrostatic interaction between the solute and ion-pair reagent. For solutes with the same kind and number of charges, there should be almost the same electrostatic free-energy change to the retention value and  $\ln k'_{ip}$  in RP-IPC, and therefore it is possible to correlate  $\ln k'_{ip}$  and  $\ln k''_{ip}$  in RP-IPC with  $\ln k'_{Rp}$  and  $\ln k''_{Rp}$  in RP-HPLC by the following equations:

$$\ln k'_{ip} = a_1 + b_1 \ln k'_{Rp} \quad (7)$$

or

$$\ln k''_{ip} = a_2 + b_2 \ln k''_{Rp} \quad (8)$$

Table VII lists the capacity factors of sixteen phenylamine- and naphthylaminesulphonic acids measured in RP-HPLC with phosphate buffer as the mobile phase. The quantitative correlations between  $\ln k'_{ip}$  at different ratios of methanol to buffer in RP-IPC and  $\ln k'_{Rp}$  in RP-HPLC for phenylamine- and naphthylaminesulphonic acids are as follows:

$$C_b = 0.325: \ln k'_{ip} = -1.492 + 0.8357 \ln k'_{Rp}; n = 15, r = 0.9388$$

$$C_b = 0.281: \ln k'_{ip} = -0.7877 + 0.8471 \ln k'_{Rp}; n = 16, r = 0.9449$$

$$C_b = 0.239: \ln k'_{ip} = -0.2558 + 0.7886 \ln k'_{Rp}; n = 15, r = 0.9548$$

$$C_b = 0.198: \ln k'_{ip} = 0.3960 + 0.7924 \ln k'_{Rp}; n = 15, r = 0.9618$$

TABLE VII

CAPACITY FACTORS OF SIXTEEN PHENYLAMINE- AND NAPHTHYLAMINESULPHONIC ACIDS WITH AQUEOUS BUFFER CONTAINING 10 mmol/l  $\text{NaH}_2\text{PO}_4$  (pH 6.8) AS THE ELUENT

Column as in Table III.

Solute	Capacity factor ( $k'$ )	Solute	Capacity factor ( $k'$ )
Phenylamine-2-sulphonic acid	2.31	6-Chlorophenylamine-3-sulphonic acid	8.64
Phenylamine-3-sulphonic acid	1.03	4-Chlorophenylamine-3-sulphonic acid	1.87
Phenylamine-4-sulphonic acid	0.484	1,3-Diaminophenyl-4-sulphonic acid	0.510
4-Methylphenylamine-2-sulphonic acid	8.29	Naphthylamine-5-sulphonic acid	4.37
4-Methylphenylamine-3-sulphonic acid	2.87	Naphthylamine-7-sulphonic acid	18.56
4-Methoxyphenylamine-2-sulphonic acid	6.86	Naphthylamine-8-sulphonic acid	29.85
4-Methoxyphenylamine-3-sulphonic acid	1.43	2-Aminonaphthalene-5-sulphonic acid	10.73
4-Nitrophenylamine-2-sulphonic acid	9.51	2-Aminonaphthalene-6-sulphonic acid	11.22

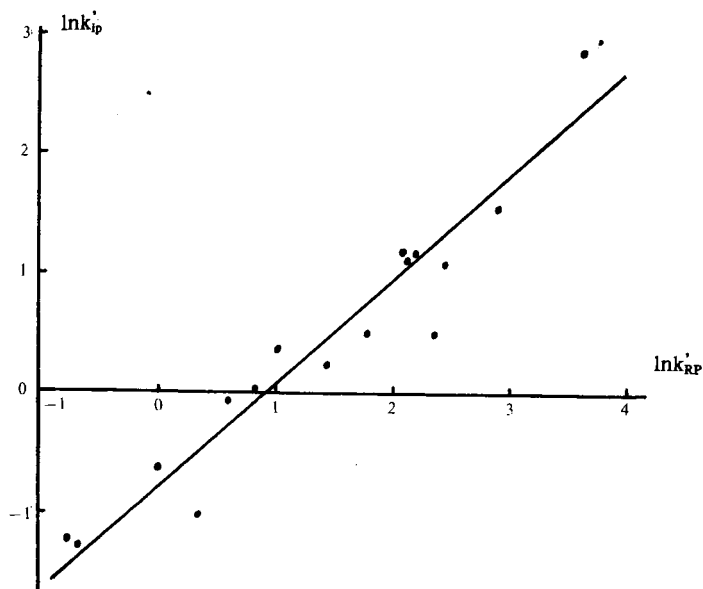


Fig. 3. Linear regression of  $\ln k'_{ip}$  in RP-IPC with methanol-phosphate buffer (0.281:0.719) containing ion-pair reagent 4 mmol/l tetrabutylammonium iodide as the eluent vs.  $\ln k'_{RP}$  shown in Table VI in RP-HPLC for sixteen phenylamine- and naphthylaminesulphonic acids.  $\ln k'_{ip} = -0.7947 + 0.8576 \ln k'_{RP}$ ;  $r = 0.9412$ .

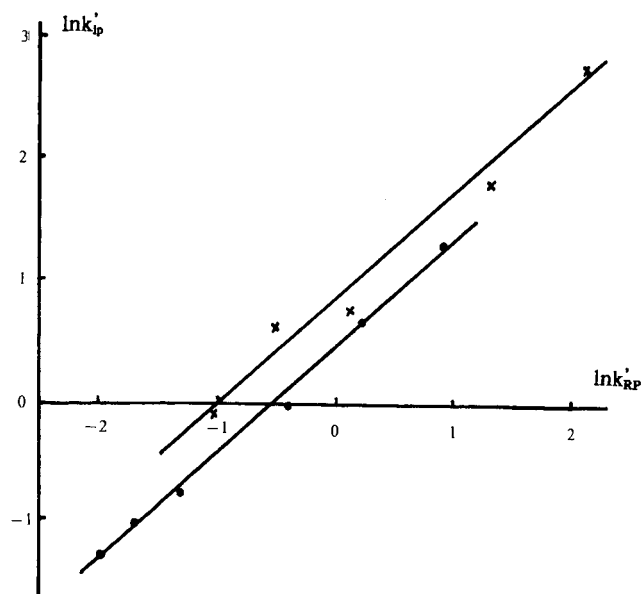


Fig. 4. Linear regression of  $\ln k'_{ip}$  in RP-IPC vs.  $\ln k'_{RP}$  in RP-HPLC. (x) For DCSA, PTSA,  $\text{BuSO}_3$ ,  $\text{HexSO}_3$  and  $\text{HepSO}_3$  with 37.5% methanol in phosphate buffer (pH 2.75) and that containing ion-pair reagent 20 mmol/l tetrabutylammonium bromide as eluent in RP-HPLC and RP-IPC, respectively.  $\ln k'_{ip} = 0.777 + 0.868 \ln k'_{RP}$ ;  $r = 0.987$ . (●) For DCSA, PTSA,  $\text{BuSO}_3$ ,  $\text{HexSO}_3$ ,  $\text{HepSO}_3$  and  $\text{OcSO}_3$  (sodium octanesulphonate) with 60% methanol in phosphate buffer (pH 3.12) and that containing ion-pair reagent 35 mmol/l tetrabutylammonium bromide as eluent in RP-HPLC and RP-IPC, respectively.  $\ln k'_{ip} = 0.433 + 0.891 \ln k'_{RP}$ ;  $r = 0.998$ . Experimental data were taken from Bartha and Vigh [17].

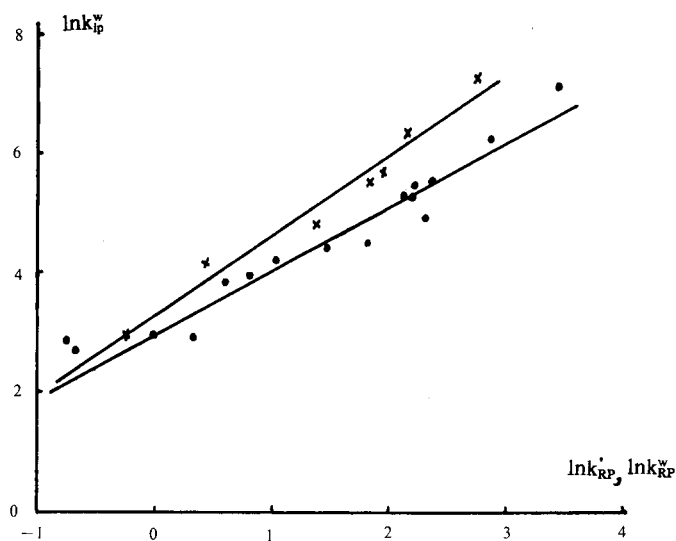


Fig. 5. Linear regression of  $\ln k_{ip}^w$  in RP-IPC vs.  $\ln k'_{Rp}$  (●; with 10 mmol/l phosphate buffer (pH 6.8) as eluent) and  $\ln k''_{Rp}$  (×) in RP-HPLC for sixteen and seven phenylamine- and naphthylaminesulphonic acids, respectively. (●)  $\ln k_{ip}^w = 3.076 + 1.009 \ln k'_{Rp}$ ;  $r = 0.9563$ . (×)  $\ln k_{ip}^w = 3.256 + 1.282 \ln k''_{Rp}$ ;  $r = 0.9710$ .

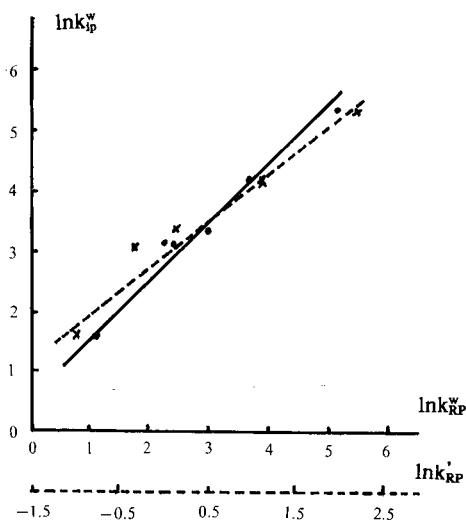


Fig. 6. Linear regression of  $\ln k_{ip}^w$  in RP-IPC shown in Table VI vs.  $\ln k'_{Rp}$  in RP-HPLC with 37.5% methanol in phosphate buffer as mobile phase for DCSA, PTSA,  $\text{BuSO}_3$ ,  $\text{HexSO}_3$  and  $\text{HepSO}_3$  (×),  $\ln k_{ip}^w = 0.400 + 2.460 \ln k'_{Rp}$ ;  $r = 0.9631$ ; and  $\ln k_{ip}^w$  in RP-IPC vs.  $\ln k''_{Rp}$  in RP-HPLC shown in Table VI (●),  $\ln k_{ip}^w = 0.716 + 0.940 \ln k''_{Rp}$ ;  $r = 0.9896$ .

It can be seen from above regression equations that there is a slight change in slope with change in organic modifier concentration, which may be caused by the fact that different column packings were used and the slight difference in pH between the two sets of experiments. The intercepts increase with decreasing methanol concentration, which implies an increase the capacity factors with decreasing methanol concentration. Figs. 3 and 4 illustrate the linear regression results of  $\ln k'_{ip}$  at  $C_b = 0.281$  in RP-IPC versus  $\ln k'_{rp}$  in RP-HPLC for sixteen phenylamine- and naphthylaminesulphonic acids, and the experimental data taken from Bartha and Vigh [17], respectively. Figs. 5 and 6 demonstrate the quantitative correlation between  $\ln k'_{ip}$  in RP-IPC and the  $\ln k'_{rp}$  and  $\ln k'_{rp}$  in RP-HPLC calculated from our experimental data and those of Bartha and Vigh [17]. It can be seen that the relationships shown in eqns. 7 and 8 should basically exist. The above results mean that the non-electrostatic free energy change of retention in RP-IPC is paralleled by that in RP-HPLC.

## REFERENCES

- 1 B. Fransson, *J. Chromatogr.*, 361 (1986) 161.
- 2 H. Zou, Y. Zhang and P. Lu, *Chromatographia*, 30 (1990) 228.
- 3 W. E. Barber and P. W. Carr, *J. Chromatogr.*, 301 (1984) 25.
- 4 W. R. Melander and Cs. Horváth, *J. Chromatogr. Sci.*, 31 (1985) 27.
- 5 A. Tilly-Melin, Y. Askemark, K. G. Wahlund and G. Schill, *Anal. Chem.*, 51 (1979) 976.
- 6 B. A. Bidlingmeyer, S. N. Deming, W. P. Prince, Jr., B. Sachok and M. Petrusek, *J. Chromatogr.*, 186 (1979) 419.
- 7 C. T. Huang and R. B. Tylor, *J. Chromatogr.*, 202 (1980) 333.
- 8 P. T. Kinnsinger, *Anal. Chem.*, 49 (1977) 883.
- 9 J. H. Knox and R. A. Hartwick, *J. Chromatogr.*, 204 (1981) 3.
- 10 S. Afrashtehfar and F. C. Cantwell, *Anal. Chem.*, 54 (1982) 2422.
- 11 J. Stahlberg, *J. Chromatogr.*, 356 (1986) 231.
- 12 J. Stahlberg, *Chromatographia*, 24 (1987) 820.
- 13 P. Lu, H. Zou and Y. Zhang, *Mikrochim. Acta*, III (1990) 35.
- 14 P. Jandera, J. Churacek and B. Taraba, *J. Chromatogr.*, 262 (1983) 121.
- 15 R. S. Deelder and J. H. M. van den Berg, *J. Chromatogr.*, 218 (1981) 327.
- 16 H. Zou, Y. Zhang, X. Wen and P. Lu, *J. Chromatogr.*, 523 (1990) 247.
- 17 A. Bartha and Gy. Vigh, *J. Chromatogr.*, 265 (1983) 171.
- 18 Cs. Horváth, W. Melander and I. Molnar, *J. Chromatogr.*, 125 (1976) 129.





## Quantification of methyl farnesoate levels in hemolymph by high-performance liquid chromatography

DAVID W. BORST\* and BRIAN TSUKIMURA

*Department of Biological Sciences, Illinois State University, Normal, IL 61761 (USA)*

(First received November 21st, 1990; revised manuscript received February 26th, 1991)

---

### ABSTRACT

Methyl farnesoate (MF) is an acyclic sesquiterpenoid that has been detected in hemolymph and other tissues of crustaceans and insects. This paper describes a rapid and sensitive method for measuring MF in crustacean hemolymph. Extracts of hemolymph samples were separated by normal-phase high-performance liquid chromatography (5- $\mu\text{m}$  silica, 250  $\times$  4.6 mm I.D., 1.3% diethyl ether in hexane) and detected by UV (220 nm). The limit of detection with this method was less than 250 pg/ml. This method should be useful for studying the physiological functions of MF in crustaceans and other arthropods.

---

### INTRODUCTION

Arthropods produce a number of sesquiterpenoids that have important physiological functions. One of these is methyl farnesoate (MF), a compound that is structurally related to insect juvenile hormone III (JH III). MF has been detected in hemolymph from embryos of the cockroach *Nauphoeta cinerea*, but its role in embryogenesis is unclear [1,2]. This compound is also an intermediate in JH III synthesis in many insects [3]. MF has been detected in the hemolymph and other tissues of crustaceans [4,5]. Recent reports suggest that MF has important roles in crustacean development and reproduction [6–10], roles that are analogous to those of JH in insects [11]. Such studies would be aided by measurements of MF levels in animals at different physiological states.

The most sensitive and specific method for quantifying MF levels uses gas chromatography–mass spectrometry (GC–MS) with selected ion-monitoring (SIM) [4]. This method has proven useful for the identification of MF in hemolymph and other tissues of several crustaceans [4, 5, 12]. However, the preparation and analysis of samples by GC–SIM–MS is time-consuming and cumbersome, and does not lend itself to the routine analysis of many samples.

Other methods, such as high-performance liquid chromatography (HPLC), also hold potential for quantifying MF. For example, reversed-phase HPLC was used to measure MF in embryos of the cockroach *Nauphoeta cinerea* [1]. However, this procedure was not particularly sensitive, requiring MF levels over 75 ng/ml. Since the MF levels in many crustaceans are lower than this amount [4], a more sensitive HPLC

method is needed. We found that normal-phase HPLC, when coupled with a triphasic extraction procedure is a simple and reliable means of quantifying MF, with a limit of detection of less than 250 pg/ml. During the past two years, we have used this approach to quantify MF levels in hundreds of hemolymph samples from several crustaceans.

## EXPERIMENTAL

### *Experimental animals*

Male lobsters (*Homarus americanus*), female spider crabs (*Libinia emarginata*) and female green crabs (*Carcinus maenas*) were obtained from the Department of Marine Resources at the Marine Biology Laboratory, Woods Hole, MA, U.S.A. Animals were held in running sea water until used. The eyestalks of some lobsters were removed to elevate hemolymph levels of MF [13].

### *Chemicals*

Unlabeled MF was obtained from Dr. D. A. Schooley (Zoecon Research Institute, Palo Alto, CA, USA) as a mixture of two isomers (approximately 70% 2*E*,6*E* and 30% 2*Z*,6*E*). The 2*E*,6*E* isomer was purified by normal-phase HPLC using the conditions described below for MF analysis. Radiolabeled [ $10^{-3}$ H]MF (2*E*,6*E*) with a specific activity of 1.44 Ci/mmol [14] was obtained from Dr. G. D. Prestwich (Dept. of Chemistry, SUNY, Stony Brook, NY, USA). HPLC grade acetonitrile and diethyl ether, iso-octane (99 mol% pure), and Optima-grade hexane were obtained from Fisher Scientific (Pittsburgh, PA, USA). Ethyl farnesoate (EF: used as an internal standard) was prepared from all *trans*-methyl farnesoate as described [4].

### *Sample preparation*

Culture tubes with PTFE-lined screw caps were used to extract MF from hemolymph. The tubes were filled with 2.5 ml of acetonitrile, 0.5 ml hexane, 5 ng of EF and sufficient saline (0.9% NaCl) to give a final aqueous volume of 2.0 ml after the addition of hemolymph. Hemolymph (0.3 to 2 ml) was collected from individual animals, added to a culture tube, rapidly mixed, and chilled on ice. After a brief centrifugation (1000 g  $\times$  5 min), three phases were observed in each tube: a clear, upper layer containing hexane; a middle yellow-colored layer containing primarily acetonitrile; and a bottom aqueous layer. In samples from animals in late premolt, the middle phase was occasionally small or absent. Acetonitrile was added to these sample until the middle and lower layers were approximately equal in volume. The top (hexane) layer was removed, a second volume of hexane added, and the extraction repeated. The second hexane layer was removed and added to the first. In some cases the volume of the combined hexane layers was reduced with a Savant Speed-Vac concentrator so the entire sample could be analysed in a single injection.

### *High-performance liquid chromatography*

Samples were injected manually or with an autosampler (Spectra-Physics 8780) and analyzed by normal-phase HPLC using a silica column (Econosil SI: 5  $\mu$ m, 250  $\times$  4.6 mm I.D.; Alltech, Deerfield, IL, USA) with a silica precolumn. Eluting material was detected with a Beckman 166 programmable detector (220 nm) and the output

analyzed by either a Beckman System-Gold or a Jandel JCL6000 chromatography data program. The solvent (1.3% diethyl ether in hexane, 2.5 ml per min) was selected to give a retention time for MF of about 5 min. The retention times of MF and EF were determined every 2 or 3 h by injecting MF and EF standards. Because this method has a low limit of detection, small amounts (usually 2 ng each) of MF and EF were used to calibrate the column. This avoided the contamination of unknown samples that can occur when large amounts of standard are used for calibration [15]. After each sample, the column was rinsed with an additional 50 ml of the eluting solvent to remove contaminants.

The amount of MF in each sample was determined by comparing either the peak height or the peak area of the sample to that of EF. In some cases, the eluate was collected from the beginning of the EF peak to the end of the MF peak. After reducing the solvent volume to  $< 50 \mu\text{l}$  with a Speed-Vac, each sample was dried manually with nitrogen and resuspended in  $5 \mu\text{l}$  of octane for analysis by GC-MS.

#### *Gas Chromatography-mass spectroscopy*

The GC-MS analysis was similar to that described previously [4]. An aliquot ( $0.5 \mu\text{l}$ ) of the resuspended sample was injected into a Hewlett-Packard MSD (Model 5790A/5970) with an Alltech RSL-150 ( $0.25 \mu\text{m}$  film,  $0.25 \text{ mm}$  I.D.,  $25 \text{ m}$ ) capillary column. EF was used as an internal standard. MF levels were determined by selected ion monitoring (SIM) using an ion common to both MF and EF ( $m/z$  69) and the analogous ion pair ( $m/z$  114 and 128).

## RESULTS

Initial studies indicated that normal-phase HPLC could detect and quantify low levels of MF standards. However, the quantification of MF in total lipid extracts [16] of hemolymph proved difficult due to the presence in interfering (*i.e.* UV-absorbing) compounds. As a solution to this problem, other extraction procedures were tested. We found that the treatment of hemolymph with acetonitrile, saline, and hexane formed a triphasic solution which removed these interfering compounds from the upper (hexane) phase containing MF.

The effectiveness of this triphasic extraction (TE) procedure could be monitored by observing the distribution of yellow organosoluble pigments found in many of the samples. When the ratio of water to acetonitrile was high (3:1), the solution was biphasic and the yellow pigments were found in the upper (hexane) phase. When the ratio of water to acetonitrile was lower (4:5), the solution was triphasic and the yellow pigments were in the middle (acetonitrile) phase. Chilling the extract also helped reduce the amount of interfering materials in the hexane phase. The presence of methanol in the extraction increased the amount of interfering materials.

The TE procedure was compared with the total lipid extraction procedure [16] using samples ( $n = 4$ ) of lobster hemolymph. The hexane phase of the TE procedure contained  $65.7\% [\pm 6.4 \text{ (S.E.M.)}]$  of the extractable mass and  $64.9\% [\pm 9.9 \text{ (S.E.M.)}]$  of the UV-absorbing material (at  $220 \text{ nm}$ ) found in total lipid extracts. Thin-layer chromatographic analysis of the hexane phase indicated that the TE procedure removed fatty acids and sterols and reduced the level of triglycerides, all of which are quantitatively recovered in total lipid extracts. MF recovery in the hexane phase (assessed by

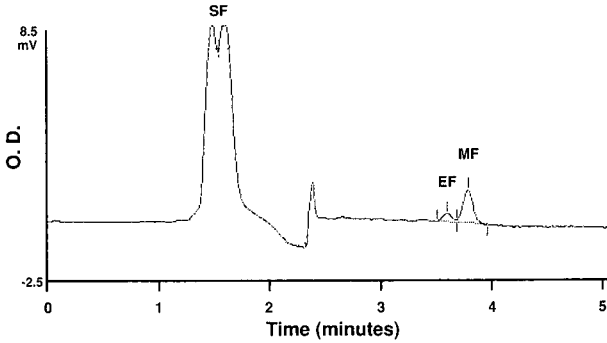


Fig. 1. HPLC detection of methyl farnesoate (MF) in lobster hemolymph. An amount of 5 ng of ethyl farnesoate (EF) was added to a hemolymph sample (0.5 ml) as an internal standard. The quantity of MF detected in this figure is approximately 1.8 ng; the concentration of MF in this animal was 18.4 ng/ml.

the addition of [ $^3\text{H}$ ]-MF) was  $>95\%$  using the TE procedure. Most important, TE coupled with normal-phase HPLC provided a sensitive method for quantifying MF in hemolymph samples (Fig. 1). MF and EF were resolved by normal phase HPLC, allowing the latter to be used as an internal standard.

The quantification of MF by this method was tested in several ways. Its linearity was examined by extracting multiple samples (from 0.1 to 2 ml) of hemolymph from each of three lobsters. The amount of MF detected increased linearly with increasing amounts of hemolymph, indicating that the quantification of MF was not affected by the volume of hemolymph used (Fig. 2). This method was further validated by comparing the amount of MF detected by normal-phase HPLC with the amount detected by GC-MS. As shown in Fig. 3, an excellent correlation ( $r = 0.963$ ) was obtained between these two methods for hemolymph samples from three crustacean species.

The accuracy of this method was determined by measuring MF standards over a wide range of levels. MF was accurately measured between 250 pg and 25 ng per

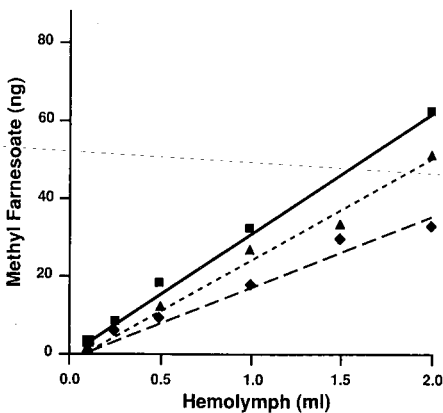


Fig. 2. Linearity of methyl farnesoate detection. Increasing volumes of hemolymph from each of three lobsters were analyzed separately by normal-phase HPLC.

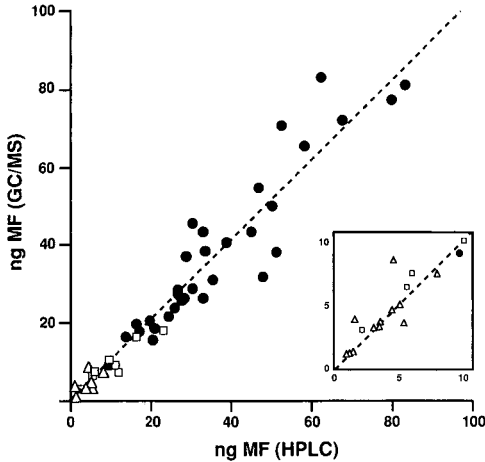


Fig. 3. Correlation between methyl farnesoate values determined by HPLC and by GC-MS. Hemolymph samples from *Homarus americanus* ( $n=32$ ; ●), *Libinia emarginata* ( $n=12$ ; △), and *Carcinus maenas* ( $n=8$ ; □) were analyzed by normal-phase HPLC and by GC-MS. The correlation coefficient was 0.983, and the slope of the line was 1.03.

injection (Table I). In all cases, the amount of MF injected and detected differed by less than 10%. The precision of this method was examined by collecting hemolymph from three lobsters with low, intermediate and high levels of MF (ca. 2, 15, and 43 ng/ml, respectively). The hemolymph from each animal was divided into three equal aliquots, which were separately extracted and analyzed for MF. As shown in Table II, the data showed small coefficients of variation (1.2 to 5.3) for the replicate aliquots from each animal.

## DISCUSSION

This paper describes and validates a sensitive normal-phase HPLC method for measuring MF levels in the hemolymph of crustaceans. This method is simple and rapid, allowing the MF level of a single sample to be determined within an hour of

TABLE I  
ACCURACY OF METHYL FARNESOATE DETECTION

Samples of methyl farnesoate standard were analyzed by HPLC. The amount of MF detected ( $\pm$  S.E.M.,  $n=3$ ) is indicated.

Injected (ng)	Detected (ng)	% Difference
0.25	0.27 $\pm$ 0.01	8.0
0.50	0.52 $\pm$ 0.04	4.0
1.00	1.07 $\pm$ 0.01	7.0
5.00	5.30 $\pm$ 0.13	6.0
25.00	23.55 $\pm$ 0.34	6.0

TABLE II  
PRECISION OF METHYL FARNESOATE DETECTION

Hemolymph samples were collected from three lobsters (A, B and C), and each sample divided into three 1-ml aliquots. Each aliquot was analyzed once by HPLC, and the amount of MF in each hemolymph sample ( $\pm$  S.E.M.,  $n=3$ ) calculated.

Sample	MF detected (ng/ml)	Coefficient of variation
A	2.1 $\pm$ 0.03	1.5
B	15.3 $\pm$ 0.8	5.3
C	43.3 $\pm$ 0.5	1.2

collection. When used with an autosampler and an automatic data collection system, over 40 samples a day can be quantified. In hemolymph samples from three crustacean species, the data obtained by HPLC were comparable to those obtained by the more selective and rigorous method of GC-MS. In addition, the accuracy and precision of HPLC were similar to GC-MS methods for related compounds [17].

Part of the precision of this method results from the use of an internal standard in each sample, a strategy that has also been used in a GC-MS method for MF [4]. Though we used EF in our studies, it seems likely that other compounds such as the 2Z,6E isomer of MF, would also be useful. The addition of internal standard to each sample allowed us to correct for occasional losses that occurred during sample preparation as well as possible changes in detector sensitivity. However, the efficiency of the extraction procedure (>95% recovery of MF) and the stability of the detector usually meant that these corrections were small. The internal standard was also useful in samples with low levels of MF (<0.5 ng), where the EF peak helped identify the MF peak.

The HPLC conditions used caused MF and EF to elute rapidly (<5.0 min) and resolved the two compounds satisfactorily for purposes of quantification. Better resolution of MF and EF can be obtained with solvents containing a lower percentage of diethyl ether in hexane. However, this approach increases the cycle time and raises the limit of detection of the procedure, making it difficult to detect MF in samples with low levels of this compound.

The internal standard (5 ng of EF) was added to each sample. This amount allowed the reliable quantification of MF at levels between 0.25 ng and 25 ng of MF per injection. Since the retention times of EF and MF are close, higher quantities of MF tend to obscure the EF peak. For samples that have consistently high levels of MF, this problem can be resolved by using larger amounts of EF. Alternately, the quantity of MF can be calculated by comparing the size of the MF peak in an unknown sample to that of the MF standard. Of course, this approach does not allow correction for losses during sample preparation or for changes in detector sensitivity.

The low limit of detection achieved by this HPLC method is partly the result of the extinction coefficient of MF, which is sufficiently high to allow small amounts (<0.25 ng) of this compound to be detected after separation on normal-phase HPLC. In addition, the entire sample can be analyzed by normal-phase HPLC. Thus, the overall detection limit of this method is similar to that of GC-MS where only a small fraction of the sample is usually injected.

Probably the most important factor in achieving high sensitivity by this method was the elimination of interfering compounds. This was accomplished using the TE procedure. Samples prepared by other extraction methods were unsatisfactory due to these compounds. Although the reduction in the extractable mass and UV-absorbing materials was modest (30% and 40%, respectively), the TE procedure succeeded in removing those contaminants from hemolymph that interfered with MF quantification.

Nevertheless, the extracts still contained major contaminants which elute after MF. These contaminants were removed by rinsing the column between samples. Since the eluting solvent was used during this rinsing period, the retention times of MF and EF were not affected. Most contaminants appeared to be removed during the rinse, but some did remain on the column. These eventually decreased column resolution. However, most silica columns remained useful for over 1000 injections, especially when care was taken during sample preparation to avoid the underlying acetonitrile phase when the hexane phase was removed. Although this rinsing procedure lengthened the time required for the analysis of each sample, it required no further manipulation of the sample after pooling the two hexane extracts. An alternate approach would be to remove these contaminants with a mini-column separation prior to HPLC. In our experience, the time and expense required to remove the contaminants outweigh the advantages of a shorter analysis time.

It should be noted that this method does not provide the experimenter with a rigorous identification of MF, since UV detectors are relatively non-specific. We have found that this method gives good results for several crustaceans, but it may prove unusable for other species. Thus, it is advisable to validate this HPLC method by GC-MS or some other means for each new species. Nevertheless, we suspect that this HPLC method, with perhaps some minor modifications, will prove useful for many, if not most, crustaceans. We have also used a modification of this method to measure JH levels in insect hemolymph [18]. Thus, normal-phase HPLC coupled with the TE procedure proved to be a valuable analytical approach for the study of MF and related compounds in many arthropods.

#### ACKNOWLEDGEMENTS

This work was supported in part by grants from the NIH (1-R15-HD22677-01), the NSF (DCB88-13472), and the National Sea Grants College Program, Department of Commerce (COMM NA85AA-083N-RA2). We express our appreciation to Drs. D. A. Schooley and F. C. Baker for unlabeled MF, to Dr. G. D. Prestwich for radiolabeled [ $10\text{-}^3\text{H}$ ]MF, and to all three for their comments on this manuscript.

#### REFERENCES

- 1 E. Bruning, A. Saxer and B. Lanzrein. *Int. J. Invertebr. Reprod. Dev.*, 8 (1985) 269.
- 2 E. Bruning and B. Lanzrein, *Int. J. Invertebr. Reprod. Dev.*, 12 (1987) 29.
- 3 D. A. Schooley and F. C. Baker, in G. A. Kerkut and L. I. Gilbert (Editors), *Comprehensive Insect Physiology, Biochemistry, and Pharmacology, Vol. 7, Endocrinology*, Pergamon Press, Oxford and Elmsford, NY, 1985, p. 363.
- 4 D. W. Borst, H. Laufer, M. Landau, E. S. Chang, W. A. Hertz, F. C. Baker and D. A. Schooley, *Insect Biochem.*, 17 (1987) 1123.

- 5 H. Laufer, D. W. Borst, F. C. Baker, C. Carrasco, M. Sinkus, C. C. Reuter, L. W. Tsai, and D. A. Schooley, *Science (Washington, D. C.)*, 235 (1987) 202.
- 6 C. R. Paulson and D. M. Skinner, *Am. Zool.*, 28 (1988) 83a.
- 7 B. Tsukimura and F. I. Kamemoto, *Am. Zool.*, 28 (1988) 63a.
- 8 M. D. Brody and E. S. Chang, *Am. Zool.* 29 (1989) 62a.
- 9 J. M. Vogel and D. W. Borst, *Am. Zool.*, 29 (1989) 49a.
- 10 D. W. Borst and H. Laufer, in A. P. Gupta (Editor), *Morphogenetic Hormones of Arthropods: Discoveries, Syntheses, Metabolism, Evolution, Modes of Action, and Techniques*, Rutgers University Press, New Brunswick, NJ, 1990, p. 35.
- 11 A. K. Kumaran, in A. P. Gupta (Editor), *Morphogenetic Hormones of Arthropods: Discoveries, Syntheses, Metabolism, Evolution, Modes of Action, and Techniques*, Rutgers University Press, New Brunswick, NJ, 1990, p. 181.
- 12 S. S. Tobe, D. A. Young, H. W. Khoo and F. C. Baker. *J. Exp. Zool.*, 249 (1989) 165.
- 13 E. F. Couch, D. W. Borst, H. Laufer and J. K. Butler, *Am. Zool.*, 27 (1987) 68a.
- 14 W.-S. Eng and G. D. Prestwich. *J. Labelled Compd. Radiopharm.*, 25 (1988) 627.
- 15 F. C. Baker, in A. P. Gupta (Editor), *Morphogenetic Hormones of Arthropods: Discoveries, Syntheses, Metabolism, Evolution, Modes of Action, and Techniques*, Rutgers University Press, New Brunswick, NJ, 1990, p. 391.
- 16 J. Folch, M. Lees and G. H. Sloane Stanley, *Biol. Chem.*, 226 (1957) 497.
- 17 B. J. Bergot, M. Ratcliff and D. A. Schooley, *J. Chromatogr.*, 204 (1981) 231.
- 18 D. W. Hunnicutt and D. W. Borst, unpublished results.



## Separation and purification of oligonucleotides using a new bonded-phase packing material

P. A. D. EDWARDSON<sup>a</sup>, I. J. COLLINS, M. D. SCAWEN\* and T. ATKINSON

*Division of Biotechnology, Centre for Applied Microbiology and Research, Porton Down, Salisbury, Wiltshire SP4 0JG (UK)*

and

G. B. COX<sup>b</sup>, S. SIVAKOFF and R. W. STOUT

*E. I. Du Pont de Nemours, Inc., Medical Products Department, Glasgow Site, Wilmington, DE 19898 (USA)*

(First received October 2nd, 1990; revised manuscript received February 12th, 1991)

---

### ABSTRACT

We describe a new bonded-phase packing material, based upon surface-stabilised microparticulate silica, suitable for the rapid separation and purification of oligonucleotides. Columns packed with this material were demonstrated to give rapid separations of individual oligonucleotide species of up to 44 base units with high purity; agarose gel electrophoresis showed that the products were essentially single bands, with only trace quantities of the  $(n-1)$ -mer present. Baseline resolution of the desired oligomer from  $(n \pm 1)$ -mer was achieved under preparative loading conditions, where up to 200–300  $\mu\text{g}$  of oligonucleotide could be separated. The separation was essentially independent of structure or sequence of the oligonucleotides. The retention mechanism of the oligonucleotides was investigated, and the results used to determine the optimum column configuration and separation conditions.

---

### INTRODUCTION

The synthesis of single-stranded oligonucleotides is an area which has grown rapidly over the past few years, due to the need for DNA probes and for use in gene synthesis. Purification of the synthetic oligonucleotides is of obvious importance and there is a continuing need for methods which are rapid, preferably universal and which result in high yields of high-purity oligomer, free from the shorter-chain-length failure sequences. Probably the most used purification technique for such oligonucleotides is polyacrylamide gel electrophoresis [1]. Although this technique produces homogeneous oligonucleotides, it is time-consuming and often results in very low yields of longer oligonucleotides (greater than 20 bases in length).

Oligonucleotides can also be purified by chromatography. A mixed-mode resin, RPC-5, for low-pressure liquid chromatographic separations, was shown to be very

---

<sup>a</sup> Present address: Analytical Research and Development, Bristol Meyers-Squibb Derm UK, Tech. Base 26, New Tech. Square, Deeside Industrial Estate, Deeside, Clwyd CH5 2NU, UK.

<sup>b</sup> Present address: Prochrom Inc., 5622 West 73rd Street, Indianapolis, IN 46278, USA.

successful for separating components of single- and double-stranded nucleic acid fragments [2]. The packing consisted of a resin-based particle, coated with a quaternary ammonium compound. Both hydrophobic and ionic properties are known to be present in this material, thus creating what may be termed a hydrophobic ion-exchange medium. In addition to being unavailable commercially, this packing suffered several shortcomings such as bleed of the amine stationary phase and pressure instability [3].

More recently, high-performance liquid chromatography (HPLC) has been employed for the separation and purification of oligonucleotides. A variety of packing materials such as anion-exchange [4], reversed-phase [5], reversed-phase ion-pair [6,7] and charge transfer [8] have been used for this purpose. One of the more popular techniques is reversed-phase chromatography of the dimethyltrityl-protected oligonucleotides [9]. This suffers to some extent in that the separation is not related to the chain length of the oligonucleotide nor to its sequence, and it is difficult, therefore, to be certain that the correct product has been synthesised, is being collected, and has the desired purity. HPLC techniques are mostly useful for purifying relatively short-chain hetero-oligonucleotides of up to 20–25 bases in length. More recently, reports of the use of ion-exchange materials for the purification of longer chain materials have appeared. Because the separation of oligonucleotides by ion-exchange chromatography is most effective at high pH values ( $\geq 11$ ), its use is restricted to highly charged, alkali-stable supports like Mono Q (Pharmacia). Under these conditions oligonucleotides up to 30 bases in length can be purified in a single step [8].

During the course of an investigation into potential packing materials for the separation and purification of homo- and hetero-oligonucleotides we have developed a novel, silica-based, microparticulate, bonded-phase packing material which is particularly suited to the task. The surface of the silica particles is stabilised by treatment with zirconium [10]; this enhances its stability to alkaline pH, but does not affect the separation of oligonucleotides. The packing contains both polar and hydrophobic groups in a configuration which is believed to facilitate the chromatographic separation of oligonucleotides [11]. In this report we illustrate how this packing material can be used for the separation and purification of both homo- and hetero-oligonucleotides up to and exceeding 40 bases in length. This packing material is now available commercially as the Zorbax BioSeries OLIGO column.

## EXPERIMENTAL

### *Chemicals*

Silica gel was either Zorbax PSM150 or Zorbax PSM300 spherical silica, 7  $\mu\text{m}$  diameter. 2-Aminoethanol was purchased from Sigma (Poole, UK) and acetonitrile (HPLC grade) was from Rathburn (Walkerburn, UK) or from J. T. Baker (Phillipsburg, NJ, U.S.A.). Acrylamide and methylene bisacrylamide (ultra pure) were from Bethesda Research Labs. (Cambridge, UK). Glycidoxypopyltrimethoxysilane was from Silar Labs. (Scotia, NY, U.S.A.) or from Petrarch (Bristol, PA, U.S.A.). [ $^{32}\text{P}$ ]ATP was from Amersham International (Amersham, UK) and homo-oligonucleotide standards were purchased from Pharmacia (Pisataway, NJ, U.S.A.). Other chemicals were of analytical grade or higher and obtained from BDH (Poole, UK) or Sigma. Oligonucleotides were synthesised using an Applied Biosystems Model 380B oligonucleotide synthesiser, employing cyanoamidate chemistry. The crude oligonu-

cleotides were deprotected, lyophilised and redissolved in water to a concentration of about 0.5 mg/ml. Stationary phases were prepared by reacting 2-aminoethanol with  $\gamma$ -glycidoxypropyltrimethoxysilane to give 3-[3'-(2''-hydroxyethylamino)-2'-hydroxypropoxy]propyltrimethoxysilane. This was bonded to the silica as described previously [12].

#### *Other bonded-phase materials*

Other packings similar in nature to that synthesised from 2-aminoethanol were prepared by analogous procedures, using 2-amino-2-methyl-1,3-propanediol, 2-amino-2-ethyl-1,3-propanediol, 2-amino-2-hydroxymethyl-1,3-propanediol and 2-mercaptoethanol (see Table I).

#### *Polyacrylamide gel electrophoresis*

Purified oligonucleotides (50 ng) were end-labelled with [<sup>32</sup>P]ATP using T4 polynucleotide kinase and then analysed by electrophoresis on 20% polyacrylamide gels using an aqueous 4 mM Tris, 1 mM borate and 0.1 M EDTA buffer adjusted to a pH 8.3. Bands were visualised by autoradiography (X-Omat autoradiograph film, Kodak, France).

#### *Chromatographic procedures*

Stainless-steel columns (50 mm  $\times$  4.6 mm I.D., 80 mm  $\times$  6.2 mm I.D. and 250 mm  $\times$  4.6 mm I.D.) were packed by a downward slurry technique. Separations were carried out at ambient temperatures (18 to 24°C) using either a Waters LC system (Model 510) (Waters Assoc., Hartford, UK) or an LKB gradient pumping system (Model 2150/2152, LKB Gaithersburg, MD, U.S.A.)

The solvent systems used were as follows. pH 6: 20 mM dipotassium phosphate in 20% (v/v) aqueous acetonitrile, adjusted to pH 6.0 with 1 M potassium dihydrogenphosphate. The elution buffer was prepared by adding KCl (1 or 2 M) to this buffer. pH 7: 20 mM disodium phosphate in 20% (v/v) aqueous acetonitrile adjusted to pH 7.0 with 1 M sodium dihydrogenphosphate. The elution buffer was prepared by adding 1 M NaCl to this buffer.

The gradients used were as follows. (A) 0.15 M NaCl, 20% acetonitrile, pH 7.0 to 0.75 M NaCl, 20% acetonitrile, pH 7.0 over 40 min at 1 ml/min: (B) 20% acetonitrile, pH 6.0 to 1 M KCl, 20% acetonitrile, pH 6.0 over 40 min at 1 ml/min. (C) 0.35 M NaCl, 20% acetonitrile, pH 7.0 to 0.6 M NaCl, 20% acetonitrile, pH 6.0 over 90 min at 1 ml/min. (D) 20% acetonitrile, pH 6.0 to 2 M KCl, 20% acetonitrile, pH 6.0 over 120 min at 1 ml/min.

The capacity factor,  $k'$ , defined as  $(V_e - V_0)/V_0$ , where  $V_e$  is the elution volume of the peak and  $V_0$  is the void volume of the column.  $V_0$  was determined by injecting a sample of acetonitrile and measuring its retention time.

Oligonucleotides eluting from the columns were collected manually at the detector outlet. Before analysis by electrophoresis, the fractions were desalted by gel filtration on Sephadex G25 and lyophilised.

## RESULTS AND DISCUSSION

*Influence of bonded phase*

The retention of oligonucleotides increased with the increasing number of hydroxyl groups on the bonded phase. Table I shows the retention times of the homo-oligonucleotides dA<sub>14</sub> and dA<sub>15</sub> on the different stationary phases prepared. Increasing the number of hydroxymethyl groups on the carbon atom adjacent to the amino group increased retention. It is not clear whether this is due to the enhancement of the ion-exchange character of the secondary amine, or if there are secondary interactions between the hydroxyl group and the phosphate ester or other polar groups in the oligonucleotide. Increasing the hydrophobic nature of the bonded phase also increases the retention time; substituting an ethyl group for a methyl group leads to a slightly longer retention time. This substitution would obviously increase any reversed-phase interactions, but would also be expected to reduce the ionic nature of the amino group due to the increase in electron-releasing character of the alkyl functionality. The presence of the amino function is essential, as was demonstrated by the use of 2-mercaptoethanol, when no retention of the oligonucleotides was observed.

*Influence of column dimensions*

The effect of column length on the gradient separation of macromolecules by reversed-phase chromatography has been shown to be relatively small, once a certain molecular size is exceeded. In the case of both polystyrene [13] and peptides and proteins [14], the slopes of plots of  $\log k'$  against solvent composition increase rapidly with molecular size. With these molecules the peak width is more a function of the gradient profile rather than of the column length, as is the case with small molecules. Similar effects have been observed under ion-exchange conditions [15]. Since it was anticipated that oligonucleotides would behave similarly, a range of columns of differing lengths was studied. As shown in Fig. 1, the separation of a 10-mer hetero-oligonucleotide from its associated impurities was improved on changing from a 50-mm column through an 80-mm column to a 250-mm column. The improvement was small for the transition to the longest column, so the 80 mm  $\times$  6.2 mm I.D. format was chosen for subsequent investigations, as it had sufficient capacity for the

TABLE I

INFLUENCE OF BONDED PHASE ON THE RETENTION TIME OF THE OLIGONUCLEOTIDES dA<sub>14</sub> AND dA<sub>15</sub>

The oligonucleotides were chromatographed using gradient B.

Bonded phase	Structure	$k'$	
		dA <sub>14</sub>	dA <sub>15</sub>
2-Aminoethanol	H <sub>2</sub> NCH <sub>2</sub> CH <sub>2</sub> OH	28.8	30.6
2-Amino-2-methyl-1,3-propanediol	HOCH <sub>2</sub> CNH <sub>2</sub> (CH <sub>3</sub> )CH <sub>2</sub> OH	41.2	43.8
2-Amino-2-ethyl-1,3-propanediol	HOCH <sub>2</sub> CNH <sub>2</sub> (C <sub>2</sub> H <sub>5</sub> )CH <sub>2</sub> OH	43.3	45.2
2-Amino-2-hydroxymethyl-1,3-propanediol	HOCH <sub>2</sub> CNH <sub>2</sub> (CH <sub>2</sub> OH)CH <sub>2</sub> OH	Not eluted	
2-Mercaptoethanol	HSCH <sub>2</sub> CH <sub>2</sub> OH	0	0

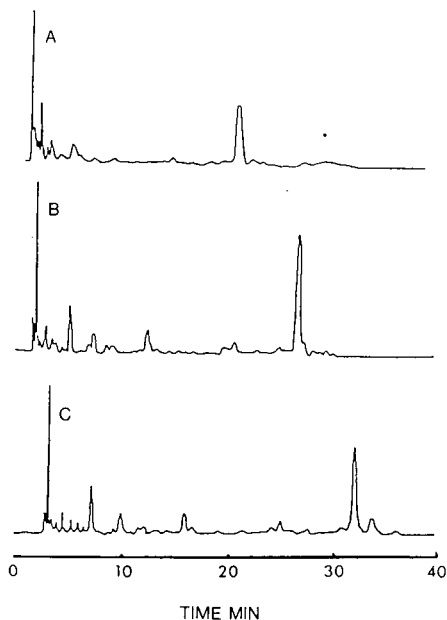


Fig. 1. Effect of column dimensions on the chromatography of an 18-mer. A 10- $\mu$ g amount of the oligonucleotide d(TCTAATACTTCGGGATGGTG) was loaded and eluted using gradient A; a.u.f.s. = 0.1.

quantities of oligonucleotide generally purified and showed adequate resolution for the oligonucleotides of interest.

#### *Solvent system parameters*

The effects of varying the pH of the buffer, the nature and concentration of the organic modifier, the buffer concentration and the temperature at which the separation was carried out were investigated.

The influence of pH on the separation was investigated using a buffer of constant ionic strength over the pH range 3–8. This was prepared from dipotassium hydrogenphosphate–citric acid mixtures and the ionic strength adjusted by the addition of potassium chloride to a final value of 0.2 *M*. A short oligonucleotide (dA<sub>4</sub>) was chromatographed isocratically using this mobile phase. A plot of  $k'$  against pH is shown in Fig. 2. The reason for the apparent increase in retention time at about pH 7 is not clear; there is, however, a general trend of reduced retention at higher pH values for both small and large oligonucleotides. The oligonucleotide dA<sub>4</sub> was not eluted at pH values below 4.

The concentration of acetonitrile in the mobile phase was investigated by the chromatography of dA<sub>4</sub> in 20 mM phosphate, pH 6.0, over a range of solvent compositions from 5% (v/v) to 50% (v/v). A plot of  $\log k'$  against the concentration of organic modifier (not shown) was linear, showing classical reversed-phase behaviour. A concentration of 20% was chosen, as representing a reasonable compromise between retention and peak shape. The concentration of the buffer system was

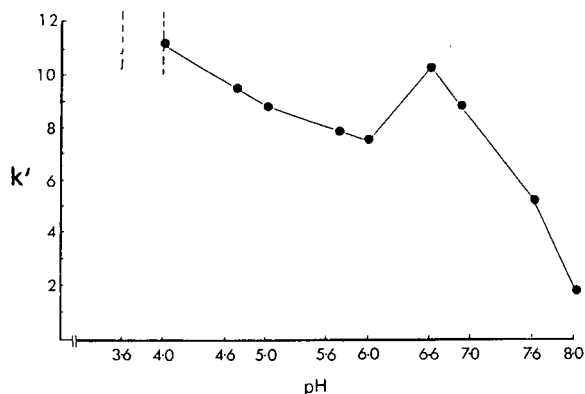


Fig. 2. Effect of pH on the chromatography of  $dA_4$ . The column was 80 mm  $\times$  6.2 mm I.D. and was eluted isocratically at a flow-rate of 1 ml/min using potassium phosphate-citric acid buffers of constant ionic strength (0.2  $M$ ).  $k'$  = Capacity factor; a.u.f.s. = 0.2.

investigated similarly, using  $dA_4$  over a range of buffer concentrations from 10 to 50 mM. A plot of  $k'$  against the inverse of buffer concentration (not shown) was linear, demonstrating the ionic nature of the separation.

Acetonitrile, methanol and tetrahydrofuran were chosen as examples of solvents exhibiting quite different selectivities [16]. These were used in the mobile phase at concentrations of 20, 30 and 10% (v/v) respectively, values which approximately reflect their relative solvent strengths in reversed-phase chromatography [16]. A sample of  $dA_{15}$  which contained appreciable concentrations of the lower oligomers was used in the gradient separation. Fig. 3 shows the plot of  $k'$  against the number of bases in the oligonucleotide. There was little difference between the solvents, apart

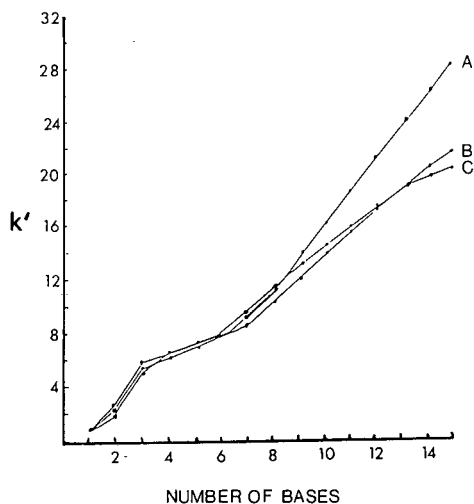


Fig. 3. Effect of organic modifier on the chromatography of oligo- $dA_n$  ( $n = 1-15$ ). The organic modifiers were (a) methanol at 30% (v/v), (b) acetonitrile at 20% (v/v) and (c) tetrahydrofuran at 10% (v/v). The column was eluted using gradient B; a.u.f.s. = 0.2.

from the greater retention seen with methanol because of its relatively lower solvent strength in this system. As the nature of the organic modifier was not critical, 20% (v/v) acetonitrile was used for the remainder of this work.

The effect of temperature on the retention of  $dA_{15}$  was also investigated by running the column in an oven over a range of temperatures from 30 to 75°C. As shown in Fig. 4, retention fell rapidly with increasing temperature.

#### *Loading capacity and recovery*

The capacity of the packing for oligonucleotides was investigated by increasing the sample load and observing the effect on the chromatography of a pure oligonucleotide. Using the 80 mm × 6.2 mm I.D. column the amount of pure 18-mer loaded was increased to 140 μg, with no appreciable change in the elution profile. With amounts greater than this, the UV absorbance was too great to monitor the separation; such 100-μg quantities, however, are more than sufficient for hybridisation experiments. In order to assess the recovery of oligonucleotides approximately 10-μg amounts were chromatographed. The eluting peak was collected, and the total amount present was estimated from the UV absorbance at 260 nm. The recoveries of all oligonucleotides, up to 38 bases in length, were in excess of 95%.

#### *Separation of homo-oligonucleotides*

In order to demonstrate the separation of the  $n-1$  oligonucleotide, the homo-oligonucleotides  $dA_{14}$ ,  $dA_{15}$ ,  $dT_{24}$  and  $dT_{25}$  were synthesised, and the separation of each oligomer pair was examined. As shown in Fig. 5A and B, baseline

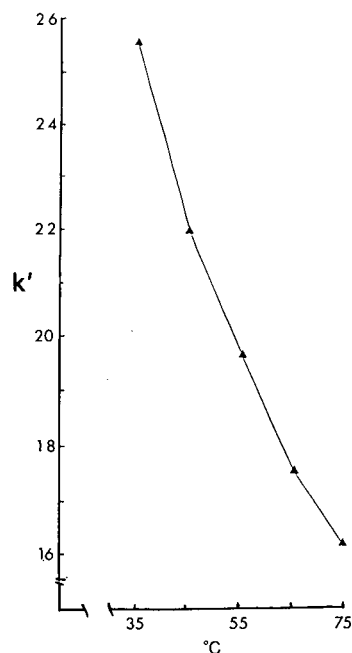


Fig. 4. Effect of temperature on the chromatography of  $dA_{15}$ . The column was eluted using gradient B; a.u.f.s. = 0.2.

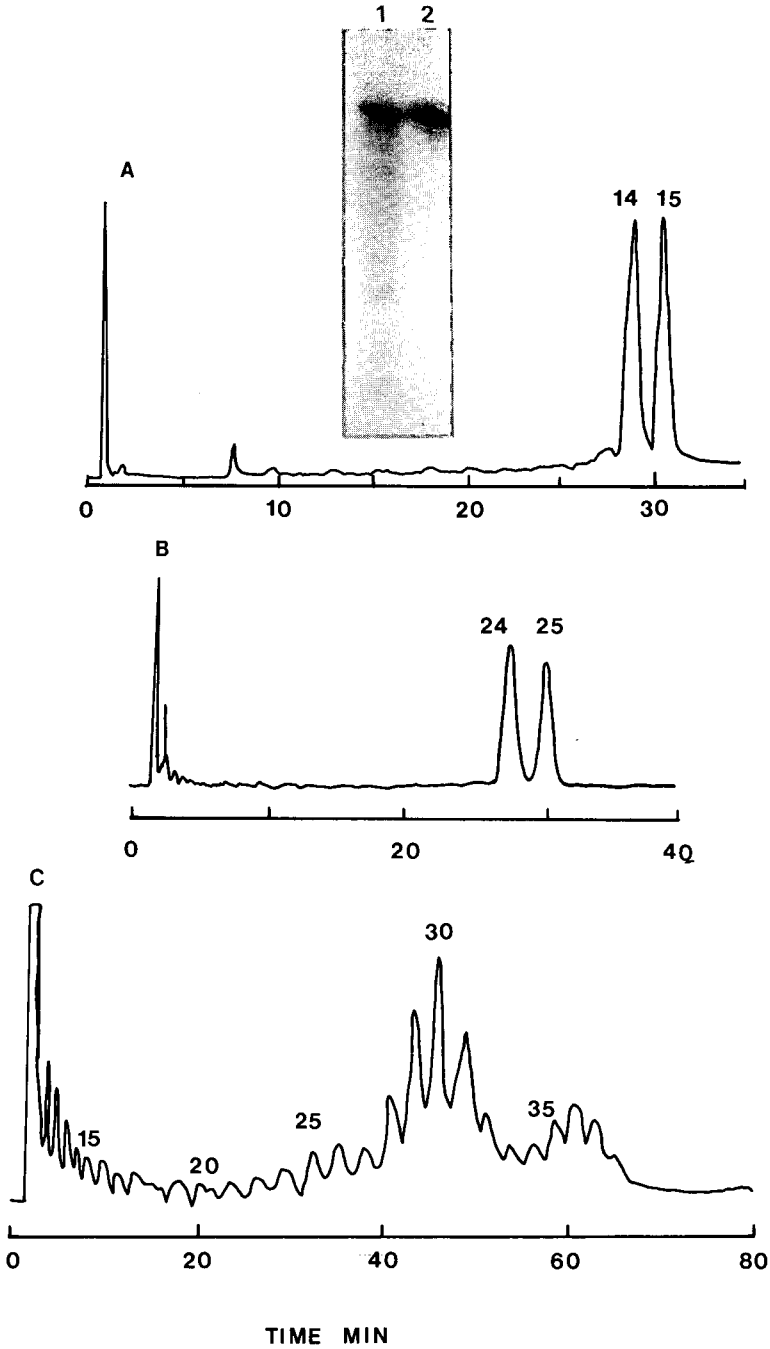


Fig. 5. Chromatography of mixed homo-oligonucleotides. (A) Separation of  $dA_{14}$  and  $dA_{15}$  using gradient B; (B) separation of  $dA_{24}$  and  $dA_{25}$  using gradient C; (C) chromatography of a failed synthesis of  $dT_{40}$  using gradient C; a.u.f.s. = 0.2. The inset in (A) shows the electropherogram of  $dA_{15}$  (1) before and (2) after chromatography.



resolution was obtained in each case. The inset to Fig. 5A shows the electropherogram obtained from  $dA_{15}$  before and after chromatography. Fig. 5C shows the chromatogram obtained from a failed synthesis of  $dT_{40}$ . The large number of peaks are indicative of the truncated sequences present in the synthesis product. Peaks can be discerned up to  $dT_{38}$ , although the complex nature of the mixture reduces the resolving power of the system.

#### *Separation of hetero-oligonucleotides*

To investigate the effect of length and nucleotide sequence on the resolution of hetero-oligonucleotides a number of 17- and 18-mer oligomers were synthesised and chromatographed. The retention times and structures of some of these are given in Table II. Although the majority of the oligonucleotides eluted with retention times close to the mean value, some were retained much longer. This may be due to the presence of sequences which allow self-hybridisation of the oligonucleotides, leading to a change in the apparent molecular size of the chromatographing species, which results in an increased retention time and peak distortion. Fig. 6 illustrates the elution profiles of some 18-mer hetero-oligonucleotides; Fig. 6D shows clearly the typical increased retention and skewed peak thought to be due to self-hybridisation of the

TABLE II  
RETENTION TIMES OF 17-MER AND 18-MER OLIGONUCLEOTIDES

Oligonucleotide sequence	<i>n</i>	Retention time (min)	Mean retention time (min)
ATGGTCTTGTGTGATAA	17	30.5	30.8 (S.D. = 1.65)
CCTTTGTAAGTGCTAAA	17	30.4	
CTTCGATAATGTCTTGA	17	30.3	
AAGTGAGCGGACAAATA	17	33.8	
TGAACCTCAGAAGTAGA	17	33.8	
TAGAATAGTGCTTCACA	17	29.9	
TCTACTGGTGTATAAAC	17	30.1	
TGGATAAGTACAAGTTA	17	29.8	
TTTCTTATGGGTAGCAAG	18	31.2	
ACCGGAAAGATTAATCAG	18	36.9	
CACCATCGAAGTATTAGA	18	32.5	31.8 (S.D. = 1.82)
AAATTTCGAACTGACGCA	18	33.8	
CTTCAAACAGGGTGTTT	18	31.4	
CTTGCAGGAACAAAATGA	18	31.4	
ACTTCCTATCTAGAAAGGA	18	33.5	
GCGATTATGAGAGTGAAT	18	29.8	
AATCGTCTCGTCTTATTA	18	29.8	
GATTAACCCAGCACATA	18	32.3	
TCTAATACTTCGATGGTG	18	31.5	
TCATTTTGTTCCTGCAAG	18	30.3	
CAGGAACAACATGAAGAA	18	32.1	
CCCTTCGTTCAACAAAAT	18	30.5	
CGCTTGGTTCTGGTTCAC	18	31.5	
AATCGTCTCGTCTTATTA	18	31.5	
TCCTTCTAGATAGGAAGT	18	31.0	

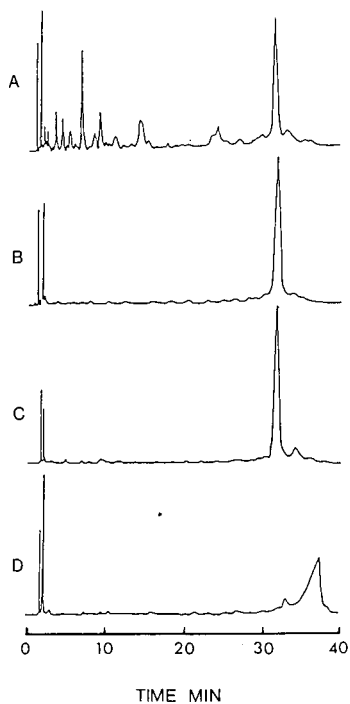


Fig. 6. Chromatography of 18-mer hetero-oligonucleotides. (A) d(TCTAATACTTCGATGGTG); (B) d(CTTGCAGGAACAAAATGA); (C) d(ATTTTGGTTGAACGAAGGG); (D) d(ACCGAAAAGATTA-ATCAG). The column was eluted using gradient C; a.u.f.s. = 0.2.

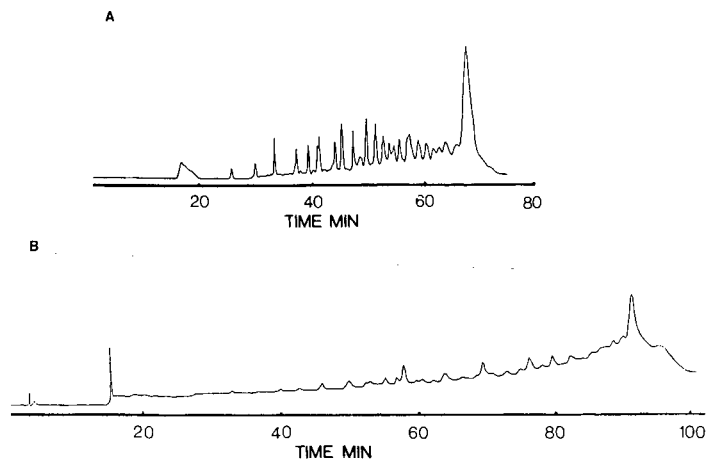


Fig. 7. Chromatography of longer oligonucleotides. (A) 27-mer; (B) 44-mer. The column was eluted using gradient D; a.u.f.s. = 0.2.

oligonucleotides, leading to a change in the apparent molecular size of the chromatographing species, which results in an increased retention time and peak distortion.

In order to investigate the effect of increasing chain length, a number of longer oligonucleotides were purified. Fig. 7 shows the elution profiles of 27-mer and 44-mer hetero-oligonucleotides. To improve the separation of these longer molecules the gradient time was increased to 120 min and the flow-rate reduced to 0.5 ml/min. Gel electrophoresis of the eluted oligonucleotides showed single bands and clearly demonstrated the removal of shorter-failure sequences. Larger oligonucleotides of this type could be isolated in greater than 90% purity, with gel electrophoresis showing only traces of the  $(n-1)$ -mer (data not shown).

## CONCLUSIONS

A novel bonded-phase packing is reported which allows the rapid purification of both homo- and hetero-oligonucleotides. The matrix is believed to interact with the oligonucleotides by a mixed-mode mechanism involving both polar and hydrophobic interactions. Rapid separations of oligonucleotides were obtained with high recoveries and purities in excess of 90% over a size range up to 44 base units in length. Baseline resolution between  $n$ - and  $(n-1)$ -mer oligomers was achieved under normal preparative loading conditions. Loading studies indicated that sufficient oligonucleotide for normal hybridisation requirements could be isolated from a single chromatographic run.

## ACKNOWLEDGEMENT

P. A. D. E., I. J. C., M. D. S. and T. A. thank E.I. Du Pont de Nemours, Inc., for support.

## REFERENCES

- 1 R. Frank, D. Miller and G. Wolff, *Nucleic Acids Res.*, 9 (1981) 4967.
- 2 G. C. Walker, O. C. Uhlenbeck, E. Bedows and R. I. Gumpert, *Proc. Natl. Acad. Sci. U.S.A.*, 72 (1975) 122.
- 3 R. D. Wells, C. Hardies, G. T. Horn, B. Kelin, J. E. Larson, S. K. Nevendorf, R. W. Patient and E. Selsing, *Methods Enzymol.*, 65 (1980) 327.
- 4 W. Haupt and A. Pingoud, *J. Chromatogr.*, 260 (1983) 419.
- 5 A. M. Delort, R. Derbyshire, A. M. Duplaa, A. Guy, D. Molko and R. Teoula, *J. Chromatogr.*, 283 (1984) 462.
- 6 J. M. Egly, *J. Chromatogr.*, 215 (1981) 243.
- 7 H. Schott, R. Semmler and H. Eckstein, *J. Chromatogr.*, 389 (1987) 165.
- 8 M. V. Cubalis and G. Marion, *J. Chromatogr.*, 329 (1985) 406.
- 9 C. R. Becken, J. W. Efcavitch, C. R. Heiner and N. F. Kaiser, *J. Chromatogr.*, 326 (1985) 293.
- 10 R. W. Stout, *U.S. Pat.*, 4 600 646 (1986).
- 11 G. B. Cox, A. Atkinson, P. A. D. Edwardson and M. D. Scawen, *U.S. Pat.*, 4 767 670 (1988).
- 12 R. W. Stout and J. J. Stefano, *J. Chromatogr.*, 326 (1985) 63.
- 13 J. P. Larman, J. J. Stefano, A. P. Goldberg, R. W. Stout, L. R. Snyder and M. A. Stadalius, *J. Chromatogr.*, 325 (1983) 163.
- 14 M. A. Stadalius, M. A. Quarry and L. R. Snyder, *J. Chromatogr.*, 327 (1985) 93.
- 15 R. W. Stout, S. I. Sivakoff, R. D. Ricker and L. R. Snyder, *J. Chromatogr.*, 353 (1986) 439.
- 16 L. R. Snyder, *J. Chromatogr. Sci.*, 16 (1978) 223.



## **Optimized high-performance liquid chromatographic procedure for the separation and determination of the main folacins and some derivatives**

### **II. Extraction method and application to rat liver**

A. HAHN, K. H. FLAIG and G. REHNER\*

*Institute of Nutrition, Justus Liebig University, Wilhelmstrasse 20, D-6300 Giessen (Germany)*

(First received October 9th, 1990; revised manuscript received January 10th, 1991)

---

#### **ABSTRACT**

Different methods for the extraction of folacins from biological materials and the hydrolysis of pteroylpolyglutamates prior to high-performance liquid chromatography were investigated. Acetone precipitation of proteins led to higher extraction rates of folates from biological materials as examined by using an endogenous labelling technique. It also caused less destruction of some folates but could not be combined with subsequent hydrolysis of pteroylpolyglutamates. Pteroylpolyglutamates were hydrolysed by a partially purified suspension of pteroylpolyglutamates hydrolase (PPH). Comparative studies on the folate content of rat liver revealed that complete hydrolysis of polyglutamates could also be achieved by incubating the homogenized tissue at 37°C to allow endogenous PPH to act. This procedure causes interconversions of folates and is therefore not suitable for the analysis of biological materials.

---

#### **INTRODUCTION**

The determination of folacins is still an analytical problem because of the high lability of the substances and their low content in biological materials. The chromatographic system we presented in a previous paper [1] allows the fast and sensitive separation and determination of the main folacin monoglutamates and the synthetic derivatives dichlorofolic acid and methotrexate which were used as internal standards.

In this paper we review critically the methods for the extraction of folacins from biological materials and the hydrolysis of the pteroylpolyglutamates because many problems in folacin analysis arise directly from disturbances caused by the extraction method and by the hydrolysis of the pteroylpolyglutamates [2]. On the one hand the folates should be liberated quantitatively from protein binding during the extraction procedure, and on the other hand the rate of conversion to degradation products or to other metabolites should be minimal. For this reason all media must contain stabilizing agents, *i.e.*, antioxidants such as ascorbic acid [3–8], mercaptoethanol [9–

13] or a combination of both [14]. Nevertheless as some folates show lability towards oxygen, a certain loss of substances can always be observed [13,15].

The most common technique used for the extraction of folates from biological materials is heat treatment at 80–100°C for 2–60 min [5–8,13,14]. The precipitation of proteins by trichloroacetic acid [16,17] or acetone [9] and freezing the tissue for cell cracking [13] has been used in only a few instances.

The pteroylpolyglutamates which represent the active forms of folacins must be converted into the corresponding monoglutamates before their chromatographic analysis [1]. The glutamyl residues are linked by the unique  $\gamma$ -peptide bond which is not attacked by conventional exo- and endopeptidases. The hydrolysis can only be achieved by pteroylpolyglutamate hydrolases (PPH, 'conjugases', E.C. 3.4.12.10), enzymes that are found in many tissues but which are not commercially available [18,19]. For this reason, folates are usually hydrolysed by incubating the homogenized tissue before heating [6,8] or by adding a more or less purified suspension of PPH [7,11,20].

The aim of this study was to test the applicability of heat treatment and acetone precipitation for the extraction of folates and their suitability for a subsequent hydrolysis of pteroylpolyglutamates. The application of the overall method to biological samples is reported.

## EXPERIMENTAL

For the extraction buffer in all experiments we used a minor modification of the buffer proposed by Gregory *et al.* [7]. It contained 0.1 M sodium acetate (pH 4.9) and 1% of sodium ascorbate as an antioxidant and was prepared freshly on the day of use.

### *Determination of the extraction efficiency*

'Everted sacs' from rat small intestine [21] were incubated for 1 h in 25 ml of Krebs's hydrogencarbonate solution containing 5 mM glucose and 1  $\mu$ M potassium 3',5',7,9-[<sup>3</sup>H]pteroylglutamate ([<sup>3</sup>H]PteGlu, specific activity 1660 GBq/mmol) (Amersham, Braunschweig, Germany). The radiochemical purity was examined by high-performance liquid chromatography (HPLC) [1] and found to be 97%. When incubations were terminated the segments (ca 10 cm long) were opened, blotted on paper, homogenized in a glass-Teflon homogenizer with acetate buffer and adjusted to a final volume of 5 ml.

For acetone extraction, 1 ml of the homogenate was placed in a reagent tube and mixed with 2 ml of ice-cold acetone for 1 min. After flushing with nitrogen for 30 s, the tube was closed tightly and centrifuged for 30 min at 10 000 g. The resulting supernatant was transferred to a second tube and the organic solvent was removed under a stream of nitrogen while the tube was kept in the cold. The radioactivity in the supernatant was measured by liquid scintillation counting and compared with that in the untreated homogenate.

Heat-treatment experiments were carried out in parallel with 1 ml of the same homogenates. The sample was heated in a water-bath at 95°C for 60 min after having been flushed with nitrogen. Subsequently it was immediately cooled on ice and centrifuged under the conditions mentioned above. The extraction efficiency was calculated in the same manner as in the acetone precipitation experiments.

In an additional series of experiments, heat treatment was performed prior to homogenization. In this instance the tissue was coarsely cut with scissors, covered with the buffer solution and immediately homogenized after heating.

### *Stability studies*

Determinations of the substrate stability during the extraction procedure were carried out with standard solutions of different folates. Pteroylglutamic acid (Pte-Glu), dihydrofolic acid (DHF), tetrahydrofolic acid (THF), sodium 5-methyltetrahydrofolate (5-CH<sub>3</sub>-THF), calcium 5-formyltetrahydrofolate (5-CHO-THF), methotrexate (MTX) and 3',5'-dichlorofolic acid (DCF) were obtained from Sigma (Deisenhofen, Germany) and were dissolved in the extraction buffer to final concentrations of 50 pmol/ml for 5-CH<sub>3</sub>-THF and 250 pmol/ml for all others. Volumes of 5 ml of these solutions were heated or mixed with acetone as described above. The contents of the different folates in the resulting supernatant were measured by HPLC with fluorimetric detection [1] and were compared with the folate content of untreated samples that had been assayed immediately.

### *Hydrolysis of pteroylpolyglutamates*

A PPH suspension was prepared according to methods described previously [7,22]. The suspension (16 mg/ml of protein) was assayed by HPLC and found to be free from any folate compounds. In incubation experiments 0.4 ml of enzyme suspension was added to 1 ml of acetate buffer containing 2 pmol of different folates and incubated for 30–120 min.

The hydrolytic capability of the enzyme suspension was tested by incubating extracted homogenates from cabbage and rat liver. A volume of 1 ml of the extraction supernatant was mixed with 0.4 ml of hog PPH and incubated for 30–90 min at 37°C. The increase in monoglutamates was measured by HPLC and compared with the monoglutamate content of samples that were assayed immediately after homogenization.

### *Application of the method to biological tissues*

To show the validity of the overall method we determined the folate content of rat liver. The analysis was monitored using internal standards, DCF and MTX, both of which were added to each sample prior to extraction. Fig. 1 summarizes the extraction scheme used. For comparison we also analysed rat liver by a modified procedure: the liver was homogenized in the extraction buffer and then incubated for 60 min at 37°C to make it possible for the endogenous PPH to hydrolyse the pteroylpolyglutamates. The homogenate was then heated at 95°C for 60 min to liberate the folates, centrifuged (10 000 g, 30 min, 4°C) and the supernatant was analysed by HPLC.

In all instances determinations were performed using an external calibration graph. The results were corrected for the incomplete extraction and for the loss of substances as a consequence of heat destruction.

## RESULTS AND DISCUSSION

### *Extraction procedure*

Table I gives the results of the experiments concerning the extraction efficiency,

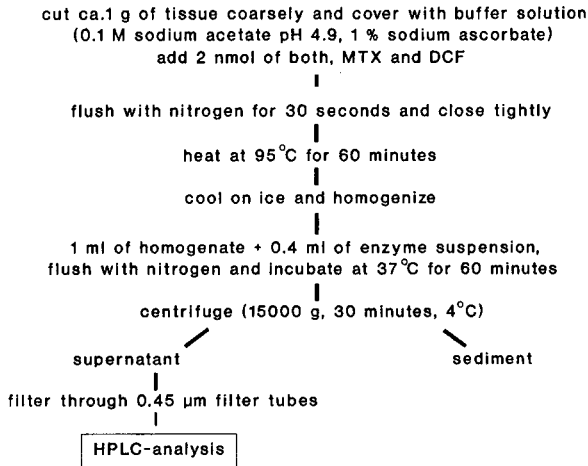


Fig. 1. Extraction of folates from biological samples and subsequent hydrolysis of polyglutamates. If it is intended to determine the content of "free" folate, *i.e.*, the folacin monoglutamates, 1 ml of the homogenate must be treated in the same way as described except for the hydrolysis with pteroylpolylglutamathydrolase.

indicating that acetone extraction was significantly better than heat treatment of the sample for extraction of folates from tissue. As can be seen, there was no significant difference between heating before and after homogenization.

The extraction efficiency is one important factor responsible for the precision of a method, but it is difficult to determine [23]. We chose an endogenous labelling technique to evaluate the extraction efficiency using intestinal tissue as a model matrix because our method was designed primarily to determine the folate content of the gut wall [24]. Chromatographic studies revealed that more than 75% of the original substrate [ $^3\text{H}$ ]PteGlu had been converted into other folacin derivatives (Fig. 2), in-

TABLE I

EXTRACTION EFFICIENCY<sup>a</sup> OBTAINED BY HEAT TREATMENT OF THE SAMPLE COMPARED WITH AN ACETONE PRECIPITATION TECHNIQUE

Experiments were carried out as described under Experimental.

Method <sup>b</sup>	Extraction efficiency (%) ( $\pm$ S.D., $n=11$ )
Acetone precipitation	95.8 $\pm$ 10.7
Heat treatment <sup>c</sup>	78.7 $\pm$ 6.1
Heat treatment <sup>d</sup>	77.3 $\pm$ 7.2

<sup>a</sup> Extraction efficiency is the amount of  $^3\text{H}$ -labelled folates found in the supernatant after centrifugation compared with the radioactivity of the whole sample.

<sup>b</sup>  $P \leq 0.001$  between acetone precipitation and the two heat-treatment techniques.

<sup>c</sup> Heating was performed after homogenization of the tissue.

<sup>d</sup> Tissue was homogenized after heat treatment (final method).



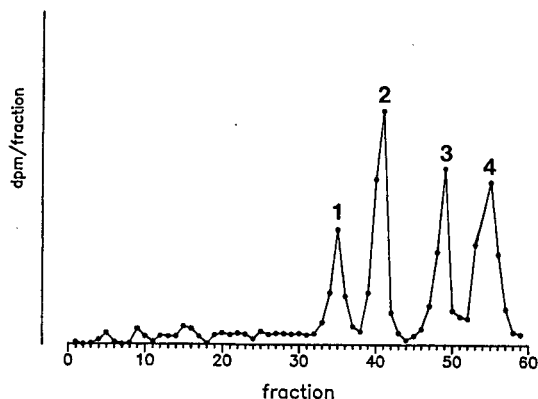


Fig. 2. Separation of radiolabelled folates from "everted sacs" of rat small intestine. Intestinal tissue had been incubated for 60 min with  $1 \mu\text{M}$  [ $^3\text{H}$ ]PteGlu and extracted as shown in Fig. 1. Separation conditions: column, Shandon Hypersil ODS ( $3 \mu\text{m}$ ,  $250 \times 4.6 \text{ mm}$  I.D.); mobile phase, gradient of (A)  $5 \text{ mM}$  potassium phosphate (pH 2.3) and (B) acetonitrile, from 7 to 13% B in 15 min and from 13 to 19% B in 3 min; flow-rate,  $0.9 \text{ ml/min}$ ; temperature ambient. The solvent stream was collected in fractions of  $0.3 \text{ ml}$  and assayed by liquid scintillation counting. Peaks were identified by comparison with chromatograms that had been recorded using UV detection at  $295 \text{ nm}$ . Peaks: 1 = THF; 2 =  $5\text{-CH}_3\text{-THF}$ ; 3 =  $5\text{-CHO-THF}$ ; 4 = PteGlu.

dicating that the substrate was at least partially equilibrated with the endogenous folates.

Up to now only one attempt to determine the extraction efficiency for folates from rat liver has been described [11]. Using  $1.5 \text{ M}$  2-mercaptoethanol as an extraction medium, about 90% of the activity was found in the supernatant after heat treatment of the sample.

We favour the endogenous labelling technique over the generally given 'recovery rates', which are easier to determine but which involve several problems. For example, they do not reflect the efficiency by which protein bonds are cleared because substrates added to tissue homogenate just before the extraction cannot be expected to behave like the endogenous substances. Further, as pointed out by others [7], the amounts of substrate usually added are often much higher than the natural substance content of the sample. Therefore, the recovery might increase because the relative amount of substrate included in the precipitate falls when higher substrate concentrations are used.

Our results confirm this assumption. After adding a very small amount ( $3.3 \text{ pmol}$ ) of [ $^3\text{H}$ ]PteGlu to a homogenate of intestinal tissue,  $70.9 \pm 3.55\%$  ( $n = 16$ ) of the activity was found after heat treatment. In contrast, when  $300 \text{ pmol}$  of substrate had to be extracted  $78.7 \pm 6.1\%$  ( $n = 11$ ,  $p \leq 0.001$ ) was found in the supernatant. However, additional results revealed that there were no significant differences when various folate contents between  $300$  and  $2000 \text{ pmol/ml}$  had to be extracted. Within this range the extraction efficiency was nearly constant and only showed non-directed variations between  $76.2\%$  and  $80.1\%$ . For this reason, the extraction efficiency can be assumed to be constant under these conditions. It should be mentioned that liver samples treated as shown in Fig. 1 contained about  $2000 \text{ pmol/ml}$  of folates in homogenate.

The efficiency of the extraction process, as judged by the amount of radioactivity in the supernatant, does not give any information about the loss of substances as a consequence of thermal or chemical degradation processes. We examined the stability of the different derivatives during the extraction procedure (Table II), which is the second factor determining the suitability of an extraction process.

The results indicate that PteGlu, DHF and 5-CHO-THF were destroyed less during acetone treatment. During heat treatment and also acetone precipitation no measurable increase in different folates could be observed, indicating that the loss of certain derivatives was due to complete degradation of these substances. The most labile derivative was found to be DHF, which was significantly better preserved using acetone treatment but which was nevertheless considerably destroyed. Additional studies showed that the extent of thermal destruction of DHF was about 90% after 10 min of heating, and the derivative could no longer be detected after 20 min. The fact that this compound was labile even under the relatively mild conditions during acetone treatment explains why it could hardly be found in natural materials [25]. Only Clifford and Clifford [10] have reported that DHF was the main folate in some foods, although they used heat treatment of the samples to extract tissue folates. We assume that these results are incorrect owing to the use of an inappropriate chromatographic system, *i.e.*, with a peak half-width of about 5 min and UV detection at 280 nm. Our data are consistent with those of O'Broin *et al.* [26], who reported that DHF was too labile to carry out systematic studies on its stability.

#### *Hydrolysis of the pteroylpolyglutamates*

Chromatographic analysis of pteroylpolyglutamates requires their hydrolysis to the corresponding monoglutamates [1]. This can be achieved by two general techniques. The fact that many tissues contain PPH allows the sample to be incubated after homogenization with its endogenous PPH [6,8]. Although this procedure leads

TABLE II

STABILITY<sup>a</sup> OF DIFFERENT FOLATE DERIVATIVES AFTER HEATING OR ACETONE TREATMENT

Experiments were carried out as described under Experimental.

Derivative	Stability (%) ( $\pm$ S.D., $n = 3-5$ )		Difference <sup>b</sup>
	Heating	Acetone treatment	
PteGlu	93.6 $\pm$ 1.6	99.1 $\pm$ 2.2	$p \leq 0.001$
DHF	0	27.5 $\pm$ 5.4	$p \leq 0.001$
THF	95.1 $\pm$ 3.6	99.4 $\pm$ 2.9	n.s.
5-CH <sub>3</sub> -THF	101.0 $\pm$ 1.6	98.9 $\pm$ 1.3	n.s.
5-CHO-THF	91.5 $\pm$ 1.8	102.9 $\pm$ 4.2	$p \leq 0.001$
MTX	91.7 $\pm$ 7.2	98.5 $\pm$ 0.9	n.s.
DCF	94.3 $\pm$ 4.6	90.0 $\pm$ 6.3	n.s.

<sup>a</sup> Stability is the amount of substrate found after carrying out the experiments compared with samples that had been assayed immediately.

<sup>b</sup> Statistical differences between the two procedures as judged by Student's *t*-test; n.s. = not significantly different.

to complete hydrolysis, it is not suitable for the analysis of folates. Because of the activity of other enzymes of folacin metabolism which are also liberated during the sample preparation, interconversions between several folates can be observed [19].

The second method for the hydrolysis of polyglutamates is to inactivate all cellular enzymes to fix the folate pattern and to add a purified PPH preparation [7,11,13,14,20]. This method minimizes the possible interconversions between different folacins described and was therefore chosen by us (Fig. 1).

Our comparative studies in which the pteroylpolyglutamates were hydrolysed by incubating the homogenized tissue for 60 min led to a different folate pattern compared with the use of a purified PPH (Table III). This emphasizes that the first technique produces artefacts. To prevent such faults the tissue must therefore be cut only coarsely and must be heated before homogenization. This step is necessary to inactivate the enzymes responsible for changes in the folate pattern and, further, enables the state of 'free folate' to be fixed. The differentiation between 'free folate', *i.e.*, the monoglutamates, and 'total folate', which includes mono- and polyglutamate forms, is of nutritional interest. The bioavailability of folacin monoglutamates is higher than that of the polyglutamates because the latter must be hydrolysed prior to intestinal absorption and they are therefore only partially utilized [27,28].

Pretests revealed that hydrolysis of polyglutamates failed when samples which had been extracted with acetone were incubated, even though the organic solvent had been removed under a stream of nitrogen. We assume that traces of acetone that remained in solution denatured the enzyme.

The experiments with PPH suspension revealed that complete hydrolysis of polyglutamates from cabbage and liver was achieved rapidly. After 30 min no further increase in monoglutamates could be measured. Additional studies in which solutions of several folacins were incubated with the PPH suspension showed that no con-

TABLE III

FOLATE CONTENT ( $\pm$ S.D.) AND FOLATE PATTERN OF RAT LIVER AS DETERMINED BY VARIOUS HPLC PROCEDURES WITH DIFFERENT DETECTION SYSTEMS

Where necessary the original data have been changed to nmol/g liver.

Detection after chromatography	THF (nmol/g)	% <sup>a</sup>	5-CH <sub>3</sub> -THF (nmol/g)	% <sup>a</sup>	CHO-THF <sup>b</sup> (nmol/g)	% <sup>a</sup>	Total (nmol/g)	Ref.
Microbiological assay	11.46 $\pm$ 1.78	42	10.20 $\pm$ 1.71	39	5.64 $\pm$ 1.58	19	27.3	11
Microbiological assay	4.63 $\pm$ 1.39	33	5.12 $\pm$ 1.85	37	4.04 $\pm$ 1.39	30	13.8	14
UV	1.30 $\pm$ 0.39	22	3.53 $\pm$ 1.02	61	0.93 $\pm$ 0.22	17	5.8	20
UV	5.70 $\pm$ 1.00	36	7.34 $\pm$ 1.20	48	2.37 $\pm$ 0.70	16	15.4	29
Fluorimetry	9.64 $\pm$ 0.58	43	5.51 $\pm$ 1.65	25	7.10 $\pm$ 0.53	32	22.3	7
Fluorimetry	3.61 $\pm$ 0.24	29	7.69 $\pm$ 0.60	61	1.27 $\pm$ 0.24	10	12.6	8
Fluorimetry	3.15 $\pm$ 0.43	29	5.21 $\pm$ 0.47	49	2.40 $\pm$ 0.52	22	10.8	This work <sup>c</sup>
Fluorimetry	3.31 $\pm$ 0.37	30	6.24 $\pm$ 0.59	57	1.43 $\pm$ 0.33	13	11.0	This work <sup>d</sup>

<sup>a</sup> Percentage of total folate.

<sup>b</sup> CHO-THF is the sum of 10- and 5-CHO-THF.

<sup>c</sup> Using a purified PPH suspension to hydrolyse the pteroylpolyglutamates.

<sup>d</sup> Incubating the homogenized tissue for 60 min at 37°C for liberating the pteroylpolyglutamates by endogenous PPH.

version of the substrate to other metabolites occurred within 2 h, thus indicating that the suspension was free from any side activities which might have led to interconversion between several folates.

#### *Analysis of rat liver folates*

Fig. 3 shows a typical chromatogram of rat liver folates. Stop-flow spectra of the sample peaks recorded at the peak maxima were compared with those of standard folates and found to be identical, thus indicating the suitability of the analytical procedure. The small shoulder peak near THF could be discriminated by integration. Table III lists the folate contents determined by our procedure as shown in Fig. 1 in comparison with other data, indicating that our results are within the same range. The internal standards MTX and DCF, which were used to monitor the extraction and chromatography, could be recovered to the extent  $70.5 \pm 4.5\%$  for MTX and  $75.3 \pm 4.2\%$  for DCF. These correspond to the amounts of these two substances that were expected to be recovered: taking into account the mean extraction efficiency for folates under these conditions (77.3%, Table I) and the thermal destruction of DCF and MTX (Table II), it can be calculated that about 70.9% of MTX and 72.9% of DCF should be recovered by the analytical procedure.

Table IV shows the reproducibility of the overall method as determined by fivefold analysis of the same sample, demonstrating that the procedure shows good reproducibility. When interpreting these small variations it should not be overlooked that these discrepancies might even be due to an inhomogeneity of the sample itself, five small pieces of liver having to be analysed separately.

The discrepancies of about 500% between different methods even with the same detection system (Table III) can be attributed to a certain extent to differences in

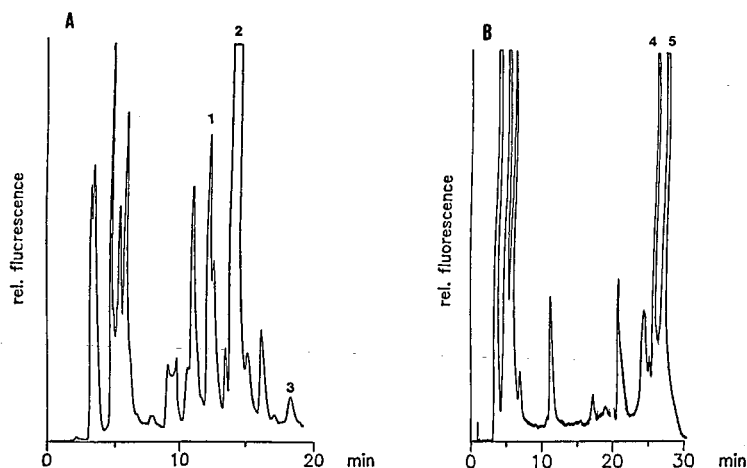


Fig. 3. Typical chromatogram of rat liver folates. Separation conditions as in Fig. 2. Detection: (A) native fluorescence of reduced folates with excitation at 295 nm and emission at 356 nm; (B) fluorescence (excitation at 365 nm, emission at 450 nm) of the products obtained by oxidation of several folates using post-column derivatization with 1% potassium peroxodisulphate. Reagent was pumped in the eluent stream leaving the first detector at a flow-rate of 0.3 ml/min. Peaks: 1 = THF; 2 = 5-CH<sub>3</sub>-THF; 3 = 5-CHO-THF; 4 = MTX; 5 = DCF.

TABLE IV

## PRECISION OF THE WHOLE ANALYTICAL PROCEDURE AS DETERMINED BY FIVEFOLD ANALYSIS OF THE SAME LIVER SAMPLE

Extraction, hydrolysis of pteroylpolyglutamates and HPLC analysis were carried out with five small pieces obtained from one liver. Values given are the means  $\pm$  S.D.

Derivative	Content (nmol/g liver)
THF	3.05 $\pm$ 0.26
5-CH <sub>3</sub> -THF	5.35 $\pm$ 0.23
CHO-THF <sup>a</sup>	2.55 $\pm$ 0.17

<sup>a</sup> CHO-THF is the sum of 10- and 5-CHO-THF.

breed, age and nutritional state of the animals used [7]. However, it should be assumed that they are mostly caused by the analytical procedure itself. Duch *et al.* [20], for example, used a prolonged extraction and sample clean-up procedure which included cation-exchange chromatography, lyophilization and a storage of the samples in buffer of pH 8.3 at 4°C for 3 h, which explains the very low contents that they obtained.

Table III also shows that the folate patterns found by several authors are different. In this context it is interesting to consider the results published previously by Gounelle *et al.* [8], who found only 10% of the whole folate activity in the formyl derivatives. They used a technique to convert 10-formyl-THF to 5-formyl-THF, with subsequent measurement of the latter, and concluded that their results were due to incomplete conversion of the 10- to 5-formyl derivative. The technique of heat conversion that they used was first described by Gregory *et al.* [7], who reported a conversion rate of 99% within 1 h. Therefore, the objections raised by Gounelle *et al.* [8] do not seem to explain this result. On the other hand, the latter group hydrolysed the polyglutamates by incubating the homogenized tissue, which might have led to interconversions such as we observed when applying the same technique. This supports the view that only purified PPH suspensions should be used in folacin analysis.

## ACKNOWLEDGEMENTS

These investigations were sponsored by the Deutsche Forschungsgemeinschaft (Re 437/5-2). The authors are grateful to Professor Dr. E. L. Sattler for giving them the opportunity to work in the laboratories of the Radiation Centre (Central Department) of the Justus Liebig University, Giessen.

## REFERENCES

- 1 A. Hahn, J. Stein, U. Rump and G. Rehner, *J. Chromatogr.*, 540 (1991) 207.
- 2 A. Hahn and G. Rehner, *Ernähr.-Umsch.*, 37 (1990) 356.
- 3 B. A. Allen and R. A. Newman, *J. Chromatogr.*, 190 (1980) 241.
- 4 S. D. Wilson and D. W. Horne, *Proc. Natl. Acad. Sci. U.S.A.*, 80 (1983) 6500.
- 5 S. K. Chapman, B. C. Greene and R. R. Streiff, *J. Chromatogr.*, 145 (1978) 302.
- 6 B. P. Day and J. F. Gregory, *J. Agric. Food Chem.*, 29 (1981) 374.
- 7 J. F. Gregory III, D. B. Sartain and B. P. F. Day, *J. Nutr.*, 114 (1984) 341.

- 8 J.-C. Gounelle, H. Ladjimi and P. Progmom, *Anal. Biochem.*, 176 (1989) 406.
- 9 M. Kohashi, K. Inoue, H. Sotobayashi and K. Iwai, *J. Chromatogr.*, 382 (1986) 303.
- 10 C. K. Clifford and A. J. Clifford, *J. Assoc. Off. Anal. Chem.*, 69 (1977) 1248.
- 11 K. E. McMartin, V. Virayotha and T. R. Tephly, *Arch. Biochem. Biophys.*, 209 (1981) 127.
- 12 L. S. Reed and M. C. Archer, *J. Chromatogr.*, 121 (1976) 100.
- 13 S. A. Kashani and B. A. Cooper, *Anal. Biochem.*, 146 (1985) 40.
- 14 S. D. Wilson and D. W. Horne, *Anal. Biochem.*, 142 (1984) 529.
- 15 J. M. Scott and D. G. Weir, *Clin. Haematol.*, 5 (1976) 547.
- 16 C. Wegner, M. Trotz and H. Nau, *J. Chromatogr.*, 378 (1986) 55.
- 17 J. Lankelma, E. van der Klein and M. J. T. Lansens, *J. Chromatogr.*, 182 (1980) 35.
- 18 R. L. Kisliuk, *Mol. Cell. Biochem.*, 39 (1981) 331.
- 19 C. L. Krumdieck, T. Tamura and J. Eto, *Vitam. Horm. (N.Y.)*, 40 (1983) 45.
- 20 D. S. Duch, S. W. Seaton and C. A. Nichol, *Anal. Biochem.*, 130 (1983) 385.
- 21 T. H. Wilson and G. Wiseman, *J. Physiol.*, 123 (1954) 106.
- 22 T. Brody, J. E. Watson and E. L. R. Stokstad, *Biochemistry*, 21 (1982) 276.
- 23 J. F. Gregory, *Food Technol.*, 13 (1983) 75.
- 24 A. Hahn, *Zum Mechanismus der intestinalen Aufnahme von Pteroylmonoglutaminsäure*, Wissenschaftlicher Fachverlag, Giessen, 1990.
- 25 R. L. Blakley, *The Biochemistry of Folic Acid and Related Pteridines*, Elsevier/North-Holland, Amsterdam, 1969.
- 26 J. D. O'Broin, I. J. Temperley, J. P. Brown and J. M. Scott, *Am. J. Clin. Nutr.*, 28 (1975) 438.
- 27 T. Tamura and E. L. R. Stokstad, *Br. J. Haematol.*, 25 (1973) 513.
- 28 C. M. Baugh, C. L. Krumdieck, H. J. Baker and C. E. Butterworth, *J. Clin. Invest.*, 50 (1971) 2009.
- 29 T. Rebello, *Anal. Biochem.*, 166 (1987) 55.

## Optimization of chromatographic selectivity of twelve sulphonamides in reversed-phase high-performance liquid chromatography using mixture designs and multi-criteria decision making

J. WIELING\*, J. SCHEPERS, J. HEMPENIUS, C. K. MENSINK and J. H. G. JONKMAN

*Pharma Bio-Research International B.V., P.O. Box 147, NL-9400 AC Assen (The Netherlands)*

(First received October 3rd, 1990; revised manuscript received January 22nd, 1991)

---

### ABSTRACT

For the optimization of the reversed-phase high-performance liquid chromatographic separation of twelve sulphonamides using a quaternary mobile phase, quadratic regression models were calculated. The three pseudo-components were buffer–methanol, buffer–acetonitrile and buffer–tetrahydrofuran and had identical solvent strengths. The capacity factors of the sulphonamides were determined at ten mobile phase compositions. The calculated regression models were used to optimize the resolution of the mobile phase and to simulate a chromatogram under optimum mobile phase conditions. The simulated optimum separation showed great similarity with a chromatogram measured under optimum conditions.

---

### INTRODUCTION

Reversed-phase high-performance liquid chromatography (RP-HPLC) is probably the most frequently utilized method in chromatography. Several structurally related compounds in a sample may be separated by the high selectivity of RP-HPLC. The most difficult part of the separation of multi-solute samples is finding the optimum experimental conditions for the separation. Mobile phase optimization is the most commonly utilized method.

By application of chemometric techniques, optimization by trial and error can be avoided and optima will (often) be reached faster. Criteria to be optimized are mostly the capacity factor of the last-eluting solute and the separation power (resolution or selectivity) of the system. The capacity factor of the last-eluting solute ( $k'_{\max}$ ) should be minimized and the separation power (here expressed by the resolution  $R_{i,j}$  [1]) should be maximized ( $R_{s_{\min}}$ ).  $R_{s_{\min}}$  is the resolution of the worst-separated pair of peaks in a chromatogram. Similarly, it is possible to calculate the minimum selectivity  $\alpha_{\min}$  of a chromatogram. However, when calculating the selectivity  $\alpha_{i,j}$  of two solutes  $i$  and  $j$ , the influence of the capacity factor on the separation is not taken into account: higher capacity factors of two solutes  $i$  and  $j$  may result in equal  $\alpha_{i,j}$  values (*i.e.*, the quality of the chromatogram due to this criterion remains constant), whereas the resolution  $R_{i,j}$

decreases (*i.e.*, the quality of the chromatogram decreases owing to this criterion, which is actually the case, as bands broaden as a result of increasing capacity factors). We prefer minimum resolution  $R_{s,\min}$  to the minimum selectivity  $\alpha_{\min}$ , as the former corrects for band broadening.

Schoenmakers [2] introduced the “calibrated normalized resolution product” (CNRP), which is the product of the separation factor of each peak pair ( $2R_{i,j}$  for one plate) divided by the mean separation factor. Chromatograms in which all peaks are equally spaced give optimum values for CNRP. This criterion has the disadvantage of not being specific; it is a relative criterion (relative to the mean of the separation factors), whereas the resolution is an absolute criterion.

Glajch *et al.* [3] combined a mixture design statistical technique and the solvent strength and selectivity theory of Rohrschneider [4] and Snyder [5,6] to obtain a systematic method for optimizing the mobile phase composition in RP-HPLC, which they called “overlapping resolution mapping” (ORM). This ORM technique has been modified since then and adapted to new approaches of mobile phase optimization [7,8].

A recent paper [9] discussed the theory of application of mixture experimental design techniques and criteria used in mobile phase optimizations. Previous papers showed a quadratic effect of mobile phase composition on retention behaviour [9–11]. An equation was given to describe the retention behaviour of one solute in a quaternary system. The quadratic equation for one solute in a ternary system is

$$\ln k' = a_1x_1 + a_2x_2 + a_3x_3 + a_{12}x_1x_2 + a_{13}x_1x_3 + a_{23}x_2x_3 + e \quad (1)$$

In special cubic models an additional term is used ( $a_{123}x_1x_2x_3$ ). Three variables represent the composition of a mobile phase; they are introduced here as  $x_1$ ,  $x_2$  and  $x_3$  and represent the fractions of the (pseudo-)components in the mobile phase.  $a_1$ – $a_{123}$  are the regression coefficients to be estimated. The residual error is given by  $e$ . For estimation of the quadratic model at least seven (six coefficients plus an error term) experiments (design points) are needed; the special cubic model requires eight experiments.

The experiments to be carried out are planned previously according to some experimental design. The experimental results are collected and then any response criterion selected can be modelled. These methods of data processing are called simultaneous optimization methods. The experiments of such simultaneous methods have to be carried out at random.

For future research concerning studies on liquid–liquid extraction of sulphonamides with determination by HPLC, a mobile phase composition had to be selected that separates the sulphonamides within an acceptable period of time and with acceptable resolution. This paper discusses the simultaneous optimization of the separation of a mixture of twelve sulphonamides using mobile phase selectivity optimization in an isoelutropic RP-HPLC system with mixture design statistical techniques and “multi-criteria decision making” (MCDM). Criteria used for selecting an optimum mobile phase are the capacity factor and the resolution.



## EXPERIMENTAL

*Instruments and instrumental conditions*

The assay was performed with an HPLC system consisting of a Spectra-Physics (San Jose, CA, U.S.A.) Model SP8700 solvent delivery system used at a flow-rate of 1.0 ml min<sup>-1</sup> and a Kratos (Ramsey, NJ, U.S.A.) Model 757 UV detector, wavelength 260 nm, range 0.005 a.u.f.s., rise time 1 s.

Injections of sulphonamide standard solutions into a Zymark (Hopkinton, MA, U.S.A.) Z 310 HPLC injection station, equipped with an electrically controlled Rheodyne valve and a 20- $\mu$ l sample loop, were performed by a Zymate II robot system. A Zymark Z 310 analytical instrument interface was used to control the HPLC injection station. The analytical column was a 100  $\times$  4.6 mm I.D. Microsphere 3- $\mu$ m C<sub>18</sub> cartridge system (Chrompack, Middelburg, The Netherlands). Data analysis was performed by means of a Spectra-Physics Chromjet SP4400 computing integrator.

Calculations were performed on an IBM PS/2 Model 60 computer using the POEM (predicting optimum eluent mixtures) software package written in Pascal [9]. This package calculates mixture models using multiple linear regression, performs validation of the models by ANOVA for judging descriptive capability, and cross-validation ("leave one out method", LOOM) to give a mean predicted error sum of squares (mPRESS [12]):

$$\text{mPRESS} = \frac{1}{n} \sum_i^n (y_i - \hat{y}_{(i)})^2$$

where  $n$  is the number of observations,  $\hat{y}_{(i)}$  represents the predicted value of the  $i$ th observation with the use of a model in which the  $i$ th observation is not incorporated and  $y_i$  is the experimental value of the  $i$ th observation. With mPRESS the predictive power of a model can be judged.

*Chemicals and reagents*

Twelve sulphonamides were supplied by Sigma (St. Louis, MO, U.S.A.): sulphacetamide (AC), sulphamethoxazole (OX), sulphamethizole (MT), phthalyl-sulphacetamide (PT), sulphisomidine (SO), sulphathiazole (TH), sulphapyridine (PY), sulphamerazine (ME), sulphamethoxypyridazine (MP), sulphachloropyridazine (CP), sulphaguanidine (GU) and sulphanilamide (AN). Acetonitrile (ACN), tetrahydrofuran (THF) and methanol were supplied by Labscan (Dublin, Ireland) and were of HPLC grade. Acetic acid (100%) (HA<sub>c</sub>), triethylamine (TEA), phosphoric acid (85%) (H<sub>3</sub>PO<sub>4</sub>) and potassium dihydrogenphosphate (KH<sub>2</sub>PO<sub>4</sub>) were all of analytical-reagent grade and supplied by Merck (Darmstadt, Germany). Water was purified by using Milli-RO-15 and Milli-Q water purification systems (Millipore, Bedford, MA, U.S.A.). Unless stated otherwise, water of Milli-Q quality was used.

A phosphate buffer (pH 3.0; 0.05 M) was prepared by dissolving 6.80 g of KH<sub>2</sub>PO<sub>4</sub> in 1000 ml of water. The pH was adjusted at 3.0 using concentrated phosphoric acid. To this buffer 4.15 ml of TEA and 10 ml of acetic acid were added. This buffer was used to prepare binary mobile phases with an organic modifier. Before use, the mobile phases were filtered through a Millipore Type HVLP filter (0.45  $\mu$ m) and degassed before use by ultrasonification for 15 min.

Stock solutions of sulphonamides were prepared by dissolving 100 mg of the compounds in 100 ml of methanol to give concentrations of 1000.0 mg l<sup>-1</sup>. These solutions were stored at +4°C.

A test solution was prepared containing all twelve sulphonamides. The concentration of each sulphonamide was 500 µg l<sup>-1</sup>. This solution was used to select solvent strength and to compare predicted and measured chromatograms. The solution was stored at +4°C.

### Peak identification

As different mobile phases with different organic modifiers may cause changes in elution order, peak identification was necessary. Separate injection of all sulphonamide standard solutions in each mobile phase is very time consuming. A method was selected for the separate identification of the components after injection of a mixture of solutes.

Snyder *et al.* [13] recommended a number of methods of peak tracking. Some of these methods require diode-array detectors or detection at two wavelengths. Other techniques use two samples in which each solute has a different concentration. Peak-height or peak-area ratios for a given compound are then predictable. They are equal to the concentration ratio in each sample.

We divided the twelve sulphonamides into four groups. Within each group, concentrations of sulphonamides in the standard solutions were made such that peak areas had a ratio of 1:2:4:8. Even if two or more solutes overlap each other completely in the chromatogram, a unique new peak area is measured. Table I gives the different sulphonamide mixtures and their concentrations.

### Optimization of solvent strength

The suitable solvent strength was determined by eluting a test mixture containing all solutes in mobile phases with different fractions of ACN in phosphate

TABLE I  
TEST MIXTURES FOR PEAK IDENTIFICATION

Test mixture	Component	Peak area	Stock solution in 100 ml (µl)
1	Sulphisomide	15 000	22
	Sulphapyridine	60 000	85
2	Sulphaguanidine	15 000	16
	Sulphacetamide	30 000	50
	Sulphathiazole	60 000	90
3	Sulphamerazine	15 000	30
	Sulphanilamide	30 000	52
	Sulphamethizole	60 000	110
4	Sulphamethoxypyridazine	7500	10
	Sulphachloropyridazine	15 000	30
	Phthalylsulphacetamide	30 000	68
	Sulphamethoxazole	60 000	110

buffer. A suitable fraction of ACN in buffer (*i.e.*, a mixture of ACN in buffer in which the capacity factors of the solutes eluted satisfy the restriction  $1 \leq k' \leq 10$ ) can be read from a plot of the logarithm of the capacity factor of the first- and last-eluting solute *versus* the fraction of ACN. Binary mixtures of buffer and methanol or buffer and THF with equal solvent strength to maintain roughly equal capacity factors can be calculated using the nomograph of Snyder *et al.* [13]. This nomograph is an approximation and was adapted from empirical data of Schoenmakers *et al.* [14,15]. The three pseudo-components obtained ( $x_1$ ,  $x_2$  and  $x_3$ ) can be placed at the vertices in a mixture triangle (Fig. 1). All mixtures of  $x_1$ ,  $x_2$  and  $x_3$  result in equal solvent strengths (isoeluotropic plane) and (theoretically) equal maximum analysis times.

### Experimental design

Design points have to be distributed evenly in the factor space  $x_1$ ,  $x_2$  and  $x_3$ . Eight design points suffice to investigate both quadratic and special cubic models. However, we decided to create some extra degrees of freedom for an intensive evaluation of the models; in this investigation ten design points were measured. Fig. 2 illustrates the design points used. Corresponding fractions of  $x_1$ ,  $x_2$  and  $x_3$ , buffer, ACN, methanol and THF are given in Table II. Experiments 4, 5, 6, 7 and 8 were repeated to investigate system reproducibility.

## RESULTS AND DISCUSSION

### Optimization of solvent strength

The first-eluting solute in the test mixture was sulphaguanidine in mixtures of 2%, 5% and 10% ACN in buffer. With mobile phases compositions of 2% and 5% ACN in buffer, the analysis time for the last-eluting solute, sulphamethoxazole, was very long. For this reason, this solute was introduced into mobile phases with 10%, 15% and 20% ACN, respectively.

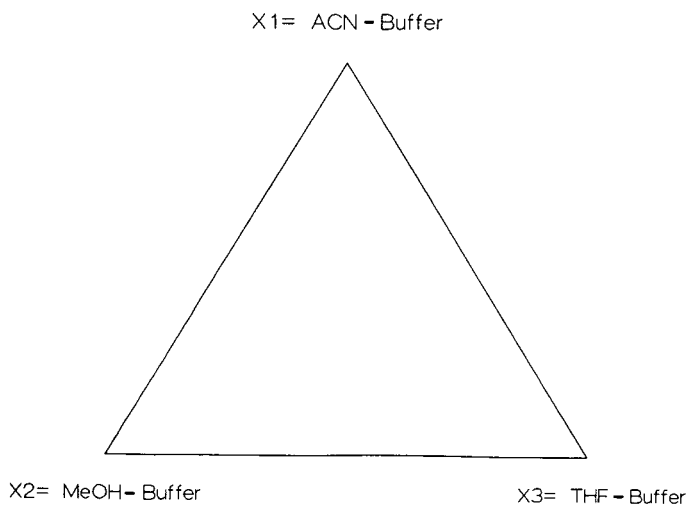


Fig. 1. Isoeluotropic mixture triangle with three pseudo-components of buffer with ACN, methanol (MeOH) and THF.

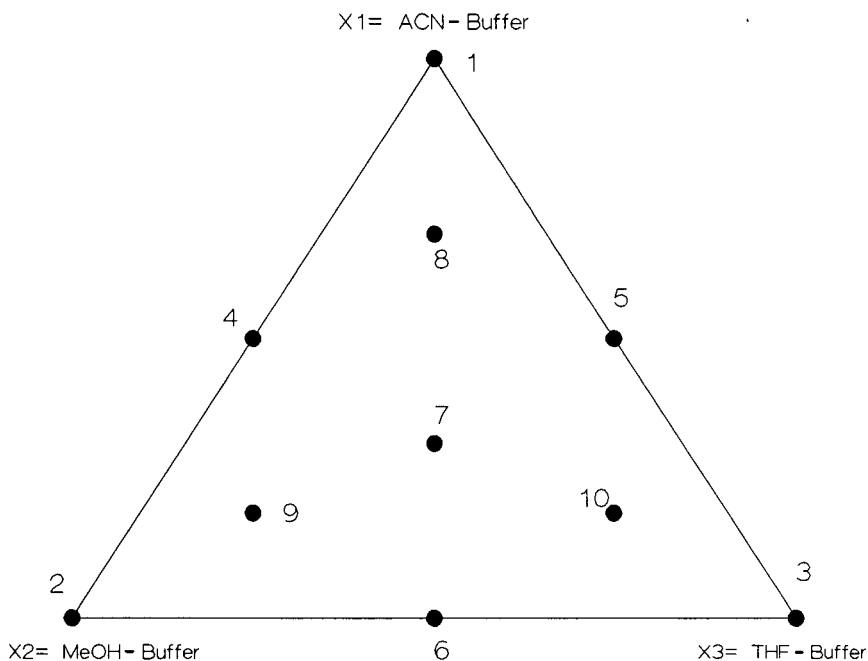


Fig. 2. Experimental design for the optimization of the separation of the twelve sulphonamides. For corresponding fractions of the solvents, see Table II.

The dead time of the HPLC system was determined to be 65 s and the plate number of the column was 6300. The results of the determination of the isoelectrotopropic HPLC system are given in Table III. In Fig. 3, a plot of the logarithm of the capacity factor *versus* the fraction of ACN leads to a buffer-ACN mixture where  $k'$  varies from *ca.* 1 to 10. A mixture of 10% ACN in buffer gives the best compromise for this restriction. With this mobile phase composition, the capacity factors of the sulphon-

TABLE II  
EXPERIMENTAL DESIGN FOR THE SEPARATION OF TWELVE SULPHONAMIDES

No.	Pseudo-component fractions			Solvent fractions			
	$x_1$	$x_2$	$x_3$	Buffer	ACN	Methanol	THF
1	1.0000	0.0000	0.0000	0.9000	0.1000	0.0000	0.0000
2	0.0000	1.0000	0.0000	0.8500	0.0000	0.1500	0.0000
3	0.0000	0.0000	1.0000	0.9200	0.0000	0.0000	0.0800
4	0.5000	0.5000	0.0000	0.8750	0.0500	0.0750	0.0000
5	0.5000	0.0000	0.5000	0.9100	0.0500	0.0000	0.0400
6	0.0000	0.5000	0.5000	0.8850	0.0000	0.0750	0.0400
7	0.3333	0.3333	0.3333	0.8900	0.0333	0.0500	0.0267
8	0.6667	0.1667	0.1667	0.8950	0.0667	0.0250	0.0133
9	0.1667	0.6667	0.1667	0.8700	0.0167	0.1000	0.0133
10	0.1667	0.1667	0.6667	0.9050	0.0167	0.0250	0.0533

TABLE III

ANALYSIS TIMES AND CAPACITY FACTORS OF THE FIRST-ELUTING (SULPHAGUANIDINE) AND LAST-ELUTING (SULPHAMETHOXAZOLE) SOLUTES

Parameter	Sulphaguanidine			Sulphamethoxazole		
	2% ACN	5% ACN	10% ACN	10% ACN	15% ACN	20% ACN
$t_r$	127	106	86	868	565	320
$k'$	0.95	0.63	0.32	12.35	7.69	3.92
Log $k'$	-0.02	-0.20	-0.50	1.09	0.89	0.59

amides vary from 0.32 to 12.4. Corresponding proportions of methanol and THF were 15% and 8%, respectively.

#### Optimization of solvent selectivity

Retention times of the twelve sulphonamides were determined and capacity factors were calculated for every design point. Table IV gives the capacity factors of all solutes in the mobile phase system used. The data demonstrate that the transfer rules of the solvent strength theory do not guarantee a constant analysis time. Binary mixtures

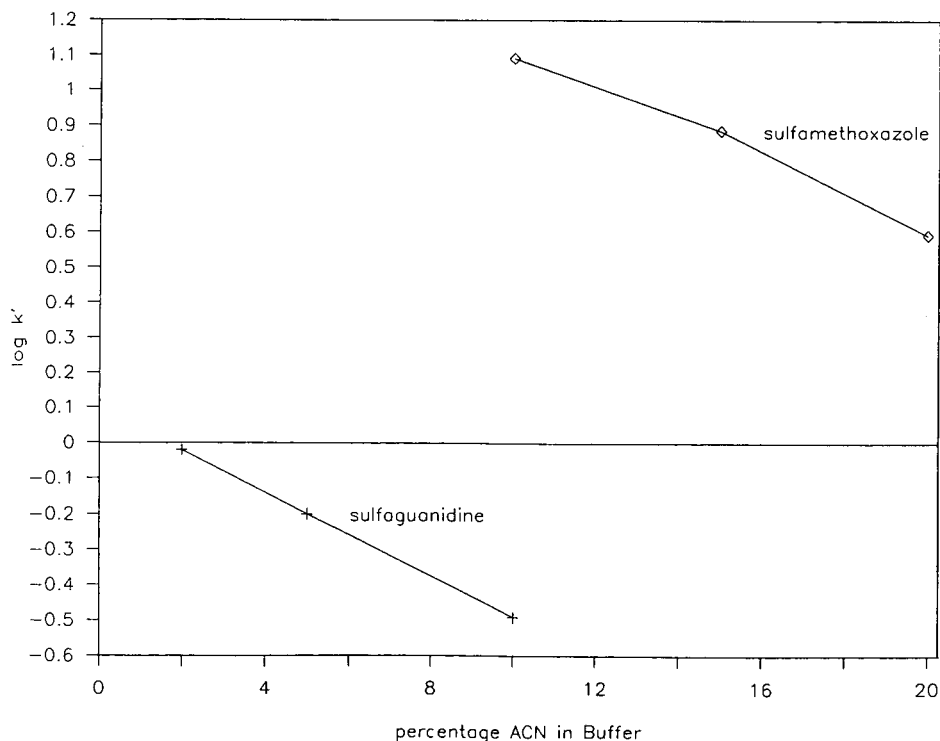


Fig. 3. Determination of the isoeutropic HPLC system. Sulphaguanidine and sulphamethoxazole were used to determine the suitable solvent strength.

TABLE IV  
MEASURED CAPACITY FACTORS OF TWELVE SULPHONAMIDES WITH TEN DIFFERENT MOBILE PHASE COMPOSITIONS

No.	Capacity factor ( $k'$ ) <sup>a</sup>										CP					
	Mobile phase fraction of															
	Buffer	ACN	Methanol	THF	GU	SO	AC	TH	PY	ME	AN	MT	MP	PT	OX	
1	0.900	0.100	0.000	0.000	0.37	1.48	1.58	3.14	3.35	3.80	5.49	6.95	7.58	13.77	15.14	11.09
2	0.850	0.000	0.150	0.000	0.23	1.83	1.03	2.45	2.87	3.45	5.69	6.06	7.75	17.08	10.09	8.62
3	0.920	0.000	0.000	0.080	0.20	0.72	1.28	1.63	1.63	2.05	2.28	3.32	3.08	7.55	11.55	8.92
4	0.875	0.050	0.075	0.000	0.29	1.77	1.35	3.00	3.34	3.83	6.03	7.11	8.31	17.98	13.52	10.62
5	0.910	0.050	0.000	0.040	0.18	0.77	1.14	1.74	1.74	2.15	1.89	3.62	3.62	6.46	10.17	7.31
6	0.885	0.000	0.075	0.040	0.23	0.92	1.25	1.83	1.83	2.18	1.83	3.80	3.80	9.22	10.51	8.08
7	0.890	0.033	0.050	0.027	0.22	0.95	1.17	1.88	1.95	2.34	2.34	4.14	4.14	9.06	10.20	7.77
8	0.895	0.067	0.025	0.013	0.26	1.14	1.34	2.49	2.49	2.94	3.51	5.45	5.60	11.86	12.72	10.43
9	0.870	0.017	0.100	0.013	0.18	1.06	1.06	1.88	2.02	2.37	2.82	4.29	7.46	10.86	9.55	7.46
10	0.905	0.017	0.025	0.053	0.18	0.74	1.17	1.63	1.63	2.05	1.51	3.37	3.25	7.48	10.23	7.80

<sup>a</sup> For abbreviations, see *Chemicals and reagents*.

of methanol in buffer and THF in buffer with presumed isoelutotropic compositions as compared with 10% ACN in buffer resulted in other  $k'$  ranges:  $k'_{\max}$  varies from 10.2 to 18.0. For our application this was of minor importance, as in the MCDM procedure it is possible to minimize  $k'_{\max}$  simultaneously with maximizing  $R_{s_{\min}}$ .

The reproducibility of the HPLC system under the conditions examined was acceptable. The mean relative standard deviation (R.S.D.), of the capacity factors for replicate design points was 1.4%. The logarithm of the capacity factor is modelled as a function of mobile phase compositions for both quadratic and special cubic models. Table V gives the statistical evaluation of both models. The values are averages for the twelve solutes. The R.S.D. of the difference between model-predicted and measured values ( $RSD_{(j-y)}$ ) was little better for the quadratic model. Although the special cubic model explains more variations of the data than the quadratic model, the descriptive power of the quadratic model is better with respect to the adjusted correlation coefficient. The adjusted correlation coefficient is the multiple correlation coefficient  $R^2$  corrected for the number of model coefficients. In this way, the descriptive power of different model types can be compared. The mPRESS value of the quadratic model was approximately 63% of that of the special cubic model. This indicates that the predictive power of the quadratic model is also better. The mPRESS value of sulphamethoxypyridazine was about 50% worse than those of the other solutes.

It was concluded that the quadratic model was the best model to use for the prediction of optimum mobile phase compositions for the separation of these twelve sulphonamides. The model coefficients of the quadratic models of the twelve solutes were used to calculate a minimum resolution plot: for every mobile phase composition (in steps of 1% of the mixture components) in the factor space a minimum resolution is calculated. This is the resolution of the worst-separated solute pair. This minimum resolution plot is given in Fig. 4.

Although the maximum capacity factor for every mobile phase composition should be about constant as a result of the solvent strength optimization, a  $k'_{\max}$  plot (Fig. 5) demonstrates that this assumption is not completely correct. Both measured and predicted values of  $k'_{\max}$  vary from 9.5 to 18.0. This variation is a result of the fact that the solvent strength theory of Snyder is an approximation, as stated before.

Although it is not typical to optimize both the minimum (min)  $k'_{\max}$  and maximum (max)  $R_{s_{\min}}$  in isoelutotropic ternary mobile phase systems we performed MCDM [9, 16], in which min- $k'_{\max}$  and max- $R_{s_{\min}}$  were weighed against each other. Fig. 6 gives an MCDM plot of  $R_{s_{\min}}$  versus  $k'_{\max}$ . A mixture composition of 1%  $x_1$ , 93%  $x_2$  and 6%  $x_3$  corresponding to an  $R_{s_{\min}}$  of 1.8 and a  $k'_{\max}$  of 14.8 (analysis time 17 min) was chosen as the optimum mobile phase composition. A chromatogram was simulated

TABLE V

STATISTICAL EVALUATION (MEAN VALUES) OF QUADRATIC AND SPECIAL CUBIC MODELS FOR TWELVE SULPHONAMIDES

Model	Explained variation (%)	$R^2_{\text{adjusted}}$	R.S.D. (%) ( $j-y$ )	mPRESS
Quadratic	94.81	0.8915	8.29	0.0538
Special cubic	95.94	0.8781	8.50	0.0847

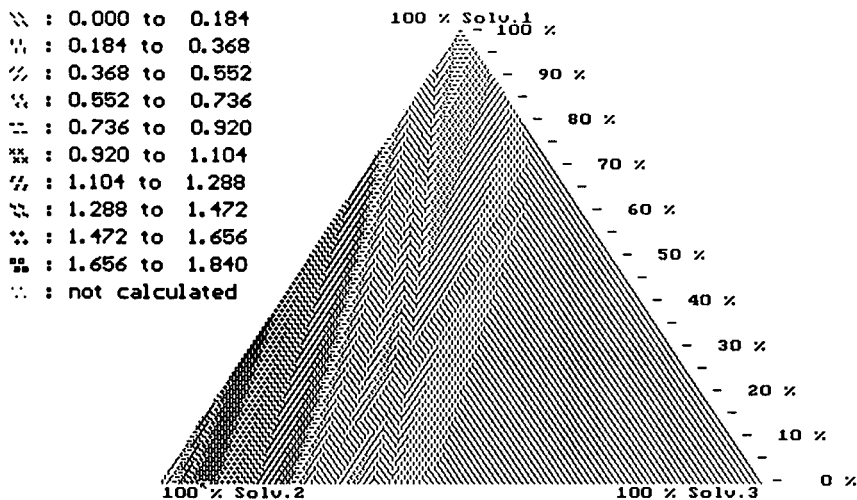


Fig. 4. Minimum resolution plot of the optimization of the separation of the twelve sulphonamides in the ternary isoelutropic HPLC system.

with this mobile phase with the regression coefficients of the quadratic models (Fig. 7). A  $\max-R_{s\min}$  of 1.8 and a  $\min-k'_{\max}$  of 14.8 were predicted under these conditions. The measured chromatogram with the same mobile phase conditions (Fig. 8) showed great similarity with the predicted chromatogram. Table VI gives measured and predicted retention times for all the sulphonamides. The retention times in the measured chromatogram are slightly shorter (0–8%) compared with the simulated chromatogram, with only sulphamethoxypyridazine having a large deviation (18.4%). This

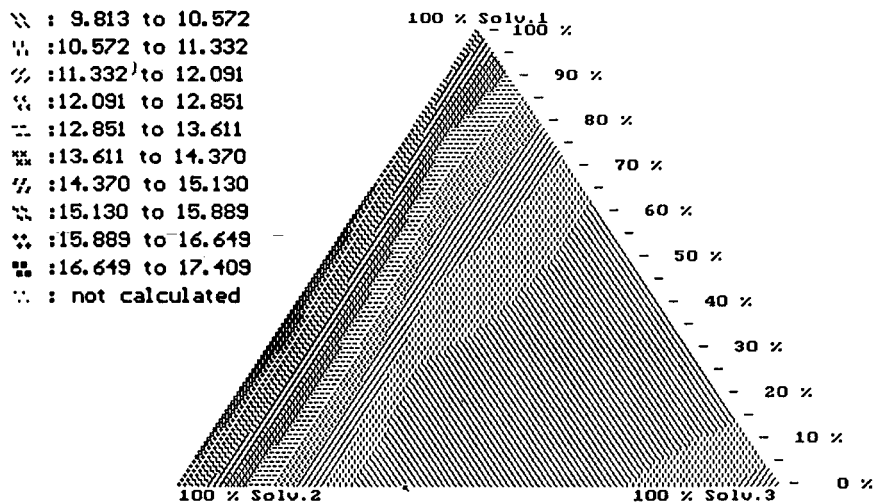


Fig. 5. Maximum capacity factor plot of the optimization of the separation of the twelve sulphonamides in the ternary isoelutropic HPLC system.



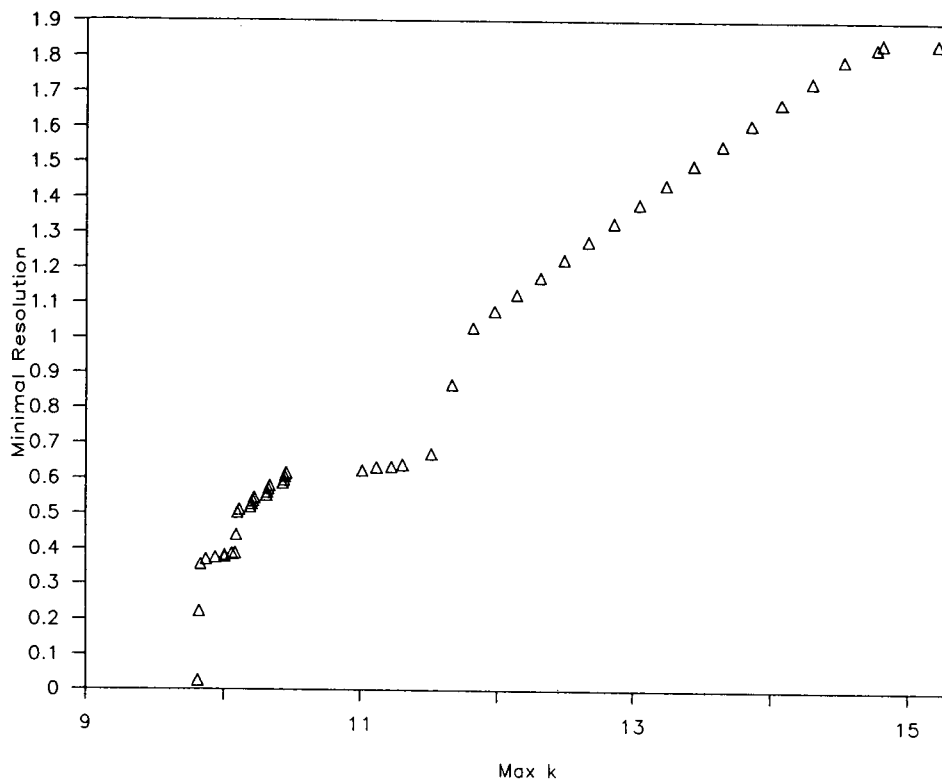


Fig. 6. MCDM plot of the minimum resolution *versus* the maximum capacity factor. Pareto-optimum points are given.

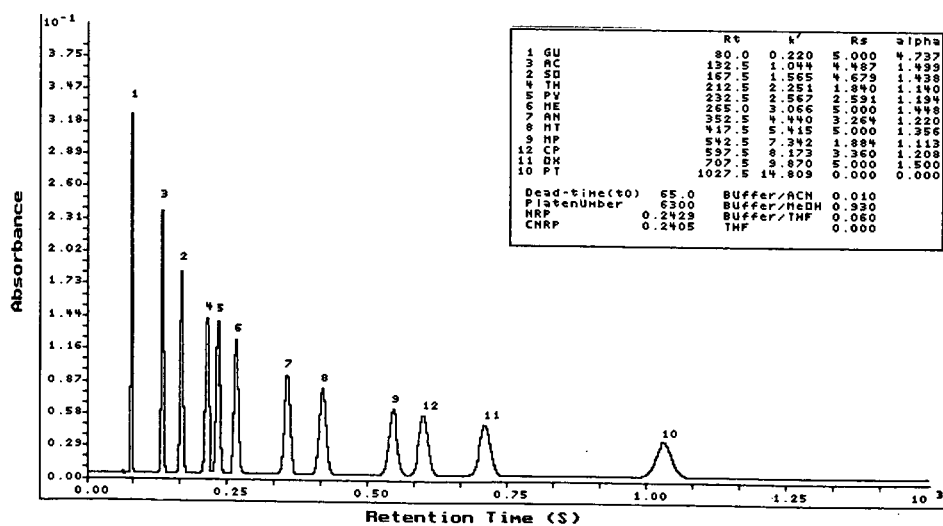


Fig. 7. Predicted chromatogram with the optimum mobile phase composition (1%  $x_1$ , 93%  $x_2$  and 6%  $x_3$ ). Data are given in Table VI.  $N = 6300$ ;  $t_0 = 65$  s. Rt = Retention time.

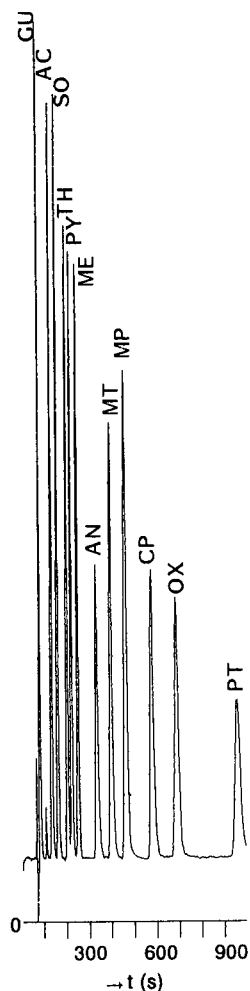


Fig. 8. Measured chromatogram with the optimum mobile phase composition (1%  $x_1$ , 93%  $x_2$  and 6%  $x_3$ ). Data are given in Table VI.

deviation may be due to the fact that the predictive power (expressed by mPRESS) of the model for sulphamethoxypyridazine is low. The peak orders in the simulated and measured chromatograms were the same.

## CONCLUSIONS

Optimization of solvent strength and solvent selectivity for the separation of twelve sulphonamides using isoelectroic eluents in mixture design optimization techniques was performed. It was concluded that the transfer rules of the solvent strength theory do not guarantee a constant analysis time. Isoelectroic mobile phases in accordance with Snyder's theory did not result in equal maximum capacity factors.

TABLE VI

MEASURED AND PREDICTED RETENTION TIMES FOR THE TWELVE SULPHONAMIDES IN THE OPTIMUM MOBILE PHASE COMPOSITION (1%  $x_1$ , 93%  $x_2$  AND 6%  $x_3$ )

Solute <sup>a</sup>	$t_R$ (s)		$\Delta t_R$ (s)	$\Delta t_R$ (%)
	Measured	Predicted		
GU	79	80	1	1.3
AC	132	132.5	0.5	0.4
SO	159	167.5	8.5	5.3
TH	201	212.5	11.5	5.7
PY	220	232.5	12.5	5.7
ME	248	265	17	6.9
AN	330	352	22	6.7
MT	393	417.5	24.5	6.2
MP	458	542.5	84.5	18.4
CP	574	597.5	25.5	4.4
OX	683	707.5	24.5	3.6
PT	952	1027.5	75.5	7.9

<sup>a</sup> For abbreviations, see *Chemicals and reagents*.

The separation of twelve solutes using statistical mobile phase optimization techniques is readily possible from both an analytical point of view (resolution) and an economic point of view (analysis time). The logarithm of the capacity factor was modelled in a ternary pseudo-component mobile phase system. The best predictive and descriptive power can be achieved by fitting quadratic models to these retention data. The quadratic models were used to optimize both maximum capacity factor and resolution and to predict an optimum chromatogram. Predicted and measured chromatograms show great similarity. The analysis time was optimized to 17 min.

The peak orders in the simulated and measured chromatograms were the same. Although the predicted analysis time for one compound had a large deviation from the experimental analysis time, this had no influence on the quality of the final chromatogram.

## ACKNOWLEDGEMENT

The authors thank the Chemometrics Research Group, Department of Analytical Chemistry and Toxicology, University of Groningen, The Netherlands, for using their mobile phase optimization software package POEM.

## REFERENCES

- 1 J. R. Gant, J. W. Dolan and L. R. Snyder, *J. Chromatogr.*, 185 (1979) 153.
- 2 P. J. Schoenmakers, *J. Liq. Chromatogr.*, 10 (1987) 1865.
- 3 J. L. Glajch, J. J. Kirkland, K. M. Squire and J. M. Minor, *J. Chromatogr.*, 199 (1980) 57.
- 4 L. Rohrschneider, *Anal. Chem.*, 45 (1973) 1241.
- 5 L. R. Snyder, *J. Chromatogr.*, 92 (1974) 223.
- 6 L. R. Snyder, *J. Chromatogr. Sci.*, 16 (1978) 223.
- 7 P. J. Schoenmakers, A. J. H. C. Drouen, H. A. H. Billiet and L. de Galan, *Chromatographia*, 15 (1982) 688.

- 8 J. W. Weyland, C. H. P. Bruins and D. A. Doornbos, *J. Chromatogr. Sci.*, 22 (1984) 31.
- 9 P. M. J. Coenegracht, A. K. Smilde, H. J. Metting and D. A. Doornbos, *J. Chromatogr.*, 485 (1989) 195.
- 10 R. Tijssen, H. A. H. Billiet and P. Schoenmakers, *J. Chromatogr.*, 122 (1976) 185-203.
- 11 J. W. Weyland, *Thesis*, State University Groningen, Groningen, 1986.
- 12 D. W. Osten, *J. Chemometr.*, 2 (1988) 39.
- 13 L. R. Snyder, J. L. Glajch and J. J. Kirkland, *Practical HPLC Method Development*, Wiley, New York, 1988, p. 32.
- 14 P. J. Schoenmakers, H. A. H. Billiet and L. de Galan, *J. Chromatogr.*, 185 (1979) 179.
- 15 P. J. Schoenmakers, H. A. H. Billiet and L. de Galan, *J. Chromatogr.*, 218 (1981) 259.
- 16 A. K. Smilde, A. Knevelman, P. M. J. Coenegracht, *J. Chromatogr.*, 369 (1986) 1.

CHROM. 23 107

## Separation and estimation of small amounts of the enantiomers of carbidopa and methyldopa on a chiral stationary phase with L-phenylalanine as selector in ligand-exchange chromatography

B. LAUSECKER\*\*<sup>a</sup>

*Central Institute of Organic Chemistry, Department of Central Analytics, Rudower Chaussee 5, O-1199 Berlin (Germany)*

and

F.-M. ALBERT

*ISIS-Chemie GmbH, Breithauptstrasse 3–5, O-9541 Zwickau (Germany)*

(First received November 16th, 1990; revised manuscript received January 4th, 1991)

---

### ABSTRACT

The chiral stationary phase with L-phenylalanine as selector was used for the separation of the enantiomers of carbidopa and methyldopa in ligand-exchange chromatography. The influence of pH, organic modifier and copper(II) salt concentration in the eluent on capacity and separation factors has been shown. The applicability of this method to the detection of small amounts of S-methyldopa and R-carbidopa in S-carbidopa has been demonstrated.

---

### INTRODUCTION

S-Carbidopa [(S)-(-)-2-hydrazino-2-(3,4-dihydroxybenzyl)propionic acid] is a drug used in combination with S-DOPA [(S)-(-)-2-amino-3-(3,4-dihydroxyphenyl)propionic acid] for the therapy of Parkinson disease; the S-form of carbidopa is the biologically active one, whereas the R-form is toxic. In the manufacturing process S-methyldopa [(S)-(-)-2-amino-2-(3,4-dihydroxybenzyl)propionic acid] is N-aminated by 3,3-pentamethyleneoxaziridine to give S-carbidopa [1]. If S-methyldopa contains some R-methyldopa or if racemization occurs during the N-amination, R-carbidopa may be produced. Gelber and Neumeyer [2] resolved the enantiomeric carbidopa and methyldopa with L-phenylalanine in the eluent on a C<sub>18</sub> RP column. The disadvantage of this method is the high noise level of the eluent in the detector which is caused by the L-phenylalanine in the eluent. Secondly, impurities of D-phenylalanine in L-phenylalanine may lead to errors in the results of the analysis.

---

<sup>a</sup> Present address: Fa. Hoffmann-La Roche AG, Department of Clinical Kinetics, Grenzacher Strasse, CH-4002 Basle, Switzerland.

In this paper we describe the synthesis of a stationary phase with L-phenylalanine as selector using a procedure similar to the procedure employed by Gübitz *et al.* [3]. The data for the phases are given below. The influence of modifier, copper concentration and pH on the capacity and separation factors of the enantiomeric carbidopa and methylidopa are shown. The sensitivity of this method in the detection of 0.03% *S*-methylidopa and 0.03% *R*-carbidopa in 99.97% *S*-carbidopa has been demonstrated with a precision of 25% for *R*-carbidopa and 29% for *S*-methylidopa when 200  $\mu\text{g}$  of *S*-carbidopa were injected.

## EXPERIMENTAL

The chiral stationary phase was synthesized in a similar fashion to the procedure of Gübitz *et al.* [3].

L-Phenylalanine was converted into the sodium salt with sodium hydroxide. The sodium phenylalanate was dried over phosphorus pentoxide, and an excess of sodium phenylalanate was placed in a flask with a magnetic stirrer and condenser together with (3-glycidoxypropyl)triethoxysilane in absolute ethanol. The reaction was carried out at 76°C for 2 h. The silica gel was dried in vacuum at 130°C for 12 h. The silica gel and the [3-N-(L)-phenylalanine-2-(*R,S*)-hydroxypropyloxypropyl]triethoxysilane together with dry toluene were then placed in a flask with a stirrer and condenser with water separator and boiled until ethanol was no longer separated. After filtration the silica gel was washed with methanol, acetone, water and again with methanol and then dried in vacuum at 65°C for 5 h. Then the silica gel was again suspended in dry toluene and treated with hexamethyldisilazane for 4 h. The silica gel was filtered and washed as described before.

The elemental analysis of the stationary phase is: C = 11.53%, H = 2.02% and N = 0.50%. The surface coverage is 2.04  $\mu\text{mol}/\text{m}^2$  calculated on the basis of the nitrogen value of the elemental analysis. The stationary phase was filled in a stainless-steel column of 300  $\times$  4 mm I.D. The silica gel was therefore suspended in 2-propanol and packed with ethanol.

### Chemicals

L-Phenylalanine was purchased from Reanal (Budapest, Hungary) and hexamethyldisilazane and (3-glycidoxypropyl)triethoxysilane were obtained from Chemiewerk Nünchritz (Nünchritz, Germany); silica gel, obtained from Leuna-Werke (Leuna, Germany), had the following properties: mean particle diameter, 7.6  $\mu\text{m}$ ; surface, 250  $\text{m}^2/\text{g}$ ; spheric particles. Methanol, ethanol and toluene were analytical-grade reagents from Laborchemie Apolda (Apolda, Germany) and dried as usual. *R*-Carbidopa and *S*-carbidopa as well as *R*- and *S*-methylidopa were obtained from ISIS-Chemie (Zwickau, Germany) and had the following properties:

Substance	Molecular rotation, $[\alpha]_{\text{D}}^{20}$	
<i>R</i> -Methylidopa Al 1276	+ 26.35°	$c = 4.4$
<i>R</i> -Carbidopa Al 1278	+ 23.8°	$c = 1$
<i>S</i> -Methylidopa lab. charge	- 26.0°	$c = 4.4$
<i>S</i> -Carbidopa Al 1201	- 24.8°	$c = 1$
<i>S</i> -Carbidopa Al 1279	- 24.86°	$c = 1$
<i>S</i> -Carbidopa 020788	- 24.8°	$c = 1$

All measurements were performed in  $\text{AlCl}_3\text{-H}_2\text{O}$  (19.65:80.35, w/w) and the pH was adjusted to 1.5 with NaOH (corresponding to United States Pharmacopeia XXI).

### Chromatography

The chromatographic system consisted of a Knauer HPLC pump type 64.00, a Knauer injection valve (20  $\mu\text{l}$ ), a Knauer variable-wavelength detector set at 280 nm (Dr. H. Knauer, Wiss. Gerätebau, Bad Homburg, Germany) and a CR 6 A integrator from Shimadzu (Duisburg, Germany), or a liquid chromatographic system had been used consisting of two Knauer high-performance liquid chromatography pumps type 64.00, a 20- $\mu\text{l}$  injection valve (Rheodyne type 7215), a Knauer variable-wavelength detector set at 280 nm, an Epson PC AX2e and Knauer software version 2.2. The eluent consisted of methanol-water with 1 mM  $\text{CuSO}_4$ . The pH value was adjusted with sulphuric acid and measured with an MV 870 digital pH meter (Präcitronic, Dresden, Germany) with a glass electrode vs. Ag/AgCl reference electrode. Solutes were dissolved in 0.1 M HCl. The dead time was determined with 0.1 M HCl.

Due to the peak asymmetry the discussion is based on the separation factor instead of the resolution.

## RESULTS AND DISCUSSION

The chiral stationary phase with L-proline or with L-hydroxyproline as selector is the most common one in ligand-exchange chromatography. All attempts to resolve the enantiomers of carbidopa on this column failed. We varied the pH, the type and amount of organic modifier and the temperature of the chromatographic process. In all cases resolution could not be achieved. Gelber and Neuneyer [2] resolved the enantiomers of carbidopa and methyldopa with L-phenylalanine in the eluent, but not in the same run. While the enantiomers of methyldopa were resolved with methanol-water, those of carbidopa were resolved with 0.1% HCl.

We synthesized a chiral stationary phase with L-phenylalanine as selector similar to the procedure developed by Gübitz *et al.* [3] as described above.

Attempts to resolve the enantiomers of carbidopa with several amounts of acetonitrile as modifier in the eluent did not lead to resolution but with methanol as modifier resolution was achieved. Table I (*R* and *S*-methyldopa) and Table II (*R* and *S*-carbidopa) demonstrate the dependence of the capacity factors  $k'$  and the separation factor  $\alpha$  on the methanol content in the eluent. Further chromatographic conditions are: eluent containing 1 mM  $\text{CuSO}_4$ , pH adjusted to 3.2 with sulphuric acid; temperature, 25°C; flow-rate, 1 ml  $\text{min}^{-1}$ . It is not possible, however, to take more than 70% methanol in the eluent at pH 3.2 as the copper sulphate is insoluble at this concentration. It must be noted that the  $k'$  values and separation factors of enantiomeric carbidopa were more strongly influenced by the increasing amount of methanol than those of enantiomeric methyldopa. In the case of enantiomeric carbidopa good baseline separation was achieved from 30% up to 70% methanol. For enantiomeric methyldopa the separation factor increased up to 1.40 at 65% methanol in the eluent; however, no baseline resolution was achieved. The best compromise between resolution, time consumption and detection limit of small amounts of *R*-carbidopa and *S*-methyldopa seems to be at pH 3.2 with 65% methanol in the eluent. For other chromatographic conditions see above. A typical chromatogram of the

TABLE I

CAPACITY FACTORS ( $k'$ ) AND SEPARATION FACTORS [ $\alpha = k'(S)/k'(R)$ ] OF (*R*)- AND (*S*)-METHYLDOPA VERSUS METHANOL CONTENT IN ELUENT

Methanol content (%)	$k'$		
	<i>R</i> -Methyldopa	<i>S</i> -Methyldopa	$k'(S)/k'(R)$
20	1.23	1.53	1.24
30	1.20	1.50	1.25
40	0.89	1.25	1.40
50	0.90	1.20	1.33
60	0.88	1.19	1.35
65	0.86	1.20	1.40
70	1.80	2.21	1.23

resolution of the enantiomers of carbidopa and methyldopa with 65% methanol in the eluent (other chromatographic conditions as above) is demonstrated in Fig. 1.

The dependence of the capacity and separation factors of enantiomeric methyldopa and enantiomeric carbidopa on the pH value is demonstrated in Tables III and IV. For enantiomeric carbidopa at pH 2.7, baseline separation is achieved and the capacity factors for *R*- and *S*-carbidopa increased up to 6.14 and 13.71, respectively, at pH 3.5, whereas for enantiomeric methyldopa at pH values from 2.7 to 2.9 no separation has been achieved. From pH 3.0 to 3.5 the capacity and the separation factors slightly increased, leading to  $k'$  values of 1.35 and 1.78 for *R*- and *S*-methyldopa, respectively, and to a separation factor of 1.32. The chromatographic conditions for these experiments were 65% methanol and 1 mM CuSO<sub>4</sub>. Using an eluent consisting of 50% methanol with a pH of 4.5 (for other conditions see above) the  $k'$  of the methyldopa enantiomers increased to 3.36 and 5.1 for *R* and *S*, respectively, but the *R*- and *S*-carbidopa became unstable in this pH range and eluted as three identical peaks at  $k'$  ranging from 3.0 to 6.2. Therefore, it is necessary to use an acidic eluent within the pH range 3.0–3.3 to separate both the enantiomers of carbidopa and the enantiomers of methyldopa.

TABLE II

CAPACITY FACTORS ( $k'$ ) AND SEPARATION FACTORS [ $\alpha = k'(S)/k'(R)$ ] OF (*R*)- AND (*S*)-CARBIDOPA VERSUS METHANOL CONTENT IN ELUENT

Methanol content (%)	$k'$		
	<i>R</i> -Carbidopa	<i>S</i> -Carbidopa	$k'(S)/k'(R)$
20	1.60	2.20	1.38
30	1.76	2.80	1.59
40	2.44	4.26	1.75
50	2.43	4.73	1.95
60	2.42	5.83	2.41
65	2.70	6.61	2.45
70	6.33	14.12	2.23



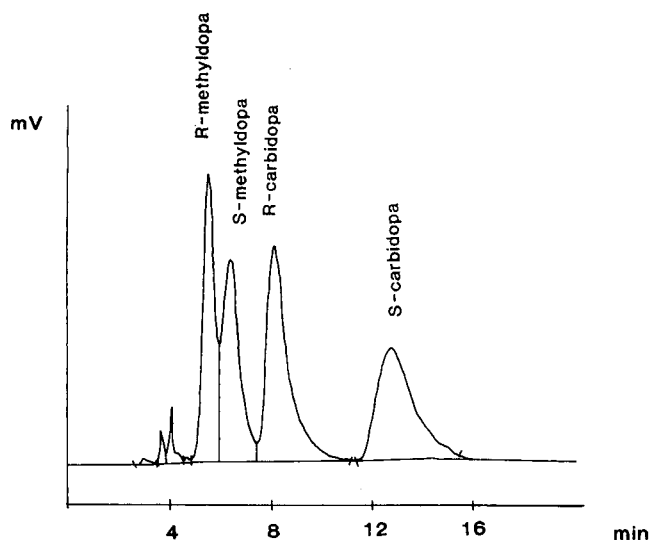


Fig. 1. Separation of the enantiomers of carbidopa and methylidopa. Amounts found: 2.5  $\mu\text{g}$  of *R*-methylidopa, 2.5  $\mu\text{g}$  of *S*-methylidopa, 3  $\mu\text{g}$  of *R*-carbidopa, 3  $\mu\text{g}$  of *S*-carbidopa.

TABLE III

CAPACITY FACTORS ( $k'$ ) AND SEPARATION FACTORS [ $\alpha = k'(S)/k'(R)$ ] OF (*R*)- AND (*S*)-METHYLDOPA VERSUS pH

pH	$k'$		
	<i>R</i> -Methylidopa	<i>S</i> -Methylidopa	$k'(S)/k'(R)$
2.7	0.06	0.06	1.00
2.9	0.21	0.21	1.00
3.1	0.68	0.93	1.37
3.2	0.86	1.20	1.40
3.3	1.16	1.50	1.29
3.5	1.35	1.78	1.32

TABLE IV

CAPACITY FACTORS ( $k'$ ) AND SEPARATION FACTORS [ $\alpha = k'(S)/k'(R)$ ] OF (*R*)- AND (*S*)-CARBIDOPA VERSUS pH

pH	$k'$		
	<i>R</i> -Carbidopa	<i>S</i> -Carbidopa	$k'(S)/k'(R)$
2.7	0.31	0.91	2.94
2.9	0.85	2.00	2.35
3.1	2.86	7.00	2.45
3.2	3.46	7.93	2.29
3.3	4.70	10.65	2.27
3.5	6.14	13.71	2.23

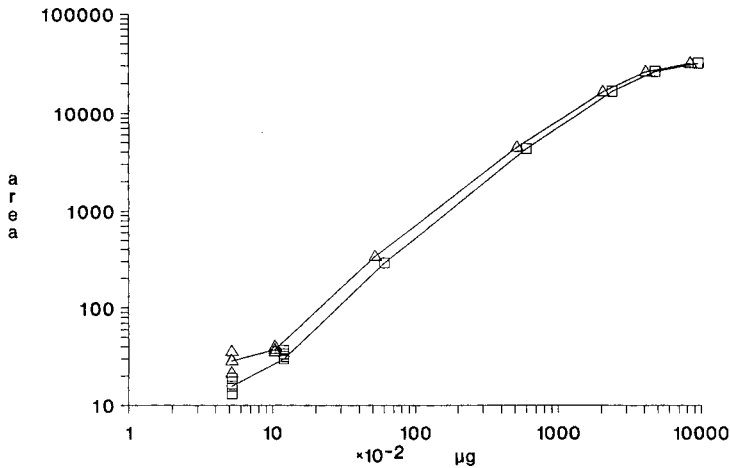


Fig. 2. Calibration curve for the estimation of ( $\Delta$ ) *S*-methyldopa and ( $\square$ ) *R*-carbidopa.

We also investigated the influence of the concentration of copper(II) salt in the eluent on the separation factors. We varied the concentration from 0.01 to 1 mM copper sulphate and found that with 0.01–0.1 mM copper(II) in the eluent (other conditions: methanol–water, 65:35, v/v, pH 3.2, adjusted with sulphuric acid) no resolution of enantiomeric methyldopa was achieved. Enantiomeric carbidopa was slightly resolved with 0.1 mM copper(II). With 0.25 mM copper in the eluent both enantiomers of carbidopa and methyldopa were resolved. We increased the concentration of copper(II) up to 1 mM but the transparency of the eluent decreased drastically so that 0.25 mM seems to be the optimal concentration for the estimation of small amounts.

In Fig. 2 the calibration curve for *S*-methyldopa and *R*-carbidopa in the range 0.05–100  $\mu\text{g}$  is shown. At 50–100  $\mu\text{g}$  the signal is not proportional to the concentra-

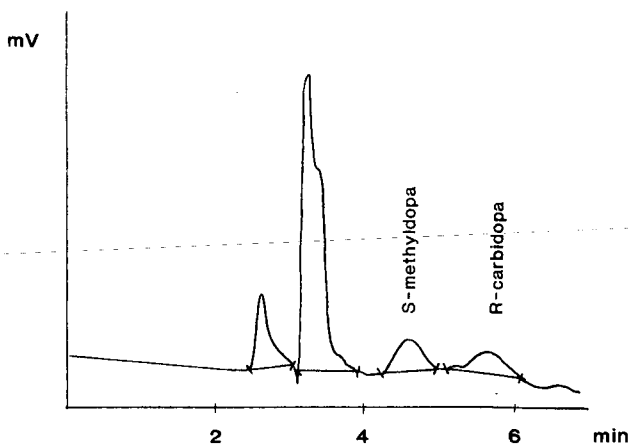


Fig. 3. Separation of 0.103  $\mu\text{g}$  of *S*-methyldopa and 0.1035  $\mu\text{g}$  of *R*-carbidopa.

TABLE V  
S-METHYLDOPA CONTENT IN COMMERCIAL S-CARBIDOPA

Brand of <i>S</i> -carbidopa	Amount injected ( $\mu\text{g}$ )	<i>S</i> -Methylidopa found				
		Area			$\mu\text{g}$	%
		Mean ( $n=4$ )	S.D.	R.S.D. (%)		
AI 1279	203	444.4	26.2	5.9	0.58	0.3
AI 1201	197	31.3	7.6	24.3	0.06	0.03
020788	201	753.1	38.4	5.1	1.0	0.5

tion because of the limited linearity of the detector, and at about  $0.05 \mu\text{g}$  the precision decreased. The standard deviation increased to 25% for *R*-carbidopa and 29% for *S*-methylidopa at a concentration of  $0.05 \mu\text{g}$ . At  $0.1 \mu\text{g}$  the standard deviation decreased to 5.9% for *R*-carbidopa and to 5.1% for *S*-methylidopa. Fig. 3 shows a chromatogram of the mixture of  $0.103 \mu\text{g}$  of *S*-methylidopa and  $0.1035 \mu\text{g}$  of *R*-carbidopa used for calibration. Chromatographic conditions for these experiments were: eluent, methanol-water (65:35, v/v) containing  $0.25 \text{ mM}$  copper(II), pH 3.13, adjusted with sulphuric acid; temperature,  $35^\circ\text{C}$ , flow-rate,  $1 \text{ ml/min}$ .

Finally, we investigated some samples of *S*-carbidopa from ISIS-Chemie Zwickau produced by *N*-amination of *S*-methylidopa as described above. The results are shown in Table V. In these investigations we could not find any *R*-carbidopa at a concentration of more than 0.03% in the *S*-carbidopa. In Figs. 4 and 5 two chromatograms of commercial products are shown designated as AI 1279 and AI 1201 with 0.3 and 0.03% *S*-methylidopa in *S*-carbidopa, respectively. As can be seen, no adsorption was detected for *R*-carbidopa at a retention time of 5 min 35 s.

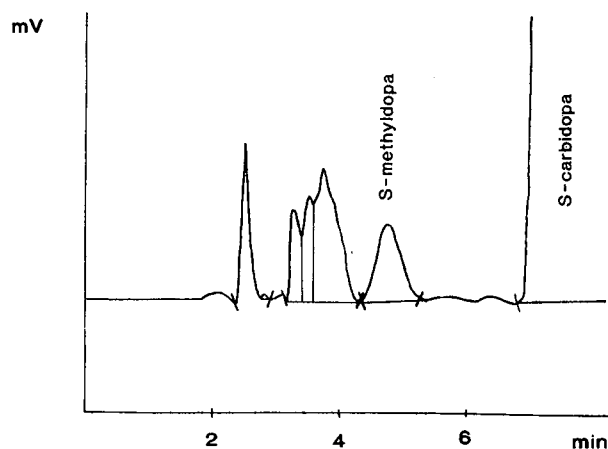


Fig. 4. Chromatogram of the commercial product AI 1279, containing  $0.58 \mu\text{g}$  of *S*-methylidopa (see text for chromatographic conditions).

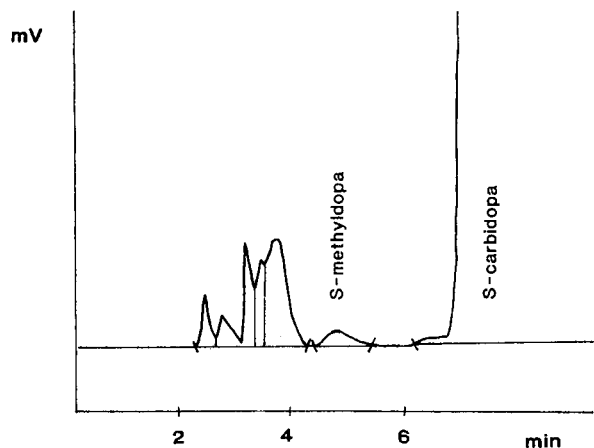


Fig. 5. Chromatogram of the commercial product Al 1201, containing 0.06  $\mu\text{g}$  of *S*-methyldopa (see text for chromatographic conditions).

#### CONCLUSIONS

Ligand-exchange chromatography with *L*-phenylalanine as selector on the stationary phase is a sensitive method for the determination of small amounts of *S*-methyldopa and *R*-carbidopa in *S*-carbidopa. With this method it is possible to estimate 0.05  $\mu\text{g}$  of *R*-carbidopa and 0.05  $\mu\text{g}$  of *S*-methyldopa in 200  $\mu\text{g}$  of *S*-carbidopa injected. It has been shown that in the products investigated no *R*-carbidopa and only very small amounts of *S*-methyldopa could be found. This means that the *S*-methyldopa used in the synthesis did not contain *R*-methyldopa above the detection limit of 0.03%. Moreover, no racemization was observed in the course of synthesis.

#### REFERENCES

- 1 S. Andreae, E. Schmitz, S. Schramm, F.-M. Albert and D. Lohman, *G.D.R. Pat.*, 230 865 (1986); *C.A.*, 105 (1986) 227 301j.
- 2 L. R. Gelber and J. N. Neumeyer, *J. Chromatogr.*, 257 (1983) 317–326.
- 3 G. Gübitz, W. Jellenz and W. Santi, *J. Liq. Chromatogr.*, 4 (1981) 701–712.

CHROM. 23 146

## **Anomalous bandspreading of ethylenediaminetetraacetato-chromium(III) ion in reversed-phase high-performance liquid chromatography**

### **An example of slow equilibrium kinetics**

JOHN H. KNOX\* and MASAMI SHIBUKAWA<sup>a</sup>

*Wolfson Liquid Chromatography Unit, Department of Chemistry, University of Edinburgh, West Mains Road, Edinburgh EH9 3JJ (UK)*

(First received November 16th, 1990; revised manuscript received January 30th, 1991)

---

#### ABSTRACT

As part of a more general study of the high-performance liquid chromatography of ethylenediaminetetraacetate (EDTA) complexes of transition metal ions, it was noted that the EDTA complex of chromium(III) (Cr(III)-edta) gave broad, but symmetrical, peaks in reversed-phase chromatography on alkyl-modified silica (Hypersil C<sub>8</sub>), whereas other metal-edta complexes exhibited normal narrow peaks. The plots against linear flow velocity for Cr(III)-edta are straight lines with slopes which depend strongly on the nature and the concentration of the electrolyte used as buffer. The results obtained are interpreted in terms of the Giddings' model for slow reactions leading to equilibration and indicate that the relative slowness of ligand substitution reactions of Cr(III)-edta with anions in the mobile phase and stationary phases is the dominant contributor to the axial dispersion of this solute. Rate constants and activation energies for ligand substitution are estimated.

---

#### INTRODUCTION

It is well known that slow kinetic processes involved in sorption and desorption may contribute to spreading of solute bands. Giddings [1,2] has derived several useful equations based on various kinetic schemes which may be relevant in real chromatographic systems. However, very few, if any, real examples of slow equilibration leading to significant excess band dispersion have been reported.

In a wider study of the high-performance liquid chromatography (HPLC) of ethylenediaminetetraacetate (EDTA) complexes of transition metal ions, it was noted that the EDTA complex of chromium(III), (Cr(III)-edta), gave extremely broad, but symmetrical, peaks in reversed-phase ion-pair chromatography. These were in striking contrast to the narrow peaks exhibited by the other metal-edta complexes.

---

<sup>a</sup> Present address: Department of Chemistry, St. Marianna University School of Medicine, 2-16-1 Sugao, Miyamae-ku, Kawasaki 213, Japan.

We felt that this characteristic phenomenon most probably reflected the slow kinetics of some reaction of Cr(III)-edta and that this system provided an opportunity to demonstrate the effect of slow chemical change on the spreading of the solute bands in line with Giddings' theory. It will be shown in the present paper that the bandspreading of Cr(III)-edta can indeed be interpreted in terms of the Giddings' model and that the experimental results are consistent with predictions based upon known equilibrium and kinetic data.

## EXPERIMENTAL

### *Materials*

[Cr(Hedta) (H<sub>2</sub>O)] [3], Na[Co(edta)] [4], Na<sub>2</sub>[Co(edta)] [4], Na[Fe(edta) (H<sub>2</sub>O)] [5] and [Cu(H<sub>2</sub>edta)] [6] were prepared according to literature. The compounds were identified by their UV and visible absorption spectra. Cetrimide (cetyltrimethylammonium bromide) was obtained from BDH (Poole, UK), HPLC-grade acetonitrile from FSA Laboratory Supplies (Loughborough, UK) and doubly distilled water was used to prepare the sample solutions and the eluent.

### *Chromatographic conditions*

The chromatographic equipment comprised a Waters Assoc. (Croydon, UK) Model M6000 pump, a Rheodyne injection valve, a 125 × 5 mm I.D. stainless-steel column (Shandon Southern Products, Runcorn, UK) and a Kratos (NJ, USA) Spectroflow 773 UV absorbance photometer. The detection signal was fed into a Hewlett-Packard reporting integrator Model 3390A (Bracknell, UK).

Columns were slurry packed in the laboratory with 5- $\mu$ m octyl silica, Hypersil C<sub>8</sub> (Shandon Southern Products), at 400 kg cm<sup>-2</sup> using 2-propanol followed by water-methanol (50:50, v/v). The column was thermostatted by an air-circulated oven (Shandon Southern Products).

Eluents were 10% (w/v) acetonitrile-water containing 0.1 mM cetrimide. pH and ionic strength were adjusted using phosphate (H<sub>3</sub>PO<sub>4</sub>, NaH<sub>2</sub>PO<sub>4</sub> and Na<sub>2</sub>HPO<sub>4</sub>) or acetate (CH<sub>3</sub>COOH and CH<sub>3</sub>COONa). Sample solutions (0.1-4 mM) were prepared by dissolving the metal-edta complexes in solutions whose compositions were the same as those of the eluents used.

Portions (5  $\mu$ l) of the sample solutions were injected into the column. Preliminary experiments showed that neither retention volume nor height equivalent to a theoretical plate (HETP) depended upon the volume injected in the range between 1 and 10  $\mu$ l. The volumetric flow-rate,  $f_v$  (ml min<sup>-1</sup>), was accurately measured using the burette designed to prevent vaporization of solvent.

### *Determination of column parameters*

The volume of the empty column,  $V_{\text{column}}$ , was determined to be 2.41 ml by filling the column with methanol from a burette. The extra column volume,  $V_{\text{extra}}$ , was determined to be 0.076 ml by measuring the elution volume of a sample solute through the system from which the column had been removed.

The mobile phase volume,  $V_m$ , was assumed to be the smallest retention volume of Cu(II)-edta. This was obtained by elution with 10% (w/v) acetonitrile-water containing 0.1 M NaCl and gave  $V_m = 1.48$  ml.

## RESULTS AND DISCUSSION

Figs. 1 and 2 show chromatograms of several metal(II,III)-edta complexes obtained by elution with eluents containing phosphate buffers of pH 4.5 and 7.0, respectively. As can be seen, Cr(III)-edta exhibits remarkably broad peaks which are in a striking contrast to the normal narrow peaks of the other analytes.

In order to clarify the dominant factor contributing to the bandspreading of Cr(III)-edta, the HETP was measured as a function of the linear flow velocity,  $u$  ( $\text{mm s}^{-1}$ ), which was calculated by eqn. 1.

$$u (\text{mm s}^{-1}) = \frac{f_v}{a_m} = \frac{f_v(V_{\text{column}} + V_{\text{extra}})}{a_{\text{column}} V_m} = 1.43 f_v (\text{ml min}^{-1}) \quad (1)$$

where  $a_{\text{column}}$  and  $a_m$  are the cross-sectional areas of the column and the mobile phase within the column, respectively.

Fig. 3 illustrates plots of HETP against  $u$  for Co(III)-edta and Cu(III)-edta; both give normal curves having a minimum. The HETP of these metal-edta complexes are nearly independent of pH, ionic strength, temperature (30–50°C) and the nature of the electrolyte used as buffer.

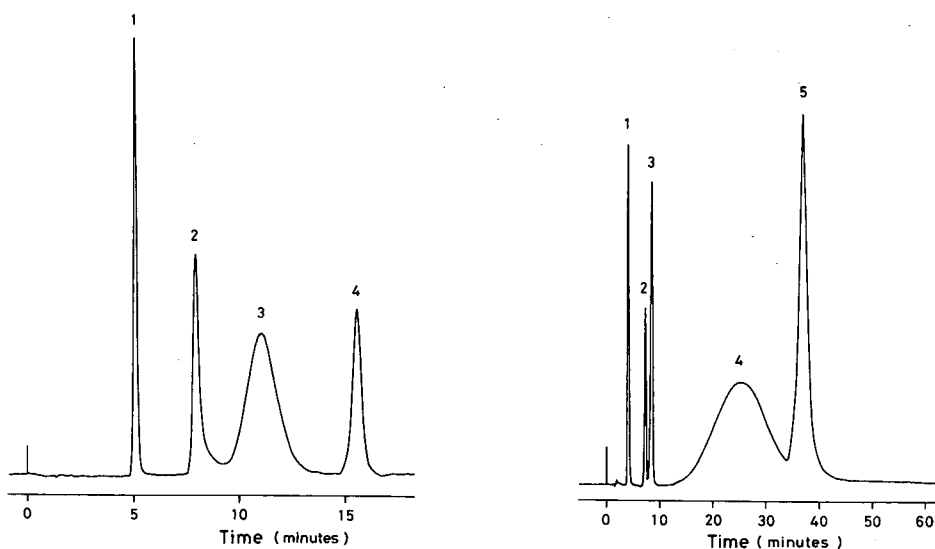


Fig. 1. Chromatogram of metal(II,III)-edta complexes. Eluent, 0.1 mM cetrimide and 10% (w/v) acetonitrile in aqueous phosphate buffer (pH 4.5, ionic strength,  $I = 0.1 M$ ); flow-rate,  $1.03 \text{ ml min}^{-1}$ ; detection wavelength, 230 nm; temperature,  $30^\circ\text{C}$ . Peaks: 1 = Co(III)-edta; 2 = Fe(III)-edta; 3 = Cr(III)-edta; 4 = Cu(II)-edta.

Fig. 2. Chromatogram of metal(II,III)-edta complexes. Eluent, 0.1 mM cetrimide and 10% (w/v) acetonitrile in aqueous phosphate buffer (pH 7.0,  $I = 0.1 M$ ); flow-rate,  $1.03 \text{ ml min}^{-1}$ ; detection wavelength, 230 nm; temperature,  $30^\circ\text{C}$ . Peaks: 1 = Co(III)-edta; 2 = Co(II)-edta; 3 = Cu(II)-edta; 4 = Cr(III)-edta; 5 = Fe(III)-edta.

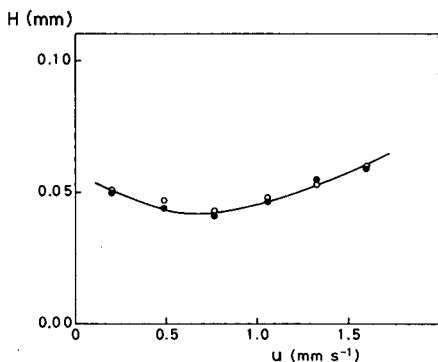


Fig. 3. Plots of HETP vs. linear flow velocity for Co(III)-edta and Cu(II)-edta. Eluent, 0.1 mM cetrinide and 10% (w/v) acetonitrile in aqueous phosphate buffer (pH 7.0,  $I = 0.1 M$ ); temperature, 30°C. ● = Co(III)-edta; ○ = Cu(II)-edta.

By contrast, the plots for Cr(III)-edta were straight lines in almost all cases whose slopes depended strongly upon the composition of the eluent. Figs. 4 and 5 show the effects of ionic strength,  $I$ , and pH on the plots of HETP against  $u$  for Cr(III)-edta, while Fig. 6 shows that the slope depends on the nature of the buffer.

In general, a linear relationship must exist between the HETP and the linear velocity for any contribution to HETP arising from slow equilibration of the analyte between the mobile and stationary phases. Such contributions are, of course, covered by the C-term in the van Deemter equation. Giddings [1] has indicated that there are six slow processes which may produce dispersion of solute zones, namely: (i) single-step sorption and desorption; (ii) diffusion through the stationary or mobile phase; (iii) adsorption on heterogeneous surfaces; (iv) simultaneous partition and adsorption; (v)

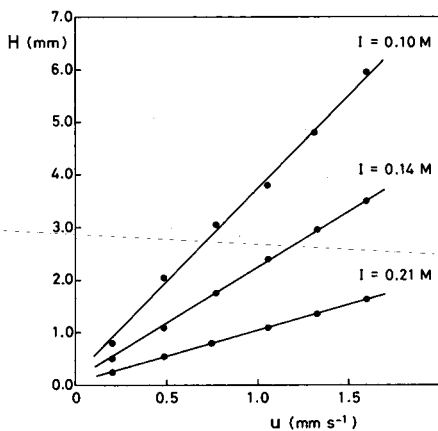


Fig. 4. Effect of ionic strength on the plot of HETP vs. linear flow velocity for Cr(III)-edta. Eluent, 0.1 mM cetrinide and 10% (w/v) acetonitrile in aqueous phosphate buffer (pH 7.0); temperature, 30°C.

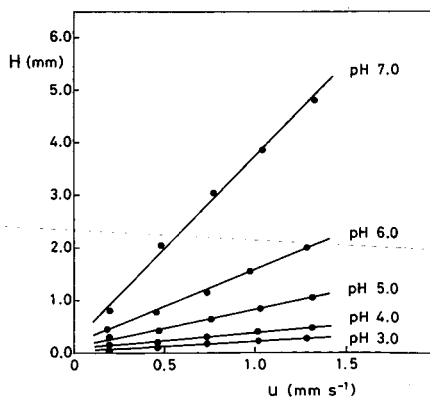


Fig. 5. Effect of pH on the plot of HETP vs. linear flow velocity for Cr(III)-edta. Eluent, 0.1 mM cetrinide and 10% (w/v) acetonitrile in aqueous phosphate buffer ( $I = 0.1 M$ ); temperature, 30°C.



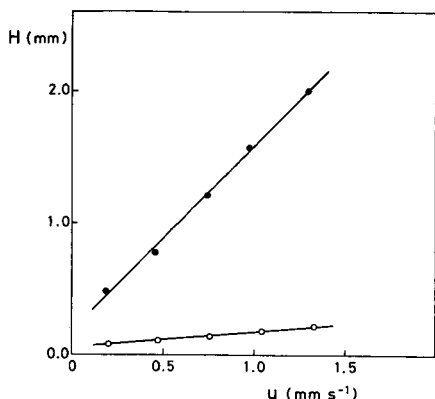


Fig. 6. Effect of the type of the electrolyte used as buffer on the plot of HETP vs. linear flow velocity for Cr(III)-edta. Eluent, 0.1 mM cetrinide and 10% (w/v) acetonitrile in aqueous buffer (pH 6.0,  $I = 0.1 M$ ); temperature, 30°C. ● = Phosphate; ○ = acetate.

adsorption of large molecules; and (vi) chemical reactions not directly related to sorption.

It is not likely that any of the processes (i)-(v) plays a predominant role in the spreading of Cr(III)-edta zones because Cr(III)-edta is considered to have basically a size and structure similar to other metal(III)-edta complexes, especially as Co(III)-edta whose peaks are narrow. Slow chemical reaction (vi) is thus the most likely cause.

Generally, aqueous Co(III) and Cr(III) ions are both kinetically inert. However, it has been found in recent years that one of the coordination sites of Cr(III)-edta is relatively labile and undergoes unexpectedly rapid substitution reactions [7-9] with some anions as shown in reaction A.



Similar ligand substitution reactions have also been observed for several other metal(III)-edta or related complexes, such as Fe(III) [9] and Co(III) [10,11]. But while the reactions of the Fe(III) complex are too fast to cause spreading of solute zones in chromatography [9], the substitution reactions of the Co(III) complex are much too slow [11-14]. In addition, aqueous solutions of  $[\text{Co}(\text{edta})\text{L}]^{(n+1)-}$  are thermodynamically unstable and eliminate  $\text{L}^{n-}$  forming  $[\text{Co}(\text{edta})]^-$  [10] so that the ligand substitution reaction of  $[\text{Co}(\text{edta})]^-$  may be ignored in the present context.

Accordingly, it is most likely that process (vi), that is, the slowness of the substitution reactions of Cr(III)-edta with co-existing anions in the eluent such as  $\text{H}_2\text{PO}_4^-$  and  $\text{CH}_3\text{COO}^-$  is responsible for the spreading of Cr(III)-edta zones.

The general scheme of chemical reaction and sorption-desorption of Cr(III)-edta complexes can be represented by Fig. 7 (charges on ions are omitted) where  $k'_w$  and  $k'_l$  are the distribution coefficients (capacity ratios) for the forms  $[\text{Cr}(\text{edta})\text{H}_2\text{O}]^-$  and  $[\text{Cr}(\text{edta})\text{L}]^{(n+1)-}$  while  $K_M$  and  $K_S$  are the equilibrium ratios for the two forms of the complex (reaction A) in the mobile and stationary phases, respectively. Definitions of

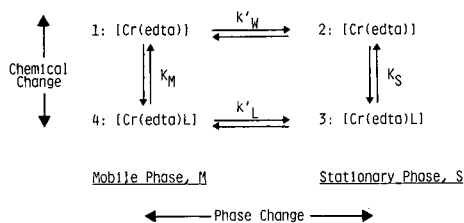


Fig. 7. Phase and chemical equilibria involved in the chromatography of Cr-edta complexes.

the various equilibrium and rate constants used in this paper are given in Table I. The following definitions apply where  $X_1$ ,  $X_2$ ,  $X_3$  and  $X_4$  refer to the fractions of analyte (the Cr-edta complex) in each of the four possible forms (numbered 1: to 4:) shown in the reaction scheme:

$$\text{Capacity ratios} \quad k'_W = X_2/X_1 \quad (2)$$

$$k'_L = X_3/X_4 \quad (3)$$

TABLE I

DEFINITIONS OF EQUILIBRIUM AND RATE CONSTANTS

Equilibrium constants

*Chromatographic distribution equilibria*

- $k'$  Overall capacity ratio of Cr(edta) irrespective of ligand (eqn. 6)
- $k'_W$  Capacity ratio of uncomplexed Cr(edta) between mobile and stationary phases (eqn. 2)
- $k'_L$  Capacity ratio of Cr(edta)L between mobile and stationary phases (eqn. 3)

*Chemical equilibria*

- $K_M$  Equilibrium distribution ratio between Cr(edta) and Cr(edta)L in mobile phase, *i.e.*,  $K_M = [\text{Cr(edta)L}]/[\text{Cr(edta)}]$  (eqn. 4)
- $K_S$  Equilibrium distribution ratio between Cr(edta) and Cr(edta)L in stationary phase (eqn. 5)

Rate constants

- $k_M$  First-order rate constant for conversion of Cr(edta) to Cr(edta)L in mobile phase (eqn. 8)
- $k_S$  First-order rate constant for conversion of Cr(edta) to Cr(edta)L in stationary phase (eqn. 8)
- $k_f$  Second-order rate constant for reaction B in forward direction
- $k_b$  First-order rate constant for reaction B in reverse direction

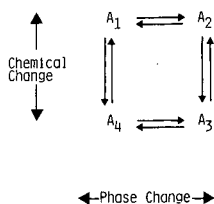


Fig. 8. Giddings' scheme for slow chemical and interphase equilibration.

$$\text{Chemical equilibria} \quad K_M = X_4/X_1 \quad (4)$$

$$K_S = X_3/X_2 \quad (5)$$

The overall  $k'$  value for the Cr(III)-edta complex as a whole is then

$$k' = \frac{X_2 + X_3}{X_1 + X_4} = \frac{k'_W + K_M k'_L}{1 + K_M} \quad (6)$$

and the relative migration rate is

$$R = \frac{1}{1 + k'} = (X_1 + X_4) \quad (7)$$

Giddings [1,2] considered several chemical systems involving slow chemical equilibration including the combination of slow mass transfer of analyte between phases and slow equilibration of two forms of analyte within the mobile and stationary phases. The relevant equilibria are given in Fig. 8, which is seen to be formally identical to our Fig. 7 for the Cr(III)-edta system.

When mass transfer between phases is rapid, as we assume in our case, but chemical equilibration is slow, Giddings' formulation gives a contribution to the plate height,  $H$ , represented by eqn. 8 where the  $X_i$ , as defined above, are the fractions of analyte in the forms  $A_i$  and where  $k_M$  and  $k_S$  are the forward rate constants for the substitution reactions in the mobile and stationary phases (*i.e.*,  $k_{14}$  and  $k_{23}$ , respectively, in Giddings' original formulation).

$$H = \frac{2(X_1 X_3 - X_2 X_4)^2}{R(k_M X_1 + k_S X_2)} u \quad (8)$$

It is then a simple matter to replace the  $X_i$  values using eqns. 2-7 to give

$$H = \frac{2}{(1 + k')^2} \frac{K_M^2}{(1 + K_M)^3} \frac{(k'_W - k'_L)^2}{(k_M + k_S k'_W)} u \quad (9)$$

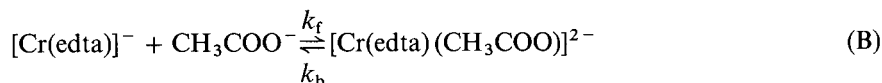
The denominator in the final factor,  $k_M + k_S k'_W$  is the overall rate constant based upon mobile phase concentrations for the substitution reaction occurring in both phases. In other words, the combined reaction rate in the two phases is given as  $(k_M + k_S k'_W)q_M$  where  $q_M$  is the quantity of analyte in the mobile phase.

In order to correlate the above expression for  $H$  with the experimental data, the various constants must either be measured experimentally or estimated. Only  $k'$ , the overall capacity factor, can be measured experimentally; however,  $k_M$  and  $k_S$ ,  $K_M$ ,  $k'_W$  and  $k'_L$  may be estimated from literature data, as discussed below.

#### Values of $K_M$ and $k_M$

Ogino and co-workers [7,9] have determined the equilibrium constant,  $K_B$ , and

the rate constants,  $k_f$  and  $k_b$ , of the reaction of Cr(III)-edta with an acetate ion in aqueous solution at 25°C and with  $I = 1.0 M$  adjusted using  $\text{NaClO}_4$  (reaction B).



( $K_B = 0.62 M^{-1}$ ;  $k_f = 3.3 \pm 0.4 M^{-1}\text{s}^{-1}$ ;  $k_b = 5.4 \pm 0.6 \text{s}^{-1}$ )

It is impossible to use the  $\text{ClO}_4^-$  ion to adjust ionic strength of the eluent in the present chromatographic system because the cetyltrimethylammonium ion added to the eluent as an ion-pairing agent precipitates when  $\text{ClO}_4^-$  is added. We have thus assumed that the equilibrium constant and the rate constants which Ogino and co-workers determined are applicable to the present system where the mobile phase consists of 10% (w/v) acetonitrile-water containing acetate buffer at an ionic strength of 0.1  $M$ . Consequently,  $K_M$  is calculated as follows

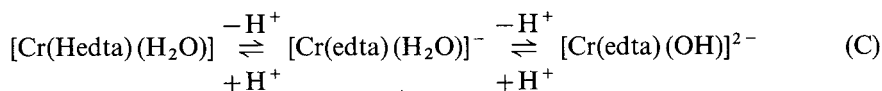
$$K_M = K_B[\text{CH}_3\text{COO}^-] = 0.1K_B = 0.062 \quad (10)$$

Unless the stationary phase accelerates the ligand substitution reaction,  $k_M$  is given by

$$k_M = k_f[\text{CH}_3\text{COO}^-] = 0.1k_f = 0.33 \text{s}^{-1} \quad (11)$$

*Capacity factors  $k'_W$  and  $k'_L$*

We have formulated the Cr(III)-edta complex as  $[\text{Cr}(\text{edta})]^-$  although there remains a problem concerning the structure of Cr(III)-edta complex in an aqueous solution of *ca.* pH 5: whether  $\text{edta}^{4-}$  in the Cr(III)-edta complex acts as a quinque-dentate ligand or as a sexidentate ligand [15-19]. It is well known that the Cr(III)-edta complex has two acid dissociation steps, which was interpreted as the loss of a proton from the uncoordinated carboxylic acid group followed by the loss of a proton from the coordinated water molecule, as shown in reaction C.



( $\text{p}K_{a1} = 1.8$ ;  $\text{p}K_{a2} = 7.39$  [7])

Thus, it was believed that the  $\text{edta}^{4-}$  remained coordinated to Cr(III) as a quinque-dentate ligand over a wide pH range. Recently, however, Wheeler and Legg [16] showed by deuterium NMR spectroscopy that  $\text{edta}^{4-}$  forms a sexidentate complex with Cr(III) between pH 3.5 and 6.5. Their view has been supported by the recent work carried out by a variety of analytical methods [17-19].

At pH 4-6 Co(III)-edta and Cr(III) have the same charge,  $-1$ , and therefore similar structures, *i.e.*,  $[\text{Co}(\text{edta})]^-$  and  $[\text{Cr}(\text{edta})]^-$ . Because it seems reasonable to assume that the affinity of  $[\text{Cr}(\text{edta})]^-$  to the stationary phase is nearly the same as that of  $[\text{Co}(\text{edta})]^-$  we assume

$$k'_W = k'_{[\text{Co}(\text{edta})]^-} \quad (12)$$

TABLE II

ESTIMATED EQUILIBRIUM CONSTANTS AND RATE CONSTANTS RELATING TO THE CHEMICAL CHANGE AND THE SORPTION OF Cr(III)-edta COMPLEX IN ACETATE BUFFER SYSTEM

pH	$k'_w$	$k'_L$	$K_M$	$k'$	$k_M$ (s <sup>-1</sup> )
5.0	2.40	23	0.062	3.6	0.33
6.0	2.60	31	0.062	4.3	0.33

On the other hand, since the overall  $k'$  is obtained experimentally,  $k'_L$  can be calculated from  $k'$ ,  $k'_w$  and  $K_M$  from eqn. 6 as

$$k'_L = \frac{k'(1 + K_M) - k'_w}{K_M} \quad (13)$$

#### Values of $k_M$ and $k_S$

The rates of substitution in the mobile and stationary phases are expected to be similar and we have assumed that  $k_M = k_S k'_w$ , that is, that the rates are identical and therefore that  $k_M + k_S k'_w = 2k_M$ . If they are not identical we would replace  $2k_M$  by  $\alpha k_M$  ( $\alpha > 1$ ), where  $\alpha$  would be a constant which could be adjusted to obtain the best fit between direct experiment and literature prediction.

The estimated equilibrium constants and the rate constants relating to the chemical change and the sorption of Cr(III)-edta complexes at pH 5.0 and 6.0 are summarized in Table II. Substituting these values into eqn. 9, we can obtain the expected slopes of the plots of HETP vs.  $u$ . The values thus obtained are listed in Table III, together with the experimental values obtained from the plots shown in Fig. 9. The experimental values are somewhat smaller than the corresponding calculated ones, but

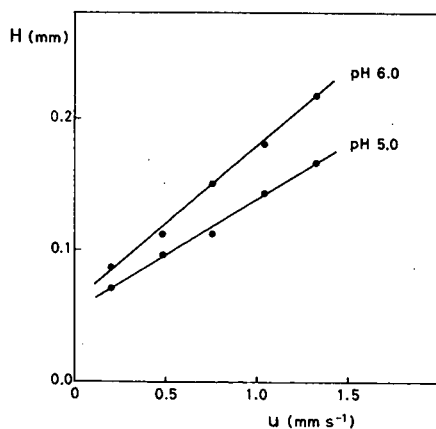


Fig. 9. Effect of pH on the plot of HETP vs. linear flow velocity for Cr(III)-edta. Eluent, 0.1 M cetrimide and 10% (w/v) acetonitrile in aqueous acetate buffer ( $I = 0.1 M$ ); temperature, 30°C.

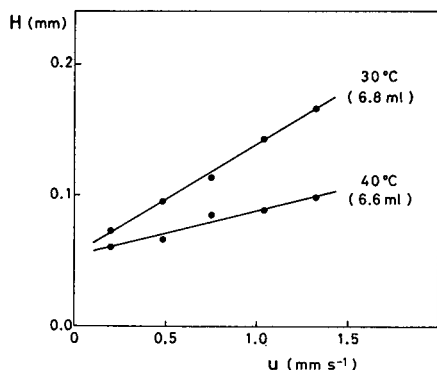


Fig. 10. Effect of temperature on the plot of HETP vs. linear flow velocity for Cr(III)-edta. Eluent, 0.1 *M* cetrimide and 10% (w/v) acetonitrile in aqueous acetate buffer (pH 5.0, *I* = 0.1 *M*). Values in parentheses are the retention volumes of Cr(III)-edta.

this discrepancy mainly results from the difference in temperature: the experimental values were obtained at 30°C while the calculated values are for 25°C.

Fig. 10 shows the effect of temperature on the plot of HETP vs. *u*. Provided the capacity factors of [Cr(edta)]<sup>-</sup> and [Cr(edta)(CH<sub>3</sub>COO)]<sup>-</sup> and the equilibrium constant of the ligand substitution reaction *K<sub>M</sub>* are independent of temperature, *T*, we can write as follows

$$H = (\text{const}/k_M)u \quad (14)$$

where both *H* and *k<sub>M</sub>* are temperature dependent. It is reasonable to assume that the capacity factors of [Cr(edta)]<sup>-</sup> and [Cr(edta)(CH<sub>3</sub>COO)]<sup>-</sup>, namely *k'<sub>w</sub>* and *k'<sub>L</sub>*, and *K<sub>M</sub>* are approximately independent of temperature between 30 and 40°C because the retention volume of Cr(III)-edta at 40°C (6.6 ml) is nearly the same as at 30°C (6.8 ml). This means that the activation energy, *E<sub>a</sub>*, can be estimated by eqn. 15

$$E_a = R \left( \frac{313 \times 303}{313 - 303} \right) \ln \left[ \frac{H(40^\circ\text{C})}{H(30^\circ\text{C})} \right] \quad (15)$$

TABLE III

COMPARISON OF THE SLOPES OF THE PLOTS OF HETP vs. *u* CALCULATED BY EQN. 10 WITH THE EXPERIMENTALLY OBTAINED VALUES

pH	Calcd. (25°C)	Exptl. (30°C) <sup>a</sup>	Exptl. (25°C) <sup>b</sup>
5.0	0.20	0.084	0.14
6.0	0.28	0.12	0.19

<sup>a</sup> Obtained from the plots shown in Fig. 9.

<sup>b</sup> Values corrected for temperature (see text for details).

where  $R$  is the gas constant.  $E_a$  at pH 5.0 is then  $71 \text{ kJ mol}^{-1}$ . From this  $E_a$  value, the slope of the  $H$  vs.  $u$  plot at  $25^\circ\text{C}$  can be estimated. The value at pH 6.0 was calculated by assuming that the activation energy of the reaction is the same at pH 6.0 as at 5.0. The estimated values are given in Table III and are in fairly good agreement with those calculated from literature. Accordingly, the spreading of Cr(III)-edta zones in reversed-phase HPLC can be interpreted in terms of the Giddings' model for slow reactions leading to equilibration where the slowness of ligand substitution reactions of Cr(III)-edta is the main contributor to the axial dispersion of this solute.

$[\text{Cr}(\text{edta})]^-$  has been found to react not only with  $\text{CH}_3\text{COO}^-$  but also with some other anions such as  $\text{SCN}^-$ ,  $\text{CrO}_4^{2-}$  and  $\text{MoO}_4^{2-}$  [9]. Although the equilibrium constants and the rate constants relating to the reaction of Cr(III)-edta with  $\text{H}_2\text{PO}_4^-$  have not yet been determined, similar ligand substitution reactions may be responsible for the bandspreading of Cr(III)-edta in the phosphate buffer system. We have found evidence that the average charge on Cr(III)-edta in a phosphate buffer solution of pH 7.0 is not  $-1$  but  $-2$  [20]. This appears to indicate that Cr(III)-edta undergoes the ligand substitution reaction with  $\text{H}_2\text{PO}_4^-$  or  $\text{HPO}_4^{2-}$ .

The dependence of the slope of the HETP vs.  $u$  plot on the ionic strength can be explained qualitatively as follows. The increase in the concentration of  $\text{L}^{n-}$  added as buffer salt results in the increase both in  $K_M$  and  $k_M$  according to eqns. 10 and 11, respectively. Furthermore, the capacity factors of  $[\text{Cr}(\text{edta})]^-$  and  $[\text{Cr}(\text{edta})\text{L}]^{(n+1)-}$  and then the difference between these two capacity factors ( $k'_L - k'_W$ ) decrease with increase in ionic strength. Consequently, the slope decreases with an increase in the ionic strength as shown in Fig. 4.

The effect of pH on the plots shown in Fig. 5 may be explained to some extent. It has been reported that the rate constant of the reaction of  $[\text{Cr}(\text{Hedta})(\text{H}_2\text{O})]$  with an acetate ion is much higher than that of  $[\text{Cr}(\text{edta})]^-$  [7]. Therefore, the overall rate constant of this kind of ligand substitution reaction is expected to increase with increase in the concentration of  $[\text{Cr}(\text{Hedta})(\text{H}_2\text{O})]$  under pH 5. At pH 5 or above, however, the concentration of  $[\text{Cr}(\text{Hedta})(\text{H}_2\text{O})]$  is so small that the effect of the reaction of the reaction of  $[\text{Cr}(\text{Hedta})(\text{H}_2\text{O})]$  on the overall reaction rate is negligible even if its high rate constant is taken into account. Changes in concentration of phosphate species in the eluent, *i.e.*,  $\text{H}_2\text{PO}_4^-$  and  $\text{HPO}_4^{2-}$ , as pH is changed may cause the result shown in Fig. 5. In order to quantitatively evaluate the effect of pH on the bandspreading of Cr(III)-edta,  $K_M$  for the reaction of  $[\text{Cr}(\text{edta})]^-$  with  $\text{H}_2\text{PO}_4^-$  and  $\text{HPO}_4^{2-}$  should be determined by means of some other method.

#### ACKNOWLEDGEMENTS

The authors gratefully acknowledge the award of a fund of the Anglo-Japanese Scientific Exchange Programme by the Japan Society for the Promotion of Science and the Royal Society to one of us (M.S.), without which support the project could not have been carried out.

#### REFERENCES

- 1 J. C. Giddings, *J. Chromatogr.*, 3 (1960) 443.
- 2 J. C. Giddings, *Dynamics of Chromatography, Part I, Principles and Theory*, Marcel Dekker, New York, 1965, p. 130.

- 3 R. E. Hamm, *J. Am. Chem. Soc.*, 75 (1953) 5670.
- 4 H. A. Weakliem and J. L. Hoard, *J. Am. Chem. Soc.*, 81 (1959) 549.
- 5 M. D. Lind, M. J. Hamor, T. A. Hamor and J. L. Hoard, *Inorg. Chem.*, 3 (1964) 34.
- 6 S. Kirschner, *J. Am. Chem. Soc.*, 78 (1956) 2372.
- 7 H. Ogino, T. Watanabe and N. Tanaka, *Inorg. Chem.*, 14 (1975) 2093.
- 8 Y. Sulfab, R. S. Taylor and A. G. Sykes, *Inorg. Chem.*, 15 (1976) 2388.
- 9 H. Ogino, M. Shimura and N. Tanaka, *Inorg. Chem.*, 18 (1979) 2497.
- 10 I. A. W. Shimi and W. C. E. Higginson, *J. Chem. Soc.*, (1958) 260.
- 11 R. Dyke and W. C. E. Higginson, *J. Chem. Soc.*, (1960) 1998.
- 12 L. Rosenhein, D. Speiser and A. Haim, *Inorg. Chem.*, 13 (1974) 1571.
- 13 H. Ogino, M. Takahashi and N. Tanaka, *Bull. Chem. Soc. Jpn.*, 47 (1974) 1426.
- 14 J. Phillips and A. Haim, *Inorg. Chem.*, 19 (1980) 1616.
- 15 H. Ogino and M. Shimura, *Adv. Inorg. Bioinorg. Mech.*, 4 (1986) 107.
- 16 W. D. Wheeler and J. I. Legg, *Inorg. Chem.*, 24 (1985) 1292.
- 17 S. Kaizaki and H. Mizu-uchi, *Inorg. Chem.*, 25 (1986) 2732.
- 18 K. Kanamori and K. Kawai, *Inorg. Chem.*, 25 (1986) 3711.
- 19 N. Miura, M. Shimura and H. Ogino, *Bull. Chem. Soc. Jpn.*, 60 (1987) 1349.
- 20 J. H. Knox and M. Shibukawa, unpublished results.



## Generalized treatment of spatial and temporal column parameters, applicable to gas, liquid and supercritical fluid chromatography

### II. Application to supercritical CO<sub>2</sub>

D. E. MARTIRE\* and R. L. RIESTER

*Department of Chemistry, Georgetown University, Washington, DC 20057 (USA)*

T. J. BRUNO

*Thermophysics Division, National Institute of Standards and Technology, Boulder, CO 80303 (USA)*

and

A. HUSSAM<sup>a</sup> and D. P. POE<sup>b</sup>

*Department of Chemistry, Georgetown University, Washington, DC 20057 (USA)*

(First received October 31st, 1990; revised manuscript received February 5th, 1991)

---

#### ABSTRACT

Equations derived in Part I [D. E. Martire, *J. Chromatogr.*, 461 (1989) 165] are used to calculate distribution functions, average densities and column profiles for supercritical fluid chromatography with carbon dioxide as the mobile phase. An approximation for the column-average capacity factor in terms of the local capacity factor is evaluated and conditions are given for its applicability.

---

#### INTRODUCTION

General equations have been derived for the spatial and temporal density distribution functions, average densities and column profiles of the mobile-phase fluid, and for the observed (apparent) capacity factors and column profiles of the solute components [1]. These equations are valid for all conditions where Darcy's law is valid, *i.e.*, as long as the flow is laminar and not turbulent. It has been shown in Part I [1] that the application of these equations is straightforward in the cases of gas and liquid chromatography. In capillary supercritical fluid chromatography (SFC), pressure drops over the length of the column are usually so small that the average density is close to the inlet density. Thus, the most interesting application is in packed-column SFC

---

<sup>a</sup> Present address: Department of Chemistry, George Mason University, Fairfax, VA 22030, USA.

<sup>b</sup> Present address: Department of Chemistry, University of Minnesota, Duluth, MN 55812, USA.

because of the large pressure drops involved and the non-ideality and compressibility of the mobile phase.

In the present study, the equations are applied to SFC with carbon dioxide as the mobile phase. In order to apply these equations, reliable density, isothermal compressibility and viscosity data for the mobile phase are needed. A modified Benedict–Webb–Rubin (BWR) equation of state [2] was used to generate densities and isothermal compressibilities; available viscosity data were used to fit a polynomial expression for viscosity in terms of density and temperature. For a given inlet pressure, the outlet pressure will depend on several variables: the column length, type and porosity of packing, type of back-pressure regulator or restrictor used, etc. In this study, various inlet and outlet pressures were assumed and distribution functions, density averages and column profiles for the mobile phase were calculated. In order to generate average capacity factors and column profiles for the solutes, an expression for the local capacity factor was assumed.

The following equations from ref. 1 (written here in reduced form) are used in this study:

The spatial distribution function  $D_x(\rho_R)$

$$D_x(\rho_R) = \eta_R^{-1} \rho_R (\partial P_R / \partial \rho_R)_T \quad (1)$$

The temporal distribution function  $D_t(\rho_R)$

$$D_t(\rho_R) = \eta_R^{-1} \rho_R^2 (\partial P_R / \partial \rho_R)_T \quad (2)$$

The spatial average mobile phase density  $\langle \rho_R \rangle_x$

$$\langle \rho_R \rangle_x = \frac{\int_{\rho_{R,0}}^{\rho_{R,i}} \rho_R D_x(\rho_R) d\rho_R}{\int_{\rho_{R,0}}^{\rho_{R,i}} D_x(\rho_R) d\rho_R} \quad (3)$$

The temporal average mobile phase density,  $\langle \rho_R \rangle_t$

$$\langle \rho_R \rangle_t = \frac{\int_{\rho_{R,0}}^{\rho_{R,i}} \rho_R D_t(\rho_R) d\rho_R}{\int_{\rho_{R,0}}^{\rho_{R,i}} D_t(\rho_R) d\rho_R} \quad (4)$$

The observed capacity factor,  $\langle k' \rangle_t$

$$\langle k' \rangle_t = \frac{\int_{\rho_{R,0}}^{\rho_{R,i}} k' D_t(\rho_R) d\rho_R}{\int_{\rho_{R,0}}^{\rho_{R,i}} D_t(\rho_R) d\rho_R} \quad (5)$$

The fractional distance,  $x/L$ , when the local mobile phase density is  $\rho_R$

$$x/L = \frac{\int_{\rho_R}^{\rho_{R,i}} D_x(\rho_R) d\rho_R}{\int_{\rho_{R,0}}^{\rho_{R,i}} D_x(\rho_R) d\rho_R} \quad (6)$$

The fractional time,  $\tau_u/t_u$ , an unretained solute has spent on the column when the local density is  $\rho_R$

$$\tau_u/t_u = \int_{\rho_R}^{\rho_{R,i}} D_i(\rho_R) d\rho_R / \int_{\rho_{R,0}}^{\rho_{R,i}} D_i(\rho_R) d\rho_R \quad (7)$$

The fractional solute migration time,  $\tau_s/t_s$ , at  $\rho_R$

$$\tau_s/t_s = \int_{\rho_R}^{\rho_{R,i}} (1 + k') D_i(\rho_R) d\rho_R / \int_{\rho_{R,0}}^{\rho_{R,i}} (1 + k') D_i(\rho_R) d\rho_R \quad (8)$$

In these equations the density ( $\rho$ ), pressure ( $P$ ) and viscosity ( $\eta$ ) are normalized to reduced variables:  $\rho_R = \rho/\rho_{cr}$ ,  $P_R = P/P_{cr}$ ,  $\eta_R = \eta/\eta^0$  where  $\rho_{cr} = 0.468 \text{ g/cm}^3$ ,  $T_{cr} = 304.2 \text{ K}$ ,  $P_{cr} = 73.84 \text{ bar}$  and  $\eta^0$  is chosen as the viscosity at one bar for a given temperature.  $L$  refers to the column length measured from the inlet,  $t_u$  the holdup time of an unretained solute,  $t_s$  the solute retention time,  $k'$  the local capacity factor; the subscripts  $i$  and  $o$  refer to inlet and outlet conditions, respectively. The quantity  $\eta_R^{-1}(\partial P_R/\partial \rho_R)_T$  which appears in both distribution functions will be referred to as the "core" of the distribution function.

The observed or apparent capacity factor is related to the local capacity factor and conditions are given for an approximation for the observed capacity factor in terms of the temporal average density. In addition, the separation factor,  $\alpha$ , for two solutes  $a$  and  $b$  is calculated from

$$\alpha = \frac{\langle k' \rangle_{t,b}}{\langle k' \rangle_{t,a}} \quad (9)$$

#### THE EQUATION OF STATE

The Jacobsen–Stewart modification [2,3] of the BWR equation of state was used to generate reliable density ( $\rho$ ) and isotherm derivative,  $(\partial P_R/\partial \rho_R)_T$ , predictions:

$$P = \rho RT + \sum_{i=1}^{32} N_i X_i \quad (10)$$

$$(\partial P/\partial \rho)_T = RT + \sum_{i=1}^{32} N_i X'_i \quad (11)$$

where  $X'_i = (\partial X_i/\partial \rho)_T$ .

The  $N_i$  coefficients for  $\text{CO}_2$  were obtained from ref. 3 and are reproduced in column 2 of Table I. Expressions for the  $X_i$  and  $X'_i$  are given in columns 3 and 4 of Table I.  $\rho$  is the density in mol/l;  $P$  the pressure in bar,  $T$  the temperature in Kelvin;  $R = 0.083144 \text{ bar} \cdot \text{l/mol} \cdot \text{K}$ . The equations are applicable for a temperature range from 215 to 1100 K and from 0 to 3000 bar with an overall accuracy of 0.3% in density [3]. Since the equation is explicit in pressure, density predictions were obtained using the bisection method [4].

TABLE I

COEFFICIENTS AND EXPRESSIONS OF EXTENDED BWR EQUATION FOR CO<sub>2</sub><sup>a</sup>

$F = \exp(-G\rho^2)$ ;  $G = 0.88999644 \cdot 10^{-2}$ ;  $F' = -2.0F\rho G$ ;  $F21 = 3.0F\rho^2 + F'\rho^3$ ;  $F22 = 5.0F\rho^4 + F'\rho^5$ ;  $F23 = 7.0F\rho^6 + F'\rho^7$ ;  $F24 = 9.0F\rho^8 + F'\rho^9$ ;  $F25 = 11.0F\rho^{10} + F'\rho^{11}$ ;  $F26 = 13.0F\rho^{12} + F'\rho^{13}$ .

<i>i</i>	<i>N</i>	<i>X</i>	<i>X'</i>
1	$-0.9818510658 \cdot 10^{-2}$	$\rho^2 T$	$2.0\rho T$
2	0.9950622673	$\rho^2 T^{1/2}$	$2.0\rho T^{1/2}$
3	$-0.2283801603 \cdot 10^2$	$\rho^2$	$2.0\rho$
4	$0.2818276345 \cdot 10^4$	$\rho^2/T$	$2.0\rho/T$
5	$-0.3470012627 \cdot 10^6$	$\rho^2/T^2$	$2.0\rho/T^2$
6	$0.3947067091 \cdot 10^{-3}$	$\rho^3 T$	$3.0\rho^2 T$
7	-0.3255500001	$\rho^3$	$3.0\rho^2$
8	4.843200831	$\rho^3/T$	$3.0\rho^2/T$
9	$-0.3521815430 \cdot 10^6$	$\rho^3/T^2$	$3.0\rho^2/T^2$
10	$-0.3240536033 \cdot 10^{-4}$	$\rho^4 T$	$4.0\rho^3 T$
11	$0.4685966847 \cdot 10^{-1}$	$\rho^4$	$4.0\rho^3$
12	-7.545470121	$\rho^4/T$	$4.0\rho^3/T$
13	$-0.381894354 \cdot 10^{-4}$	$\rho^5$	$5.0\rho^4$
14	$-0.4421929339 \cdot 10^{-1}$	$\rho^6/T$	$6.0\rho^5/T$
15	$0.5169251681 \cdot 10^2$	$\rho^6/T^2$	$6.0\rho^5/T^2$
16	$0.2124509852 \cdot 10^{-2}$	$\rho^7/T$	$7.0\rho^6/T$
17	$-0.2610094748 \cdot 10^{-4}$	$\rho^8/T$	$8.0\rho^7/T$
18	$-0.888533389 \cdot 10^{-1}$	$\rho^8/T^2$	$8.0\rho^7/T^2$
19	$0.1552261794 \cdot 10^{-2}$	$\rho^9/T^2$	$9.0\rho^8/T^2$
20	$0.4150910049 \cdot 10^6$	$\rho^3 F/T^2$	$F21/T^2$
21	$-0.1101739675 \cdot 10^8$	$\rho^3 F/T^3$	$F21/T^3$
22	$0.2919905833 \cdot 10^4$	$\rho^5 F/T^2$	$F22/T^2$
23	$0.1432546065 \cdot 10^8$	$\rho^5 F/T^4$	$F22/T^4$
24	$0.1085742075 \cdot 10^2$	$\rho^7 F/T^2$	$F23/T^2$
25	$-0.247799657 \cdot 10^3$	$\rho^7 F/T^3$	$F23/T^3$
26	$0.1992935908 \cdot 10^{-1}$	$\rho^9 F/T^2$	$F24/T^2$
27	$0.1027499081 \cdot 10^3$	$\rho^9 F/T^4$	$F24/T^4$
28	$0.3776188652 \cdot 10^{-4}$	$\rho^{11} F/T^2$	$F25/T^2$
29	$-0.3322765123 \cdot 10^{-2}$	$\rho^{11} F/T^3$	$F25/T^3$
30	$0.1791967071 \cdot 10^{-7}$	$\rho^{13} F/T^2$	$F26/T^2$
31	$0.9450766278 \cdot 10^{-5}$	$\rho^{13} F/T^3$	$F26/T^3$
32	$-0.1234009431 \cdot 10^{-2}$	$\rho^{13} F/T^4$	$F26/T^4$

<sup>a</sup> See eqns. 10 and 11.

## VISCOSITY

Viscosities were obtained by fitting tabulated viscosity data [5] to the equation

$$\eta_R = \sum_{i=0}^4 \sum_{j=0}^4 c_{i,j} T_R^j \rho_R^i \quad (12)$$

The  $c_{i,j}$  coefficients for CO<sub>2</sub> are listed in Table II. The fit is applicable for pressures from 40 to 1000 bar over the temperature range 315 to 900 K with an average error of 0.4%.

TABLE II

 COEFFICIENTS OF  $\eta_R$  VISCOSITY EQUATION FOR  $\text{CO}_2$ ,  $c_{i,j}$ <sup>a</sup>

<i>i</i>	<i>j</i>	$c_{i,j}$	<i>i</i>	<i>j</i>	$c_{i,j}$
0	0	1.984239055923858	2	3	-6.962674520424649
0	1	-1.765978814900643	2	4	0.7797272269308236
0	2	1.200587190352171	3	0	-15.836119060967
0	3	-0.3587967344551215	3	1	26.17032056108262
0	4	3.939799401399628 · 10 <sup>-2</sup>	3	2	-17.42070707993796
1	0	-6.939097844205919	3	3	5.402335087741039
1	1	12.16864979120884	3	4	-0.6352935554972202
1	2	-7.954279939480736	4	0	4.337989765743405
1	3	2.311176553431279	4	1	-7.058859850635407
1	4	-0.2499449770969321	4	2	4.866472957964851
2	0	22.0798196307882	4	3	-1.607823031693741
2	1	-35.92289143102958	4	4	0.2014049388370968
2	2	23.41530455411397			

<sup>a</sup> See eqn. 12.

For the calculation of reduced viscosity from  $\eta/\eta^0$ , a fit of  $\eta^0$  vs.  $T_R$  was completed, where  $\eta^0$  was selected as the viscosity at 1 bar. The relation is

$$\eta^0 = \sum_{j=0}^3 a_j T_R^j \quad (13)$$

The  $a_j$  coefficients are given in Table III. Figs. 1 and 2 show the relationship of viscosity to pressure and density, respectively.

#### THE CORE OF THE DISTRIBUTION FUNCTION

In order to obtain a tractable expression for the core of the distribution function for use in the integral equations, the expression  $\eta_R^{-1}(\partial P_R/\partial \rho_R)$  was evaluated using the equation of state and tabulated viscosity data [5] and fit to a seventh-order polynomial

TABLE III

 COEFFICIENTS OF  $\eta^0$  ( $10^{-6}$  Ns/m<sup>2</sup>) VISCOSITY EQUATION FOR  $\text{CO}_2$ <sup>a</sup>

<i>j</i>	$a_j$ ( $10^{-6}$ Ns/m <sup>2</sup> )
0	-1.842303556958221
1	19.94110352045899
2	-3.288620563501078
3	0.3299574285621828

<sup>a</sup> See eqn. 13.

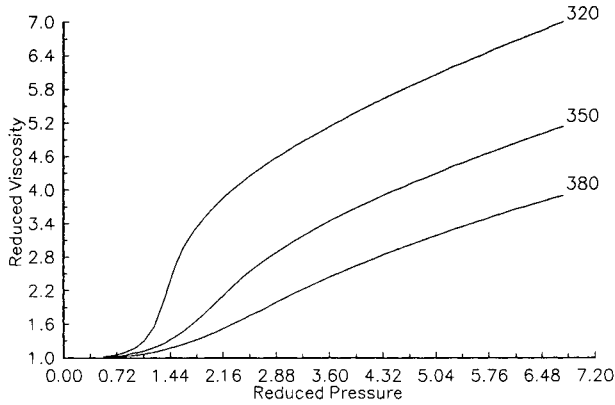


Fig. 1. Relationship between reduced viscosity and reduced pressure of CO<sub>2</sub> at 320, 350 and 380 K.

in reduced density at a given temperature. The resulting equation for the core of the distribution function is

$$\frac{1}{\eta_R} (\partial P_R / \partial \rho_R)_T = \sum_{j=0}^7 c(T)_j \rho_R^j \quad (14)$$

The coefficients for selected temperatures from 320 to 500 K are given for CO<sub>2</sub> in Table IV. This method has the advantage of yielding analytically solvable integrals for the density averages, but the disadvantage of requiring a temperature-dependent set of coefficients. The equation of state and viscosity equations may be used to calculate these coefficients at any desired temperature. Alternatively, the integrals may be evaluated numerically at any temperature and pressure using the equation of state to obtain  $(\partial P_R / \partial \rho_R)_T$  and eqn. 12 to obtain  $\eta_R^{-1}$ .

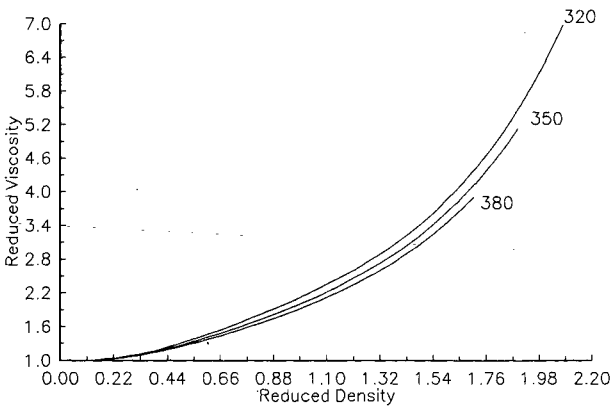


Fig. 2. Relationship between reduced viscosity and reduced density of CO<sub>2</sub> at 320, 350 and 380 K.

TABLE IV

COEFFICIENTS OF THE CORE OF THE DISTRIBUTION FUNCTION,  $\eta_R^{-1}(\partial P_R/\partial \rho_R)_T$ , FOR CO<sub>2</sub>

<i>T/j</i>	0	1	2	3	4	5	6	7
315	3.430721	-5.436177	-14.063478	50.004813	-61.078887	37.082152	-11.123848	1.315836
318	3.449651	-5.165713	-14.619629	50.386233	-61.179006	37.156443	-11.184187	1.329785
320	3.468362	-5.035216	-14.898416	50.693615	-61.520404	37.471557	-11.330728	1.354716
323	3.507241	-4.981013	-14.660994	49.710760	-60.361265	36.903599	-11.220950	1.350461
325	3.529547	-4.900966	-14.704797	49.488739	-60.065716	36.806435	-11.232691	1.357955
328	3.567610	-4.835326	-14.554064	48.740216	-59.183956	36.402942	-11.171629	1.359514
330	3.594037	-4.805044	-14.400660	48.137436	-58.477669	36.057054	-11.105119	1.357108
333	3.634926	-4.775353	-14.113013	47.128036	-57.301045	35.461413	-10.978996	1.349891
335	3.663093	-4.767234	-13.876192	46.368154	-56.417075	34.998493	-10.872244	1.341962
340	3.735941	-4.779590	-13.157321	44.218988	-53.909728	33.635421	-10.531496	1.311594
345	3.811424	-4.829204	-12.292277	41.775228	-51.034637	32.005334	-10.090694	1.266392
350	3.888584	-4.904933	-11.324438	39.117654	-47.871881	30.149953	-9.560026	1.207156
355	3.966580	-4.996535	-10.295859	36.329849	-44.511071	28.120857	-8.954059	1.135399
360	4.044703	-5.094889	-9.245997	33.495104	-41.047809	25.977564	-8.291338	1.053338
365	4.122378	-5.192201	-8.210274	30.692525	-37.578626	23.784241	-7.593386	0.963788
370	4.199161	-5.282081	-7.219233	27.994251	-34.196937	21.606888	-6.883810	0.870070
375	4.274729	-5.359553	-6.297969	25.463207	-30.989408	19.510516	-6.187295	0.775874
380	4.348880	-5.421136	-5.465210	23.149812	-28.030595	17.554815	-5.527916	0.685023
385	4.421507	-5.464634	-4.733836	21.092105	-25.381855	15.792668	-4.928420	0.601345
390	4.492589	-5.489028	-4.111053	19.315239	-23.089491	14.268038	-4.409205	0.528503
395	4.562169	-5.494315	-3.598799	17.831406	-21.183243	13.013900	-3.987211	0.469786
400	4.630341	-5.481284	-3.194661	16.641477	-19.677496	12.052323	-3.675652	0.428020
410	4.762983	-5.406185	-2.684254	15.098625	-17.853463	11.039525	-3.415627	0.403671
420	4.891684	-5.278686	-2.504810	14.525946	-17.471506	11.193787	-3.650242	0.465356
430	5.017609	-5.115442	-2.563619	14.691491	-18.248922	12.347147	-4.339176	0.612149
440	5.141729	-4.931525	-2.769727	15.344966	-19.838448	14.248806	-5.395477	0.833515
450	5.264761	-4.738747	-3.046140	16.257123	-21.891474	16.616550	-6.705176	1.111919
460	5.387171	-4.545277	-3.334909	17.241746	-24.101283	19.178477	-8.146164	1.425930
470	5.509227	-4.356014	-3.597456	18.163942	-26.227172	21.702104	-9.603891	1.753273
480	5.631051	-4.173312	-3.811609	18.937261	-28.100147	24.008383	-10.981440	2.073214
490	5.752686	-3.997791	-3.967820	19.516300	-29.618699	25.975777	-12.205201	2.368296
500	5.874126	-3.829018	-4.064945	19.885808	-30.735909	27.534386	-13.225300	2.625066
510	5.995350	-3.666042	-4.107097	20.051584	-31.446624	28.657725	-14.014026	2.834337
520	6.116340	-3.507723	-4.101016	20.032035	-31.774063	29.352199	-14.562299	2.990911
530	6.237089	-3.352985	-4.054338	19.851937	-31.758491	29.646665	-14.875213	3.092957
540	6.357602	-3.200899	-3.974493	19.538255	-31.449228	29.584628	-14.968485	3.141461
550	6.477901	-3.050744	-3.868163	19.117157	-30.897801	29.216445	-14.864230	3.139390
560	6.598021	-2.902022	-3.740895	18.612604	-30.154598	28.595194	-14.588566	3.091189
570	6.718008	-2.754413	-3.597292	18.045621	-29.266003	27.772556	-14.168946	3.002157
580	6.837917	-2.607786	-3.440735	17.433791	-28.273103	26.796665	-13.632527	2.877999
590	6.957805	-2.462108	-3.273899	16.791695	-27.211291	25.710798	-13.005036	2.724506
600	7.077740	-2.317489	-3.098509	16.130949	-26.110274	24.552744	-12.309946	2.547261

The core of the distribution function is shown as a function of pressure and density in Figs. 3 and 4, respectively.

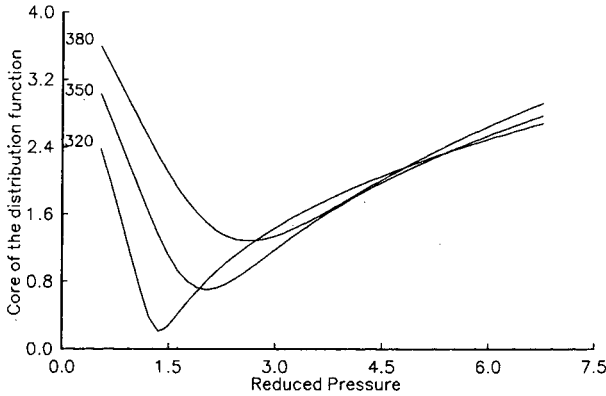


Fig. 3. Relationship between the "core" of the distribution function and reduced pressure for CO<sub>2</sub> at 320, 350 and 380 K.

COLUMN AVERAGES

Typical inlet and outlet pressures were selected and the corresponding densities calculated from the equation of state. The positional and temporal average densities were calculated using the seventh-order polynomial for the core of the distribution function (eqn. 14):

The mean density

$$\bar{\rho}_R = \frac{\rho_{R,i} + \rho_{R,o}}{2} \tag{15}$$

The spatial average density

$$\langle \rho_R \rangle_x = \frac{\sum_{j=3}^{10} c_{j-3}(\rho_{R,i}^j - \rho_{R,o}^j)/j}{\sum_{j=2}^9 c_{j-2}(\rho_{R,i}^j - \rho_{R,o}^j)/j} \tag{16}$$

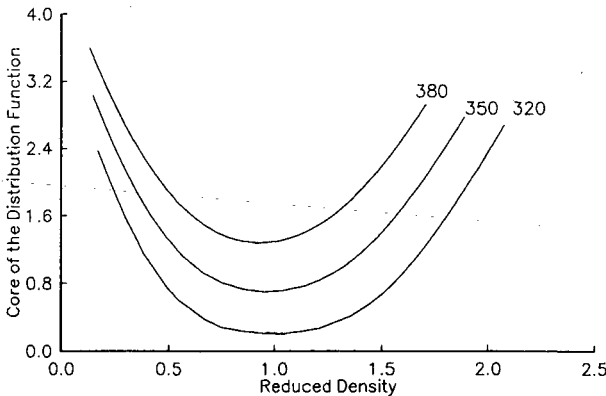


Fig. 4. Relationship between the "core" of the distribution function and reduced density for CO<sub>2</sub> at 320, 350 and 380 K.



The temporal average density

$$\langle \rho_R \rangle_t = \sum_{j=4}^{11} c_{j-4} (\rho_{R,i}^j - \rho_{R,0}^j) / j \left/ \sum_{j=3}^{10} c_{j-3} (\rho_{R,i}^j - \rho_{R,0}^j) / j \right. \quad (17)$$

Table V summarizes the results for selected outlet and inlet pressures at 320 K. Note that for a pressure drop of 50 bar, there is a significant difference between the positional and temporal average densities for low outlet densities, but they are essentially equal if the outlet density is high.

#### COLUMN AVERAGE (OBSERVED) CAPACITY FACTOR

The observed or apparent capacity factor was calculated assuming the form  $k'_{\text{local}} = k'_0 \exp(a\rho + b\rho^2)$  for the local capacity factor, where  $k'_0$  refers to the zero-density value. The constants for this expression were calculated for heptadecane and octadecane from ref. 6:

$$\ln k'_0 = -(4.43 + 0.784n) + [(1.09 + 1.676n)/T_R]$$

$$a = (0.40 + 0.595n) - (0.97 + 1.448n)/T_R$$

$$b = (0.17 + 0.260n)/T_R \quad (18)$$

TABLE V  
AVERAGE DENSITIES AT 320 K

$P_i$ (bar)	$\rho_{R,i}$	$P_0$ (bar)	$\rho_{R,0}$	$\bar{\rho}_R^a$	$\langle \rho_R \rangle_x^b$	$\langle \rho_R \rangle_t^c$
80	0.49	70	0.38	0.44	0.44	0.44
90	0.67	70	0.38	0.53	0.51	0.53
100	0.96	70	0.38	0.67	0.62	0.67
110	1.21	70	0.38	0.80	0.76	0.85
120	1.35	70	0.38	0.87	0.88	0.99
130	1.44	70	0.38	0.91	0.97	1.09
110	1.21	100	0.96	1.08	1.10	1.10
120	1.35	100	0.96	1.16	1.19	1.20
130	1.44	100	0.96	1.20	1.26	1.28
140	1.51	100	0.96	1.23	1.31	1.33
150	1.56	100	0.96	1.26	1.35	1.37
160	1.60	100	0.96	1.28	1.39	1.41
140	1.51	130	1.44	1.48	1.48	1.48
150	1.56	130	1.44	1.50	1.50	1.51
160	1.60	130	1.44	1.52	1.53	1.53
170	1.63	130	1.44	1.54	1.55	1.55
180	1.66	130	1.44	1.55	1.57	1.57
190	1.69	130	1.44	1.57	1.59	1.59

<sup>a</sup> See eqn. 15.

<sup>b</sup> See eqn. 16.

<sup>c</sup> See eqn. 17.

where  $n$  = number of carbon atoms in the alkane. The numerator in eqn. 5 was evaluated numerically using a numerical integration routine [7].

The separation factor,  $\alpha$ , for heptadecane and octadecane was calculated from

$$\alpha = \frac{\langle k' \rangle_{t,C_{18}}}{\langle k' \rangle_{t,C_{17}}} \quad (19)$$

The approximation

$$\langle k' \rangle_t \approx k_0 \exp(a \langle \rho_R \rangle_t + b \langle \rho_R^2 \rangle_t)$$

or

$$\ln \langle k' \rangle_t \approx \ln k_0 + a \langle \rho_R \rangle_t + b \langle \rho_R^2 \rangle_t \quad (20)$$

was tested. As expected [1], the estimated value is always less than or equal to the value for  $\ln \langle k' \rangle_t$  calculated from eqn. 5, and is essentially equal to the calculated value if the outlet density is close to the inlet density (as in capillary SFC) or if the outlet density is significantly greater than the critical density (Fig. 5). The estimated  $\alpha$  values are also close to the calculated values under these conditions. In general, low densities produce higher  $\alpha$  values. For a given outlet pressure, low density drops also produce higher  $\alpha$  values. Although high densities and/or high density drops lead to shorter analysis times, large density drops are undesirable because they may lead to greater band broadening [8]. As long as the chromatographic conditions are in the region where the estimates are close to the calculated values, both  $\ln \langle k' \rangle$  and  $\alpha$  can be easily estimated for a given set of conditions if the local capacity factors are known. The temporal average density can be replaced by the arithmetic mean density, thus simplifying the calculation. However, the column average density is significantly different from the inlet density, so the capacity factor cannot be approximated using the inlet density alone. The results are summarized in Table VI where column 1 is the temporal average density from Table V.

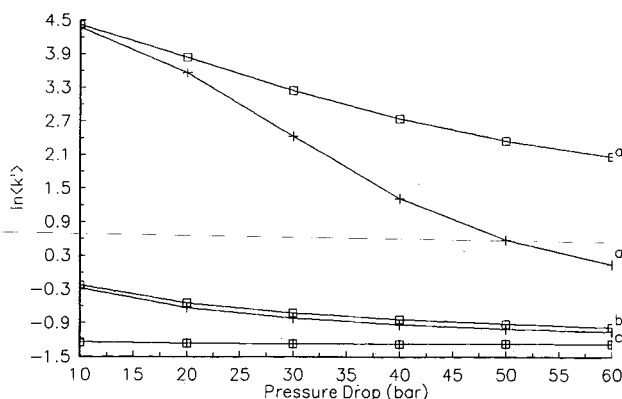


Fig. 5. Average capacity factor as a function of pressure drop. (□) Calculated from eqn. 5; (+) estimated from eqn. 20. (a)  $P_0 = 70$  bar; (b)  $P_0 = 100$  bar; (c)  $P_0 = 130$  bar.

TABLE VI  
CALCULATED AND ESTIMATED  $\ln \langle k' \rangle$  VALUES

$\langle \rho_R \rangle_t$	$\ln \langle k' \rangle$ Num. <sup>a</sup> C <sub>17</sub>	$\ln \langle k' \rangle$ Est. <sup>b</sup> C <sub>17</sub>	$\ln \langle k' \rangle$ Num. <sup>a</sup> C <sub>18</sub>	$\ln \langle k' \rangle$ Est. <sup>b</sup> C <sub>18</sub>	$\alpha$ Num. <sup>c</sup>	$\alpha$ Est. <sup>d</sup>
<i>P</i> <sub>0</sub> = 70 bar ( $\rho_{R,0}$ = 0.38)						
0.44	4.42	4.37	4.89	4.83	1.61	1.60
0.53	3.84	3.56	4.29	3.98	1.57	1.53
0.67	3.25	2.44	3.69	2.80	1.56	1.43
0.85	2.74	1.32	3.18	1.62	1.55	1.34
0.99	2.36	0.59	2.80	0.85	1.55	1.29
1.09	2.08	0.15	2.51	0.38	1.54	1.26
<i>P</i> <sub>0</sub> = 100 bar ( $\rho_{R,0}$ = 0.96)						
1.10	-0.23	-0.28	-0.02	-0.07	1.24	1.23
1.20	-0.55	-0.63	-0.35	-0.44	1.22	1.20
1.28	-0.72	-0.82	-0.54	-0.64	1.21	1.19
1.33	-0.84	-0.93	-0.66	-0.76	1.20	1.19
1.37	-0.92	-1.01	-0.74	-0.84	1.19	1.18
1.41	-0.97	-1.06	-0.80	-0.89	1.19	1.18
<i>P</i> <sub>0</sub> = 130 bar ( $\rho_{R,0}$ = 1.44)						
1.48	-1.25	-1.25	-1.09	-1.09	1.16	1.16
1.51	-1.26	-1.26	-1.11	-1.11	1.16	1.16
1.53	-1.27	-1.27	-1.12	-1.12	1.16	1.16
1.55	-1.28	-1.28	-1.12	-1.12	1.16	1.16
1.57	-1.27	-1.27	-1.12	-1.12	1.16	1.16
1.59	-1.27	-1.27	-1.12	-1.12	1.16	1.16

<sup>a</sup> Numerical integration of eqn. 5.  
<sup>b</sup> Estimated from eqn. 20.  
<sup>c</sup> Determined from numerically integrated values of  $\ln \langle k' \rangle$ .  
<sup>d</sup> Determined from estimated values of  $\ln \langle k' \rangle$ .

COLUMN PROFILES

The density decrease over the column was divided into ten equally spaced density decrements from the inlet to the outlet density. Profiles for the mobile phase were generated using eqns. 6 and 7 and the core of the distribution function:

$$x/L = \sum_{j=2}^9 c_{j-2}(\rho_{k,i}^j - \rho_k^j)/j \bigg/ \sum_{j=2}^9 c_{j-2}(\rho_{k,i}^j - \rho_{k,0}^j)/j \tag{21}$$

$$\frac{\tau_u}{t_u} = \sum_{j=3}^{10} c_{j-3}(\rho_{k,i}^j - \rho_k^j)/j \bigg/ \sum_{j=3}^{10} c_{j-3}(\rho_{k,i}^j - \rho_{k,0}^j)/j \tag{22}$$

The fractional solute migration time was calculated by numerical integration of eqn. 8. The results are summarized in Table VII. Note that when the mobile phase has spent 50% of its time on the column, it has traversed 47% of the column length. At this point, the reduced density is 1.11, compared to 1.09, the arithmetic mean density. Hence, the mobile phase spends *relatively* more time in the inlet region of the column. The solutes

TABLE VII  
COLUMN PROFILES

$T = 320$  K,  $P_0 = 100$  bar,  $P_i = 110$  bar.

$\rho_R$	$x/L^a$	$\tau_u/t_u^b$	$\tau_s/t_s^c$ $C_{17}$	$\tau_s/t_s^c$ $C_{18}$	$\alpha^d$
1.21	0.00	0.00	0.00	0.00	—
1.19	0.13	0.14	0.12	0.12	1.20
1.16	0.25	0.27	0.24	0.23	1.21
1.14	0.37	0.39	0.34	0.33	1.21
1.11	0.47	0.50	0.44	0.43	1.21
1.09	0.57	0.60	0.54	0.53	1.21
1.06	0.66	0.69	0.63	0.62	1.22
1.04	0.75	0.78	0.72	0.71	1.22
1.01	0.84	0.85	0.82	0.81	1.23
0.99	0.92	0.93	0.91	0.90	1.23
0.96	1.00	1.00	1.00	1.00	1.24

<sup>a</sup> See eqn. 21.

<sup>b</sup> See eqn. 22.

<sup>c</sup> See eqn. 8.

<sup>d</sup> See eqn. 19.

are moving relatively more quickly because they have a much smaller  $k'$  in the higher-density inlet part. The effective separation factor,  $\alpha$ , which is defined as the ratio of temporal average capacity factors of the two solutes at a given value of  $x/L$ , increases as the column is traversed. This does not necessarily imply, however, that longer columns will produce better separations. The change in  $\alpha$  is a pressure-drop-induced effect; the same pressure drop can also cause increased band spreading [8]. Indeed, it is conceivable that shorter columns could provide separations with resolution equal or superior to that from longer columns.

## CONCLUSIONS

If the pressure drop over a column is small, or if the outlet density is sufficiently greater than the critical density, the arithmetic mean density, the positional average density and the temporal average density are nearly identical. The average capacity factor can then be related to the local capacity factor and the average density using any of the density averages and eqn. 20. However, if the density drop is large and encompasses the region where the core of the distribution function goes through a minimum (Fig. 4), the average capacity factor must be calculated using eqn. 5 and a numerical integration routine. It is then difficult to relate the observed capacity factor to the local capacity factor. This problem is still under investigation. It is also possible that Darcy's law may not be applicable when pressure drops are high since high mobile-phase velocities may lead to turbulence. A simpler expression for the core of the distribution function would lead to more tractable expressions for both the density averages and the apparent capacity factor.

## ACKNOWLEDGEMENTS

This material is based upon work supported at Georgetown University by the National Science Foundation under Grant CHE-8902735, which the authors gratefully acknowledge. The Bush Sabbatical Program of the University of Minnesota is also thanked for partial support of D.P. T.B. acknowledges support of the Gas Research Institute and the U.S. Department of Energy.

## REFERENCES

- 1 D. E. Martire, *J. Chromatogr.*, 461 (1989) 165.
- 2 R. T. Jacobsen and R. J. Stewart, *J. Phys. Chem. Ref. Data*, 2 (1973) 757.
- 3 J. F. Ely, *Proceedings of the 63rd Gas Processors Association Annual Convention*, Gas Processors Association, Tulsa, OK, 1984, pp. 9-22.
- 4 G. Arfken, *Mathematical Methods for Physicists*, Academic Press, Orlando, FL, 3rd ed., 1985, p. 964.
- 5 K. Stephan and K. Lucas, *Viscosity of Dense Fluids*, Plenum Press, New York and London, 1979.
- 6 D. E. Martire and R. E. Boehm, *J. Phys. Chem.*, 91 (1987) 2433.
- 7 T. E. Sharp, *Applied Numerical Methods for the Microcomputer*, Prentice-Hall, Englewood Cliffs, NJ, 1984.
- 8 D. P. Poe and D. E. Martire, *J. Chromatogr.*, 517 (1990) 3.



## Factors governing the analytical supercritical fluid extraction and supercritical fluid chromatographic retention of polycyclic aromatic hydrocarbons

JOSEPH REIN, CINDY M. CORK and KENNETH G. FURTON\*

*Department of Chemistry, Florida International University, University Park, Miami, FL 33199 (USA)*

(First received November 13th, 1990; revised manuscript received February 19th, 1991)

---

### ABSTRACT

The molecular connectivity of polycyclic aromatic hydrocarbons (PAHs) correlates well with retention data for several supercritical fluid chromatographic systems. The quantitative effect of microextractor cell geometry on supercritical fluid extraction (SFE) efficiencies of PAHs from octadecyl-bonded sorbents is compared with that seen upon varying the fluid density for the same system. Relative recoveries were increased by up to a factor of two, for coronene, by employing short broad extraction vessels, 1:1 length:I.D., compared to using long narrow vessels, 20:1 length:I.D. The average relative recovery increase was 121% with a large dependence on compound type, increasing *ca.* linearly with fused ring number for the PAHs studied. A similar relative recoveries increase was achievable by increasing the fluid density by 0.12 g ml<sup>-1</sup> with a small dependence on the compound type (decreasing linearly with fused ring number).

---

### INTRODUCTION

Although Hannay and Hogarth [1] reported the high solvating power of supercritical fluids over a century ago, practical applications of supercritical fluids did not begin to emerge until relatively recently. Two of these techniques are supercritical fluid chromatography (SFC), introduced by Klesper *et al.* [2], and supercritical fluid extraction (SFE), first demonstrated by Zosel [3]. These techniques have received a great deal of attention in recent years as the full potential of supercritical fluids in analytical chemistry has begun to emerge [4,5]. SFE has developed into an important industrial-scale extraction technique as an alternative to distillation and traditional solvent extractions. Recently, the use of SFE on an analytical-scale has received a great deal of attention. SFE can potentially provide more rapid, efficient and selective extractions compared to conventional extraction techniques. Analytical-scale SFE using supercritical CO<sub>2</sub> has been applied to the recovery of a variety of non-polar volatiles and semi-volatiles from solids and adsorbents with up to an order of magnitude increase in the rate of extraction reported compared to conventional methods [6–12].

Supercritical fluids possess unique physicochemical properties which make them attractive as solvents for extraction and chromatography. Supercritical fluids

have densities (and solvating powers) approaching that of liquids, which are readily changed by varying the temperature and pressure. Supercritical fluids have gaslike transport properties of viscosity and intermediate diffusivity. Additionally, the zero surface tension of supercritical fluids allows for efficient penetration into macroporous materials. SFE can be used on-line, combined with gas, liquid or supercritical chromatography, to provide a complete sample extraction and analysis system, or can be employed off-line, replacing many conventional liquid solvent techniques. On-line methods provide the greatest sensitivity and, in principle, should be more accurate, due to the reduced sample handling. Off-line methods allow the greatest experimental flexibility (*e.g.* fluid type, modifiers, flow-rate, etc.) and the possibility of multiple analysis of the extract regardless of the sample conditions (*e.g.* matrix and concentration). A more thorough discussion of SFE and applications can be found in refs. [13–15].

Extraction of compounds from solid sorbents is controlled by many of the same factors which control SFC retention. These include the affinity of the compounds for the sorbent, the vapor pressure of the compounds, and the solubility and diffusion coefficient of the compounds in the supercritical fluid. Therefore, SFC retention data can be useful in predicting potential SFE recoveries for compounds or classes of compounds, and may provide insight into the processes involved in supercritical extraction. Qualitative correlations between SFC retention and supercritical fluid extractability have been reported [16,17], and, recently, we have demonstrated quantitative correlations for polycyclic aromatic hydrocarbons (PAH's) using octadecyl sorbents [18]. In addition to the above factors, SFE efficiencies are controlled by a complex relationship between many experimental variables, including the density (controlled by pressure), temperature, extraction cell geometry, compound type, fluid type, fluid modifiers, flow-rate, sample matrix, etc. Although it is well established that, to a first approximation, the solvent power of a supercritical fluid is related to its density, little is known about the relative effects of many of the other controllable variables for analytical-scale SFE. A better understanding of the relative effects of controllable SFE variables is needed to more readily allow SFE extractions to be optimized for maximum selectivity as well as maximum overall recoveries.

## EXPERIMENTAL

### *Apparatus*

The extraction apparatus used for this work was constructed from an Isco 260D syringe pump, Valco C6W valve, Fiatron heater and controller, and linear restrictors fabricated from 41  $\mu\text{m}$  I.D.  $\times$  362  $\mu\text{m}$  O.D. fused silica (polymicro Technologies, Phoenix, AZ, USA). HPLC guard columns with 2- $\mu\text{m}$  stainless steel frits (Upchurch Scientific, Oak Harbor, WA, USA) were used for the extraction cells. SFC grade carbon dioxide (Scott Specialty Gases, Plumsteadville, PA, USA) was used for all of the extractions. The packed-column supercritical fluid chromatograph used to generate the chromatographic retention data was constructed from a computer (Zenith)-controlled Isco SFC-500 high-pressure syringe pump (Lincoln, NE, USA), Valco C14W 0.5- $\mu\text{l}$  injection valve, Isco 1 mm I.D. microbore  $\text{C}_{18}$  column, Fiatron column heater and controller (Oconomowoc, WI, USA), and an Isco V<sup>4</sup> UV-Vis detector with 6000 p.s.i. flow cell. Data were collected with an E-Lab Chromatographic control and data acquisition system (OMS Tech, Miami, FL, USA).



*Reagents and procedure*

Methoxychlor, naphthalene, anthracene, fluorene, pyrene, perylene, benzo[ghi]perylene, and coronene were obtained from Aldrich (Milwaukee, WI, USA). Chloroform (Fisher 'Optima') was used to prepare all solutions. The octadecyl coated silica support from 50 1000-mg Prep Sep (Fisher) C<sub>18</sub> solid-phase extractions cartridges was used to prepare a stock packing used for all of the extractions. An amount of 50 g of the octadecyl packing containing 200 ppm of each PAH was prepared from a chloroform solution with evaporation from a packing flask using a rotary evaporator. Extractions were performed on 520-mg samples of the standard packing contained in cells of two different geometries: one short with 1.0 × 1.0 cm dimensions, and the other long, with 7.3 × 0.37 cm dimensions (length of bed × I.D.). The total volume of the sorbent beds were *ca.* 0.79 cm<sup>3</sup> for both cells, with the short cell having a 1:1 length to diameter ratio of and the long cell a 20:1 length to diameter ratio. Extractions were performed with carbon dioxide at 100.0°C at an average flow-rate of 600 μl min<sup>-1</sup>, controlled by varying the length of a linear capillary restrictor. Blockages were minimized by heating the length of the fused-silica capillary and agitating the collection vessel in an ultrasonic bath (Branson, Shelton, CT, USA). Each extraction was carried out with the same total volume of carbon dioxide. The extracted compounds were collected by inserting the end of the outlet restrictor into a 10-ml volumetric flask containing several milliliters of absolute ethanol. An amount of 2.5 μg of fluorene was added to the volumetric flask as an external standard. Identification and quantitation of the extracted standard PAHs was performed using a Hewlett-Packard Model 5890 Series II GC and a HP5971 MSD or flame ionization detection.

## RESULTS AND DISCUSSION

SFC retention data for the PAHs studies is listed in Table I, along with some physical and spectroscopic properties for these compounds. The widely differing physical and spectroscopic properties of these compounds can make their separation

TABLE I

PHYSICAL, SPECTROSCOPIC AND SFC CHROMATOGRAPHIC PROPERTIES OF PAHs STUDIED

PAH	Formula	Melting point (°C)	Boiling point <sup>a</sup> (°C)	λ <sub>max</sub> (nm)	k (C <sub>18</sub> )	k <sup>b</sup> (Al)	k <sup>c</sup> (Si)
Naphthalene	C <sub>10</sub> H <sub>8</sub>	81	218	275	0.54	0.48	0.23
Anthracene	C <sub>14</sub> H <sub>10</sub>	217	340	251	1.97	1.50	0.81
Pyrene	C <sub>16</sub> H <sub>10</sub>	150	404S	240	4.07	2.60	1.35
2,3-Benzanthracene	C <sub>18</sub> H <sub>12</sub>	347	380S	274	6.26	3.55	1.99
Perylene	C <sub>20</sub> H <sub>12</sub>	274	340S	252	14.10	5.20	—
Benzo[ghi]perylene	C <sub>22</sub> H <sub>14</sub>	278	> 500	299	26.03	—	—
Coronene	C <sub>24</sub> H <sub>12</sub>	427	525	301	50.16	10.00	5.71

<sup>a</sup> S = sublimes.

<sup>b</sup> Data from ref. 20.

<sup>c</sup> Data from ref. 21.

and identification difficult. The chromatogram for the isoconfertic (having constant density)-isothermal SFC separation of the PAHs on the C<sub>18</sub> column, used to generate the  $k$  value listed in Table I, is shown in Fig. 1. Fig. 1 illustrates the difficulty in achieving complete separation and the difficulty in finding a single UV wavelength that gives sensitive detection of all of the PAHs studied. Although considerable progress has been made in recent years, the relationships between solute properties and their retention in supercritical fluid chromatography is still not well understood. Correlations between various physicochemical parameters of solutes and their chromatographic retention (*e.g.* capacity factor,  $k$ ) may provide valuable insights into the dominant retention mechanisms and may provide useful predictive information for establishing optimum experimental parameters [19]. A variety of physical parameters have been shown to correlate with chromatographic retention. A list of several of these parameters for the PAHs studied is given in Table II.

These parameters are different measures of molecular structure for the PAHs studied. In general, molecular structure can be broken down into three primary elements; namely, the number of atoms, the kinds of atoms, and the linking pattern or bonding scheme of the atoms. Therefore, the more accurately a parameter incorporates these three elements, the more useful the parameter will be in describing molecular structure. Molecular weight and, particularly, Van der Waals volume are good indicators of the size of molecules, but may actually underestimate the bonding scheme and aromaticity contribution to molecular structure. Molecular polarizability and number of fused rings may overestimate the bonding scheme and aromaticity contribution to molecular structure. The correlation factor and molecular connectivity are indexes derived in an attempt to more accurately describe overall molecular structure. The correlation factor,  $F$ , is an index empirically derived from  $\log k$  values for PAHs on C<sub>18</sub> high-performance liquid chromatographic (HPLC) columns calcu-

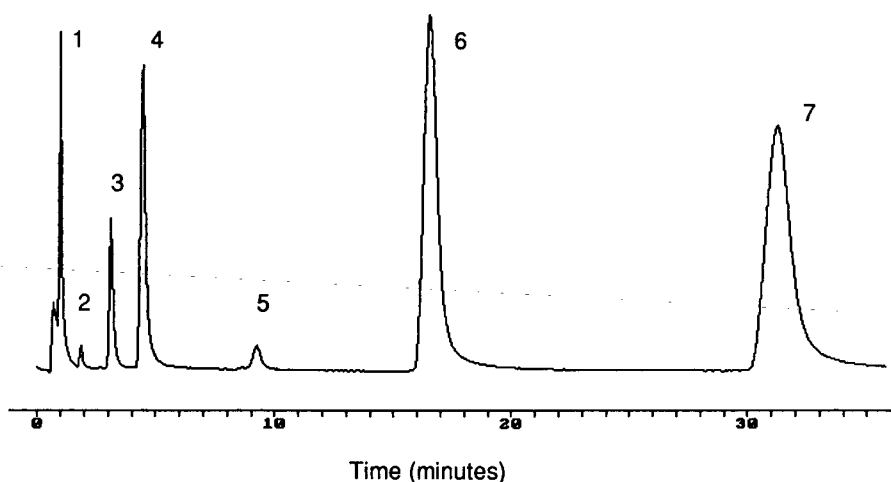


Fig. 1. A chromatogram for an isoconfertic (having constant density)-isothermal SFC separation of 1 ppm mixture of the PAHs on an octadecyl-bonded packed column with supercritical carbon dioxide mobile phase. Column temperature 100°C; UV detector at 290 nm. Peaks: 1 = naphthalene; 2 = anthracene; 3 = pyrene; 4 = 2,3-benzanthracene; 5 = perylene; 6 = benzo[ghi]perylene; 7 = coronene.

TABLE II  
VARIOUS PHYSICAL PARAMETERS FOR THE POLYCYCLIC AROMATIC HYDROCARBONS STUDIED

PAH	Molecular weight (g)	Fused ring number	Correlation factor (F)	Van der Waals volume ( $\text{\AA}^3$ )	Average molecular polarizability ( $\alpha$ )	Molecular connectivity ( $\chi$ )
Naphthalene	128.17	2	5.0	127.1	17.48	3.40
Anthracene	178.23	3	7.0	170.0	25.93	4.81
Pyrene	202.26	4	8.0	185.5	29.34	5.56
2,3-Benzanthracene	228.29	4	9.0	213.9	32.86	6.22
Perylene	252.32	5	10.0	229.0	38.84	6.98
Benzo[ghi]perylene	276.34	6	11.0	243.8	41.31	7.72
Coronene	300.36	7	12.0	259.2	42.50	8.46

lated as follows [22]:  $F = \text{number of double bonds} + \text{the number of primary and secondary carbons} - 0.5$  for a nonaromatic ring.

A more generally applicable index is molecular connectivity. Molecular connectivity has been extensively applied as a structure-based approach to biological quantitative structure-activity analysis and has proven to be a useful tool for establishing relationships between molecular structure and various physicochemical properties [23]. The term molecular connectivity is a descriptive title for indexes from molecular structure [24]. For the PAHs studied, the simplest form of the index can be used. Each carbon atom is designated by a cardinal number called the delta value,  $\delta$ , which is a count of adjacent or formally bonded carbon atoms. The molecular structure can then be dissected into all constituent bonds formed between carbon atoms  $i$  and  $j$ . Using the Randic algorithm [25], a value for each bond is computed. The molecular connectivity index,  $\chi$ , is a simple sum of these bond values over the entire molecule as follows:

$$\chi = \sum (\delta_i \delta_j)^{-0.5}$$

#### *Correlation between SFC data and various parameters*

A linear correlation has previously been reported between the logarithm of SFC capacity factors and fused ring number of PAHs [26]. Correlations between the number of fused rings and SFC retention parameters can only apply to a first approximation, as it is well known that PAHs with the same number of fused rings can have different retention characteristics as seen by the separation of pyrene (peak 3) and 2,3-benzanthracene (peak 4) in Fig. 1. However, fused ring number may be a useful parameter, particularly when comparing PAHs of similar symmetry and those with widely differing number of fused rings. For the present data, we did not observe a linear correlation between  $\log k$  and fused ring number. In fact, the correlation appears to be logarithmic with fused ring number as seen in Fig. 2 for three different types of SFC systems. The logarithmic curve fit through the data demonstrates the generally good agreement, but also illustrates the limitation in using this parameter, with the data for the four fused ring PAHs, pyrene and 2,3-benzanthracene, lying above and below the fitted line for each plot. This logarithmic relationship is not

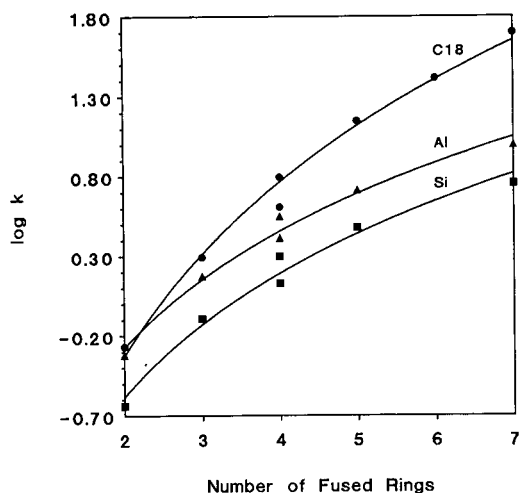


Fig. 2. Plot of  $\log k$  vs. the number of fused rings for PAHs. C<sub>18</sub> = octadecyl column, 100°C, 300 atm, supercritical carbon dioxide mobile phase; Al = alumina column, 245°C, 47 atm, supercritical isopropanol mobile phase; Si = silica gel column, 260°C, 40 atm, supercritical ethanol-hexane (10:90) mobile phase.

surprising for the alumina and silica gel systems, as it is well known that in adsorption chromatography the following equation is valid [27].

$$\log R^0 = \log V_a + aS^0$$

where  $R^0$  is the specific retention volume,  $V_a$  and  $a$  are parameters characterizing the adsorbent activity, and  $S^0$  the so-called adsorption energy of the compound. It is surprising, however, to see an apparent logarithmic relationship for the partitioning system, octadecyl column, when linear relationships with physical parameters have been reported previously (*e.g.* 19, 28).

To determine which parameters are most generally useful in predicting SFC retention, we plotted  $\log k$  vs. each parameter, as well as  $\log k$  vs.  $\log$  (parameter) for the three systems studied. The correlation coefficients for the plots are summarized in Table III in order of best to worst correlation for the parameters studied. For all of the parameters discussed above, with the exception of fused ring number, good linear correlation was seen with the retention data for the octadecyl system. A logarithmic correlation was seen for all of the parameters on the adsorbent systems, alumina and silica gel. Plots with fused ring number and average molecular polarizability, which emphasize the aromaticity of the molecule, generally showed the poorest correlation. Plots with Van der Waals volumes, which emphasize the physical size of the molecule, generally showed better correlation, and molecular weight plots yielded correlation coefficients greater than 0.998. Although the correlation factor demonstrated even better correlation than molecular weight, the parameter which yields near perfect correlation was molecular connectivity ( $r = 0.9995$  to  $0.9999$ ), as seen in Fig. 3. As molecular connectivity is relatively simple to calculate for any compound, not just PAHs, this parameter appears to be the most generally useful in describing and predicting retention in SFC.

TABLE III

CORRELATION COEFFICIENTS BETWEEN LOG  $k$  AND VARIOUS PARAMETERS FOR THREE DIFFERENT SFC SYSTEMS

Parameter	Linear plot Log plot	Column type		
		Octadecyl	Alumina	Silica
Molecular connectivity	Linear	0.9995	0.9875	0.9848
	Log	0.9903	0.9997	0.9999
Correlation factor	Linear	0.9991	0.9888	0.9865
	Log	0.9894	0.9995	0.9999
Molecular weight	Linear	0.9988	0.9896	0.9876
	Log	0.9886	0.9992	0.9998
Van der Waals volume	Linear	0.9927	0.9920	0.9919
	Log	0.9806	0.9954	0.9970
Average molecular polarizability	Linear	0.9915	0.9901	0.9953
	Log	0.9763	0.9928	0.9980
Number of fused rings	Linear	0.9872	0.9530	0.9475
	Log	0.9940	0.9925	0.9889

*Correlation between cell geometry and SFE recoveries*

To quantify the effect of extraction cell geometry on SFE efficiencies, care was taken to ensure that all of the other controllable experimental variables were kept constant. Temperature, pressure (and, therefore, density), flow-rates, and total volumes were accurately controlled and measured. Extraction conditions were purposely chosen to yield less than quantitative recovery of the PAHs to allow comparisons to

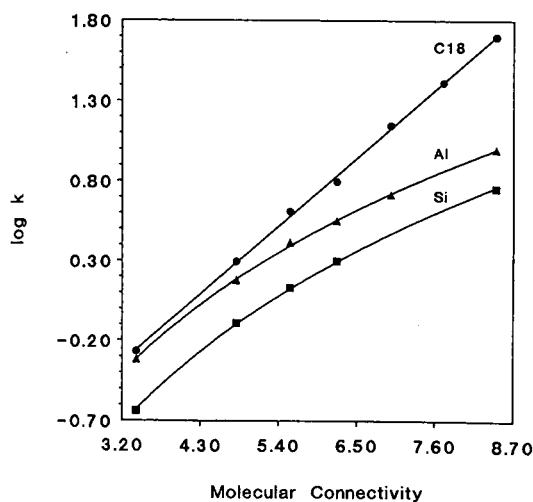


Fig. 3. Plot of  $\log k$  vs. the molecular connectivity for PAHs.  $C_{18}$  = octadecyl column, 100°C, 300 atm, supercritical carbon dioxide mobile phase; Al = alumina column, 245°C, 47 atm, supercritical isopropanol mobile phase; Si = silica gel column, 260°C, 40 atm, supercritical ethanol-hexane (10:90) mobile phase.

be made between the different extraction cell geometries. Unfortunately, conditions required to yield reproducible recoveries of coronene ( $> 1\%$ ) resulted in quantitative ( $> 90\%$ ) recoveries of naphthalene and anthracene, and, therefore, only the last four PAHs were useful for comparative purposes. The average recoveries for the PAHs from octadecyl packings for two different cell geometries have been reported previously [18]. The average percent recoveries [and standard deviations] for the compounds pyrene, perylene, benzo[ghi]perylene, and coronene using the 20:1 (length:I.D.) cell were 60.4 [0.9], 17.1 [0.6], 6.5 [0.7], and 1.7 [0.2], respectively. The average percent recoveries [and standard deviations] for the compounds pyrene, perylene, benzo[ghi]perylene, and coronene using the 1:1 (length:I.D.) cell were 80.4 [1.6], 35.8 [0.8], 15.4 [1.4], and 5.2 [0.3], respectively. Each sample was extracted at  $100.0^{\circ}\text{C}$  and 4500 p.s.i. (density =  $0.675\text{ ml}^{-1}$ ) at an average flow-rate of  $600\ \mu\text{l min}^{-1}$ , with a total of 7.5 ml of carbon dioxide.

If the dominant factors which control SFC retention are the same as those controlling SFE, one would expect to see a similar linear correlation between molecular connectivity and the logarithm of the observed recoveries. Fig. 4 shows the plots for the logarithms of the SFC capacity factors and the SFE recoveries for the two different cell geometries studied. Although there is obvious curvature with the SFE recovery data, the linear correlation coefficient appears to improve as the extraction cell geometry is increased (made more column-like). For example, a linear least squares regression analysis for the 1:1 geometry cell yields a  $r = 0.973$ ; whereas, the 20:1 cell geometry yields a  $r = 0.985$ . Surprisingly, good correlation is seen when the percent recoveries are directly correlated to molecular connectivity, although an opposite effect is seen with cell geometry. As the cell geometry is reduced (made less column-like) the linear correlation increases. For example, a linear least squares regression analysis for plots of percent recovery *versus* molecular connectivity for the

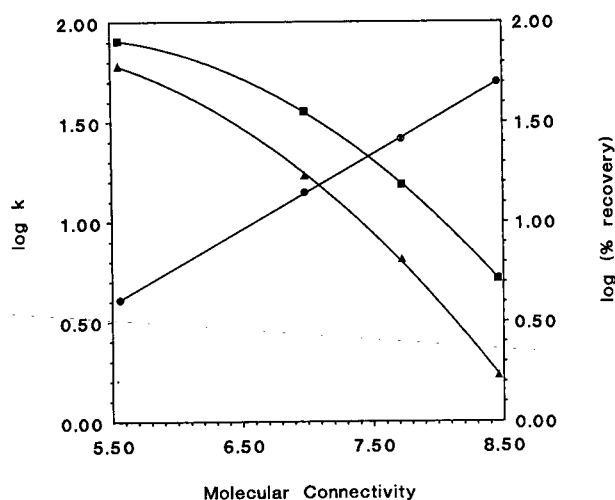


Fig. 4. Plot of  $\log k$  and  $\log (\% \text{ recovery})$  vs. molecular connectivity for pyrene, perylene, benzo[ghi]perylene, and coronene from  $\text{C}_{18}$  SFC retention data and SFE with different extraction cell geometries.  $\bullet$  = SFC;  $\blacksquare$  = SFE; 1:1 cell;  $\blacktriangle$  = SFE, 20:1 (length:I.D.) cell.

20:1 geometry cell yields a  $r = 0.962$ ; whereas the 1:1 cell geometry yields a  $r = 0.990$ . Therefore, it appears that molecular connectivity can be a useful parameter in predicting potential SFE recoveries.

The logarithms of the SFE percent recoveries show excellent linear correlation with fused ring number ( $r > 0.996$ ) for all of the extractions of the present study. Further studies are needed to determine whether there is truly a relationship between these two variables or if this is simply a fortuitous correlation. Unfortunately, the widely differing extractability of these PAHs limits the number which can be compared at a chosen set of extraction conditions, as mentioned previously. Fig. 5 shows the plots of  $\log(\% \text{ recovery})$  vs. fused ring number for PAHs using the two different cell geometries. It is obvious from this figure that PAHs with a smaller number of fused rings than those studied (*e.g.* 3) are quantitatively recovered; whereas, larger fused ring number PAHs (*e.g.* 8) are generally non-recoverable under the same experimental conditions. For all of the PAHs, a markedly higher recovery was achieved with the short broad cell (1:1) *versus* the long narrow cell (20:1). The relative increase in percent recovery using a 1:1 vs. 20:1 extraction cell geometry is 33, 109, 137, and 206% for pyrene, perylene, benzo[ghi]perylene, and coronene, respectively.

#### *Correlation between fluid density and SFE recoveries*

One of the advantages of supercritical fluids is the ease with which the density, and effectively the solvating power, of the fluid can be changed by varying the pressure at a constant temperature. Selective extractions are possible by performing extractions at successively increasing pressures while keeping the temperature constant. Data for one such extraction is given in Table IV, for successive 3.2-ml supercritical carbon dioxide extractions at 100°C and pressures of 2000 p.s.i. (density = 0.30 g ml<sup>-1</sup>), 3000 p.s.i. (density = 0.49 g ml<sup>-1</sup>), 4000 p.s.i. (density = 0.63 g ml<sup>-1</sup>), and

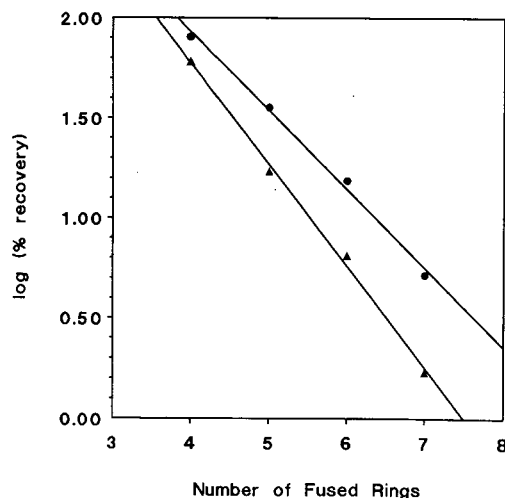


Fig. 5. Plot of  $\log(\% \text{ recoveries})$  for supercritical  $\text{CO}_2$  extractions vs. the number of fused rings for pyrene, perylene, benzo[ghi]perylene, and coronene using a 1:1 extraction cell geometry (●) and a 20:1 extraction cell geometry (▲). Extraction conditions: 100°C; 4500 p.s.i. (density = 0.675 g ml<sup>-1</sup>); flow-rate = 0.6 ml min<sup>-1</sup>; total volume of carbon dioxide used for each extraction = 7.5 ml.

TABLE IV

RECOVERY (%) OF PAHs FROM AN OCTADECYL-BONDED PACKING AT SUCCESSIVELY INCREASING PRESSURES AT 100°C

Analyte	% Recovery (ca. 5% R.S.D.) <sup>a</sup>			
	2000 p.s.i.	3000 p.s.i.	4000 p.s.i.	5000 p.s.i.
Naphthalene	61.0	>97	—	—
Anthracene	8.9	42.9	>97	—
Pyrene	0.2	18.0	48.9	>97
Perylene	0.0	7.3	18.3	34.4
Benzo[ghi]perylene	0.0	3.2	7.0	13.8
Coronene	0.0	0.0	2.1	4.0

<sup>a</sup> R.S.D. = Relative standard deviation.

5000 p.s.i. (density = 0.71 g ml<sup>-1</sup>). Again, correlation is observed between the log (% recovery) and fused ring number as seen in excellent linear correlation ( $r > 0.993$ ) for all of the compounds studied. Linear least squares regression analysis for the data yield the following equations:  $\log(\% \text{ recovery})_{\text{pyrene}} = 3.281d - 0.321$ ;  $\log(\% \text{ recovery})_{\text{perylene}} = 3.055d - 0.644$ ;  $\log(\% \text{ recovery})_{\text{benzo[ghi]perylene}} = 2.849d - 0.909$ ;  $\log(\% \text{ recovery})_{\text{coronene}} = 2.737d - 1.347$ ; where  $d$  is the density of supercritical carbon dioxide at 100°C. The relative increase in percent recovery upon increasing the supercritical carbon dioxide density 0.12 g ml<sup>-1</sup> (0.7 vs. 0.58) at 100°C is 148, 132, 120, and 113% for pyrene, perylene, benzo[ghi]perylene, and coronene, respectively (calculated from the equations above). The average relative increase in recovery, upon increasing the density 0.12 g ml<sup>-1</sup>, was 128% (standard deviation = 15%), with a

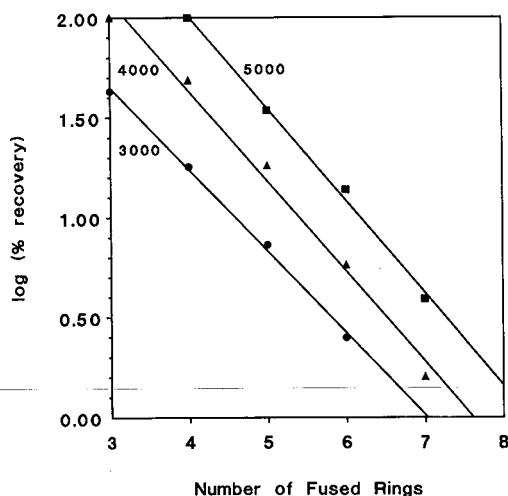


Fig. 6. Plot of log (% recoveries) for supercritical CO<sub>2</sub> extractions at 100°C vs. the number of fused rings for pyrene, perylene, benzo[ghi]perylene, and coronene at 3000, 4000 and 5000 p.s.i. Extraction conditions: 1:1 cell geometry; 100°C; flow-rate = 0.6 ml min<sup>-1</sup>; total volume of carbon dioxide used for each extraction = 3.2 ml.



small approximately linear decrease with the number of fused rings for the PAHs studied. This compares to an average relative increase in recovery, upon shortening the extraction vessel from 20:1 to 1:1 (length:I.D.), of 121% (standard deviation = 72%), with a large approximately linear increase with the number of fused rings for the PAHs studied.

The present results indicate that, of the parameters studied, molecular connectivity is the best in evaluating or predicting potential SFC retention characteristics for PAHs. For the partitioning system, octadecyl sorbent, SFC derived  $\log k$  values directly correlate with molecular connectivity; whereas, for the adsorbent systems, alumina and silica gel, linear correlation is observed with the logarithm of the molecular connectivity. The correlation of molecular connectivity with SFE recoveries of PAHs from octadecyl sorbents is dependent on the extraction cell geometry. For the long narrow extraction vessel (20:1), the molecular connectivity of the PAH shows an approximately linear correlation with the logarithm of the observed recoveries; whereas, for the short broad vessel (1:1), the molecular connectivity correlates directly with the observed recovery. Although supercritical fluid density had the greatest overall effect on achievable SFE recoveries in the present study, it is clear that other variables, including cell geometry, can have effects that are of a similar magnitude and, therefore, must be considered when optimizing a SFE system.

#### ACKNOWLEDGEMENT

Acknowledgement is made to the FIU College of Arts & Sciences Faculty Development Minigrant Program for support of this research.

#### REFERENCES

- 1 J. B. Hannay and J. Hogarth, *Proc. R. Soc. London, A*, 29 (1879) 324.
- 2 E. Klesper, A. H. Corwin and D. A. Turner, *J. Org. Chem.*, 27 (1962) 700.
- 3 K. Zosel, *Ger. Pat.* 1 493 190 (1969).
- 4 B. A. Charpentier and M. R. Sevenants (Editors), *Supercritical Fluid Extraction and Chromatography*, (ACS Symposium Series, No. 366), American Chemical Society, Washington, DC, 1987.
- 5 R. M. Smith (Editor), *Supercritical Fluid Chromatography*, The Royal Society of Chemistry, London, 1988.
- 6 M. M. Schantz and S. N. Chesler, *J. Chromatogr.*, 363 (1986) 397.
- 7 S. B. Hawthorne and D. J. Miller, *J. Chromatogr.*, 403 (1987) 63.
- 8 B. W. Wright, C. W. Wright, R. W. Gale and R. D. Smith, *Anal. Chem.*, 59 (1987) 38.
- 9 M. E. McNally and J. R. Wheeler, *J. Chromatogr.*, 435 (1988) 63.
- 10 S. B. Hawthorn, M. S. Krieger and D. J. Miller, *Anal. Chem.*, 61 (1989) 736.
- 11 J. M. Levy and A. C. Roselli, *Chromatographia*, 28 (1989) 613.
- 12 K. G. Furton and J. Rein, *Chromatographia*, 31 (1991) in press.
- 13 K. G. Furton and J. Rein, *Anal. Chim. Acta*, 236 (1990) 99.
- 14 S. B. Hawthorne, *Anal. Chem.*, 62 (1990) 633A.
- 15 M. A. McHugh and V. J. Krukonis, *Supercritical Fluid Extraction: Principles and Practice*, Butterworths, Boston, 1986.
- 16 M. E. P. McNally and J. R. Wheeler, *J. Chromatogr.*, 447 (1988) 53.
- 17 J. R. Wheeler and M. E. McNally, *J. Chromatogr. Sci.*, 27 (1989) 534.
- 18 K. G. Furton and J. Rein, *Anal. Chim. Acta*, 248 (1991) in press.
- 19 K. Jinno, M. Saito, T. Hondo and M. Senda, *Chromatographia*, 21 (1986) 219.
- 20 S. T. Sie and G. W. A. Rijnders, *Sep. Sci.*, 2 (1967) 755.
- 21 Y. Hirata, *J. Chromatogr.*, 315 (1984) 39.

- 22 J. F. Schabron and R. J. Hurtubise, *Anal. Chem.*, 49 (1977) 2253.
- 23 L. B. Kier and L. H. Hall, *Molecular Connectivity in Structure-Activity Analysis*, Wiley, New York, 1986.
- 24 L. B. Kier, L. H. Hall, W. J. Murray and M. Randic, *J. Pharm. Sci.*, 65 (1976) 1971.
- 25 M. Randic, *J. Am. Chem. Soc.*, 97 (1975) 6609.
- 26 D. Leyendecker, in R. M. Smith (Editor), *Supercritical Fluid Chromatography*, Royal Society of Chemistry, London, 1988, p. 86.
- 27 L. R. Snyder, *Principles of Adsorption Chromatography*, Marcel Dekker, New York, 1968.
- 28 K. Jinno and K. Kawasaki, *Chromatographia*, 18 (1984) 103.

## Chromatographic behaviour of diastereoisomers

### X.<sup>a</sup> Thin-layer chromatographic retentions on silica of some (*E*)- and (*Z*)-oxazolones and related cinnamates as a function of mobile phase effects or Hammett constants

M. D. PALAMAREVA\*

*Department of Chemistry, University of Sofia, Sofia 1126 (Bulgaria)*

and

B. J. KURTEV and I. KAVRAKOVA

*Institute of Organic Chemistry, Bulgarian Academy of Sciences, Sofia 1040 (Bulgaria)*

(First received August 2nd, 1990; revised manuscript received January 24th, 1991)

---

#### ABSTRACT

The thin-layer chromatographic behaviour of twenty diastereoisomeric 1,1-disubstituted 2-arylethenes [(*Z*)- and (*E*)-oxazolones and -cinnamates] on silica was studied using 40 mobile phases. The (*E*)-oxazolone and the (*Z*)-cinnamate were the stronger adsorbing isomers in all instances. The relative retentions and the retentions themselves were correlated with solvent selectivity effects or Hammett constants of the various substituents on the aryl group. Solvent selectivity effects were approximated on the basis of Snyder's theory by the parameter localization, *m*, for experiments with mobile phases of constant strength, *ε*, and by the molar fraction of one of the solvents for the experiments with binary mobile phases of increasing *ε*. According to the data obtained, electronic effects determine the model of adsorption of any *Z/E* pair and steric effects modify it, controlling the relative retention which is not affected by solvent selectivity effects and the nature of the aryl group.

---

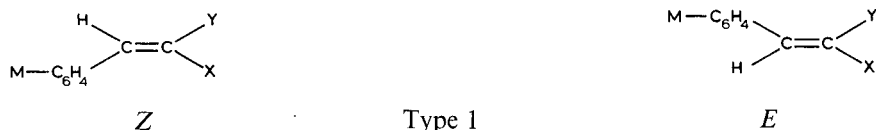
#### INTRODUCTION

This series of papers reports studies performed during the last two decades on thin-layer chromatographic (TLC) separations of over 110 diastereoisomeric pairs of tetrasubstituted ethanes and related cyclic compounds (see refs. 1 and 2 and the literature cited therein). The data obtained have been analysed on the basis of the general Snyder theory [3–5], including Soczewiński's method [6]. The relative retention of the diastereoisomers, showing which isomer is better retained, is attributed to steric hindrance control of adsorption in most instances and to mobile phase composition, or so-called solvent selectivity effects, in some particular instances. The latter

\* For Part IX, see ref. 1.

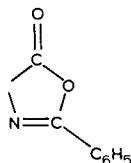
are shown to be predictable nowadays [7] on the basis of variation of the solvent localization,  $m$ , keeping the strength,  $\varepsilon$ , constant, as described in refs. 3–5. Such predictions are important in connection with the use of TLC for assigning the relative configurations of diastereoisomers [8,9]. In addition to interest in relative retention, attention has been paid to the separation  $\alpha$  (band spacing) of diastereoisomers. Maximum separation [2,7,10] corresponds to mobile phases of minimum localization,  $m$ , as predicted by the theory [5].

Broadening the type of diastereoisomers, we deal here with the TLC behaviour of  $Z$  and  $E$  isomers of 1,1-disubstituted 2-arylethenes of type 1, namely ( $Z$ )- and ( $E$ )-oxazolones and -cinnamates:



$M = \text{H}, 4\text{-Cl}, 4\text{-CH}_3, 3\text{-CH}_3\text{O}, 4\text{-CH}_3\text{O}$  or  $3\text{-NO}_2$

Cyclic compounds (oxazolones):  $X + Y =$



( $X$  is the imino group and  $Y$  is the ester group of this fragment)

Acyclic compounds (cinnamates):  $X = \text{NHCOC}_6\text{H}_5$ ,  $Y = \text{CO}_2\text{CH}_3$

This paper reports TLC retentions of twenty diastereoisomeric compounds of type 1 with 40 mobile phases which are either of constant strength,  $\varepsilon$ , or of increasing  $\varepsilon$ , being sets of binary mobile phases with various ratios of the components. The considerable database was aimed at a better understanding of the relative retention and separation of these  $Z/E$  pairs, whose TLC behaviour has been preliminarily studied [11–13]. The data obtained with mobile phases of constant  $\varepsilon$  [13] were updated using a new version of a microcomputer program [14] for the calculation of  $\varepsilon$  and  $m$  and included in this study.

## THEORY

This study used Snyder's developed displacement model [3–5] and Soczewiński's simplified model [6] concerning the mechanism in normal-phase liquid–solid chromatography (LSC).

According to Snyder's developed displacement model, the properties of mobile phases used in LSC are well understood having in mind the values of the parameter

strength,  $\epsilon$ , localization,  $m$ , and polarity,  $P'$ , being easily calculated nowadays [14]. The strength,  $\epsilon$ , is a measure of the adsorption energy of the mobile phase per unit surface area of the adsorbent and  $m$  measures the capability of the mobile phase for a given specific interaction with adsorbent sites. Polarity,  $P'$ , refers to the solvation ability of the mobile phase and is a co-parameter in determining its strength in normal-phase LSC [14].

Localization,  $m$ , is considered to be an approximation of solvent selectivity effects. The following recently derived equation describes the influence of these effects on the separation,  $\alpha$ , of a pair of compounds:

$$\log \alpha = A + Bm \quad (1)$$

where  $A$  and  $B$  are constants for a given solute pair and adsorbent. The equation has been widely verified when  $\epsilon$  is kept constant [1] or relatively constant [2,5,7,10].

Concerning diastereoisomers [1,2,7,10],  $\log \alpha$  is related to their relative retentions. Values of  $A$  correspond to the relative retention in the absence of mobile phase localization ( $m = 0$ ) and express the relative steric hindrance in diastereoisomers to adsorption [7]. According to eqn. 1, relative retention is a result of relative steric effects and relative solvent selectivity effects. On increasing the localization,  $m$ , from the minimum value up to the maximum experimental value of 1.05, relative retention will be determined by one of the two effects depending on the absolute values of the terms  $A$  and  $Bm$  in eqn. 1. The parameter  $m_{\text{crit.}} = -A/B$  obtained from eqn. 1 when  $\log \alpha$  is equal to zero indicates the intercept of the  $\log \alpha$  vs.  $m$  plot with the abscissa with a subsequent change in  $\log \alpha$  values from positive to negative and *vice versa*. Hence this value of  $m$  can predict an inversion of relative retention as a result of the dominant role of solvent selectivity effects [7].

In a simplified chromatographic system including mobile phases of two given solvents A and B in various ratios, solvent selectivity effects are approximated by the molar fraction  $N_B$  of the more polar solvent B. The basic equation proposed by Soczewiński [6] for such systems of increasing  $N_B$ , and thus increasing  $\epsilon$  [5,14], has the following two equivalent forms:

$$R_M = A - n \log X_S \quad (2)$$

$$R_M = A - n \log N_B \quad (2a)$$

where  $A$  is a constant for a given solute and set of mobile phases,  $X_S$  denotes the concentration of solvent B in the mobile phase and the slope of the plot,  $n$ , is the number of solvent molecules displaced by a solute molecule from the adsorbent surface. Eqn. 2 has been shown to be valid [9,10] for some diastereoisomers giving some information about the molecular mechanism of adsorption.

The Hammett equation [15,16], which is a tool for obtaining information on transition states in chemical reactions, seems to be applicable to the LSC of some *meta*- and *para*-substituted arenes (see ref. 3, p. 303). A convenient form of this equation for LSC systems is

$$R_{M(\text{subst.})} = R_{M(\text{unsubst.})} + \rho\sigma \quad (3)$$

where  $R_{M(\text{subst.})}$  and  $R_{M(\text{unsubst.})}$  are  $R_M$  values of *meta*- or *para*-substituted M-Ar-X and the unsubstituted arene H-Ar-X, respectively. Being the intercept of the plot,  $R_{M(\text{unsubst.})}$  presents the calculated value of  $R_M$  for the unsubstituted arene.  $\sigma$  is Hammett's constant of the substituent M, which depends mainly on its electronic effects in a corresponding position;  $\rho$  is the susceptibility of the adsorption centre X to the influence of substituent M. Positive and negative values of  $\rho$  refer to an anionic and a cationic adsorption centre X, respectively. Enhanced resonance or direct conjugation of this centre with a substituent M requires the use of the modified constants  $\sigma^-$  or  $\sigma^+$ .

## EXPERIMENTAL

The synthesis and configuration of the diastereoisomeric oxazolones **1-12** and cinnamates **13-20** in Tables II and III, respectively, have been described [12,13,17].

TLC was performed as in ref. 2 on the same type of silica. The solvents used were of analytical-reagent grade. The  $R_F$  values are arithmetic means of three to six measurements. The reproducibility of  $R_F$  was  $\pm 0.025$ . TLC with mobile phases 23-28 showed the presence of second fronts (see Table III). The diastereoisomeric pairs **7-8**, **9-10** and **11-12** were at the start with mobile phase 8 and separation was not observed, as shown in Table II. These particular data were not included in the quantitative treatments described below.

## RESULTS AND DISCUSSION

Table I lists the mobile phases used. The values of strength,  $\epsilon$ , localization,  $m$ , polarity,  $P'$ , and molar fraction,  $N_B$ , in the case of binary mobile phases were calculated by means of a microcomputer program [14] based on Snyder's theory [3-5]. The mobile phases differ significantly in their properties, based on the values of the three parameters, namely  $0.1 \leq \epsilon \leq 0.42$ ,  $-0.42 \leq m \leq 0.98$  and  $0.19 \leq P' \leq 3.79$ .

Mobile phases with strength  $\epsilon$  in the range 0.10-0.25 and 0.29-0.42 were used for TLC of oxazolones **1-12** and cinnamates **13-20**, respectively. The lower strengths  $\epsilon$  in the former instance show that cyclic compounds of type I have significantly weaker adsorption than that of acyclic compounds, and this was the reason for studying each group of compounds separately.

Tables II and III summarize the TLC data for the diastereoisomeric oxazolones and cinnamates, respectively. Except for the  $R_F$  values, they include the derived values of the separation  $\alpha$  of Z/E pairs calculated by the following equations:

$$\log \alpha = R_{M(Z)} - R_{M(E)} = A + Bm \quad (1a)$$

$$R_M = \log k' = \log (1/R_F - 1) \quad (4)$$

where  $k'$  is the capacity factor. The subscripts written in parentheses in eqn. 1a specify the isomer.

We used the definition of  $\alpha$  in eqn. 1a to express the relative retentions of the diastereoisomers in a shorter manner, namely positive and negative values of  $\log \alpha$  correspond to a stronger adsorption of Z and E isomers, respectively.

TABLE I

MOBILE PHASES STUDIED AND THE CORRESPONDING COMPUTER-CALCULATED [13,14] VALUES OF STRENGTH,  $\epsilon$ , LOCALIZATION,  $m$ , AND POLARITY,  $P'$  $N_B$  is molar fraction of the second solvent for binary mobile phases 8–16 and 29–40. Using a previous version [13] of the microcomputer program [14], the values of  $\epsilon$  were 0.233 and 0.378 for mobile phases 1–7 and 17–28, respectively.

No.	Composition (vol.%), $N_B$	$\epsilon$	$m$	$P'$
<i>For oxazolones 1–12</i>				
1	Hexane–benzene (20:80)	0.233	–0.42	2.18
2	Tetrachloromethane–diethyl ether (95:5)	0.233	0.36	1.66
3	Tetrachloromethane–ethyl acetate (98:2)	0.234	0.37	1.66
4	Hexane–chloroform–diethyl ether (68.9:30:1.1)	0.226	0.24	1.33
5	Hexane–1,2-dichloroethane (68:32)	0.233	0.14	1.19
6	Cyclohexane–toluene–tetrahydrofuran (64:35:1)	0.211	0.18	0.75
7	Toluene–methylene chloride (91.5:8.5)	0.233	0.01	2.46
8	Cyclohexane–benzene (86.6:13.4), 0.158	0.100	–0.21	0.19
9	(70.6:29.4), 0.336	0.150	–0.37	0.65
10	(44:56), 0.607	0.200	–0.41	1.42
11	(29.6:70.4), 0.743	0.220	–0.42	1.84
12	(2:98), 0.983	0.248	–0.42	2.64
13	Tetrachloromethane–chloroform (84.7:15.3), 0.180	0.150	0.03	1.98
14	(56.7:43.3), 0.481	0.200	0.08	2.68
15	(41.2:58.8), 0.634	0.220	0.09	3.07
16	(12.5:87.5), 0.895	0.250	0.10	3.79
<i>For cinnamates 13–20</i>				
17	Hexane–diethyl ether (35:65)	0.378	0.66	1.86
18	Hexane–methyl <i>tert.</i> -butyl ether (51.9:48.1)	0.377	0.81	–
19	Toluene–diethyl ether (66:34)	0.378	0.57	2.54
20	Benzene–acetone (89.8:10.2)	0.378	0.57	2.95
21	Hexane–chloroform–diethyl ether (51.2:32:16.8)	0.379	0.60	1.83
22	Hexane–chloroform–diisopropyl ether–ethyl acetate–acetone (75.8:20:2:2:0.2)	0.376	0.59	1.04
23	Cyclohexane–tetrachloromethane–benzene–tetrahydrofuran (55.3:2.5:2.5:39.7)	0.378	0.98	1.59
24	(26.6:25:25:23.4)	0.379	0.92	1.96
25	(8.2:37.5:37.5:16.8)	0.378	0.86	2.27
26	(10.1:30:45:14.9)	0.378	0.83	2.27
27	Hexane–chloroform–diisopropyl ether–ethyl acetate–acetonitrile (77.85:18:2:2:0.15)	0.364	0.59	0.96
28	Hexane–chloroform–diisopropyl ether–acetonitrile (69.6:19:10:1.4)	0.348	0.69	1.17
29	Hexane–diethyl ether (78.4:21.6), 0.256	0.290	0.64	0.68
30	(57.6:42.4), 0.479	0.330	0.65	1.25
31	(34:66), 0.708	0.380	0.66	1.88
32	(10:90), 0.918	0.420	0.66	2.53
33	Benzene–diethyl ether (92.5:7.5), 0.064	0.290	0.11	2.71
34	(82.8:17.2), 0.150	0.330	0.28	2.72
35	(62.6:37.4), 0.337	0.380	0.54	2.74
36	(8:92), 0.907	0.420	0.66	2.79
37	Benzene–acetone (97.8:2.2), 0.026	0.290	0.12	2.75
38	(94.9:5.1), 0.061	0.330	0.29	2.82
39	(89.5:10.5), 0.124	0.380	0.57	2.95
40	(81.6:18.4), 0.213	0.420	0.78	3.14

TABLE II  
EXPERIMENTAL  $R_F$  VALUES AND DERIVED VALUES OF  $\log \alpha$  FOR THE DIASTEREOMERIC OXAZOLONES 1-12 OF TYPE I

For compositions of mobile phases, see Table I. The values of  $\log \alpha$  were calculated from  $R_F$  values of the corresponding Z-E pair using eqns. 1a and 4.

M	Solute	$R_F$ for indicated mobile phase															
Config-uration	No.	1	2	3	4	5	6	7	8	9	10	11	12	13	14	15	16
4-Cl	Z	0.77	0.69	0.39	0.46	0.43	0.30	0.70	0.06	0.18	0.43	0.62	0.74	0.25	0.46	0.57	0.73
	E	0.53	0.51	0.31	0.37	0.33	0.20	0.51	0.02	0.07	0.20	0.33	0.49	0.11	0.25	0.38	0.56
H	Z	0.70	0.67	0.39	0.43	0.40	0.27	0.65	0.05	0.16	0.37	0.55	0.69	0.20	0.41	0.51	0.69
	E	0.48	0.50	0.30	0.34	0.30	0.19	0.45	0.02	0.06	0.16	0.29	0.43	0.09	0.22	0.33	0.51
4-CH <sub>3</sub>	Z	0.68	0.65	0.38	0.41	0.40	0.23	0.63	0.04	0.13	0.33	0.50	0.67	0.19	0.40	0.50	0.68
	E	0.47	0.49	0.30	0.33	0.29	0.17	0.43	0.01	0.05	0.15	0.27	0.41	0.09	0.22	0.33	0.52
3-CH <sub>3</sub> O	Z	0.53	0.50	0.30	0.31	0.25	0.18	0.48	0.01	0.05	0.17	0.33	0.52	0.08	0.22	0.32	0.51
	E	0.32	0.38	0.24	0.23	0.16	0.14	0.30	0.01	0.02	0.07	0.15	0.26	0.03	0.11	0.18	0.32
4-CH <sub>3</sub> O	Z	0.45	0.41	0.26	0.26	0.20	0.17	0.41	0	0.04	0.13	0.27	0.46	0.06	0.19	0.28	0.48
	E	0.26	0.30	0.19	0.20	0.12	0.10	0.26	0	0.01	0.05	0.12	0.23	0.03	0.09	0.15	0.30
3-NO <sub>2</sub>	Z	0.51	0.50	0.33	0.30	0.25	0.21	0.49	0.01	0.05	0.17	0.33	0.51	0.09	0.22	0.33	0.52
	E	0.31	0.39	0.25	0.23	0.16	0.15	0.30	0.01	0.02	0.08	0.15	0.26	0.05	0.12	0.20	0.34

$\log \alpha$ for indicated mobile phase																	
1-2	-0.47	-0.33	-0.16	-0.16	-0.19	-0.23	-0.35	-0.50	-0.46	-0.48	-0.52	-0.47	-0.43	-0.41	-0.33	-0.33	-0.33
3-4	-0.40	-0.31	-0.18	-0.17	-0.19	-0.20	-0.36	-0.41	-0.47	-0.49	-0.48	-0.47	-0.40	-0.39	-0.33	-0.33	-0.33
5-6	-0.38	-0.29	-0.16	-0.15	-0.21	-0.17	-0.35	-0.62	-0.45	-0.44	-0.43	-0.47	-0.37	-0.37	-0.31	-0.30	-0.30
7-8	-0.38	-0.21	-0.13	-0.17	-0.24	-0.13	-0.34	0	-0.41	-0.43	-0.44	-0.48	-0.45	-0.36	-0.33	-0.35	-0.35
9-10	-0.36	-0.21	-0.18	-0.15	-0.27	-0.26	-0.29	0	-0.62	-0.45	-0.44	-0.45	-0.32	-0.37	-0.34	-0.34	-0.34
11-12	-0.37	-0.19	-0.17	-0.15	-0.24	-0.17	-0.35	0	-0.41	-0.37	-0.44	-0.47	-0.28	-0.32	-0.29	-0.32	-0.32



Concerning  $\log \alpha$ , Tables II and III show negative values for oxazolones **1–12** and positive values for cinnamates **13–20**. These different relative retentions were independent of the type of substituent M, the nature of the mobile phase and the presence of second fronts in some instances (see Experimental).

The  $R_F$  values obtained with mobile phases 1–7 and 17–28 having constant strengths  $\epsilon$  of 0.23 and 0.38 (mean values), respectively, showed that Snyder's theory and the microcomputer program used [13,14] permit suitable mobile phases to be selected with minimum experimental effort (see details in refs. 1 and 13). The mobile phases mentioned were used to study the influence of solvent selectivity effects with the cyclic and acyclic diastereoisomers by means of eqn. 1a. The fit of the corresponding data to this equation is shown in Table IV and illustrated in Fig. 1.

The data obtained with sets of mobile phases 8–12, 13–16, 29–32, 33–36 and 37–40 of increasing  $\epsilon$  agree well with eqn. 2a as the standard deviation (S.D.) and correlation coefficient,  $R$ , show mean values of  $\pm 0.07$  and  $-0.990$ , respectively, as presented in Table V and illustrated in Fig. 2.

Examples of the data necessary to verify the Hammett eqn. 3 are shown in Table VI. Application of this equation to the corresponding data is illustrated in Fig. 3.

#### *Role of solvent selectivity effects on retention of diastereoisomers*

*Sets of mobile phases of constant strength,  $\epsilon$  (verification of eqn. 1a).* The data obtained when the mobile phase strength,  $\epsilon$ , was kept constant and the localization,  $m$ , was varied in the ranges  $-0.42 \leq m \leq 0.37$  and  $0.57 \leq m \leq 0.81$  for the oxazolones and cinnamates, respectively, correlated with eqn. 1a, as can be seen from Table IV and Fig. 1. The overall S.D. is  $\pm 0.07$ , similar to that reported earlier [2]. In addition, maximum absolute values of  $\log \alpha$  and maximum separation of diastereoisomers correspond to minimum values of  $m$ , as established also [2,7,10] for conformationally flexible diastereoisomeric compounds.

According to Table IV, the values of  $A$  are negative for the oxazolones and positive for the cinnamates. Taking into account what was said under Theory, these data show that the relative steric effects favour the stronger adsorption of (*E*)-oxazolone and (*Z*)-cinnamate then that of the corresponding isomers when solvent selectivity effects are absent. The relative steric effects are equal ( $A = -0.3$ ) for any oxazolone pair. However,  $A$  varies in the range 0.32–0.70 for the cinnamates.

The values of  $m_{\text{crit.}} = -A/B$  from Table IV exceed the maximum experimentally accessible value of  $m$  (1.05 [2]) in all instances except those concerning the pairs **1–2**, **11–12** and **7–8**, where this parameter is 0.93 or 0.87. Consequently, the relative retentions of the diastereoisomers found for oxazolones **1–12** with mobile phases 1–7 and for cinnamates **13–20** with mobile phases 17–22 are determined by relative steric effects. A change in the relative retention induced by solvent selectivity effects could occur only for oxazolones **1–2**, **11–12** and **7–8** with mobile phases whose values of  $m$  exceed 0.93 for the first two pairs and 0.87 for the third. However, it does not seem possible because of the weak adsorption of oxazolones mentioned above, which will make it difficult to find mobile phases of low  $\epsilon$  and  $m$  greater than 0.87.

*Sets of mobile phases of increasing strength,  $\epsilon$  (verification of eqn. 2a).* The construction of  $R_M$  vs.  $\log N_B$  plots was based on the sets of binary mobile phases 8–12 and 13–16 for the oxazolones and 29–32, 33–36 and 37–40 for the cinnamates,

TABLE III

EXPERIMENTAL  $R_F$  VALUES AND DERIVED VALUES OF  $\log \alpha$  FOR THE DIASTEREOISOMERIC CINNAMATES 13-20 OF TYPE IFor compositions of mobile phases, see Table I. Values of  $\log \alpha$  were calculated from  $R_F$  values of the corresponding  $Z-E$  pair using eqns. 1a and 4.

M	Solute		$R_F$ for indicated mobile phase <sup>a</sup>										
	Config-uration	No.	17	18	19	20	21	22	23	24	25	26	
4-Cl	Z	13	0.41	0.57	0.52	0.56	0.25	0.03	0.62	0.66	0.55	0.54	
	E	14	0.53	0.65	0.68	0.68	0.39	0.08	0.66	0.75	0.66	0.68	
H	Z	15	0.40	0.56	0.48	0.53	0.24	0.03	0.61	0.63	0.52	0.52	
	E	16	0.50	0.64	0.62	0.62	0.35	0.07	0.64	0.71	0.64	0.65	
4-CH <sub>3</sub> O	Z	17	0.28	0.49	0.39	0.47	0.16	0.02	0.52	0.47	0.43	0.44	
	E	18	0.37	0.56	0.52	0.55	0.22	0.03	0.55	0.57	0.53	0.57	
3-NO <sub>2</sub>	Z	19	0.27	0.49	0.43	0.50	0.14	0.01	0.52	0.44	0.44	0.45	
	E	20	0.42	0.61	0.56	0.58	0.24	0.03	0.58	0.59	0.58	0.61	
			Log $\alpha$ for indicated mobile phase										
			13-14	0.21	0.16	0.30	0.23	0.29	0.45	0.08	0.19	0.20	0.26
			15-16	0.18	0.15	0.24	0.16	0.23	0.39	0.06	0.16	0.22	0.24
			17-18	0.18	0.12	0.22	0.14	0.17	0.18	0.06	0.17	0.17	0.22
			19-20	0.29	0.22	0.22	0.14	0.29	0.49	0.11	0.26	0.24	0.28

<sup>a</sup> Second fronts were established for the following mobile phases as their  $R_F$  values are 0.52 (mobile phase 23), 0.39 (mobile phase 24), 0.24 (mobile phase 25), 0.21 (mobile phase 26), 0.12 (mobile phase 27) and 0.04, 0.23 and 0.30 (mobile phase 28).

TABLE IV

FIT OF  $\log \alpha$  FOR INDIVIDUAL DIASTEREOISOMERIC PAIRS WITH MOBILE PHASES 1-7 AND 17-22 OF CONSTANT  $\varepsilon$  TO THE EQUATION  $\log \alpha = A + Bm$  (EQN. 1a) WHERE  $m$  IS LOCALIZATION OF MOBILE PHASE

The structures of the solute pairs and their values of  $\log \alpha$  are shown in Tables II and III. The values of  $m$  were taken from Table I. The values of  $A$ ,  $B$  and the S.D. were calculated by linear regression analysis of  $\log \alpha$  vs.  $m$  data using the method of least squares. The critical values  $m_{\text{crit.}} = -A/B$  were calculated on the basis of the data for  $A$  and  $B$  from preceding columns. Mean values of  $\varepsilon$  are shown.

Solute pair	$A$	$B$	S.D.	$m_{\text{crit.}}$
<i>Oxazolones, mobile phases 1-7, <math>\varepsilon = 0.23</math>, <math>\log \alpha &lt; 0</math></i>				
1-2	-0.31	0.33	$\pm 0.08$	0.93
3-4	-0.29	0.25	0.07	1.16
5-6	-0.28	0.25	0.07	1.12
7-8	-0.27	0.31	0.06	0.87
9-10	-0.28	0.23	0.04	1.21
11-12	-0.27	0.29	0.05	0.93
<i>Cinnamates, mobile phases 17-22, <math>\varepsilon = 0.38</math>, <math>\log \alpha &gt; 0</math></i>				
13-14	0.70	-0.67	0.09	1.04
15-16	0.50	-0.43	0.09	1.16
17-18	0.32	-0.24	0.03	1.33
19-20	0.37	-0.17	0.13	2.17
overall				$\pm 0.07$

27	28	29	30	31	32	33	34	35	36	37	38	39	40
0.03	0.09	0.02	0.15	0.43	0.70	0.28	0.46	0.66	0.82	0.14	0.31	0.53	0.70
0.08	0.20	0.09	0.28	0.55	0.78	0.48	0.66	0.78	0.87	0.26	0.48	0.63	0.77
0.03	0.10	0.03	0.16	0.44	0.70	0.24	0.43	0.64	0.81	0.12	0.29	0.50	0.66
0.06	0.17	0.09	0.27	0.53	0.77	0.39	0.59	0.74	0.86	0.20	0.40	0.58	0.73
0.01	0.06	0.01	0.07	0.29	0.59	0.16	0.33	0.55	0.72	0.08	0.22	0.44	0.61
0.03	0.09	0.03	0.15	0.40	0.67	0.27	0.48	0.67	0.79	0.14	0.32	0.52	0.68
0.01	0.05	0.01	0.07	0.29	0.58	0.20	0.38	0.56	0.73	0.10	0.26	0.47	0.63
0.03	0.10	0.03	0.15	0.42	0.69	0.29	0.50	0.68	0.81	0.15	0.34	0.54	0.69
0.45	0.40	0.69	0.34	0.21	0.18	0.38	0.36	0.26	0.17	0.34	0.32	0.18	0.15
0.32	0.26	0.51	0.29	0.15	0.15	0.31	0.28	0.20	0.16	0.27	0.21	0.14	0.14
0.49	0.19	0.49	0.37	0.21	0.15	0.29	0.28	0.22	0.17	0.27	0.22	0.13	0.14
0.49	0.33	0.49	0.37	0.25	0.21	0.21	0.21	0.23	0.20	0.20	0.16	0.12	0.12

composed of cyclohexane–benzene, tetrachloromethane–chloroform, hexane–diethyl ether, benzene–diethyl ether and benzene–acetone, respectively. The molar fraction,  $N_B$ , of the second solvent was  $0.026 \leq N_B \leq 0.983$ .

The values of the slope  $n$  vary from *ca.* 1 to 4. However, the diastereoisomeric compounds show close values, which indicate that they adsorb via the same groups. As can be seen from Table V and Fig. 2, almost equal values of  $n$  and parallel plots are established for the diastereoisomers with mobile phases 8–16, which do not contain a strongly adsorbing second solvent. The remaining mobile phases, 29–40, contain a solvent such as diethyl ether or acetone and the slopes are usually not parallel. Hence the solvent selectivity effects vary with the change in molar fraction,  $N_B$ , in this instance as the maximum separation of diastereoisomers corresponds to minimum values of  $N_B$ .

When  $N_B$  approaches unity,  $A$  in eqn. 2a is equal to  $R_M$  and the relative parameter  $\Delta A = A_Z - A_E$  is equal to  $\log \alpha$ . The values of  $\Delta A$  are negative for the oxazolones and positive for the cinnamates, similarly to  $\log \alpha$ , indicating that the relative retentions found will not alter as a result of solvent selectivity effects if the mobile phase is composed mainly of the second solvent. The diastereoisomeric pair **13–14** shows a particularity with mobile phases 37–40 as  $\Delta A$  is equal to zero, *i.e.*, separation will not occur in this instance. The  $R_M$  vs.  $\log N_B$  plots for diastereoisomers do not cross and consequently a change in relative retentions is not expected for the whole range of  $N_B$  from 0 to 1.

TABLE V

FIT OF  $R_M$  OF INDIVIDUAL COMPOUNDS OBTAINED WITH BINARY MOBILE PHASES 8-16 AND 29-40 OF INCREASING  $\epsilon$  TO THE EQUATION  $R_M = A + n \text{ LOG } N_B$  (EQN. 2a), WHERE  $N_B$  IS MOLAR FRACTION OF THE SECOND SOLVENT

The structures and  $R_F$  values of oxazolones 1-12 and cinnamates 13-20 are presented in Tables II and III, respectively. The values of  $R_M$  were calculated on the basis of eqn. 4. The values of  $N_B$  were taken from Table I. The values of  $A$ ,  $n$  and the S.D. were calculated by linear regression analysis of  $R_M$  vs.  $\log N_B$  data using the method of least squares. The values of  $\Delta A = A_Z - A_E$  were calculated on the basis of  $A$  for the indicated isomer.

Solute	Config-uration	Binary mobile phases 8-12, $\epsilon = 0.100-0.248$				Binary mobile phases 13-16, $\epsilon = 0.150-0.250$			
		$A$	$n$	S.D.	$\Delta A$	$A$	$n$	S.D.	$\Delta A$
1	Z	-0.42	2.09	$\pm 0.09$	-0.49	-0.41	1.25	$\pm 0.09$	-0.33
2	E	0.07	2.09	0.08		-0.08	1.40	0.11	
3	Z	-0.31	2.05	0.08	-0.49	-0.33	1.30	0.09	-0.33
4	E	0.18	1.97	0.10		0.00	1.40	0.10	
5	Z	-0.25	2.11	0.09	-0.42	-0.31	1.31	0.09	-0.30
6	E	0.17	2.31	0.06		-0.01	1.41	0.11	
7	Z	-0.02	2.82	0.08	-0.47	-0.01	1.49	0.09	-0.32
8	E	0.45	2.68	0.08		0.31	1.65	0.07	
9	Z	0.10	2.81	0.10	-0.41	0.04	1.60	0.10	-0.40
10	E	0.51	3.20	0.07		0.44	1.51	0.15	
11	Z	-0.01	2.80	0.08	-0.44	-0.01	1.42	0.11	-0.32
12	E	0.43	2.68	0.04		0.31	1.37	0.11	
		Binary mobile phases 29-32, $\epsilon = 0.290-0.420$				Binary mobile phases 33-36, $\epsilon = 0.290-0.420$			
		$A$	$n$	S.D.	$\Delta A$	$A$	$n$	S.D.	$\Delta A$
13	Z	-0.46	3.68	$\pm 0.05$	0.10	-0.71	0.94	$\pm 0.02$	0.17
14	E	-0.56	2.73	0.11		-0.88	0.74	0.03	
15	Z	-0.43	3.36	0.08	0.09	-0.69	0.99	0.02	0.15
16	E	-0.52	2.67	0.12		-0.84	0.85	0.02	
17	Z	-0.22	3.86	0.11	0.13	-0.50	0.99	0.06	0.17
18	E	-0.35	3.23	0.09		-0.67	0.88	0.07	
19	Z	-0.21	3.83	0.10	0.19	-0.49	0.89	0.04	0.21
20	E	-0.40	3.31	0.09		-0.70	0.89	0.05	
		Binary mobile phases 37-40, $\epsilon = 0.290-0.420$							
		$A$	$n$	S.D.	$\Delta A$				
13	Z	-1.21	1.27	$\pm 0.02$	0.00				
14	E	-1.21	1.04	0.03					
15	Z	-1.15	1.27	0.01	0.02				
16	E	-1.17	1.12	0.02					
17	Z	-1.13	1.38	0.02	0.02				
18	E	-1.15	1.22	0.01					
19	Z	-1.11	1.30	0.02	0.05				
20	Z	-1.16	1.20	0.01					

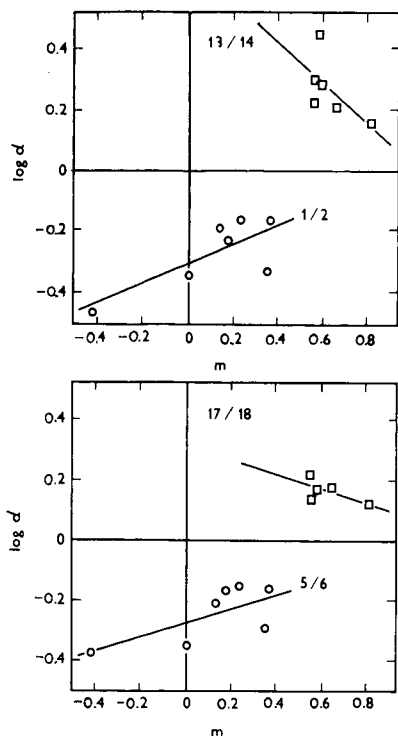


Fig. 1. Log  $\alpha$  vs. localization ( $m$ ) plots from Table IV for diastereoisomeric pairs 1-2, 5-6, 13-14 and 17-18.

TABLE VI

FOUR EXAMPLES OF DATA NECESSARY TO VERIFY THE HAMMETT EQN. 3

$R_F$  values referring to mobile phases 1 and 20 were taken from Tables II and III.  $R_M$  values were obtained by eqn. 4. The compounds are arranged in order of increasing retention. The values of  $\sigma^+$  were taken from ref. 15. See text for the deviations from eqn. 3 of *meta*-substituted derivatives 7, 11 and 19.

Z isomers	$R_F$	$R_M$	E isomers	$R_F$	$R_M$	Substituent M	$\sigma^+$ values
<i>Oxazolones, mobile phase 1</i>							
1	0.77	-0.52	2	0.53	-0.05	4-Cl	0.11
3	0.70	-0.37	4	0.48	0.03	H	0
5	0.68	-0.33	6	0.47	0.05	4-CH <sub>3</sub>	-0.31
7	0.53	-0.05	8	0.32	0.33	3-CH <sub>3</sub> O	0.05
11	0.51	-0.02	12	0.31	0.35	3-NO <sub>2</sub>	0.67
9	0.45	0.09	10	0.26	0.45	4-CH <sub>3</sub> O	-0.78
<i>Cinnamates, mobile phase 20</i>							
13	0.56	-0.10	14	0.68	-0.33	4-Cl	0.11
15	0.53	-0.05	16	0.62	-0.21	H	0
19	0.50	0	20	0.58	-0.14	3-NO <sub>2</sub>	0.67
17	0.47	0.05	18	0.55	-0.09	4-CH <sub>3</sub> O	-0.78

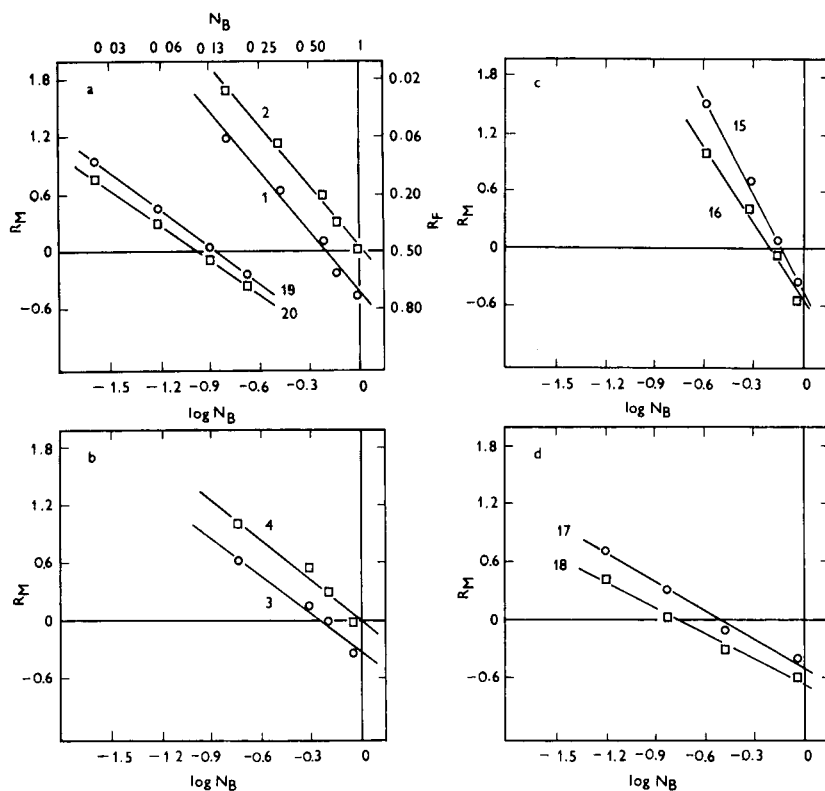


Fig. 2.  $R_M$  vs.  $\log [N_B]$  plots from Table V for indicated sets of binary mobile phases and diastereoisomers shown in parentheses: (a) set 8-12 (1-2) and set 37-40 (19-20); (b) set 13-16 (3-4); (c) set 29-32 (15-16); (d) set 33-36 (17-18).

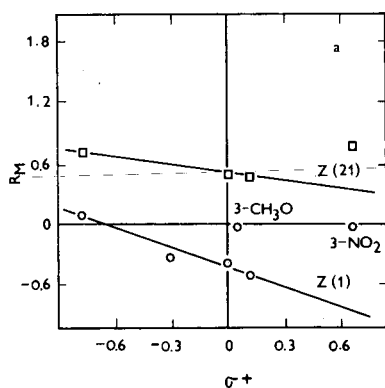


Fig. 3.  $R_M$  vs. Hammett  $\sigma^+$  plots for compounds of indicated configuration and mobile phases shown in parentheses.



As done previously [7,9], we shall look for different models of adsorption to explain the different relative retentions found for the oxazolones and cinnamates. Taking into account the above conclusion about the role of steric effects, the greater adsorption energy [3] of groups X and Y than that of M and the fact that only the oxazolones are bases, we considered that the adsorption of cyclic and acyclic compounds of type I occurs via the nitrogen atom and ester carbonyl and via amide carbonyl and ester carbonyl, respectively. Inspection of models showed that substituents M in *meta* and *para* positions are far from the adsorbing groups and the hydrogen atom in an *ortho* position in the aryl group hinders them.

The presence of an olefinic carbon atom as a member of a five-membered ring distorts the geometry of oxazolones relative to that of the usual olefins. Fig. 4 shows that the aryl group hinders more the nitrogen atom in (*Z*)-oxazolones than the ester carbonyl in the *E* isomers, which is the reason for the stronger adsorption of the latter isomers and the negative values of  $\log \alpha$  established. The amide carbonyl in the cinnamates is far from the aryl group. Hence, the ester carbonyl is not hindered in the *Z* isomers, which determines their stronger adsorption and the positive values of  $\log \alpha$  found.

#### CONCLUSIONS

The TLC behaviour of (*Z*)- and (*E*)-oxazolones (1–12) and related cinnamates (13–20) on silica was studied using 40 mobile phases, and showed a better retention of (*E*)-oxazolones and (*Z*)-cinnamates in all cases studied.

The theoretical relationship between the separation  $\alpha$  of diastereoisomers and solvent selectivity effects as measured by the localization,  $m$ , was studied when the strength,  $\epsilon$ , was kept constant. The results showed that a mobile phase-induced change in the relative retentions established cannot be obtained. In addition, the best separations were obtained with mobile phases showing minimum values of  $m$  as predicted by the theory.

Using sets of mobile phases composed of two solvents with increasing molar fraction  $N_B$  of the more polar solvent and thus increasing  $\epsilon$ , the plots of  $R_M$  vs.  $\log N_B$  were similar for the diastereoisomers, indicating that their adsorption occurs via similar groups.

Electronic effects related to the substituent M do not control the relative retentions of the diastereoisomers studied. The Hammett equation is of limited validity because of the considerable deviation of *m*-CH<sub>3</sub>O and *m*-NO<sub>2</sub> derivatives.

The relative retentions established were attributed to adsorption models including two adsorbing groups, namely the nitrogen atom and ester carbonyl for the oxazolones and the amide carbonyl and ester carbonyl for the cinnamates. Each adsorption model ensures less steric hindrance of the adsorbing groups for the better retained isomer.

#### ACKNOWLEDGEMENTS

We express our grateful thanks to Dr. L. R. Snyder for constructive ideas and comments. Thanks are due to Professors E. Soczewiński and I. Pojarliel for helpful comments on the manuscript.



## REFERENCES

- 1 M. D. Palamareva, *J. Chromatogr.*, 438 (1988) 219.
- 2 L. R. Snyder, M. D. Palamareva, B. J. Kurtev, L. Z. Viteva and J. N. Stefanovski, *J. Chromatogr.*, 354 (1986) 107.
- 3 L. R. Snyder, *Principles of Adsorption Chromatography*, Marcel Dekker, New York, 1968.
- 4 L. R. Snyder and J. J. Kirkland, *Introduction to Modern Liquid Chromatography*, Wiley-Interscience, New York, 2nd ed., 1979.
- 5 L. R. Snyder, in Cs. Horváth (Editor), *High-Performance Liquid Chromatography*, Vol. 3, Academic Press, New York, 1983, p. 157.
- 6 E. Soczewiński, *J. Chromatogr.*, 388 (1987) 91, and references cited therein.
- 7 M. D. Palamareva and L. R. Snyder, *Chromatographia*, 19 (1984) 352.
- 8 M. Palamareva, M. Haimova, J. Stefanovski, L. Viteva and B. Kurtev, *J. Chromatogr.*, 54 (1971) 383.
- 9 M. D. Palamareva, B. J. Kurtev, M. P. Mladenova and B. M. Blagoev, *J. Chromatogr.*, 235 (1982) 299.
- 10 L. R. Snyder, *J. Chromatogr.*, 245 (1982) 165.
- 11 I. Kavrakova, V. Koleva and B. Kurtev, *C.R. Acad. Bulg. Sci.*, 37 (1984) 1495.
- 12 I. Arenal, M. Bernabe and E. Fernandez-Alvarez, *An. Quim.*, 77C (1981) 56.
- 13 M. Palamareva and I. Kavrakova, *Commun. Dept. Chem., Bulg. Acad. Sci.*, 21 (1988) 218.
- 14 M. D. Palamareva and H. E. Palamarev, *J. Chromatogr.*, 477 (1989) 235.
- 15 C. D. Johnson, *The Hammett Equation*, Cambridge University Press, Cambridge, 1973.
- 16 N. S. Isaacs, *Physical Organic Chemistry*, Longman, New York, 1987.
- 17 R. L. Douglas and J. M. Gulland, *J. Chem. Soc.*, (1931) 2893.



## Resolution and concentration detection limit in capillary gel electrophoresis

J. MACEK<sup>\*a</sup>, U. R. TJADEN and J. VAN DER GREEF

*Division of Analytical Chemistry, Centre for Bio-Pharmaceutical Sciences, P.O. Box 9502, 2300 RA Leiden (The Netherlands)*

(Received January 2nd, 1991)

---

### ABSTRACT

The effects of column length and applied electric field on the column efficiency and the resolution of two oligonucleotides in capillary gel electrophoresis were examined. The best resolution was obtained by using long columns in combination with optimum (and not the highest possible) electric field. Further, the concentration detection limits were optimized; it was found that electrokinetic injection did not cause excessive peak broadening even when applied for 25 s at the operating voltage. Thus sample molecules were concentrated during the injection by isotachophoretic effects resulting in very low concentration detection limits (216 pmol/l for a dodecanucleotide with a relative molecular mass of 3707).

---

### INTRODUCTION

Capillary gel electrophoresis (CGE) is increasing in popularity, especially for the separation of oligo- and polynucleotides [1–3]. Several methods for the preparation of gel-filled capillaries have been described [1,4–6] and the separation of polynucleotides containing up to 431 nucleotide units has been reported [1]. Columns with several gel compositions have been compared [3] and very high plate numbers have been obtained on gels with relatively low monomer contents. However, little attention has been paid to the effects of other separation parameters such as column length, applied electric field and duration of electromigration injection on the resolution and the detection limit. In this work we studied these effects using two oligonucleotides as model compounds.

### EXPERIMENTAL

#### *Materials*

The oligonucleotides CTT.GTG.GTG.GG (XI, relative molecular mass 3417.6) and CTT.GTG.GTG.GGC (XII, relative molecular mass 3706.6) dissolved in

---

<sup>a</sup> Present address: Department of Clinical Biochemistry, Faculty Policlinics, Charles University, 12 111 Prague, Czechoslovakia.

water (0.4 mmol/l) were kindly supplied by CIVO-TNO Institutes (Zeist, The Netherlands) and diluted with water to the desired concentrations. N,N,N',N'-Tetramethylenediamine (TEMED) was obtained from BDH (Poole, U.K.), ammonium peroxodisulphate, acrylamide, bisacrylamide, urea and polyethylene glycol 6000 from Merck (Darmstadt, Germany), boric acid from J. T. Baker (Deventer, The Netherlands) and tris(hydroxymethyl)aminomethane (Tris) from Aldrich Chemie (Steinheim, Germany).

### Apparatus

An Alpha Series II 15-kV high-voltage power supply (Brandenburg, Thornton Heath, U.K.) was used to generate the voltage across the capillary gel column. The compounds were detected by a Spectra 100 UV-VIS detector (Spectra-Physics, San Jose, CA, U.S.A.) operating at 260 nm. Each end of the gel-filled capillary (see below) was dipped in a 15-ml vial filled with 0.1 M Tris-0.2 M boric acid buffer. Samples were injected electrokinetically into the capillary by immersing the cathodic end of the column in the sample vial and applying a voltage between 0.5 kV and the operating voltage for 1-25 s.

### Preparation of gel-filled capillaries

Before filling, a few millimetres of the polyimide coating of the fused-silica capillary (60 cm  $\times$  0.075 mm I.D.) were burned off at the distance of 15 cm from the detection end. For some experiments multiple detection windows were created.

The gel-filled capillaries were prepared as described by Yin *et al.* [1]: 4  $\mu$ l of 5% (w/v) ammonium peroxodisulphate and 4  $\mu$ l of 5% (v/v) TEMED were added to 0.5 ml of the polymerization solution containing acrylamide-bisacrylamide (T = 6%, C = 5% [5]<sup>a</sup>). The capillaries were filled with the polymerization solution by vacuum, then the ends of the capillary were sealed with silicone-rubber septa and the capillary was left in a horizontal position. The gel was formed within 1 h, but capillaries were left overnight for complete polymerization.

In some experiments the capillaries were prepared according to the method of Karger and Cohen [5], in which the gel is bonded to the capillary walls by a bifunctional silane reagent, and contains 20% of polyethylene glycol.

## RESULTS AND DISCUSSION

### Resolution

The column efficiency, characterized by the number of theoretical plates,  $N$ , and the resolution,  $R_s$  can be calculated as follows [7]:

$$N = (u_c EL)/(2D) \quad (1)$$

$$R_s = [(u_{c2} - u_{c1}) (EL)^{1/2}]/[4(2u_c D)^{1/2}] \quad (2)$$

where  $u_{c1}$  and  $u_{c2}$  are the electrophoretic mobilities of compounds 1 and 2, respec-

<sup>a</sup> C = g N,N'-methylenebisacrylamide (Bis)  $\times$  100/(g acrylamide + g Bis); T = (g acrylamide + g Bis)/100 ml of solvent.

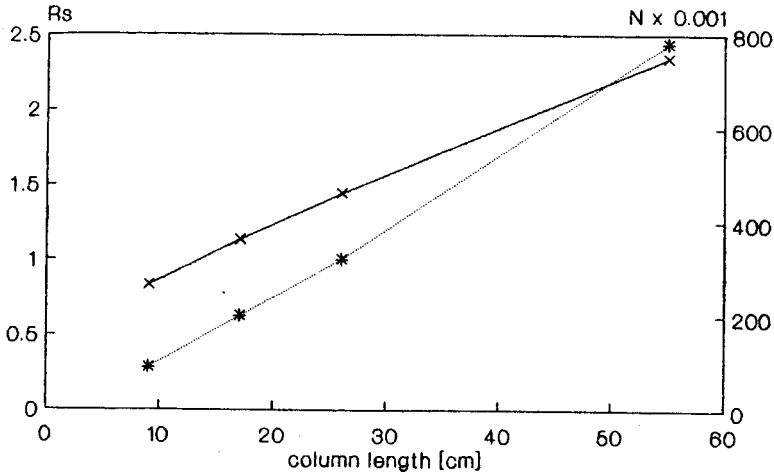


Fig. 1. Separation efficiency (\*) and resolution (x) of XI and XII ( $20 \mu\text{g/ml}$ ) as a function of the effective column length. Capillary,  $60 \text{ cm} \times 0.075 \text{ mm}$  I.D. with detection windows at 9, 17, 27 and 55 cm, filled with polyacrylamide gel, 6% T, 5% C; buffer,  $0.1 \text{ M}$  Tris- $0.2 \text{ M}$  boric acid; electric field,  $270 \text{ V/cm}$ ; current,  $10 \mu\text{A}$ ; electromigration injection, 1 s at 1 kV; detection wavelength,  $260 \text{ nm}$ ; time constant,  $0.3 \text{ s}$ .

tively,  $u_e$  is the average mobility of the two compounds,  $D$  is the diffusion coefficient,  $E$  is the electric field and  $L$  is the column length.

We examined these relationships for two oligonucleotides having 11 and 12 nucleotide units, respectively (Figs. 1 and 2). The dependence of efficiency and resolution on column length follows the theory, but in the case of an applied electric field the above-mentioned equations are not satisfied: the efficiency increases only slowly and the resolution even exhibits a maximum. This behaviour was observed on several columns differing in length and in gel composition. The limited gain in efficiency can be explained by thermally induced zone broadening [8], because at high electric fields

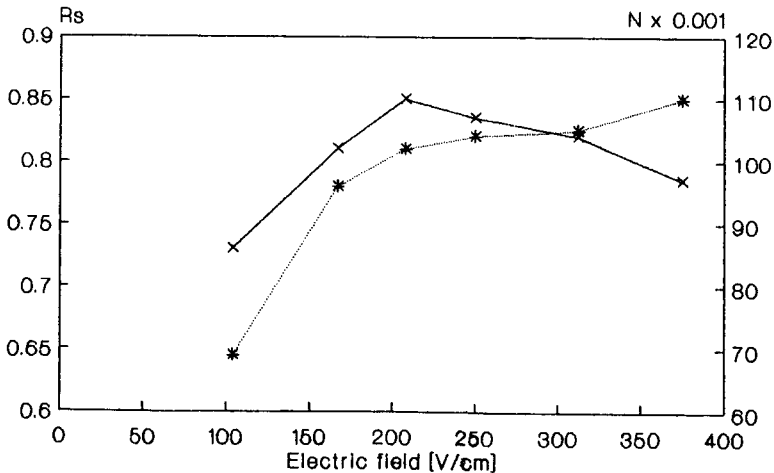


Fig. 2. Separation efficiency (\*) and resolution (x) of XI and XII ( $20 \mu\text{g/ml}$ ) as a function of electric field. Separation conditions as in Fig. 1, except for fixed effective column length, 9 cm.

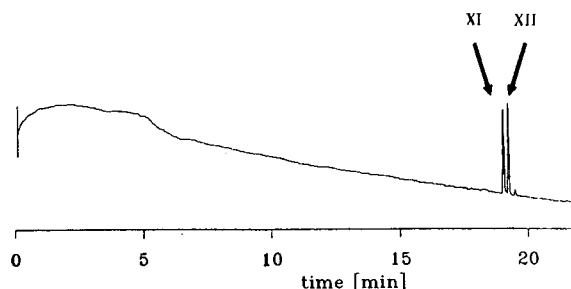


Fig. 3. CGE separation of XI and XII (20  $\mu\text{g}/\text{ml}$ ). Effective column length, 55 cm; range, 0.01 a.u.f.s.; other conditions as in Fig. 1.

the temperature increases owing to Joule heating. The maximum on the resolution–field curve is caused by the superimposition of the efficiency–field relationship and the increase in electrophoretic mobility with temperature [3] (see eq. 2). It follows that for the best resolution a long column has to be used and that the optimum voltage is not the highest possible (Fig. 3).

#### Detection limit

One of the main drawbacks of CGE is the high concentration detection limit (*i.e.*, lowest measurable concentration in the sample) usually obtained with conventional UV detection. The reasons are the absorption of the light in the capillary owing to the optical properties of the gel, the short optical pathlength in the (on-capillary) detection cell and the small amount of the sample injected into the column.

We compared the transmittance of capillaries filled with water of CGE buffer with gel-filled capillaries. It is difficult to measure the absorbance of the gel accurately, because some light always passes through only the walls of the capillary. Therefore we evaluated the ratio of the reference and sample beam intensities for different

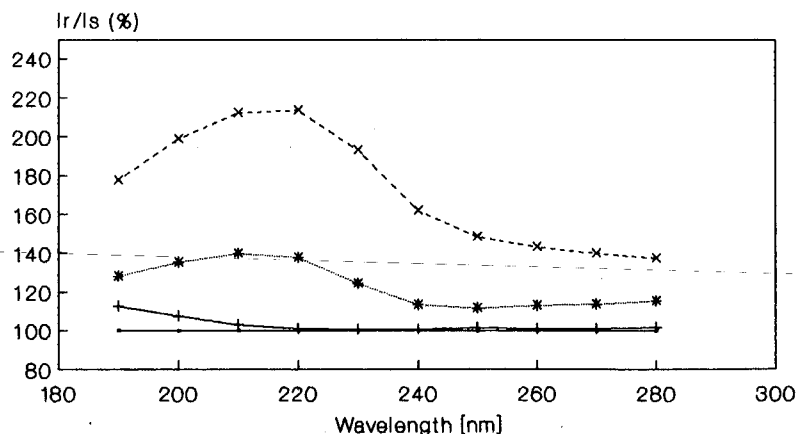


Fig. 4. Optical properties of polyacrylamide gels measured as ratio of intensities of reference and sample beam, and related to water. • = Water; \* = gel, T = 6%, C = 5%; + = CGE buffer; x = gel, T = 6%, C = 5%, 20% polyethylene glycol.

materials inside the capillary (Fig. 4). It can be seen that relative to water the intensity of the sample beam at 260 nm decreases by 15% when the column is filled with gel of  $T=6\%$ ,  $C=5\%$ . When the same gel contains 20% of polythelene glycol the intensity is even lowered by 40%. Therefore, we chose the preparation of gel-filled capillaries described by Yin *et al.* [1], because these gels do not contain polyethylene glycol. We did not observe any improvement in the stability as they described for capillaries with walls coated with polyacrylamide. Therefore, we prepared the gel-filled capillaries by the simplest method as described under Experimental. As already described [1,9], the columns are not stable for a long period and occasionally the first few millimetres of the capillary must be cut in order to restore its performance.

The amount of sample that can be injected into the capillary is limited by the requirement not to cause significant zone broadening on sample introduction. This phenomenon can be caused either by distortion of the applied electric field when the concentration of sample ions is too high [10] or simply by injecting too large a zone. However, when the sample is dissolved at low concentration in pure water, a zone-sharpening effect can occur as in isotachopheresis: we used to inject normally at a voltage equal to one tenth of the operating voltage for 1 s (Fig. 3). This is equivalent to an injection for 0.1 s at the operating voltage, *i.e.*, the zone broadening induced by

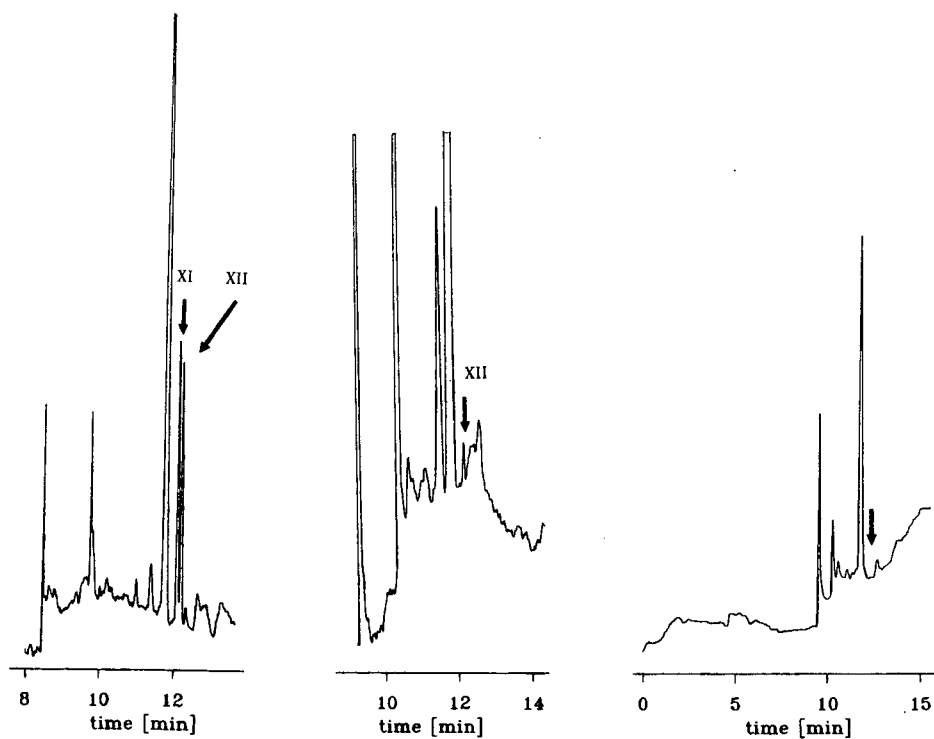


Fig. 5. CGE separation of XI and XII (4 ng/ml). Effective column length, 36 cm; electrokinetic injection, 25 s at 10 kV; range, 0.0005 a.u.f.s.; other conditions as in Fig. 1.

Fig. 6. Electropherogram of XII (800 pg/ml). Conditions as in Fig. 5.

Fig. 7. Electropherogram of pure water. Conditions as in Fig. 5, exception range, 0.002 a.u.f.s.

injection is 0.1 s in time units, which is acceptable for peaks with a width of 2 s at half-height. The concentration detection limit under such conditions is *ca.* 100 ng/ml (based on a signal-to-noise ratio of 3:1). However, on employing injections as long as 25 s at the operating voltage, no excessive peak broadening was introduced and therefore it was possible to lower the detection limit to and even below the ng/ml level without loss of resolution (Figs. 5 and 6). The peak of XII in Fig. 6 corresponds to a concentration of 216 pmol/l, which to our knowledge is the lowest concentration detection limit reported for capillary electrophoresis with conventional UV detection.

It is difficult to calculate the absolute amount injected into the capillary, because the volume fraction occupied by the gel is unknown and the electrophoretic mobilities in buffer and pure water are different [11].

Paulus and Ohms [9] observed severe distortion of oligonucleotide peak shapes after injection for 10 s at 5 kV (operating potential 10 kV), but the concentration of the compounds was 0.2 mg/ml and thus concentration overloading could occur, as discussed above. They assumed that the peak deformation was caused by the high concentration of urea (7 M) in the electrolyte solution, but similar effects have not been confirmed by others [2]. We did not observe any gain of efficiency for the tested compounds using 7 M urea and therefore we used buffers without urea.

The impurities from water are concentrated in exactly the same way as sample molecules. When only water was injected, the electropherogram showed several peaks (Fig. 7), which can also be found in the sample electropherograms (Figs. 5 and 6). The inherent advantage of CGE is that these peaks belonging to low-molecular-weight compounds are eluted rapidly and therefore they do not interfere with peaks of higher molecular weight, such as oligonucleotides. Some of these peaks might also be due to rapid changes in concentration in the buffer generated during the injection.

## CONCLUSION

Samples with concentrations down to 1 ng/ml dissolved in water can be analysed by CGE with conventional UV detection owing to the zone-sharpening effect. The presence of other compounds at high concentrations in the sample could represent a problem, and in such a case a suitable sample pretreatment would be necessary.

## REFERENCES

- 1 H.-F. Yin, J. A. Lux and G. Schomburg, *J. High Resolut. Chromatogr.*, 13 (1990) 624.
- 2 A. S. Cohen, D. R. Najarian, A. Paulus, A. Guttman, J. A. Smith and B. L. Karger, *Proc. Natl. Acad. Sci.-U.S.A.*, 85 (1988) 9660.
- 3 A. Guttman, A. S. Cohen, D. N. Heiger and B. L. Karger, *Anal. Chem.*, 62 (1990) 137.
- 4 J. A. Lux, H.-F. Yin and G. Schomburg, *J. High Resolut. Chromatogr.*, 13 (1990) 436.
- 5 B. L. Karger and A. S. Cohen, Northeastern University, *Eur. Pat.*, EP 324 539 A2, 1989.
- 6 P. F. Bente and J. Myerson, Hewlett-Packard, *Eur. Pat.*, EP 272 925 A2, 1988.
- 7 A. S. Cohen, A. Paulus and B. L. Karger, *Chromatographia*, 24 (1987) 15.
- 8 K. D. Lukacs and J. W. Jorgenson, *J. High Resolut. Chromatogr. Commun.*, 8 (1985) 407.
- 9 A. Paulus and J. I. Ohms, *J. Chromatogr.*, 507 (1990) 113.
- 10 R. A. Wallingford and A. G. Ewing, *Adv. Chromatogr.*, 29 (1989) 41.
- 11 Z. Prusik, in O. Mikeš (Editor), *Laboratory Handbook of Chromatographic and Allied Methods*, Wiley, Chichester, 1979, p. 654.



## Short Communication

---

# Peptide separation by gel filtration high-performance liquid chromatography using a gradient elution system

TOMOHIRO ARAKI\*, MAYUMI KURAMOTO and TAKAO TORIKATA

*Laboratory of Biochemistry, Faculty of Agriculture, Kyushu Tokai University, Aso, Kumamoto 869-14 (Japan)*

(First received June 5th, 1990; revised manuscript received January 11th, 1991)

---

### ABSTRACT

Peptides were separated by gel filtration high-performance liquid chromatography with gradient elution. Two gradient elution systems were applied: (1) 0 to 20% acetonitrile in 30 mM phosphate buffer, pH 8.0 and (2) 30 mM phosphate buffer, pH 8.0 to water; with the polymer-type gel filtration column we used, excellent separation of tryptic peptides from hen egg-white lysozyme was achieved within 50 min. System 2 was applied to a separation of V8 protease peptide from yam tuber chitinase and yielded two to three times higher amounts of peptides than reversed-phase high-performance liquid chromatography.

---

### INTRODUCTION

With the advances in high-performance liquid chromatographic (HPLC) techniques for separating peptides for protein structural analysis, considerable work has been reported on reversed-phase (RP) HPLC. One convenience of RP-HPLC is that the separation is done with the volatile 0.1% trifluoroacetic acid (TFA)-acetonitrile elution system, yielding salt-free peptides that are suitable for sequencing [1]. However, a few relatively hydrophobic peptides are difficult to separate with this system owing to loss by irreversible adsorption to the gel matrix. Further, some peptides which possess different amino acid sequences but have similar hydrophobicities elute as a single peak, and some of them cannot be separated with other solvents, such as phosphate buffer-acetonitrile, with a different pH [1]. In order to avoid these disadvantages, other modes of separation such as gel filtration [2], ion exchange [3], hydrophobicity [4] or combined modes [5,6] have been reported. For the sequencing of peptides, however, these methods involve the complication of pre- or post-treatment of corresponding peptides subjected to the Edman method.

In this paper, we report a simple method for the separation of peptides for sequence study employing gradient elution on gel filtration polymer-type HPLC columns.

## EXPERIMENTAL

*Carboxymethylation and enzymatic digestion*

Hen egg-white lysozyme (HEWL) (Seikagaku Kogyo, crystallized six times) and yam chitinase were reduced and carboxymethylated by the method of Crestfield *et al.* [7]. Lyophilized carboxymethylated (Cm)-lysozyme (5 mg) suspended in 1.0 ml of distilled water by ultrasonication was digested with 1/50 (w/w) trypsin (TR-TPCK) (Cooper Biomedical) at 37°C and pH 8.0 for 4 h. Cm-chitinase (8 mg) suspended in 2 ml of 5 mM ammonium hydrogencarbonate (pH 8.2) was digested with 1/50 (w/w) V8 protease (Boehringer) at 37°C for 6 h. The digests were directly subjected to HPLC analysis after removal of the insoluble materials.

*Isolation of peptides by gel filtration HPLC*

The tryptic digest of lysozyme (100  $\mu$ l, containing 0.3 mg of peptide mixture) was applied to a high-performance gel filtration (GF) HPLC column (Asahipak GS320, Asahi Chemical) using a JASCO LC-800 HPLC system (Japan Spectroscopic). The mobile phases for isocratic elution were composed of 0, 3 and 30 mM phosphate buffer (pH 8.0) and 0, 5 and 10% acetonitrile in 30 mM phosphate buffer (pH 8.0). The mobile phases for gradient elution were composed of two different solvent systems: system 1, 30 mM phosphate buffer (pH 8.0) (solvent A) and 20% acetonitrile in solvent A (solvent B); system 2, 30 mM phosphate buffer (pH 8.0) (solvent A) and distilled water (solvent B). Other conditions were as follows: monitoring wavelength, 220 nm; flow-rate, 1.0 ml/min; recording range, 0.32 a.u.f.s.

The separation of V8 peptides from yam chitinase was performed by gradient elution using solvent system 2 but ammonium hydrogencarbonate was used instead of phosphate buffer.

*Isolation of peptides by RP-HPLC*

The tryptic and V8 protease digests were applied to RP-HPLC columns (YMC C18 120A or C4 300A, Yamamura Chemical) using the same HPLC system as for GF-HPLC. The peptide elution was performed with a linear gradient of 0.1% TFA (solvent) and 60% acetonitrile in solvent 1 (solvent 2). Other conditions were the same as in GF-HPLC, except for the recording range of 0.64 a.u.f.s.

*Calculation of hydropathic value of peptides*

The hydropathic value for each tryptic peptide was calculated using the hydrophilicity value of each amino acid [8]. For carboxymethyl cysteine, the hydrophilicity value of aspartic acid was used.

*Amino acid analysis and amino acid sequence analysis of tryptic peptides*

Peptide was hydrolysed in an evacuated sealed tube at 110°C for 20 h using constant-boiling hydrochloric acid containing 0.05%  $\beta$ -mercaptoethanol. The hydrolysate was analysed with the aid of a Hitachi Model 835 amino acid analyser. Amino acid sequence analysis was performed by the method of dimethylaminoazobenzene isothiocyanate-phenylisothiocyanate double coupling manual micro-sequencing [9, 10].

## RESULTS AND DISCUSSION

The influence of the buffer concentration of the mobile phase on the separation of peptides on the GF-HPLC column was investigated using tryptic peptides of HEWL as model peptides. As shown in Fig. 1A–C, on elution with water (0 mM phosphate buffer) few peptides were retained on the column, but an increase in the buffer concentration caused longer elution times. Each peptide was separated by 30 mM phosphate buffer; however, it was not effective on account of the broad peaks.

The shortcoming of the separation of peptides with phosphate buffer was eliminated by adding an organic solvent, acetonitrile. The influence of acetonitrile concentration on the peptide separation in 30 mM phosphate buffer is shown in Fig. 1D and E. The notable feature of acetonitrile is that it reduces the retention times and the peak widths. This suggests that acetonitrile effectively acted to elute the peptides adsorbed on the gel matrix by hydrophobic interaction. These results indicate that a high buffer concentration and addition of an organic solvent are effective for the separation of peptides on a GF-HPLC column with isocratic elution. However, as some peptides were still cross-contaminated when the organic solvent was contained in the solvent, different separation modes in the first and second halves of the chromatography were considered to be effective for the separation of peptides.

Gradient elution for peptide separation on a GF-HPLC column was investigated next. The elution profile obtained by gradient elution with 30 mM phosphate buffer (pH 8.0) and 20% acetonitrile in the same buffer is shown in Fig. 2B. A linear gradient of 30 min provided a good separation, *i.e.*, the peptides that eluted during the first 10 min were separated under the influence of the buffer concentration and the peptides that eluted between 10 and 30 min were separated under the influence of the increased acetonitrile concentration. Further, the same excellent separation was obtained by a gradient from 30 mM phosphate buffer to water as shown in Fig. 2A. This result indicates that a simple gradient with or without an organic solvent results in a separation capacity equal to that obtained in RP-HPLC without prolonging the analysis time.

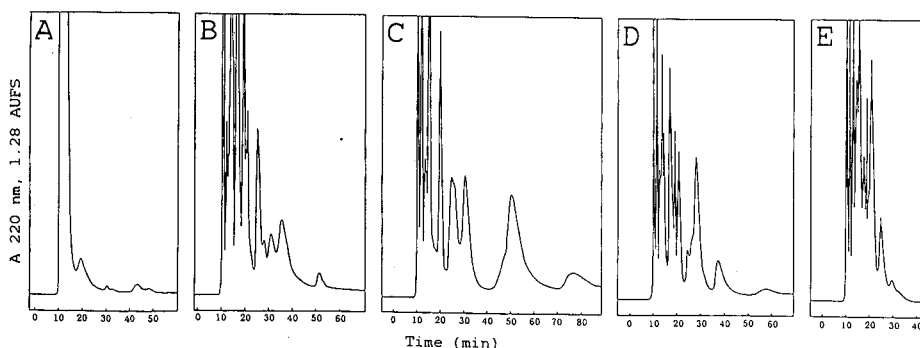


Fig. 1. GF-HPLC of tryptic peptides of lysozyme with various buffer concentrations in the mobile phase. (A) Water; (B) 3 mM phosphate buffer (pH 8.0); (C) 30 mM phosphate buffer (pH 8.0); (D) 5% acetonitrile in 30 mM phosphate buffer (pH 8.0); (E) 10% acetonitrile in 30 mM phosphate buffer (pH 8.0). For HPLC conditions, see text.

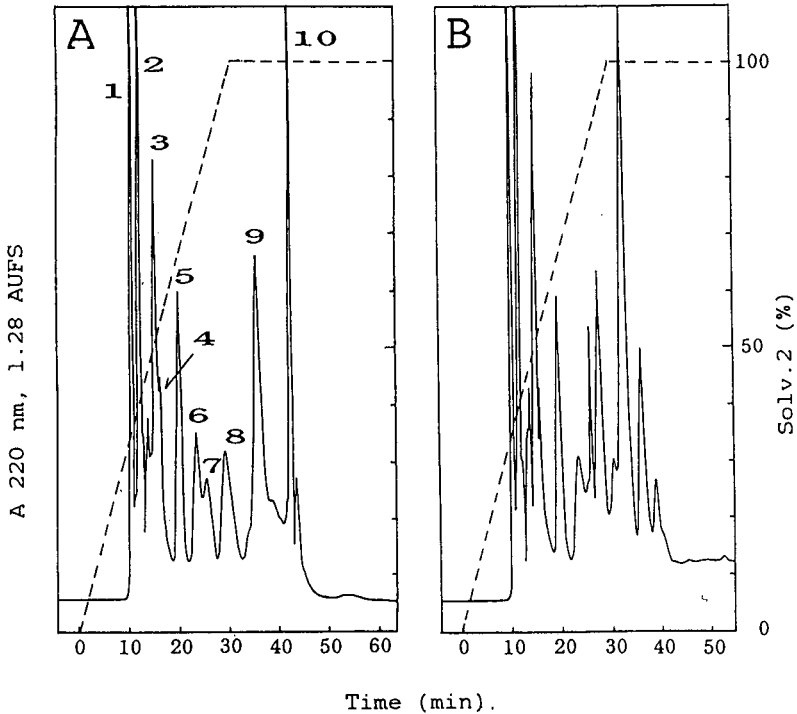


Fig. 2. Gradient elution of tryptic peptides of lysozyme on a GF-HPLC column. (A) Gradient elution from 30 mM phosphate buffer (pH 8.0) to water; (B) gradient elution from 0 to 20% acetonitrile in 30 mM phosphate buffer (pH 8.0). Peptides in the numbered peaks were analysed.

In order to elucidate the relationship between retention time and the properties of peptides, each peak obtained by gradient elution from 30 mM phosphate buffer (pH 8.0) to water was desalted by RP-HPLC using a 0.1% TFA-acetonitrile gradient system. Some peaks containing two peptides on GF-HPLC were separated by RP-HPLC. These desalted peptides were subsequently subjected to amino acid analysis, and then the amino acid sequences were determined by comparison with reported sequences [11,12]. It was found that the retention time did not depend on the number of residues. One of the reasons for this is the property of the polymer-type [poly(vinyl alcohol)] gel and another is the effect of the gradient on the gel particles. However, if the hydrophatic value of each peptide was plotted against retention time, two lines relating to the retention time were obtained by the method of least squares, as shown in Fig. 3. These results imply that the peptides on the column were separated by at least two separation modes, size exclusion and reversed phase. These two separation modes are not independent but combined under these experimental conditions.

This system was applied to separate the V8 protease digested peptides of yam tuber chitinase [13], which contain relatively high-molecular-weight peptides with up to 80 amino acid residues. The separation pattern and the yield of peptides were compared with those given by RP-HPLC. Nine peaks were obtained by RP-HPLC using a C<sub>4</sub> 300 column, as shown in Fig. 4A. However, the N-terminal peptide V10

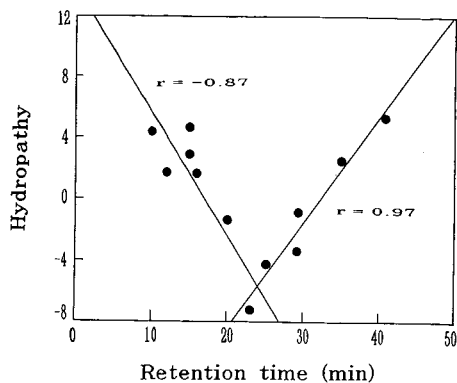


Fig. 3. Relationship between hydrophathy of peptide and retention time in gradient elution (Fig. 2A). Two lines were obtained by regression analysis and the corresponding regression coefficients are represented by  $r$ .

(N-blocked, 55 amino acid residues) was not eluted by RP-HPLC. In contrast, GF-HPLC (a volatile solvent, ammonium hydrogencarbonate, was used instead of phosphate buffer for direct sequencing) yielded seven peaks with the gradient elution system of ammonium hydrogencarbonate and water (Fig. 4B), and the amino acid composition and N-terminal sequence of each peak were analysed. High-molecular weight fragments, especially the N-terminal peptide V10, were eluted with high yields. The irreversible adsorption of peptides on RP-HPLC gel matrices, such as that of peptide V10 in this study, have often been observed, and prevent the microanalysis of peptides. However, peptide V10 was easily obtained in high yield by GF-HPLC. Gradient elution was effective for the earlier elution of small and hydrophobic peptides without peak spreading.

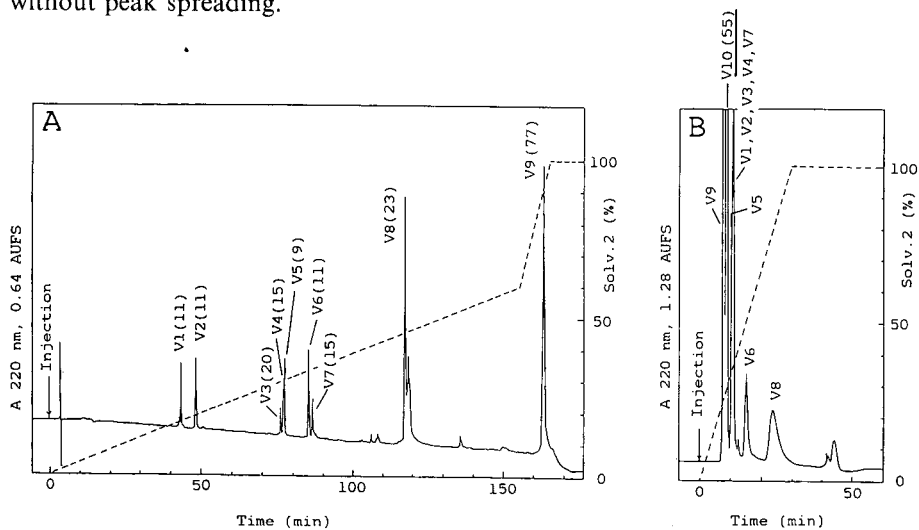


Fig. 4. V8 protease fragment separation by GF-HPLC and RP-HPLC. V8 protease digest of Cm-chitinase was separated on (A) an RP-HPLC column ( $C_4$ -300,  $250 \times 4.6$  mm I.D.) using a linear gradient elution system of 0.1% TFA and 60% acetonitrile in 0.1% TFA and (B) a GF-HPLC column (GS-320,  $500 \times 7.6$  mm I.D.) using a linear gradient elution system of 30 mM ammonium hydrogencarbonate and water.

TABLE I

## COMPARISON OF PEPTIDE RECOVERIES ON RP-HPLC AND GF-HPLC COLUMNS

The yields of V8 peptides from Cm-chitinase (10 mg) were measured by amino acid analysis. The peptides obtained with insufficient separation by GF-HPLC were analysed after rechromatography by RP-HPLC.

Peptide	Yield (nmol)	
	RP-HPLC	GF-HPLC
V1	112.1	242.2
V2	130.5	305.6
V3	85.4	127.1
V4	33.9	165.5
V5	158.5	94.9
V6	120.6	310.8
V7	81.5	91.9
V8	44.4	114.5
V9	48.8	130.2
V10	0.0	164.0

The yield of each peptide in RP-HPLC and GF-HPLC are summarized in Table I. The results show that the yields of the peptides in RP-HPLC are relatively low when the peptides are hydrophobic or of high molecular weight, whereas the yields of such peptides in GF-HPLC are high.

Combining these results, we conclude that the GF-HPLC method is advantageous for long-chain, hydrophobic peptides that are difficult to recover by RP-HPLC. The gradient system enables peptides that have strong gel matrix interactions to elute easily without peak spreading. Further, the GF-HPLC gradient system is well suited for biologically active peptides that cannot be subjected to organic solvents.

## REFERENCES

- 1 C. Y. Yang, E. Pauly, H. Kratzin and N. Hilschmann, *Hoppe-Seyler's Z. Physiol. Chem.*, 362 (1981) 1131.
- 2 T. Araki, Y. Yoshioka and G. Funatsu, *Biochim. Biophys. Acta*, 872 (1986) 277.
- 3 H. Nika and T. Hultin, *Methods Enzymol.*, 91 (1983) 359.
- 4 S. Hjerten, *J. Chromatogr.*, 87 (1973) 325.
- 5 N. Hirata, M. Kasai, Y. Yanagishita and K. Noguchi, *J. Chromatogr.*, 434 (1988) 71.
- 6 N. Takahashi, Y. Takahashi and F. W. Putnam, *J. Chromatogr.*, 266 (1983) 511.
- 7 A. M. Crestfield, W. H. Stein and S. Moore, *J. Biol. Chem.*, 238 (1963) 622.
- 8 T. P. Hopp and K. R. Woods, *Proc. Natl. Acad. Sci. U.S.A.*, 78 (1981) 3824.
- 9 J. Y. Chang, D. Brauer and B. Wittman-Liebold, *FEBS Lett.*, 93 (1978) 205.
- 10 C. Y. Yang, *Hoppe-Seyler's Z. Physiol. Chem.*, 360 (1979) 1673.
- 11 J. Jollès, J. Jaregui-Adell, I. Bernier and P. Jollès, *Biochim. Biophys. Acta*, 78 (1963) 668.
- 12 R. E. Canfield, *J. Biol. Chem.*, 238 (1963) 2698.
- 13 T. Araki, M. Kuramoto and T. Torikata, *Proc. Fac. Agric. Kyushu Tokai Univ.*, 8 (1989) 29.

## Short Communication

---

### Use of chromatofocusing for separation of $\beta$ -lactamases

#### IX. Analytical chromatofocusing for the separation of a chromosomal cephalosporinase from *Proteus vulgaris* 1028

SUSANNE GÁL, ANDREA TAR, BELA L. TOTH-MARTINEZ\* and FERENC J. HERNADI

Chemotherapy Section, Department of Pharmacology, University Medical School of Debrecen, Debrecen H-4012 (Hungary)

(First received January 29th, 1990; revised manuscript received October 30th, 1990)

---

#### ABSTRACT

Simultaneous purification and isoelectric point (*pI*) determination was carried out at analytical scale of the chromosomal cephalosporinase from the *Proteus vulgaris* 1028 strain. Comparison of the enzyme to the purification results with *m*-aminophenylboronic acid–agarose affinity chromatography with sodium dodecyl sulphate–polyacrylamide gel electrophoresis revealed that minute amounts of accompanying proteins having identical *pI* values but different molecular masses were found in the chromatofocused preparation. The molecular mass of the enzyme was 24 000 dalton. The *pI* was found to be 8.3.

---

#### INTRODUCTION

The frequent  $\beta$ -lactam resistance of *Proteus vulgaris* strains is due to their intense  $\beta$ -lactamase production. *P. vulgaris* is usually resistant to ampicillin, first-generation cephalosporins and cefuroxime, and there are some isolates that exhibit resistance against ureidopenicillins and third-generation cephalosporins [1]. The  $\beta$ -lactamase enzymes produced by *P. vulgaris* spp. were classified by Richmond and Sykes [2] as class I enzymes, but owing to their physico-chemical properties and their substrate profile they should be reclassified as class III enzymes.

The *P. vulgaris*  $\beta$ -lactamases have a wide range of isoelectric points (*pI*) but their substrate specificities are very similar [3]. Matsubara *et al.* [4] characterized a special *P. vulgaris* enzyme that had a molecular mass of 29 000 dalton and alkaline *pI* of 8.8. As the enzyme was able to hydrolyse cefuroxime very rapidly, Matsubara *et al.* classified it

separately under the name cefuroximase. The  $V_{\max}$  value for penicillins is lower, but penicillins exhibit a higher affinity to the *P. vulgaris* enzyme. Thus resistance can be explained by hydrolysis. Tajima *et al.* [5] described another specific enzyme with a molecular mass of 28 000 dalton and  $pI = 7.8$ , which did not hydrolyse the 7- $\alpha$ -methoxy-substituted congener cephalosporins. Okonogi *et al.* [3] investigated *P. vulgaris* clinical isolates and found the  $pI$  values of these  $\beta$ -lactamases to be within the range 6.9–9.0. According to Aspiotis *et al.* [1], the *P. vulgaris* specific  $\beta$ -lactamases can be grouped into three classes according to three  $pI$  values: 7.4, 8.8 and 9.5. Yang and Livermore [6] found five clinical isolates with inducible  $\beta$ -lactamases; their production could be stably derepressed in the basal mutants and the enzymes had  $pI$  values of 7.8, 8.0, 8.2, 8.6 and 8.9. Pagani *et al.* [7] investigated *P. vulgaris* 85, which proved to be strongly resistant against the new generation cephalosporins and its  $\beta$ -lactamase was acidic with  $pI = 5.6$ .

According to Matthew and co-workers [8,9], analytical isoelectric focusing is a suitable method for the identification of  $\beta$ -lactamases and for bacterium taxonomic purposes. As minute changes in the amino acid composition in the *Proteus* spp. enzymes by mutation can result in significant changes in the  $pI$  values without essential changes in the substrate profile, the above observation does not seem to apply to that species [3].

We have been able to use the chromatofocusing technique successfully in a comparative methodological project for the assessment of  $pI$  values of  $\beta$ -lactamases, and therefore we carried out the present experiments with the same aim of establishing at the same time whether this technique is suitable for the isolation and purification of the cephalosporinase from crude extracts of *P. vulgaris* 1028.

## EXPERIMENTAL

### *Bacterial strain*

Constitutive cephalosporinase-producing *P. vulgaris* 1028 strain was kindly provided by Dr. R. Then (Hoffmann-La Roche, Basle, Switzerland).

### *Crude enzyme preparation, purification of the $\beta$ -lactamase, chromatofocusing, enzyme assay and protein determination*

In order to obtain a crude enzyme preparation, the strain was cultured in nutrient broth at 37°C with low-speed shaking (80 rpm). Portions of 150 ml of medium were inoculated in 500-ml conical flasks and cultured overnight. The cells were spun down and treated by freezing–thawing three times. Complete disruption of the cells was achieved in a Braun Labsonic 2000 sonifier by 30-s sonications at 0°C three times with 1-min cooling intervals. Cells debris was ultracentrifuged at 105 000  $g$  for 60 min in a Janetzki VAC-601 ultracentrifuge. The supernatant was regarded as crude enzyme.

In order to prepare pure enzyme, *m*-aminophenylboronic acid–agarose affinity chromatography was used (type B column) according to Cartwright and Waley [10]. A 3  $\times$  0.9 cm I.D. column was used. The enzyme was applied to the column in 20  $mM$  triethylamine hydrochloride–0.5  $M$  sodium chloride buffer (pH 7.00). The affinity material was pre-equilibrated with the same buffer. The column was then washed with the above buffer until accompanying protein-free eluates were collected, however,



elution of the enzyme was carried out with 0.5 M borate–0.5 M sodium chloride elution buffer (pH 7.00). Enzyme fractions of 3 ml were collected and the high specific activity fractions were pooled for chromatofocusing.

Chromatofocusing was carried out in a Pharmacia C10/20 column with PBE 94 in the pH range 9.00–6.00 [11]. Fractions of 4 ml were collected. The starting buffer was 0.025 M ethanolamine–acetic acid (pH 9.6) and the elution buffer was Polybuffer 96 in tenfold dilution (pH 6). Enzyme activity, pH and protein content were monitored.

$\beta$ -Lactamase activity was determined with nitrocefin (NC) as substrate at 486 nm according to O'Callaghan *et al.* [12]. One unit was that amount of enzyme which was capable of hydrolysing 1  $\mu$ mol of NC per minute at 37°C.

Protein was measured according to Lowry *et al.* [13].

Sodium dodecyl sulphate–polyacrylamide gel electrophoresis (SDS-PAGE) was performed according to the method of Weber and Osborn [14] and used for molecular mass determination. A molecular mass standard mixture (SDS-7) was purchased from Sigma (St. Louis, MO, U.S.A.).

The stability of the  $\beta$ -lactams was measured according to Ross and O'Callaghan [15].

## RESULTS AND DISCUSSION

The chromosomal  $\beta$ -lactamase enzyme produced by our *P. vulgaris* 1028 strain belongs to class III of the Richmond–Sykes classification system. The substrate profile data, shown in Table I, support this conclusion.

For the purification of the crude enzyme, *m*-aminophenylboronic acid–agarose affinity chromatography was used. According to our experience, N-acetyl-D-penicillamine–Sepharose 4B gel was capable of binding only penicillinase character  $\beta$ -lactamases [16].

Fig. 1 shows the results of the purification of the enzyme on a type B *m*-aminophenylboronic acid–agarose affinity column. In 2 ml, 3.3 U of crude enzyme were administered to the column. Unbound enzyme was not detected in the wash. About 96% of the activity was eluted from the column with the elution buffer. The affinity material is able to purify the enzyme in a single step by eliminating the accompanying proteins, as opposed the multi-step classical methods.

TABLE I

STABILITY OF THE  $\beta$ -LACTAM ANTIBIOTICS AGAINST THE ISOLATED AND PURIFIED *PROTEUS VULGARIS* 1028  $\beta$ -LACTAMASE

$\beta$ -Lactam <sup>a</sup>	Rel. $v_{\max}$ <sup>b</sup>	$\beta$ -Lactam <sup>a</sup>	Rel. $v_{\max}$ <sup>b</sup>
AMP	60	CTA	25
CPH	120	CPER	30
CXI	<1	CTRI	75
CMA	150	CTAZ	<1
CFUR	150		

<sup>a</sup> AMP = ampicillin; CPH = cephalotin; CXI = ceftioxin; CMA = cefamandole; CFUR = cefuroxime; CTA = cefotaxime; CPER = cefoperazone; CTRI = ceftriaxone; CTAZ = ceftazidime.

<sup>b</sup> Rel  $v_{\max}$  = relative to cephaloridine = 100.

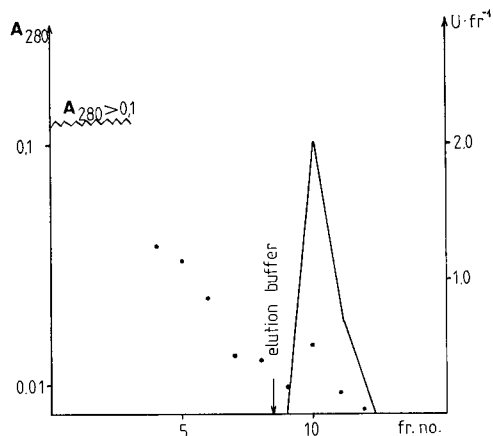


Fig. 1. Elution profile of the crude extract of  $\beta$ -lactamase from *P. vulgaris* 1028 strain on a type B phenylboronic acid-agarose affinity column. Protein (dots) and activity (solid line) monitoring were as described under Experimental; fr.no. = fraction number;  $U\text{ fr}^{-1}$  = units per fraction.

In order to establish whether chromatofocusing was suitable not only for  $pI$  determination but also for the purification of this chromosomally coded cephalosporinase, the crude enzyme sample was chromatofocused. Fig. 2 depicts the chromatogram of 2.83 U of crude enzyme preparation in a 2-ml volume. The activity was eluted in four fractions: No. 8, 0.29 U; No. 9, 1.55 U; No. 10, 0.70 U; and No. 11, 0.18 U. These represent 96% of the total activity applied to the column. Fig. 2 demonstrates that the majority of the accompanying proteins were separated from

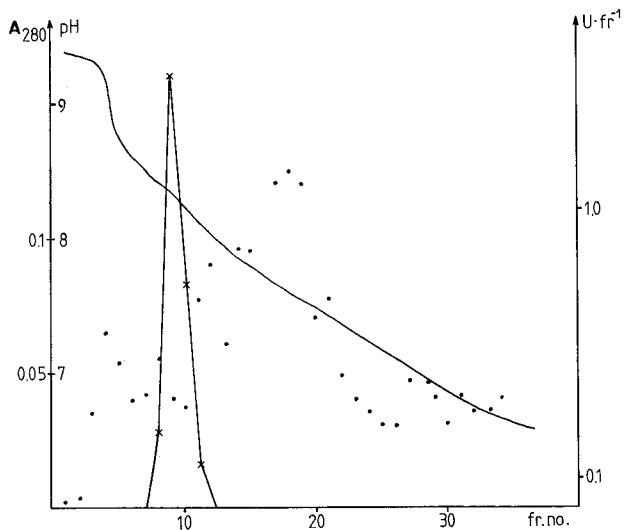


Fig. 2. Elution profile of the crude *P. vulgaris* 1028 enzyme after analytical chromatofocusing. Elution conditions: solid line, pH;  $\times$ , activity; and dots, protein monitoring as described under Experimental; fr. no. = fraction number;  $U\text{ fr}^{-1}$  = units per fraction.

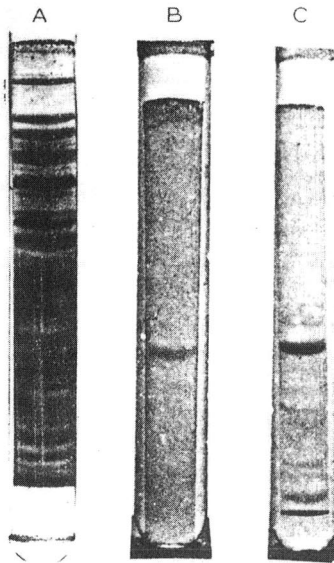


Fig. 3. SDS-PAGE of *Proteus vulgaris*  $\beta$ -lactamase. (A) Crude extract (200  $\mu\text{g}$  of protein); (B) sample of the enzyme purified by affinity chromatography (30  $\mu\text{g}$  of protein); (C) sample of the chromatofocused  $\beta$ -lactamase (50  $\mu\text{g}$  of protein). The gels were subjected to 110 V, 70 mA for 4 h. Protein was detected with Coomassie Brilliant Blue R-250. The anode was at the bottom of the gels.

the activity according to their different  $pI$  values. The main fraction emerged from the column at pH 8.32.

The purity of the enzyme preparations was determined by SDS-PAGE (Fig. 3). Fig. 3 reveals that both (Fig. 3B and C, respectively) methods resulted in the production of pure enzymes. Two faint bands of the chromatofocused sample indicate the presence of minute amounts of accompanying proteins having identical  $pI$  values but different masses of the enzyme. The molecular mass of the enzyme was 24000.

Table II shows specific activity data ( $\text{U mg}^{-1}$ ) expressing the extent of purification related to the crude enzyme.

In order to check the  $pI$  value obtained with the crude enzyme, chromatofocusing of the purified  $\beta$ -lactamase from the affinity gel was also performed. Fig.

TABLE II

COMPARISON OF PURITY PARAMETERS OBTAINED BY AFFINITY CHROMATOGRAPHY AND CHROMATOFOCUSING OF THE *PROTEUS VULGARIS* 1028 ENZYME

Parameter	Crude extract	Affinity chromatography	Chromatofocusing
Specific activity ( $\text{U mg}^{-1}$ ) <sup>a</sup>	0.47	28	22
Purification (fold)	1	60	47

<sup>a</sup> Specific activity was calculated as the number of units per mg of total protein.

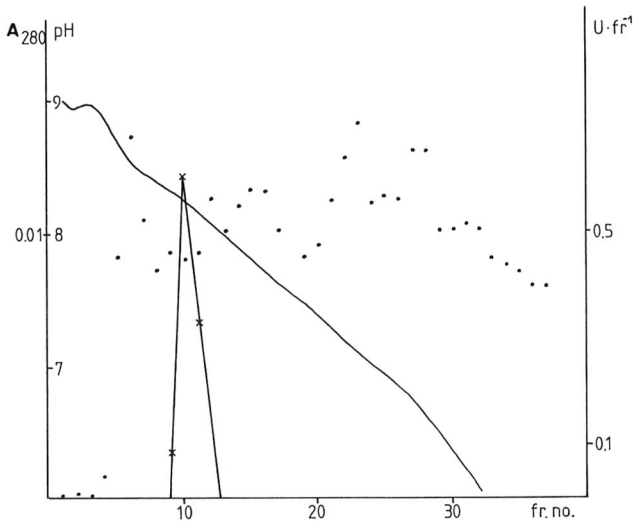


Fig. 4. Elution profile of the pure *P. vulgaris* 1028 enzyme after analytical chromatofocusing. Elution conditions: solid line, pH; ×, activity; and dots, protein monitoring as described under Experimental; fr. no. = fraction number; U fr<sup>-1</sup> = units per fraction.

4 shows the chromatogram of the purified enzyme. The very low absorbances at 280 nm are due to the Polybuffer ampholytes as described in ref. 11. These values overall are negligible on comparing them with the absorbance values at 280 nm in Fig. 2, which represent Polybuffer ampholyte values together with those of the protein fractions. A 1.03 U amount of enzyme was applied to the PBE 94 column in 2 ml, and it emerged in three fractions: No. 9, 0.07 U; No. 10, 0.6 U; No. 11, 0.34 U; altogether 98% of the total activity was regained. The peak enzyme fraction had  $pI = 8.26$ .

The  $pI$  values for the purified and the crude enzyme preparations agree well, and therefore we may conclude that the cephalosporinase of the *P. vulgaris* 1028 strain has its  $pI$  value at 8.3.

Finally we concluded that both affinity chromatography and chromatofocusing are suitable methods for the purification of this enzyme, but chromatofocusing also provides the  $pI$  value.

Our previous experiments with standard  $\beta$ -lactamases [17–20] demonstrated that  $pI$  values determined using other methods provided data identical with those obtained with chromatofocusing. Therefore, we may conclude that the  $pI$  value of *P. vulgaris* 1028  $\beta$ -lactamase is also independent of other factors, *i.e.*, only its  $pI$  is decisive during chromatofocusing.

## REFERENCES

- 1 A. Aspiotis, W. Cullmann, W. Dick and M. Stieglitz, *Chemotherapy*, 32 (1986) 236.
- 2 M. H. Richmond and R. B. Sykes, *Adv. Microb. Physiol.*, 9 (1973) 31.
- 3 K. Okonogi, M. Kuno and E. Higashide, *J. Gen. Microbiol.*, 132 (1986) 143.
- 4 N. Matsubara, A. Yotsuji, K. Kumano and M. Inoue, *Antimicrob. Agents Chemother.*, 19 (1981) 185.
- 5 M. Tajima, Y. Takenouchi, S. Ohya and S. Sugawara, *Microbiol. Immunol.*, 26 (1982) 531.
- 6 Y. Yang and D. M. Livermore, *Antimicrob. Agents Chemother.*, 32 (1988) 1385.

- 7 L. Pagani, M. Perduca and E. Romero, *Microbiologica*, 6 (1983) 163.
- 8 M. Matthew, A. M. Harris, M. J. Marshall and G. W. Ross, *J. Gen. Microbiol.*, 88 (1975) 169.
- 9 M. Matthew and A. M. Harris, *J. Gen. Microbiol.*, 94 (1976) 55.
- 10 S. J. Cartwright and S. G. Waley, *Biochem. J.*, 221 (1984) 505.
- 11 *Chromatofocusing with Polybuffer<sup>TM</sup> and PBE<sup>TM</sup> (Technical Handbook)*. Pharmacia, Uppsala, 1980.
- 12 C. H. O'Callaghan, A. Morris, M. Kirby and A. H. Shingler, *Antimicrob. Agents Chemother.*, 1 (1972) 283.
- 13 O. H. Lowry, N. J. Rosenbrough, A. L. Farr and R. J. Randall, *J. Biol. Chem.*, 193 (1951) 265.
- 14 K. Weber and M. Osborn, *J. Biol. Chem.*, 244 (1969) 4406.
- 15 G. W. Ross and C. H. O'Callaghan, *Methods Enzymol.*, 33 (1975) 69.
- 16 L. Kiss, A. Tar, S. Gál, B. L. Tóth-Martinez and F. J. Hernádi, *J. Chromatogr.*, 448 (1988) 109.
- 17 B. L. Toth-Martinez, S. Gál and L. Kiss, *J. Chromatogr.*, 262 (1983) 373.
- 18 B. L. Toth-Martinez, S. Gál, F. Hernádi, L. Kiss and P. Nánási, *J. Chromatogr.*, 287 (1984) 413.
- 19 L. Kiss, B. L. Toth-Martinez, S. Gál and F. Hernádi, *J. Chromatogr.*, 333 (1985) 244.
- 20 A. Tar, S. Gál, B. L. Toth-Martinez, F. Hernádi and L. Kiss, *J. Chromatogr.*, 368 (1986) 427.

## Short Communication

---

# Separation of ribosomal subunits on Trisacryl GF 2000

DEENA BHOOLIA and KEITH L. MANCHESTER\*

*Department of Biochemistry, University of the Witwatersrand, Johannesburg (South Africa)*

(Received December 6th, 1990)

---

### ABSTRACT

The separation of rat liver and *E. coli* ribosomal subunits was attempted on Trisacryl GF 2000. Contrary to experiments with Sepharose 4B and Bio-Gel A-15 the 60S mammalian subunit did not bind to the resin at 4°C but eluted within the column volume ahead of the 40S subunit. Puromycin, however, used to prepare the subunits, which on the agarose gels had eluted at the total column volume, exhibited anomalous retardation on the Trisacryl resin. Trisacryl therefore behaves as the more non-polar resin, and the binding of 60S subunits to agarose gels is a result of hydrophilic interaction.

---

### INTRODUCTION

Ribosomal subunits, so-called 40S and 60S for eukaryotes, of relative molecular mass ( $M_r$ )  $1.5 \cdot 10^6$  and  $3.0 \cdot 10^6$  [1], are normally separated from each other during preparation by centrifugation on sucrose gradients and subsequent fractionation of the gradient [2]. In a previous study [3], it was shown that rat liver 40S and 60S subunits could be separated from each other by column chromatography on Sepharose 4B or Bio-Gel A-15. This separation, however, was not the consequence of gel exclusion chromatography, but because at 4°C the 60S subunit, although not the 40S, bound to the gel matrix. After elution of the 40S peak, and of puromycin used in the preparation of the subunits at around the total column volume, the 60S subunit could be eluted if the temperature was raised to 25°C or above. At this temperature in other experiments the individual subunits eluted in the order to be expected based on their respective  $M_r$ , but too close to be easily resolved.

The explanation for the binding of the 60S to the gel at 4°C is not known. It is not critically dependent on gel pore size, as a similar phenomenon is observed with Sepharose 2B and 6B (unpublished observations) and the large RNA of the 60S subunit, 28S RNA, also behaves in an anomalous manner on Sepharose gels [4–6]. In an attempt to explore this phenomenon further, we examined the behaviour of the subunits on the synthetic matrix Trisacryl GF 2000, which is formed by copolymerization of a hydroxylated acrylic monomer and N-acryloyl-2-amino-2-hydroxy-

methyl-1,3-propanediol. The makers (Reactifs IBF) describe it as possessing a separation range of  $1.2 \cdot 10^5$ – $1.5 \cdot 10^7$  dalton.

## EXPERIMENTAL

The behaviour of 40S and 60S ribosomal subunits was studied on columns of Trisacryl GF 2000 of length 30 and 135 cm (1.2 cm I.D.), which were loaded and equilibrated with buffer A [500 mM KCl–2 mM MgCl<sub>2</sub>–0.2 mM EDTA–20 mM 4-(2-hydroxyethyl)-1-piperazineethanesulphonic acid (HEPES), pH 7.8, supplemented with 5 mM melanocyte-stimulating hormone (MSH) when in use with ribosomal components]. Elution was monitored at 254 nm and the flow-rate was normally 3 ml/h. Experiments were carried out at either 4 or 20°C. The void volume was determined with glycogen and the volume of the stationary phase with either acetone or <sup>3</sup>H<sub>2</sub>O.

Ribosomes were prepared from rat liver as described previously [7] and for dissociation into subunits were incubated at 37°C for 15 min with 1 mM puromycin in buffer A. Separation and collection of subunits by centrifugation were as described previously [8].

## RESULTS

Ribosomal subunits aggregate readily, particularly at low temperatures [2,8]. This aggregation is in part prevented by a high concentration of monovalent cations and a low concentration of Mg<sup>2+</sup>. The use of 500 mM KCl and 2 mM MgCl<sub>2</sub> is a compromise between seeking to maximize dissociation without producing conditions so stringent that the subunits are stripped of proteins and/or unfold and become denatured.

The first striking feature about chromatography of the rat liver subunits on Trisacryl 2000 is that, unlike the behaviour of the 60S subunit on Sepharose or Bio-Gel, both subunits elute at 4°C within a column volume and show no signs of anomalous retardation. Initial experiments with the 30-cm column showed only a slight shift in the elution position for the two subunits at either 4 or 20°C, although at 20°C the peaks were sharper than at 4°C. This would be consistent with less dimerization of 40S to 55S at that temperature and of 60S to 90S [8]. All subsequent experiments were performed with the longer column.

The elution profile of the individual subunits prepared from rat liver and of a mixture of subunits at 4 and 20°C is shown in Fig. 1. The individual subunits eluted with peaks at both 4 and 20°C with  $K_d = 0.19$  and  $0.13$  for the 40S and 60S, respectively (Fig. 1a), the 60S showing a clear shoulder at 4°C which at 20°C resolved into a distinct peak with  $K_d = 0.22$  (Fig. 1b). The solution representing this peak is brown and is believed to be due to ferritin, which is a normal contaminant of rat liver ribosomes as conventionally prepared. Preparations of rabbit reticulocyte ribosomal subunits behaved virtually identically with the rat liver subunits except that no ferritin peak was observed (not shown).

The profile for the mixture of subunits obtained by treatment with puromycin shows three peaks at essentially the positions expected for 40S, 60S and ferritin (Fig. 1c and d). Not shown in the elution profiles is the unexpected observation that puromycin did not elute as expected near the total column volume, but at a position corresponding

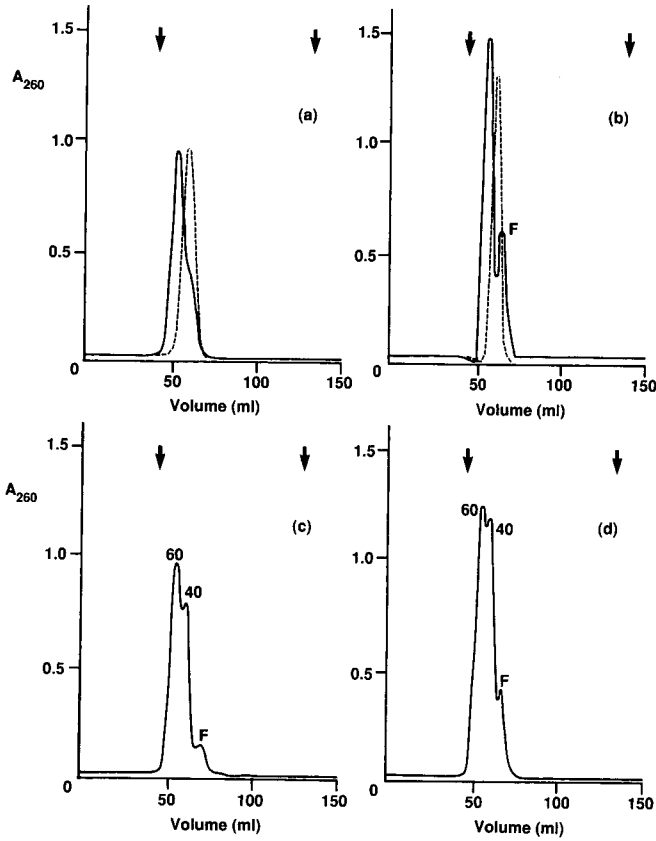


Fig. 1. Elution profiles of rat liver ribosomal subunits on a 135-cm column of Trisacryl GF 2000 equilibrated and eluted with buffer A at (a) and (c) 4°C and (b) and (d) 20°C as described under Experimental: (a) and (b) *ca.* 20  $A_{260}$  units of isolated subunits; (c) and (d) *ca.* 20  $A_{260}$  units of ribosomes treated with puromycin. Arrows on the left-hand side indicate  $V_0$  and on the right  $V_1$ .

to a  $K_d \approx 1.6$ . Krauss and Schmidt [9] observed retardation of nucleotides on Trisacryl GF 05. The separated subunits showed activities in poly-U directed protein synthesis comparable to subunits isolated on Sepharose 4B or by sucrose gradient centrifugation.

Fig. 2 shows the behaviour of ribosomal subunits from *Escherichia coli* on Trisacryl GF 2000. At 4°C both subunits eluted in the order expected (Fig. 2a), but despite the lower molecular masses than for mammalian subunits their  $K_d$  values were smaller (0.11 and 0.15) than for the liver and reticulocyte subunits. The 30S subunit shows a small peak at  $V_0$ , which could be reassociated 70S if the 30S fraction were contaminated with a small amount of 50S during preparation. Under the conditions used, a mixture of the 30S and 50S subunits appeared to elute as 70S couples and excess 30S (Fig. 2b).



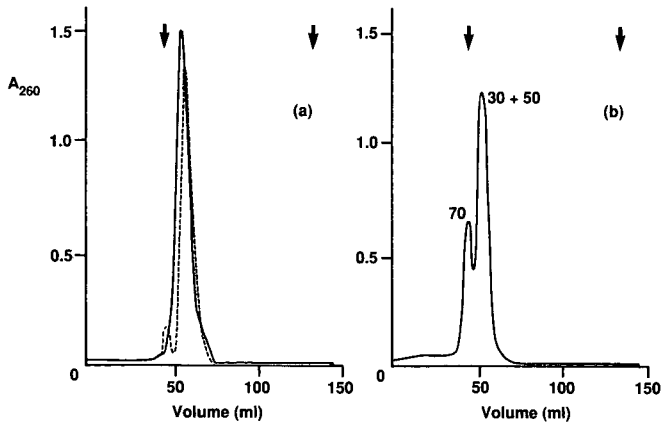


Fig. 2. Elution profiles of *E. coli* ribosomal subunits at 4°C on a 135-cm column of Trisacryl GF 2000 equilibrated and eluted with buffer containing 6 mM KCl, 0.2 mM MgCl<sub>2</sub> and 25 mM Tris-HCl (pH 7.6). (a) Ca. 20  $A_{260}$  units of 30S (---) and 50S (—) subunits prepared from *E. coli* ribosomes by density gradient centrifugation; (b) ca. 20  $A_{260}$  units of *E. coli* ribosomes. Arrows on the left-hand side indicate  $V_0$  and on the right  $V_t$ .

## DISCUSSION

According to the manufacturer, the separation range of Trisacryl GF 2000 is  $1.2 \cdot 10^5$ – $1.5 \cdot 10^7$  dalton. Theoretically, if the separation range were linear, two solutes of  $M_r$   $3.0 \cdot 10^6$  and  $1.5 \cdot 10^6$  would elute with  $K_d = 0.33$  and 0.48, respectively. On Sepharose 4B the 40S subunit had previously been found to possess a  $K_d$  of 0.43 [3], consistent with an  $M_r$  of  $1.3 \cdot 10^6$  based on the supplier's claim of an exclusion range for the gel of  $6 \cdot 10^4$ – $2 \cdot 10^7$  dalton. A 98% separation should be possible if the plate number ( $N$ ) is not less than 800 for the peak for the 60S subunit and 600 for that for the 40S subunit;  $N$  for the 40S subunit was only 180 [3]. For  $^3\text{H}_2\text{O}$  on the Trisacryl a value of  $N \approx 1300$  was obtained with the 30-cm column and 1800 with the 135-cm column, which indicate that a resolving power in excess of 600–800 is possible (use of acetone as opposed to  $^3\text{H}_2\text{O}$  to determine the total column volume showed both a slightly smaller volume and a lower value of  $N$ ).

In the event, the rat liver ribosomal subunits eluted much earlier than the above calculations suggest, at  $K_d \approx 0.13$  for the 60S and 0.19 for the 40S at both 4 and 20°C. These values approximate to apparent  $M_r$  of  $8.0 \cdot 10^6$  for the 60S and  $6.0 \cdot 10^6$  for the 40S, which are several times greater than those normally quoted [1]. For the ferritin peak where  $K_d = 0.22$  the apparent  $M_r$  is  $5.1 \cdot 10^6$ . It is possible that under the conditions used the ribosomal subunits exhibit anomalous  $M_r$ , but the same conclusion would have to be drawn for ferritin with an  $M_r$  normally considered to be about  $5 \cdot 10^5$  [10]. More likely, the relationship of  $K_d$  to  $\log M_r$  is not linear and the gel pore size is not optimum for the separation of these molecular species.

By the same reasoning as for the eukaryote subunits, the apparent  $M_r$  of the *E. coli* subunits would be  $8.7 \cdot 10^6$  and  $7.3 \cdot 10^6$ , but we believe that these results can be discounted. It is apparent, however, that factors other than  $M_r$  determine the elution behaviour of the ribosomes, as the smaller bacterial subunits elute ahead of the larger

mammalian subunits. A distinction between the *E. coli* and mammalian ribosomes may be the difference in the protein to RNA ratio, being 0.67 for the former and 1.0 for the latter, but more important in the present instance is the dissociation of the bacterial ribosomes by low  $Mg^{2+}$  concentrations under low ionic strength conditions, which is likely to lead to greater unfolding of the structure and therefore higher apparent  $M_r$  than in the case of the mammalian ribosomes dissociated and eluted with high ionic strength buffer.

For two solutes with  $K_d$  values of 0.13 and 0.19 to achieve a 98% separation, one needs a value of  $N$  of about 2700, which appears unrealistic. The  $N$  value for the two peaks of liver subunits was in practice about 320 for the 60S and 800 for the 40S. An effective if not 98% separation of ferritin from 60S subunits is possible.

In conclusion, it can be said that, comparing the agarose and Trisacryl resins, the latter did not exhibit the binding phenomenon with the 60S subunit observable with the agarose, although there was interaction with puromycin so as to give retardation, which was not observed on agarose. These observations suggest that the Trisacryl gel is more apolar than the Sepharose and therefore that the 60S subunit binds to agarose at 4°C mainly by hydrogen bonding; its release at higher temperatures bears this out. The compactness of the peaks (theoretical plates) was consistently better on the Trisacryl than on the agarose gels.

#### ACKNOWLEDGEMENTS

We are grateful to the Foundation for Research Development for support for this work and to Dr. R. M. McGrath for helpful comments.

#### REFERENCES

- 1 M. G. Hamilton, A. Pavlovec and M. L. Petermann, *Biochemistry*, 10 (1971) 3424.
- 2 T. E. Martin, I. G. Wool and J. J. Castles, *Methods Enzymol.*, 20 (1971) 417.
- 3 K. L. Manchester and J. E. Manchester, *FEBS Lett.*, 110 (1980) 177.
- 4 S. Petrovic, M. Novakovic and J. Petrovic, *Biochim. Biophys. Acta*, 254 (1971) 493.
- 5 S. L. Petrovic, J. S. Petrovic and M. B. Novakovic, *Biochim. Biophys. Acta*, 308 (1973) 317.
- 6 M. Zeichner and R. Stern, *Biochemistry*, 16 (1977) 1378.
- 7 K. L. Manchester and T. Alford, *Biochim. Biophys. Acta*, 563 (1979) 155.
- 8 K. L. Manchester, *Biochim. Biophys. Acta*, 781 (1984) 279.
- 9 F. Krauss and A. Schmidt, *J. Chromatogr.*, 264 (1983) 111.
- 10 C. F. A. Bryce and R. R. Crichton, *J. Biol. Chem.*, 246 (1971) 4198.

## Short Communication

---

# Determination of vitamin D<sub>2</sub> in shiitake mushroom (*Lentinus edodes*) by high-performance liquid chromatography

KAZUNORI TAKAMURA\* and HIROKO HOSHINO

*Seitoku Junior College of Nutrition, 1–4–6, Nishi-shinkoiwa, Katsushika-ku, Tokyo, 124 (Japan)*

TATSUYUKI SUGAHARA

*Kagawa Nutrition College, 3–24–2, Komagome, Toshima-ku, Tokyo, 170 (Japan)*

and

HISAO AMANO

*Toho University School of Medicine, 5–21–16, Ohmori-nishi, Ohta-ku, Tokyo, 143 (Japan)*

(First received January 8th, 1991; revised manuscript received February 13th, 1991)

---

### ABSTRACT

The total content of vitamin D<sub>2</sub> (ergocalciferol) in shiitake mushroom (*Lentinus Edodes*) was determined by high-performance liquid chromatography. The vitamin D<sub>2</sub> content fluctuated considerably in different years of harvest and according to the brands and the quality of grades; the reason may be that most shiitake mushroom are cultivated under natural climatic conditions.

---

### INTRODUCTION

Ergocalciferol (vitamin D<sub>2</sub>; D<sub>2</sub>) is contained in shiitake (*Lentinus edodes*), a kind of edible mushroom cultivated widely in Japan [1], and its determination is therefore important from the nutritional point of view.

D<sub>2</sub> has been determined in shiitake by spectrophotometric [2,3] gas-liquid chromatographic [4] and high-performance liquid chromatographic (HPLC) procedures [5,6]. However, significant differences in D<sub>2</sub> contents in shiitake were reported, because a small number of samples were taken for determination, the determinations were not conducted on samples taken in consecutive years of harvest but at random, different kinds of pretreatment of the samples were applied or very sensitive detectors (absorbance  $1 \cdot 10^{-3}$ ), generally not in common (sensitivity  $1 \cdot 10^{-2}$ ) use, were used<sup>a</sup>.

In this work, the above differences in D<sub>2</sub> contents in shiitake obtained using HPLC procedures were investigated. The results obtained for the determination of D<sub>2</sub> in shiitake by HPLC procedure are discussed with regard to the quality of grades, the consecutive years of harvest and the various brands.

---

<sup>a</sup> The mobile phase of D<sub>2</sub> determination by HPLC used mainly a solution of *n*-hexane. It is difficult to detect high sensitivity for an unstable baseline.

## EXPERIMENTAL

The test samples used were obtained from cultivated Japanese shiitake mushroom, harvested and heated to dryness in the years 1986–88. The  $D_2$  contents in the samples were determined by applying the HPLC procedure in the year of harvest. A 10-g sample was homogenized in a blender and an aliquot of *ca.* 3 g of the homogenate was placed in a digestion flask. After the addition of 40 ml of aldehyde-free ethanol, 4 g of pyrogallol and 10 ml of 50% potassium hydroxide solution the sample was decomposed at 80°C for 30 min. After the mixture had cooled completely it was extracted with 100 ml of benzene. The benzene fraction was washed once each with 100 ml of 1 and 0.5 *M* potassium hydroxide solution and four times with 30 ml of distilled water and then filtered through Whatman 1PS filter-paper. An aliquot of 90 ml of the filtrate was evaporated to dryness below 35°C. The residue was dissolved in 1 ml of methanol–acetonitrile (1:1) and the solution obtained served as the test material for the determination of  $D_2$  by HPLC.

A 200- $\mu$ l volume of the solution was injected onto a LiChrosorb RP-18 column (250 mm  $\times$  7.5 mm I.D.) and eluted with methanol–acetonitrile (1:1) at a flow-rate of 2.2 ml/min. The fraction obtained was evaporated to dryness and the residue was dissolved in 0.5 ml of the HPLC eluent. For the determination of  $D_2$  by HPLC an aliquot (30  $\mu$ l) of the solution was injected onto to a Nucleosil 100-5 column (150 mm  $\times$  4.6 mm I.D.) and eluted with hexane containing 0.1% of *n*-amyl alcohol and 0.4% of isopropyl alcohol at a flow-rate of 1 ml/min. An NSLC Model 100A HPLC unit (Nippon Seimitsu Kagaku) was used; reagents used were obtained from Wako Junyaku Kogyo.

## RESULTS AND DISCUSSION

A chromatogram obtained from the test material by preparative HPLC is shown in Fig. 1. A fraction containing  $D_2$  was obtained with a retention time of 18–22 min, and before and after this fraction other benzene-soluble substances were eluted. As shown in Fig. 2, when the fraction containing  $D_2$  (*ca.* 50 ng) was subjected to HPLC, a single peak of  $D_2$  with a retention time of 7.6 min was obtained. From the results obtained, it is evident that  $D_2$  is separated satisfactorily on the 150-mm column and the sensitivity of the absorbance detector was  $1 \times 10^{-2}$ . The results of a recovery test with authentic  $D_2$  are shown in Table I. Takeuchi *et al.* [7] reported that  $D_2$  detected in dried shiitake was mostly in the free form and the esterified form was not detected. From these results, it may be better to apply a direct saponification method than an extraction method [6] for crude fat in-test material.

*Determination of total vitamin D<sub>2</sub> content in dried shiitake*

The results of the determination of total  $D_2$  content ( $D_2$  + pre-ergocalciferol) in dried shiitake obtained in consecutive years and according to the brand and the quality of the grades are shown in Table II. Kiribuchi [6] reported that  $D_2$  was contained in some samples of dried shiitake but not in others. In this work, however, the existence of  $D_2$  in all the samples tested was confirmed but the yearly fluctuations of the total content of  $D_2$  were significant.

According to the report of Takeuchi *et al.* [7], the total content of  $D_2$  was higher

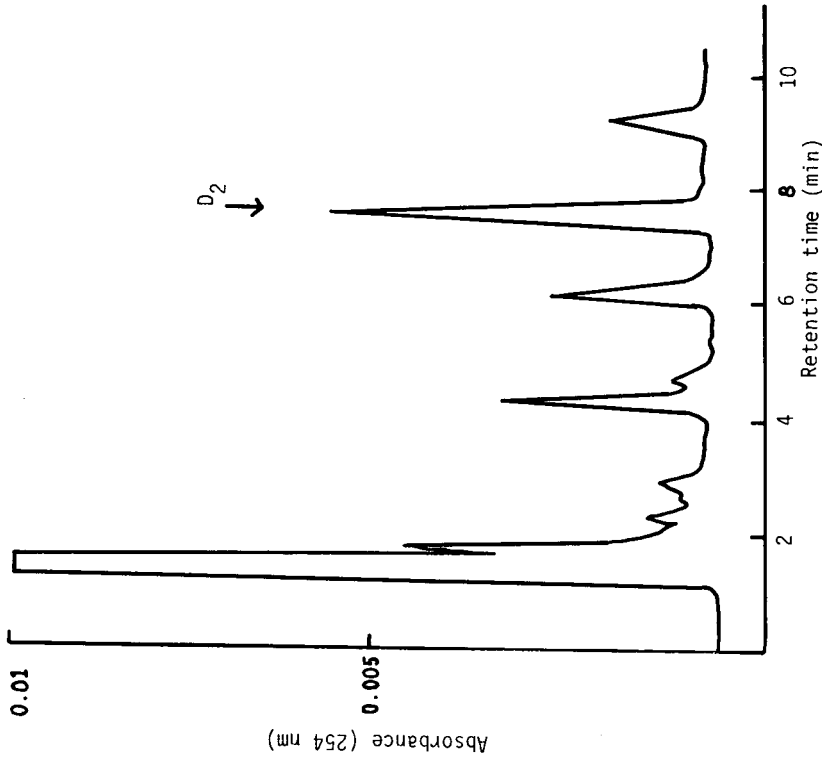


Fig. 1. HPLC of  $D_2$  in crude extract of dried shitake, obtained with clean-up procedure. LiChrosorb RP-18 column, 250 mm  $\times$  7.5 mm I.D.; mobile phase, methanol-acetonitrile (1:1); flow-rate, 2.2 ml/min. Hatched area: the fraction with the same retention time as that of the standard sample was collected.

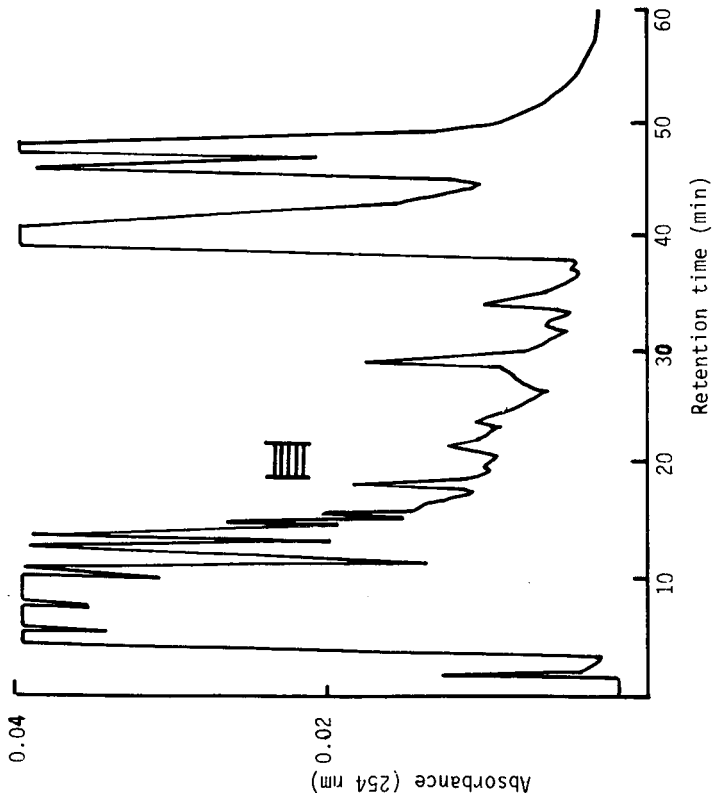


Fig. 2. HPLC of purified  $D_2$  fraction obtained from dried shitake. Nucleosil 100-5 column, 150 mm  $\times$  4.6 mm I.D.; mobile phase, *n*-hexane containing 0.1% *n*-amyl alcohol and 0.4% isopropyl alcohol; flow-rate, 1 ml/min; UV detection at 254 nm.

TABLE I  
DETERMINATION AND RECOVERY TEST OF VITAMIN D<sub>2</sub> IN DRIED SHIITAKE BY HPLC

Trial No.	Vitamin D <sub>2</sub> (IU per 100 g)		Recovery (%)
	Added	Total present <sup>a</sup>	
1	1500	3206	94.8
2	1500	2906	74.8
3	1500	2960	78.4
4	1500	3118	88.9
5	1500	3014	82.0
Mean ± S.D.			83.8 ± 7.2

<sup>a</sup> Without addition of vitamin D<sub>2</sub>, mean ± S.D. (n=5) = 1784.4 ± 108.1 IU per 100 g.

TABLE II  
CONTENTS OF VITAMIN D<sub>2</sub> IN DRIED SHIITAKE BY HPLC

Brand name <sup>a</sup>	Vitamin D <sub>2</sub> (IU per 100 g dry wt.) <sup>b</sup>		
	1986	1987	1988
Jyo-donko	1516 ± 932	1752 ± 568	1090 ± 154
Nami-donko	2767 ± 285	873 ± 68	1397 ± 346
Kotsubu-donko	3102 ± 928	1457 ± 260	1182 ± 396
Jyo-koshin	2026 ± 792	4382 ± 379	1809 ± 158
Nami-koshin	2062 ± 570	1762 ± 411	1607 ± 99
Chayori	1828 ± 83	1871 ± 437	2148 ± 560

<sup>a</sup> Jyo, high grade; Nami, middle grade; Kotsubu and Chayori, low grade.

<sup>b</sup> Values are means ± S.D. for 15 samples.

in Koshin (mushroom with large pileus) than in Donko (mushroom with small pileus) and this tendency was observed in general, but no significant differences were observed. The reason why the total contents of D<sub>2</sub> in the dried shiitake fluctuate significantly in different years of cultivation and according to the brands and quality of grades may be that most shiitake mushrooms are cultivated under natural climatic conditions.

#### REFERENCES

- 1 K. Takamura, H. Hoshino, N. Harima, T. Sugahara and H. Amano, *J. Chromatogr.*, 543 (1991) 241.
- 2 K. Arimoto, T. Ttakano, K. Matsuoka, G. Saimon, T. Yamashita, K. Katoh, T. Ono, N. Tosane, K. Mori and C. Miyashita, *Nippon Kosyu Eisei Zasshi*, 14 (1967) 1201.
- 3 A. Fujita, S. Tokuhisa and K. Michinaka, *Bitamin*, 40 (1969) 121.
- 4 T. Kobayashi, A. Adachi and K. Furuta, *Bitamin*, 50 (1976) 421.
- 5 A. Takeuchi, T. Okano, S. Teraoka, Y. Murakami, M. Sayamoto, S. Sawamura and T. Kobayashi, *Bitamin*, 58 (1984) 439.
- 6 T. Kiribuchi, *Nippon Kaseigaku Kaishi*, 41 (1990) 395.
- 7 A. Takeuchi, T. Okano, M. Sayamoto, S. Sawamura and T. Kobayashi, *Bitamin*, 58 (1984) 589.

## Short Communication

---

# High-performance liquid chromatography of rubber antidegradants with diode-array detection

E. BRANDŠTETEROVÁ\*

*Department of Analytical Chemistry, Slovak Technical University, Radlinského 9, 812 37 Bratislava (Czechoslovakia)*

M. ŠTUBŇA

*Institute of Rubber Technology, Gumárne Púchov, 020 01 Púchov (Czechoslovakia)*

and

J. LEHOTAY and D. DERNESCHOVÁ

*Department of Analytical Chemistry, Slovak Technical University, Radlinského 9, 812 37 Bratislava (Czechoslovakia)*

(First received April 17th, 1990; revised manuscript received December 28th, 1990)

---

## ABSTRACT

High-performance liquid chromatography (HPLC) using diode-array detection is described for the separation and determination of antioxidants applied in tyre production.

An octadecyl silica column was used with a methanol–0.05% ammonia solution as the mobile phase. The extraction recoveries were determined for the rubber samples with contents of the antioxidants N-phenyl-N'-isopropyl-*p*-phenylenediamine (CD), N-phenyl- $\beta$ -naphthylamine (PBN) and 2,2,4-trimethyl-1,2-dihydroquinoline (TMQ).

The influence of weather conditions on the contents of CD and PBN in tyre samples was evaluated and the stability changes were compared for rubber samples before and after vulcanization procedures.

The HPLC method has also been applied to the determination of the antioxidant PBN contents in rubber samples used as the raw materials. Detection limits were 0.26, 0.14 and 0.41 mg/kg for CD, PBN and TMQ, respectively.

---

## INTRODUCTION

Antidegradants are commonly used in the rubber and plastics industry to improve the dynamic characteristics of rubber products and prevent their degradation. The analysis of different types of antioxidants has been described [1–4]. Thin-layer and gel permeation chromatography have been applied to the analysis of additives used for the stabilization and vulcanization for rubbers [5,6] after their extraction with polar solvents (acetone, diethyl ether, ethanol, isopropanol). Typical amine stabilizers used

in rubber production have been determined [7] using a polystyrene gel chromatograph with tetrahydrofuran as the solvent.

The application of silica columns to the antidegradants separation has been described [8,9]. It was stated that adsorption chromatography is not suitable for this purpose as aromatic diamines (*e.g.*, *p*-phenylenediamine) are chemisorbed on active hydroxyl groups on the surface of the adsorbent.

The high-performance liquid chromatographic (HPLC) separation of antioxidants from rubber and plastics with the macroporous gel Separon SE and methanol and acetonitrile as eluents has been reported [10]. The samples of rubber were Soxhlet extracted for 24 h in acetone and the extract was evaporated to dryness and the residue dissolved in methanol. Methanol–water, acetonitrile–water and tetrahydrofuran–water were tried as mobile phases but methanol–diethyl ether–water (80:10:10) was recommended. UV detection was applied at 254 nm. The determination of secondary aromatic amine antioxidants (*e.g.*, phenyl-1-naphthylamine) and the isolation and identification of their intermediate oxidation products (dimer, trimer, tetramer) after 24 h at 190°C have been described [11]. Liquid chromatography was used for separation, with identification of the intermediate products by mass spectrometry and determination using gas chromatography with a thermionic detector.

We described in previous papers [12–14] the application of HPLC for the control of the stability of dialkyldithiocarbamates (dimethyl and dibutyl derivatives, which have been used as antioxidants in the plastics and rubber industry), with their simultaneous separation together with the main degradation products (tetraalkylthiuram disulphides, monosulphides and dialkylthiourea).

The aim of this work was to develop a control method for the determination of antidegradants applied in tyre production. An HPLC method using diode-array detection was applied in the combination with extraction procedures. This method can be recommended for control analyses in rubber factories (control of standards purity, contents of antidegradants before and after the vulcanization process) and it has been applied in studies of stability changes under the influence of oxygen, temperature and time.

## EXPERIMENTAL

### *Apparatus*

All experiments were carried out on a Waters Assoc. modular HPLC system with a Model 990 a diode-array detector. A Separon C<sub>18</sub> (5 μm) glass column (150 × 3.2 mm I.D.) with a short C<sub>18</sub> (7 μm) precolumn (30 × 3.2 mm), both from Tessek (Prague, Czechoslovakia), were used with methanol–0.05% ammonia solution (pH 7.2) (85:15) as the mobile phase.

### *Chemicals*

Antidegradants used for tyre production, CD (N-phenyl-N'-isopropyl-*p*-phenylenediamine), PBN (N-phenyl-β-naphthylamine) and TMQ (2,2,4-trimethyl-1,2-dihydroquinoline), were obtained as standards from the Institute of Rubber Technology (Gumárne Púchov, Czechoslovakia). Their purity was verified by elemental analysis using a Model 1108 Elemental Analyser (Carlo Erba, Milan, Italy). All solvents were of analytical-reagent grade from Lachema (Brno, Czechoslovakia).



### Procedures

Extractions were made with acetone according to a published procedure [5,10] or directly on 0.1-g rubber samples by extraction with four 10-ml volumes of methanol. The extracts were filtered using Tessek cellulose filters and injected in volumes of 20  $\mu$ l into the chromatographic column.

### RESULTS AND DISCUSSION

The purities of the antidegradants CD, PBN and TMQ were checked by elemental analysis and the results are given in Table I. Three different standards of TMQ were analysed and compared [Matoflex (Czechoslovakia), Naogard (Hungary) and Flectol (Germany)]. For all three standards the chromatograms are shown in Fig. 1. The three chromatograms confirmed that TMQ is a mixture of different monomers eluted at about 4.5, 6.3 and 8.1 min.

TABLE I  
RESULTS OF ELEMENTAL ANALYSIS OF THE ANTIDEGRADANTS

Antidegradant	Theoretical (%)			Found (%)		
	C	H	N	C	H	N
CD	79.26	8.37	12.34	79.37	7.99	12.49
PBN	87.27	6.36	6.35	87.05	5.95	6.52
TMQ (Matoflex)	83.24	8.67	8.09	82.82	8.50	7.93
TMQ (Naogard)	83.24	8.67	8.09	83.31	8.63	8.02
TMQ (Flectol)	83.24	8.67	8.09	82.99	8.59	7.77

The optimum mobile phase for the separation of CD, PBN and TMQ was methanol-0.05% ammonia solution (pH 7.2) (85:15). A flow rate of 0.3 ml/min resulted in a simultaneous separation with good resolution ( $R_{ij} > 1.25$ ). The elution times for CD and PBN were 3.6 and 5.7 min, respectively. The resolution values for CD and PBN was  $R_{ij} = 1.92$  and that for CD and TMQ was  $R_{ij} = 2.86$ . This means that combinations of the antidegradants CD-PBN and CD-TMQ can be evaluated quantitatively without problems.

The main reason for the use of TMQ instead of PBN in tyre production is the possible carcinogenicity of PBN. Rubber mixtures before vulcanization and vulcanized rubber products (different types of tyres produced in Gumarne Púchov) were extracted according to the procedures described under Experimental. The average extraction recoveries (for five parallel experiments) were for CD  $95.4 \pm 2.1\%$ , for PBN  $97.3 \pm 1.9\%$  and for TMQ  $84.2 \pm 3.1\%$ .

Comparing the results of HPLC analysis of rubber samples before and after vulcanization procedures it was found that in many instances the antidegradant concentrations were lower after vulcanization. Using diode-array detection it was found that in some rubber samples after vulcanization CD was degraded and a new peak was observed in the chromatogram (retention time 4.4 min). The absorption maxima for CD and its degradation product were 206.4 and 288.0 nm, respectively.

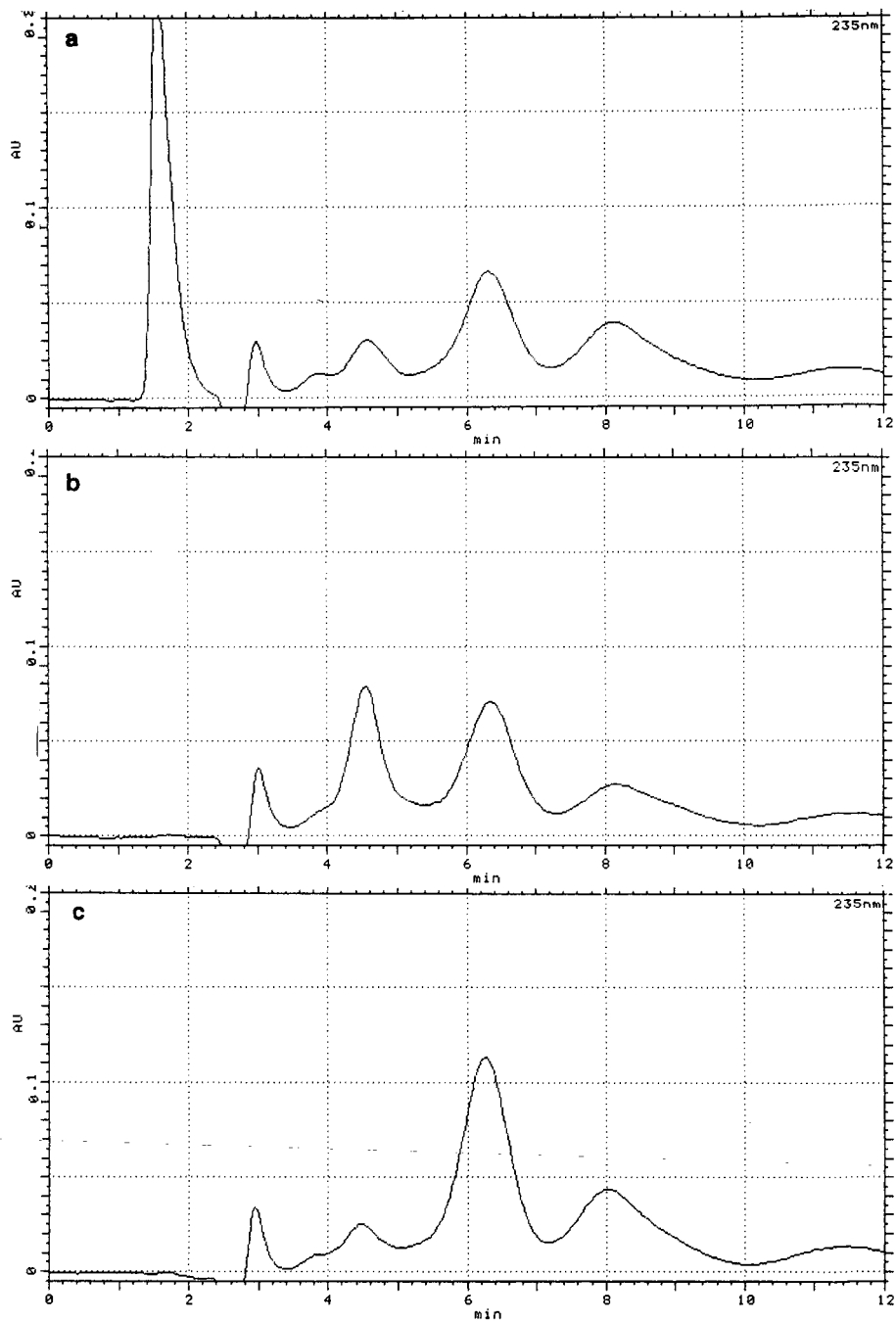


Fig. 1. HPLC of TMQ samples: (a) Matoflex; (b) Naogard; (c) Flectol. Column: Separon C<sub>18</sub> (5  $\mu$ m) (150  $\times$  3.2 mm I.D.). Mobile phase: methanol-0.05% ammonia solution (85:15). Flow-rate: 0.3 ml/min.

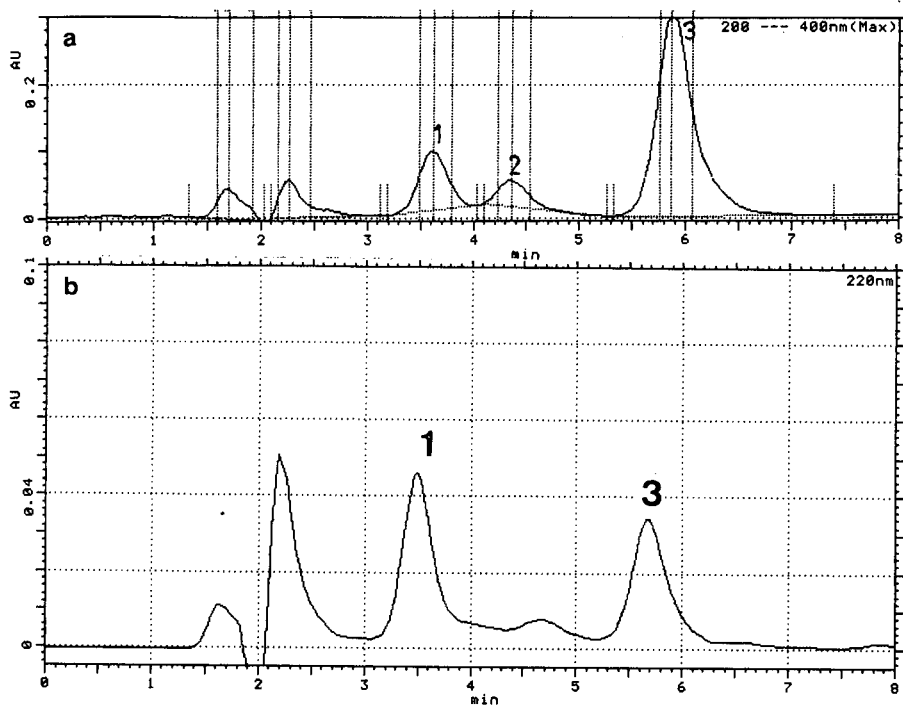


Fig. 2. HPLC of (a) a vulcanized rubber product extract and (b) a non-vulcanized rubber mixture. Peaks: 1 = CD; 2 = degradation product of CD; 3 = PBN.

The HPLC separations of the extract of the vulcanized rubber product and the rubber mixture before vulcanization are illustrated in Fig. 2. The contents of CD and PBN in rubber samples before and after vulcanization are given listed in Table II.

HPLC was also applied to the determination of the antidegradant contents in rubber used as the raw materials. It was found that some of rubber additives used contain small amounts of PBN (Fig. 3) and for this reason PBN was also identified using diode-array detection in the extracts of tyres prepared without the direct addition of PBN (Fig. 4).

The results of the determination of CD and PBN in tyres produced in Gumárne Púchov are given in Table III. Three samples with known amounts of both antidegradants were evaluated after subtraction of the concentrations of PBN found in

TABLE II

CONTENTS OF CD AND PBN IN RUBBER BEFORE AND AFTER VULCANIZATION

Antidegradant	Before vulcanization (%)	After vulcanization (%)
PBN	0.634	0.560
CD	0.890	0.814

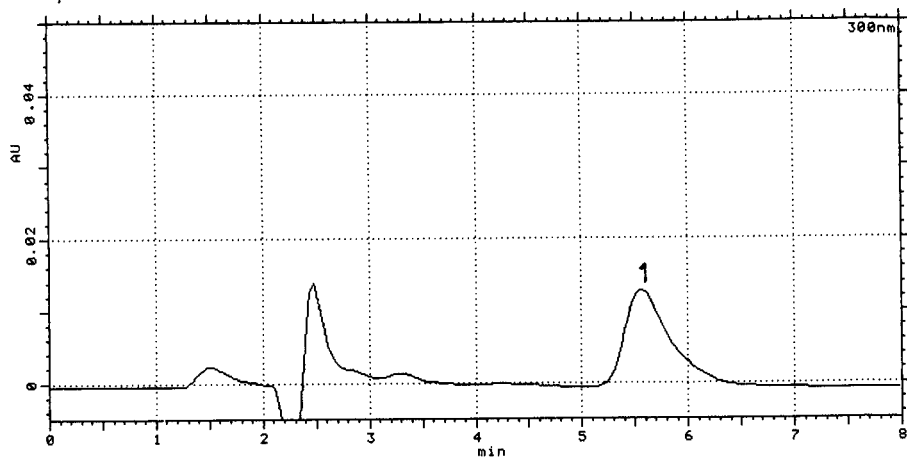


Fig. 3. HPLC separation of an extract of rubber (SKI-3). Conditions as in Fig. 1. Peak 1 = PBN.

the rubber samples without PBN (blank). The average value was also subtracted from the results obtained for unknown samples (Nos. 19 and 208). The content of PBN in rubber (SKI-3) was about 0.2%.

The data were evaluated using linear regression according to the calibration graph  $y = 2.06 + 89.4x$ , where  $y$  is the peak area ( $\text{mm}^2$ ) and  $x$  the concentration ( $\mu\text{g/g}$ ); the correlation coefficient was  $r = 0.9962$ . The response of the detector was linear for antidegradant concentrations in rubber samples in the range 0.1–10  $\mu\text{g/ml}$  (five parallel experiments for one determination); relative standard deviations are given in Table III. The detection limits were CD 0.26, PBN 0.14 and TMQ 0.41  $\text{mg/kg}$ .

The influence of weather conditions on the contents of CD and PBN in two samples (Nos. 05 and 12) was studied by analysing the samples immediately after

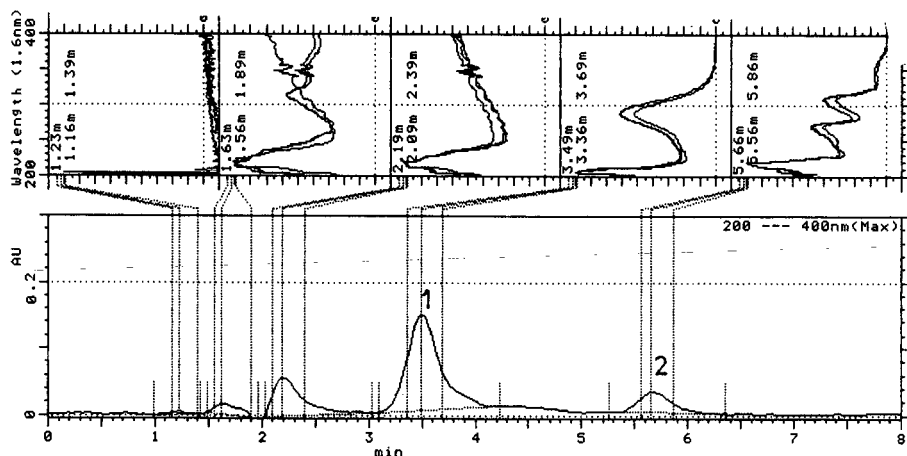


Fig. 4. HPLC separation of an extract of vulcanized rubber tyres prepared without PBN. Conditions as in Fig. 1. Peaks: 1 = CD; 2 = PBN.

TABLE III  
CONTENTS OF CD AND PBN IN EXTRACTS OF TYRES

Sample No.	Antidegradant	Content (%)	Extraction recovery (%)	R.S.D. <sup>a</sup> (n=5) (%)
05-20	PBN	0.582	96.52	2.2
	CD	0.814	95.29	2.0
15-07	PBN	0.506	97.27	1.8
	CD	0.498	95.57	2.1
90-15	PBN	0.516	98.01	1.7
	CD	0.799	94.85	2.4
19	PBN	0.498	—	—
	CD	0.466	—	—
208	PBN	0.528	—	—
	CD	0.501	—	—

<sup>a</sup> Relative standard deviation.

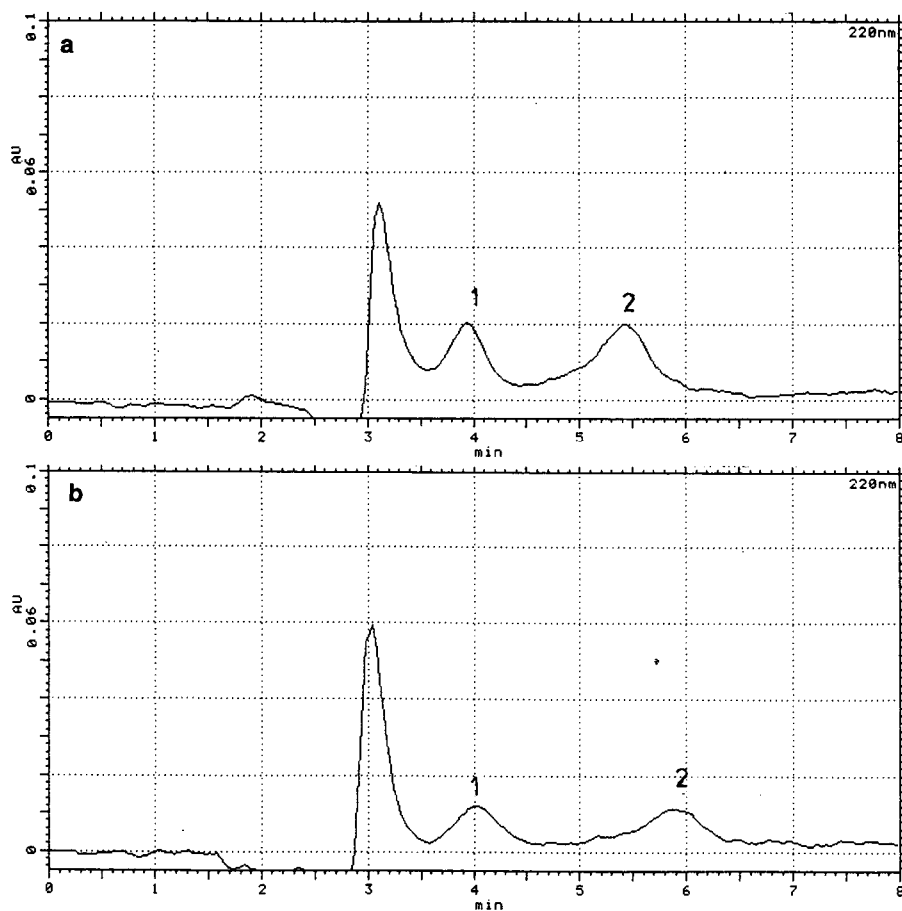


Fig. 5. HPLC of tyre sample 05 (a) before and (b) after exposure to weather for 4 months. Conditions as in Fig. 1. Peaks: 1 = CD; 2 = PBN.

TABLE IV

CONTENTS OF CD AND PBN (%) IN SAMPLES 05 AND 12 BEFORE AND AFTER THE EXPOSURE TO WEATHER CONDITIONS

Sample No.	Antidegradant	Time of exposure (months)		
		0	4	5
05	PBN	0.549	0.169	0.093
	CD	0.806	0.159	0.095
12	PBN	0.315	0.051	0.050
	CD	1.139	0.251	0.236

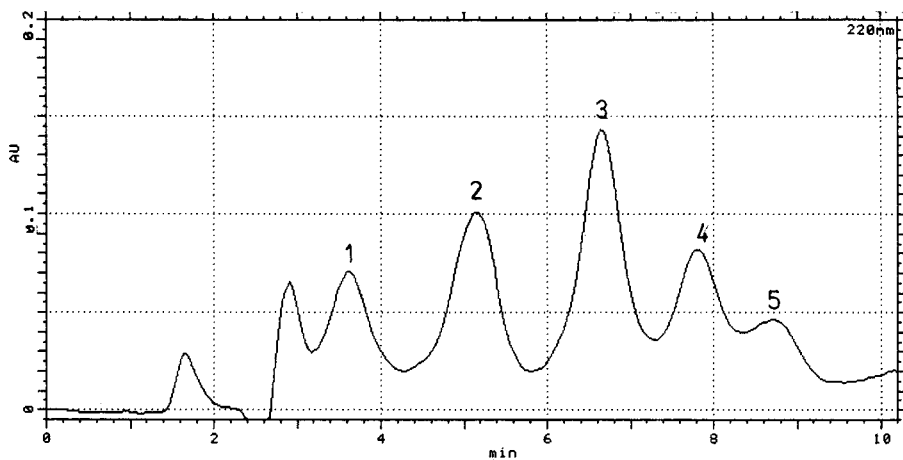


Fig. 6. HPLC of an extract of a rubber sample with CD and TMQ added. Conditions as in Fig. 1. Peaks: 1 = CD; 2 = PBN; 3 = TMQ; 4,5 = degradation products of TMQ.

production and after 4 and 5 months of exposure. The results are given in Table IV and chromatograms of sample 05 before and after exposure are shown in Fig. 5. It is obvious that the concentrations of both antidegradants decreased rapidly during exposure (June–October).

Fig. 6 is a chromatogram of the extract of a rubber sample (No. 276) with CD and TMQ added. This separation also illustrates the simultaneous determination of CD, PBN and TMQ, because PBN was originally used as an additive in the rubber.

In conclusion, this method achieves the rapid simultaneous separation (12 min) of antidegradant applied in tyre production (CD, PBN and TMQ) together with the degradation products before and after vulcanization.

#### REFERENCES

- 1 J. Pospíšil, *Antioxidants*, Academia, Prague, 1968.
- 2 J. Čoupek, S. Pokorný, J. Holčík, M. Karvaš and J. Pospíšil, *J. Chromatogr.*, 65 (1972) 279.
- 3 J. Čoupek, S. Pokorný, L. Jiráčková and J. Pospíšil, *J. Chromatogr.*, 75 (1973) 87.
- 4 R. B. Sleight, *Chromatographia*, 61 (1973) 3.

- 5 J. Protivová, J. Pospíšil and J. Holčík, *J. Chromatogr.*, 92 (1974) 361.
- 6 B. Uchytíl, *J. Chromatogr.*, 93 (1974) 447.
- 7 J. Protivová, J. Pospíšil, *J. Chromatogr.*, 88 (1974) 65.
- 8 A. W. Wims and J. J. Swarin, *J. Appl. Polym. Sci.*, 19 (1975) 1243.
- 9 B. L. Karger, J. R. Grant, A. Hartkopf and R. H. Weiner, *J. Chromatogr.*, 728 (1976) 65.
- 10 P. Šmejkal, M. Popl and A. Čihová, *J. Polym. Sci.*, 68 (1980) 145.
- 11 M. A. Keller and C. S. Saba, *J. Chromatogr.*, 409 (1987) 325.
- 12 O. Liška, J. Lehotay, E. Brandšteterová and G. Guiochon, *J. Chromatogr.*, 171 (1979) 153.
- 13 E. Brandšteterová, J. Lehotay, O. Liška and J. Garaj, *J. Chromatogr.*, 291 (1984) 439.
- 14 E. Brandšteterová, J. Lehotay, J. Garaj and P. A. Leclercq, *J. Chromatogr.*, 404 (1987) 359.

## Short Communication

---

# Multiple-development high-performance thin-layer chromatography of organochlorine pesticides

GAETANO LODI\* and ADALBERTO BETTI

*Department of Chemistry, University of Ferrara, Via L. Borsari 46, I-44100 Ferrara (Italy)*

and

YASSIN DUALE KAHIE and AHMED MOHAMUD MAHAMED

*Department of Chemistry, Somali National University, P.O. Box 1081, Mogadishu (Somalia)*

(Received December 4th, 1990)

---

### ABSTRACT

Gradient multiple development on silica gel high-performance liquid chromatographic plates has been employed in this work to separate organochlorine pesticides. This method, even when performed with a limited number of development steps as in the present case, seems to give higher spot capacity and lower detection limits. Thus, wider screening possibilities for pesticide residue analysis can be expected to be introduced in the future employing multiple development gradients performed by automated techniques.

---

### INTRODUCTION

The application of thin-layer chromatography (TLC) to the separation, identification and determination of organochlorine pesticides (OC) is well documented [1–6]. Among the various sorbents employed, silica gel and alumina [7] are the most popular. Plates with preadsorbent or concentration zones have been recommended because they allow sharper separations and higher sensitivity [8–10]. Many chromogenic reagents have been proposed [1,2,11–14]. For screening purposes silver nitrate, *o*-toluidine and 3,5,3',5'-tetramethylbenzidine (TMB) seem to be the most suitable, the visual detection sensitivities ranging from 50 to 300 ng for many OC pesticides [13,15,16] and the lowest being obtained on silica gel plates with preadsorbent zones [16].

The coupling of a very efficient preconcentration technique with TLC separation allows the detection of OC pesticides at trace levels. Sherma [16] and Junk and Richard [17], for instance, showed that using C<sub>18</sub> solid-phase extraction it is possible, assuming 80% recovery, to achieve a detection limit of 0.06 ppb (10<sup>9</sup>) for methoxychlor, lindane, endrin and DDT using a 1000-ml water sample. If lower detection limits are not



required, modern TLC [18] may play a role in pesticide residue analysis for both screening and quantitative purposes [16].

In this paper, the gradient multiple development of some selected OC pesticides on high-performance (HP) TLC plates is described. In the multiple development process, the plate is repeatedly developed in the same direction with either the same or a different solvent, with drying of the solvent between runs. Each subsequent development moves the trailing edge of the zone closer to the front, resulting in narrower bands. This effect improves the spot capacity and sensitivity [19]. Gradient multiple development on silica gel plates is expected to enhance the visual detection limits, thus allowing improved screening analyses.

## EXPERIMENTAL

### *Materials*

Merck (Darmstadt, Germany) 5641 silica gel 60 HPTLC precoated plates, 10 × 20 cm, without fluorescence indicator, prewashed with dichloromethane-methanol (1:1) and then with pure methanol, were used. The solvents employed were *n*-heptane and dichloromethane of HPLC grade (Carlo Erba, Milan, Italy). The OC insecticides methoxychlor, dieldrin, endosulfan, lindane, *p,p'*-DDD, *p,p'*-DDE and aldrin were obtained from Supelco (Bellefonte, PA, U.S.A.) and used as received and dissolved in ethyl acetate to give 50–1000-ppm solutions.

### *Sample application*

Standard solutions were applied to the plates as 10 mm wide bands with a Linomat IV (Camag, Muttentz, Switzerland) (1–3  $\mu$ l; delivery speed 0.25  $\mu$ l/s).

### *Chromatographic conditions*

Ascending, one-dimensional, stepwise multiple development in a twin chamber (Camag), without chamber saturation, was applied. The temperature was 21–23°C and the relative humidity 60–65%.

The mobile phases were *n*-heptane-dichloromethane in the following proportions, with the distances run in each development step as indicated: (1) 55:45, 14 mm; (2) 65:35, 28 mm; (3) 75:25, 42 mm; (4) 85:15, 56 mm; (5) 95:5, 70 mm. After each development the plate was dried in a stream of nitrogen for 2 min. The time for a complete run was about 50 min.

### *Detection*

The developed plates were dipped either in 0.5% ethanolic solutions of silver nitrate containing 5% concentrated ammonia solution or 0.1% acetone solutions of 3,5,3',5'-tetramethylbenzidine (TMB).

The dried plates were irradiated with short-wavelength UV light for 30 min. The pesticides were detected on the layer as black-brown spots on a white background with silver nitrate and yellow-brown spots on a clear background with TMB. The spots obtained in both instances remain stable for several days if the dipped layer is kept in a refrigerator.

The derivatized layers were scanned with a Camag Scanner II equipped with a Merck-Hitachi chromato-integrator. The reflectance was measured at 550 nm.

## RESULTS

The choice of the solvent for multiple development depends on the width of the polarity range of the sample components. Samples with wide polarity ranges require so-called "universal gradients" that are useful for general purposes [18]. They consist of solvent mixtures starting with a very polar and ending with a very non-polar solvent, *e.g.*, methanol–dichloromethane–*n*-hexane.

In the present instance, owing to the relatively narrow polarity range of the OC insecticide mixture, a two-component solvent, one of medium polarity and the other of low polarity, proved to be appropriate. Dichloromethane was chosen from other possible medium-polarity solvents because, in addition to showing good selectivity, it could be used in a relatively wide composition range (from 45% to 5%) in mixtures with *n*-heptane. *n*-Heptane was chosen as a non-polar solvent because it showed a better mobility (20%) than *n*-hexane.

Some isocratic runs were carried out as preliminary steps for the gradient set-up. The results of these experiments are shown in Fig. 1 as plots of  $R_M$  versus volume fraction ( $\varphi$ ) of dichloromethane for the eight OC insecticides. These isocratic data and those with multiple development were obtained under unsaturated conditions; better separations took place under these conditions than under saturated conditions, as observed previously by Gocan and Marutoiu [20].

It is noteworthy that in the experimental conditions adopted (relative humidity 60–65% and no preadsorption of the solvent vapour on the layer), a linear relationship between  $R_M$  and volume fraction,  $\varphi$ , of dichloromethane was obtained, as shown in Fig. 1. In contrast, a linear relationship between  $R_M$  and  $\log \varphi$ , generally expected in normal-phase liquid chromatography, was found for the eight insecticides if the layers were allowed to preequilibrate with the solvent vapour before the development.

From the plots in Fig. 1, it is apparent that solvents with  $\varphi \geq 0.40$  should be used

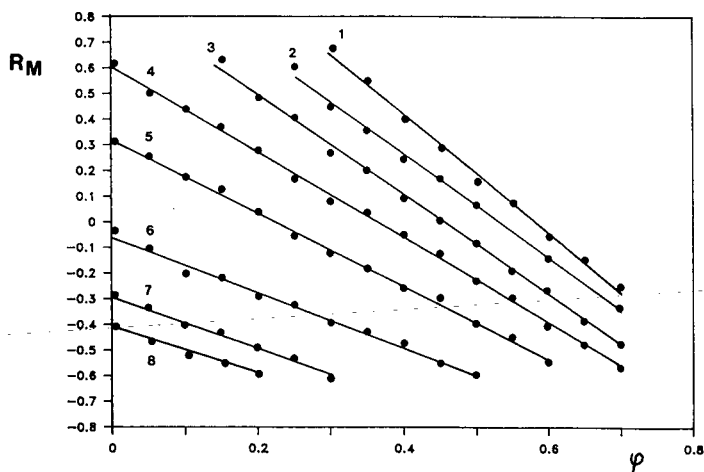


Fig. 1. Plot of  $R_M$  versus volume fraction of dichloromethane ( $\varphi$ ) on HPTLC silica gel layers. OC insecticides as listed in Table I.

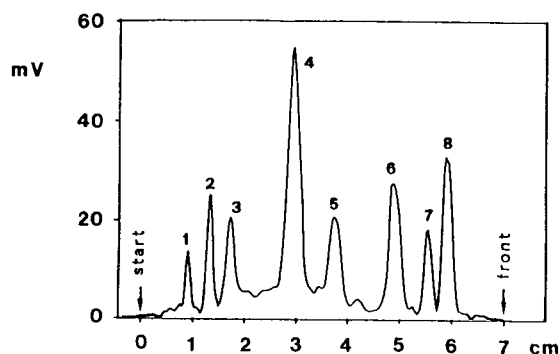


Fig. 2. HPTLC of OC insecticides. Densitogram of HPTLC plate after multiple development and derivatization with ethanolic silver nitrate, according to Sherma [16]. OC insecticides as in Table I. Amount of insecticide applied from 50 ng to 1  $\mu$ g per spot.

as a first step in the gradient development in order to move appreciably methoxychlor, the most polar of the insecticides. On the other hand, a solvent of low polarity must be used in the last steps of the gradient in order to separate aldrin and *p,p'*-DDE. This separation is only possible in chromatographic zones not too close to the solvent front [21].

A few experiments were sufficient to devise the five-step optimized gradient described under Experimental. Fig. 2 shows the densitogram of the eight standards, well separated into narrow bands with a homogeneous distribution in the chromatographic space. An appreciable band reconcentration effect may be observed here and in Table I, where the limits of visual detection of the OC are reported.

In conclusion, multiple development on silica gel HPTLC plates increases the screening possibilities in pesticides residue analysis. Further, the results can be significantly improved by using gradients with a larger number of development steps as performed by automated techniques [6,18].

TABLE I

VISUAL DETECTION LIMITS OF ORGANOCHLORINE PESTICIDES (ng/mm<sup>2</sup>)

No.	Compound	Silver nitrate + UV	TMB + UV
1	Methoxychlor	1	10
2	Dieldrin	15	15
3	$\alpha$ -Endosulfan	50	2
4	Lindane	5	5
5	<i>p,p'</i> -DDD	15	25
6	<i>p,p'</i> -DDT	1	3
7	<i>p,p'</i> -DDE	5	10
8	Aldrin	10	25

## REFERENCES

- 1 J. Sherma, in G. Zweig and J. Sherma (Editors), *Analytical Methods for Pesticides and Plant Growth Regulators*, Vol. VII, Academic Press, New York, 1973, p. 3.
- 2 J. Sherma, in G. Zweig and J. Sherma (Editors), *Analytical Methods for Pesticides and Plant Growth Regulators*, Vol. XI, Academic Press, New York, 1980, p. 79.
- 3 V. N. Mallet, in J. Harvey and G. Zweig (Editors), *Pesticide Analytical Methodology (ACS Symposium Series, No. 136)*. American Chemical Society, Washington, DC, 1980, p. 137.
- 4 M. E. Getz, *Paper and Thin-Layer Chromatography of Environmental Toxicants*, Heyden, London, 1980.
- 5 J. Sherma, *J. Liq. Chromatogr.*, 5 (1982) 1013.
- 6 J. Sherma, in G. Zweig and J. Sherma (Editors), *Analytical Methods for Pesticides and Plant Growth Regulators*, Vol. XIV, Academic Press, New York, 1986, p. 1.
- 7 J. M. Follweiler and J. Sherma, *Handbook of Chromatography —Pesticides*, Vol. 1, CRC Press, Boca Raton, FL, 1984.
- 8 J. Sherma, *Am. Lab. (Fairfield, Conn.)*, 10 (1980) 105.
- 9 J. C. Touchstone and S. S. Levin, *J. Liq. Chromatogr.*, 3 (1980) 1853.
- 10 H. E. Hauck and E. Amadori, in J. Harvey and G. Zweig (Editors), *Pesticide Analytical Methodology (ACS Symposium Series, No. 136)*, American Chemical Society, Washington, DC, 1980, p. 159.
- 11 V. M. Adamovic, *J. Chromatogr.*, 23 (1966) 274.
- 12 M. Beroza, J. Sherma and J. F. Thompson, *Analysis of Pesticide Residues in Human and Environmental Samples*, U.S. Environmental Protection Agency, Triangle Park, 1977.
- 13 J. Makhubalo, A. Mainga and A. Phiri, *J. Chromatogr.*, 284 (1984) 518.
- 14 J. Sherma, in G. Zweig and J. Sherma (Editors), *Analytical Methods for Pesticides and Plant Growth Regulators*, Vol. XIV, Academic Press, New York, 1986, p. 14.
- 15 A. Amrus, E. Hargital, G. Karoly, A. Fulop and J. Lantos, *J. Assoc. Off. Anal. Chem.*, 64 (1981) 743.
- 16 J. Sherma, *J. Liq. Chromatogr.*, 11 (1988) 2121.
- 17 G. A. Junk and J. J. Richard, *Anal. Chem.*, 60 (1988) 451.
- 18 D. E. Jaenchen, *J. Liq. Chromatogr.*, 11 (1988) 1941.
- 19 C. F. Poole and S. K. Poole, *Anal. Chem.*, 61 (1989) 1257A.
- 20 S. Gocan and C. Marutoiu, *Rev. Chim. (Bucharest)*, 32 (1981) 166.
- 21 F. Geiss, *Fundamentals of Thin-Layer Chromatography (Planar Chromatography)*, Hüthig, Heidelberg, 1987, p. 321.

## Book Review

---

*Chromatographic analysis of pharmaceuticals*, edited by J. A. Adamovics, Marcel Dekker, New York, 1990, IX + 688 pp., price US\$ 125.00, ISBN 0-8247-7953-3.

Interest in the chromatography of drugs is currently reflected in the number of monographs devoted to this topic. After the voluminous four-part monograph by R. M. Gupta, *Handbook of Chromatography, Drugs* [reviewed in *J. Chromatogr.*, 564 (1991) 355], this book by Adamovics has now been published. This author, similarly to Gupta, has selected the format of a tabular survey. While Gupta emphasized drug analysis in biological materials (about 90% of the data are related to this type of material), the book by Adamovics is devoted exclusively to drug analysis, either as bulk drugs or in pharmaceutical preparations with respect to Pharmacopoeia requirements.

The contents of this book are divided into four large chapters. The first deals with Regulatory considerations for the chromatographer. It surveys various regulatory stages of a candidate drug with considerable attention being paid to validation methods. The second part deals with the problems of sample pretreatment of various drug formulations including both manual techniques and robotics. In the third part, the current situation in individual chromatographic techniques is described: thin-layer chromatography (TLC), gas chromatography (GC), headspace analysis of pharmaceuticals and high-performance liquid chromatography (HPLC). The fourth and main part deals with applications: here the basic data about chromatographic procedures for 1280 drugs in different formulations are summarized (formulation, chromatographic techniques, sample pretreatment, sorbent, mobile phase, detection, comments, reference). This part contains 1137 references from the period 1961–1987 (however, of these, *e.g.*, the book by Florey is quoted 141 times!).

From the viewpoint of an analyst concerned with pharmaceutical analysis, the most fruitful chapters are I, II and IV, while the survey of current chromatographic techniques (excluding headspace analysis) does not differ much from many reviews already available. Most space is allotted to applications presented in tabular form. Although this part will, no doubt, be attractive for most readers, several objections can be raised against its presentation. First, it is my opinion that it does not reflect correctly the extent to which chromatographic techniques are currently exploited in pharmaceutical analysis: about 48% of the described procedures use TLC, 42% HPLC and only 10% GC. According to my statistics, the situation in 1988 was such that out of all papers published on the chromatography of drugs, 65% dealt with HPLC, 17.5% with planar techniques and 17.5% with GC. Similarly, in Gupta's book HPLC strongly predominates, with only 2% dealing with TLC. Such a disproportion is, perhaps, caused by the fact that Adamovics took considerable material from Pharmacopoeias, (mainly the US 1985 and the Japanese 1981), in which articles are regularly delayed

behind current developments. Although the chapter on applications contains almost 1000 references, 69% of all the data about drug chromatography are taken from only four sources: A. H. Stead *et al.*, *Analyst (London)*, 107 (1982) 1106, R. W. Ardrey and A. C. Moffat, *J. Chromatogr.*, 220 (1981) 195, I. Jane *et al.*, *J. Chromatogr.*, 323 (1985) 191 and *US Pharmacopeia*, 21st Revision, 1985. Applications-related references are arranged in a rather confusing way: they are presented neither with an alphabetical arrangement according to authors nor in the order in which they occur in the tables (only a non-sequential arrangement according to alphabetical order of the drugs can be sensed). With regard to the fact that the book lacks an author index, looking for a particular reference is almost impossible. Even reference quotations in tables are not very lucid because they are presented both under Comments and in the References column. For individual bulk drugs only a single technique is reported: the author should have specified in the Introduction to this chapter what the reason for this was (is it considered the most suitable technique according to his own experience? I would place serious doubt on this in many instances). It is certainly my opinion that in recommending techniques papers from the area of biomedical applications should have been considered also, because in working out a particular assay every worker starts with bulk drug first.

In addition to these drawbacks, it is necessary to emphasize some minor errors. I should certainly mention the alphabetical location of compounds in tables (*e.g.*, sodium nitroprusside is under N, but sodium fusidate under S; nitroglycerine can be found both as nitroglycerine and under glycerine trinitrate); amino acid analysers were not introduced in the early 1960s but in 1958; a European reader will certainly be surprised that the whole chapter on TLC does not mention the name of Egon Stahl, the founder of modern TLC: he is the originator of fundamental equipment and sorbents for TLC, he pioneered the application of TLC in pharmaceutical analysis and last but not least he is the author of the first monograph on TLC.

If we compare this book by Adamovics with that by Gupta, it can be concluded that they are complementary and the material contained in the tables does not overlap. The advantages of Adamovics' book for pharmaceutical analysis are, no doubt, its first two parts dealing with regulatory considerations for chromatographers and the sample treatment for various drug formulations, headspace analysis of pharmaceuticals and data about individual drug formulations in the tables. The advantage of Gupta's book is the greater emphasis on modern column chromatographic techniques, considerably more information contained in the tables (the tables frequently allow one to work without consulting the original literature) and, finally, well arranged references. With the provisos specified in this review, the book by Adamovics can be recommended as a primary source of information for drug analysis in different drug forms.

*Prague (Czechoslovakia)*

KAREL MACEK

## Book Review

---

*Chromatographic analysis of alkaloids (Chromatographic Science Series, Vol. 53)*, by M. Popl, J. Fährnich and V. Tatar, Marcel Dekker, New York, 1990, VIII + 667 pp., price US\$ 150.00 (U.S.A. and Canada), US\$ 180.00 (all other countries), ISBN 0-8247-8140-6.

Alkaloids represent one of the largest groups of natural products, many being used as medicine and others being known drugs of abuse. As a result, the analysis of these compounds has been the subject of numerous publications. In 1983 and 1984 Baerheim Svendsen and Verpoorte reviewed the thin-layer chromatography (TLC), gas chromatography (GC) and high-performance liquid chromatography (HPLC) of alkaloids. Since then, new applications and improved methods have been reported for their separation. This book by Popl *et al.* in part covers the literature previously reviewed and in part covers the more recent literature on this subject. Moreover, it reviews some general aspects of alkaloids and the various chromatographic methods.

In the first chapter, the authors discuss the problems of the classification of alkaloids in very general terms. The next chapter deals with the properties of alkaloids relevant for chromatography, *e.g.*,  $pK_a$  values in different solvents, solubility, UV absorption and electrochemical properties. The third chapter is a very general chapter on chromatography. In the next three chapters this is followed by a more detailed discussion of GC, HPLC and TLC, respectively. The chapter on GC first deals with general aspects, followed by a series of selected applications which are arranged according to the classification as discussed in Chapter 1. Compared with the following chapter on LC, the GC chapter is rather superficial. For example, the stationary phases used in GC are only very briefly described, whereas the stationary phases applied in LC are discussed in great detail, although the specially developed reversed phases for the LC of basic compounds deserved more attention. The various separation principles, *e.g.*, reversed-phase, ion-pair and ion-exchange, are discussed separately and illustrated with a number of examples. The chapter ends with an assessment of the various detection methods suitable for alkaloids.

The chapter on TLC is again constructed like the chapter on GC, with first a very general discussion of the method, followed by a series of applications arranged according to the classification scheme of alkaloids.

The first six chapters comprise 300 pages of text. Chapter 7, on applications, fills another 330 pages. This chapter contains 23 tables; the first five concern sample preparation from plant materials and biological fluids and subsequent tables summarize a number of applications. For each major group of alkaloids GC, TLC and LC separations are summarized together in a table. Sufficient details are given to allow the reader to reproduce the separations.

At the end of the book an index is given, in which among others entries on

alkaloid names, alkaloid classes, plant species and methods can be found. The usual confusion with synonyms is also found in this publication (*e.g.*, diamorphine/heroin, hyoscine/scopolamine, hyoscyamine/atropine).


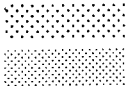
A total of about 1200 references are cited, but according to the authors this is far from comprehensive. However, one can find sufficient information to solve most known separation problems. For developing new methods, ideas and directions can be found in the chapters describing the different chromatographic techniques.

As the book covers the topic from undergraduate level (general theory) to specialist level (specific separations), it is an important handbook which deserves a place in each chemical and pharmaceutical library.

*Leiden (The Netherlands)*

R. VERPOORTE





journal of  
**chromatography news section**

## **COURSE**

**NATO ASI COURSE ON THEORETICAL ADVANCEMENT IN CHROMATOGRAPHY AND RELATED SEPARATION TECHNIQUES, FERRARA, ITALY, AUGUST 18–30, 1991**

The aim of the course is to discuss and disseminate information on the latest theoretical developments in chromatography and related separation techniques, including:

- Generalized theory of separation processes;
- Theory of chromatography;
- Thermodynamics of chromatography and transport phenomena;
- Supercritical fluid chromatography (SFC);
- Field flow fractionation (FFF);
- Electrophoretic techniques;
- Chemometrics of chromatography;
- and poster and discussion sessions

The working language of the Institute will be English. The course involves lectures, seminars and discussions and it will have the character of a training course.

Scientists and engineers in university, industry and government establishments who are interested in chromatography and separation science are invited to apply for participation. The minimum educational level is Dipl. Ing. or MS degree.

Applications should be sent to: Professor F. Dondi, NATO ASI Theoretical Advancement in Chromatography and Related Separation Techniques, Department of Chemistry, University of Ferrara, I-44100 Ferrara, Italy. Tel.: (+ 39 0) 532-207346/206228; Fax: (+ 39 0) 532-40709.

## **ANNOUNCEMENTS OF MEETINGS**

**INTERNATIONAL ION CHROMATOGRAPHY SYMPOSIUM 1991, DENVER, CO, U.S.A., OCTOBER 6–9, 1991**

This three-day international meeting provides an opportunity for scientists from a variety of disciplines to exchange ideas and results on current ion chromatography methods and procedures. Podium and poster presentations will report original work in a variety of topic areas, such as: fundamental principles and general aspects of IC, modes of detection; on-line analysis; gradient separations; ion exclusion chromatography; sample handling and pretreatment; novel applications; post-column treatment; industrial problem-solving; separations using novel stationary and mobile phases; capillary ion analysis.

Many different analytical areas will be considered including environmental applications; industrial applications; analysis of food and plant materials; clinical, biochemical, and pharmaceutical applications; industrial hygiene; and ultra-pure water analysis.

The registration fee (US\$ 550.00) includes a welcome reception, three continental breakfasts, two luncheons, a buffet dinner on Monday, all technical presentations and a copy of the published proceedings.

For program details and registration information, write or call: Century International Inc., P.O. Box 493, Medfield, MA 02052, U.S.A. Tel.: (508) 359-8777; Fax: (508) 359-8778.

#### FREDERICK CONFERENCE ON CAPILLARY ELECTROPHORESIS, FREDERICK, MD, U.S.A., OCTOBER 15-16, 1991

The focus of this meeting is on the scientific exchange and dissemination of the technical aspects of capillary electrophoresis (CE). Discussion of established methodologies as well as creative and innovative new approaches and techniques are invited. The format will include workshops, oral and poster presentations by individual conference participants, and optional enrollment in a definitive CE course to be held on October 14th. Invited speakers will provide expert overviews of the basic aspects and applications of CE including, but not limited to, instrument and column design, detection, the role of the buffer and factors that influence mobility, selectivity, resolution and optimization. Also, the application of CE to the separation of small ions as well as large biomolecules will be presented and discussed.

There is no registration fee; however, registration is mandatory to ensure participation. A nominal fee of \$100.00 will be charged for participation in the CE course. State-of-the-art equipment displays and literature will be made available to participants by the leading manufacturers of CE instrumentation.

For further information on registration, abstract submittal, and course participation, please contact: Margaret L. Fanning, Conference Coordinator, PRI, NCI-FCRDC, P.O. Box B, Frederick, MD 21702-1201, U.S.A. Tel.: (301) 846-1089; Fax: (301) 846-5866.

#### 30th ANNUAL EASTERN ANALYTICAL SYMPOSIUM AND EXPOSITION, SOMERSET, NJ, U.S.A., NOVEMBER 11-14, 1991

The 1991 EAS will be held at the Somerset Hilton and the Garden State Convention & Exhibition Center

The technical program will include the following topics: good manufacturing practices; chemometrics; two-dimensional NMR; laboratory automation; clinical chemistry; molecular fluorescence; electron & optical spectroscopy; forensic science; capillary electrophoresis; gas chromatography; bioanalytical chemistry; mass spectrometry; high-performance liquid chromatography; high resolution NMR; near-infrared spectroscopy; X-ray crystallography; Fourier transform IR; transform methods in chemistry; microscopy; protein characterization; atomic spectroscopy; supercritical fluid extraction; imaging NMR; microwave techniques; ion chromatography; chiral separations; therapeutic drug monitoring; process analytical chemistry; chemical sensors; bioanalytical chemistry; and much more.

The EAS program will consist of contributed and invited papers, which will be presented in oral or poster format. Prospective authors should submit a 150-200 word abstract of the proposed presentation, indicating preference for oral or poster format, to the program committee. In keeping with tradition, the program will include symposia honoring the recipients of the several EAS Awards.

The exposition will feature a 250-booth array of manufacturers exhibiting the latest analytical technology.

For further details contact: EAS 1991 Program Committee, P.O. Box 633, Montchanin, DE 19710-0633, U.S.A. Tel.: (302) 453-0785; Fax: (302) 738-5275.

1992 WINTER CONFERENCE ON PLASMA SPECTROCHEMISTRY, SAN DIEGO, CA, U.S.A.,  
JANUARY 6-11, 1992

The scientific program and symposia of the 1992 Winter Conference on Plasma Spectrochemistry will include:

- automation, expert systems, and robotics with plasma spectroscopy;
- chemometric applications in plasma spectrochemistry;
- chromatography with plasma source detection;
- flow injection plasma spectrometry;
- glow discharge and low pressure plasma atomic and mass spectrometry;
- laser assisted plasma spectrochemistry;
- mechanisms and process in plasma sources;
- modern sample preparation and calibration techniques;
- new instrumentation for plasma spectrochemistry;
- plasma source mass spectrometry;
- process control, remote, and on-line plasma analysis;
- sample introduction techniques and phenomena;
- spectrochemical applications of plasma sources;
- transform spectroscopy, interferometry for plasma sources.

Short courses highlighting special topics will be offered January 3-5. A three-day exhibition of spectroscopic instrumentation and accessories will also be included.

Titles and 50-words abstracts for submitted lecture or poster papers are solicited by 1 July, 1991. Extended conference abstracts are requested by 7 October, 1991.

For further information please contact: Dr. R. Barnes, c/o ICP Information Newsletter, Department of Chemistry, CRC Towers, University of Massachusetts, Amherst, MA 01003-0035, U.S.A. Tel.: (413) 545-2294; Fax: (413) 545-4490; Bitnet: RBARNES@UMASS.

PREP-92, 9th INTERNATIONAL SYMPOSIUM ON PREPARATIVE AND INDUSTRIAL CHROMATOGRAPHY, NANCY, FRANCE APRIL 6-8, 1992

The scientific program will include plenary lectures (45 min), oral communications (20 min) and poster presentations. An exhibit of modern instrumentation will be organized.

The symposium aims to reflect the most recent progress in preparative and industrial chromatography with gas, liquid or supercritical eluents, including:

- modeling and simulation - physico-chemical interactions between stationary and mobile phases;
- equipment design and optimization - new stationary phase developments;
- process integration and cost estimation;
- applications and development case stories.

The official languages are: English and French.

The registration fee is: 2800 FF (taxes and proceedings included). The deadline for submission of abstracts is 1 October, 1991 and for submission of full papers 1 February, 1992. The proceedings will be published in advance of the conference and will be delivered to participants on registration.

For further details contact: PREP-92 Secretary, E.N.S.I.C.-L.P.C.I., 1 rue Grandville, B.P. 451, F-54001 Nancy Cedex, France. Tel.: (33) 83 30 02 76; Fax: (33) 83 35 08 11.

22nd INTERNATIONAL ROLAND W. FREI SYMPOSIUM ON ENVIRONMENTAL ANALYTICAL CHEMISTRY AND WORKSHOP ON DETECTION PRINCIPLES IN ENVIRONMENTAL ANALYSIS, DORTMUND, GERMANY, JUNE 9-12, 1992

This symposium will be 22nd in a series of successful meetings initiated by the late Roland W. Frei in Halifax, Canada in 1971.

Major topics to be treated during the 1992 Symposium will be: environmental standards in a unified Europe; emission control; analytical chemistry in biotechnology; surface and depth profile anal-

ysis; analytical laser spectroscopy; chemical sensors.

The registration fee for the symposium will be: DM 400, DM 350 for members of the IAEAC, and DM 100 for students.

For further details contact: M. Frei-Hausler, Symposium Office IAEAC, P.O. Box 46, CH-4123 Allschwil 2, Switzerland. Tel.: (+41 61) 632789; Fax: (+41 61) 4820805.

**SAC 92, AN INTERNATIONAL CONFERENCE ON ANALYTICAL CHEMISTRY, READING, U.K., SEPTEMBER 20-26, 1992**

This is the tenth in the series of triennial Conferences originally started by the Society for Analytical Chemistry (hence SAC), and on this occasion also celebrates the 150th anniversary of the founding of The Laboratory of the Government Chemist (LGC). The scientific program will be organised around plenary, invited and contributed papers and posters covering the whole field of analytical chemistry. The language of the conference will be English. The program will include workshops, where research workers can demonstrate new apparatus and techniques. An opportunity will be made for all participants to visit The Laboratory of the Government Chemist and other scientific establishments.

A limited number of bursaries will be available from the Analytical Chemistry Trust Fund for student members of the Royal Society of Chemistry, The Laboratory of the Government Chemist will also provide bursaries for a limited number of younger research workers. Participants are encouraged to register for the whole week. Special concessionary rates will be offered to student, retired and unemployed members of The Royal Society of Chemistry.

For details concerning the program or submission of papers contact: The Secretary, Analytical Division, Royal Society of Chemistry, Burlington House, Piccadilly, London W1 OBN, U.K.

Announcements are included free of charge. Information on planned events should be sent well in advance (preferably 6 months or more) to: Journal of Chromatography, News Section, P.O. Box 330, 1000 AH Amsterdam, The Netherlands, Fax: (31) 20-5862845.

## CALENDAR OF FORTHCOMING EVENTS

June 3-7, 1991  
Basel, Switzerland

**HPLC '91, 15th International Symposium on Column Liquid Chromatography**

Contact: Secretariat HPLC '91, Convention Center Basel, Congress Department, P.O. Box, CH-4021 Basel, Switzerland. (Further details published in Vol. 477, No. 2.)

June 4-6, 1991  
Egham, U.K.

**5th International LIMS Conference**

Contact: The Conference Registrar, 5th International LIMS Conference, P.O. Box 341, High Wycombe, Buckinghamshire HP11 2QG, U.K. Tel.: (0494) 24769.

June 9-14, 1991  
Bergen, Norway

**XXVII Colloquium Spectroscopicum Internationale**

Contact: Secretariat XXVII CSI, HSD Congress-Conference, P.O. Box 1721 Nordnes, N-5024 Bergen, Norway. Tel.: (475) 318414; Telex: 42607 hsd n, Fax: (475) 324555. (Further details published in Vol. 508, No. 2.)

June 10–13, 1991  
San Francisco,  
CA, U.S.A.

**5th Annual Seminar on Analytical Biotechnology**

Contact: Janet E. Cunningham, Barr Enterprises, P.O. Box 279, Walkersville, MD 21793, U.S.A. Tel.: (301) 898-3772; Fax: (301) 898-5596.

July 8–12, 1991  
Amsterdam, The  
Netherlands

**4th Amsterdam HPLC Summercourse**

Contact: Dr. J.C. Kraak, Laboratory of Analytical Chemistry, University of Amsterdam, Nieuwe Achtergracht 166, 1018 WV Amsterdam, The Netherlands. Tel.: (31 20) 5256515; Fax: (31 20) 5255698.

July 8–12, 1991  
Loughborough, U.K.

**\* Short Course on High-performance Liquid Chromatography**

Contact: Mrs. S. Maddison, Department of Chemistry, Loughborough University of Technology, Loughborough, Leics. LE11 3TU, U.K. Tel. (0509) 222575; Fax: (0509) 233163. (Further details published in Vol. 540.)

July 15–16, 1991  
Ithaca, NY, U.S.A.

**\* Short Course on LC–MS, SFC–MS, IC–MS, CE–MS**

Contact: Dr. J. Henion, Drug Testing and Toxicology Program, NY State College of Veterinary Medicine, Cornell University, 925 Warren Drive, Ithaca, NY 14850, U.S.A. Fax: (607) 255-3235. (Further details published in Vol. 540.)

July 16–18, 1991  
London, U.K.

**Two-Dimensional Polyacrylamide Gel Electrophoresis**

Contact: Conference Secretariat 2-D PAGE 1991, Department of Cardiothoracic Surgery, National Heart & Lung Institute, Dovehouse Street, London SW3 6LY, U.K. (Further details published in Vol. 504, No. 2.)

July 17–19, 1991  
Ithaca, NY, U.S.A.

**\* 8th (Montreux) Symposium on Liquid Chromatography–Mass Spectrometry (LC–MS, SFC–MS, CE–MS, IC–MS)**

Contact: Dr. J. Henion, Drug Testing and Toxicology Program, NY State College of Veterinary Medicine, Cornell University, 925 Warren Drive, Ithaca, NY 14850, U.S.A. Fax: (607) 255-3235. (Further details published in Vol. 540.)

Aug. 5–9, 1991  
Vienna, Austria

**\* 2nd International Congress on Amino Acids and Analogues**

Contact: Gert Lubec, University of Vienna, Department of Pediatrics, Währinger Gürtel 18, A-1090 Vienna, Austria. Tel. (222) 2340424 or (222) 404003229; Fax: (222) 404003238.

Aug. 12–15, 1991  
Phoenix, AZ,  
U.S.A.

**\* 105th Annual International Meeting of the Association of Official Analytical Chemists**

Contact: AOAC, Suite 400, 2200 Wilson Boulevard, Arlington, VA 2201-3301, U.S.A. Tel.: (703) 522-3032; Fax: (703) 522-5468.

Aug. 17–22, 1991  
Budapest, Hungary

**33rd IUPAC Congress**

Contact: 33rd IUPAC Congress, E. Pungor, c/o Hungarian Academy of Sciences, Gellért ter 4, H-1111 Budapest, Hungary.

Aug. 18–21, 1991  
York, U.K.

**Capillary Electrophoresis Training Course**

Contact: Dr. Carys Calvert, Short Course Coordinator, Department of Chemistry, University of York, YO1 5DD, U.K. Tel. (0904) 432576/432511; Fax: (0904) 432516/433433.

Aug. 19–30, 1991  
Ferrara, Italy

**\* NATO ASI Course on Theoretical Advancement in Chromatography and Related Separation Techniques**

Contact: Prof. Francesco Dondi, Department of Chemistry, University of Ferrara, via L. Borsari 46, I-44100 Ferrara, Italy. Tel.: (+39 352) 207346 or 206228; Fax: (+39 352) 40709.

Aug. 21–24, 1991  
Kumamoto, Japan

**5th International Conference on Flow Analysis**

Contact: Professor Ishibashi, Department of Applied Analytical Chemistry, Faculty of Engineering 36, Kyushu University, Hokazaki, Higashiku, Fukuoka 812, Japan. (Further details published in Vol. 475.)

Aug. 25–31, 1991  
Makuhari, Japan

**ICAS '91, IUPAC International Congress on Analytical Sciences**

Contact: ICAS '91 Secretariat, The Japan Society for Analytical Chemistry, 1-26-2 Nishigotande, Shinagawa, Tokyo 141, Japan. Tel.: (813) 490-3351; fax: (813) 490-3572. (Further details published in Vol. 483.)

Sept. 1–6, 1991  
Heslington, U.K.

**4th European Conference on the Spectroscopy of Biological Molecules**

Contact: Prof. R.E. Hester, ECSBM '91 Chairman, Department of Chemistry, University of York, Heslington, York YO1 5DD, U.K. (Further details published in Vol. 523.)

Sept. 1–6, 1991  
Lubeck-Travemunde,  
Germany

**8th International Conference on Fourier Transform Spectroscopy**

Contact: Gesellschaft Deutscher Chemiker, Abt. Tagungen, P.O. Box 900440, D-6000 Frankfurt 90, Germany. Tel.: 17-366/360; Fax: (79) 17475; Telex: 4170497 gdch d.

Sept. 2–6, 1991  
Warsaw, Poland

**8th Danube Symposium on Chromatography**

Contact: 8th Danube Symposium on Chromatography, Janusz Lipkowski, Institute of Physical Chemistry of the Polish Academy of Sciences, Kasprzaka 44/52, 01-224 Warsaw, Poland. (Further details published in Vol. 502, No. 2.)

Sept. 3–6, 1991  
Guildford, U.K.

**\* Symposium on Bioanalysis of Drugs, including Anti-allergics and Anti-asthmatics**

Contact: Dr. E. Reid, Guildford Academic Associates, 72 The Chase, Guildford, Surrey GU2 5UL, U.K. Tel.: (0483) 65324. (Further details published in Vol. 540.)

Sept. 9–13, 1991  
Loughborough, U.K.

**\* Workshop on Liquid Scintillation Counting**

Contact: Dr. P. Warwick, Nuclear Chemistry Laboratories, Loughborough University of Technology, Loughborough, Leics. LE11 3TU, U.K. Tel.: (0509) 222585.

Sept. 4-6, 1991  
Bilthoven, The  
Netherlands

**3rd Workshop on Chemistry and Fate of Modern Pesticides**  
Contact: Pesticides Workshop Office, Dr. P. van Zoonen, RIVM, P.O. Box 1, 3720 Bilthoven, The Netherlands. (Further details published in Vol. 472, No. 2.)

Sept. 23-25, 1991  
Somerset, NJ,  
U.S.A.

**\* National Symposium on Planar Chromatography: Modern Thin-Layer Chromatography**  
Contact: Ms. Janet Cunningham, Symposium Manager, Barr Enterprises, P.O. Box 279, Walkersville, MD 21793, U.S.A. Tel.: (301) 898-3772; Fax: (301) 898-5596. (Further details published in Vol. 537.)

Sept. 24-25, 1991  
Baden Baden,  
Germany

**Short Course on Sample Handling in Liquid Chromatography**  
Contact: Workshop Office, IAEAC, M. Frei-Häusler, Postfach 46, CH-4123 Allschwil 2, Switzerland. Tel.: (004161) 632789 and (004161) 732950.

Sept. 24-28, 1991  
Yokohama, Japan

**9th International Symposium on Affinity Chromatography and Biological Recognition**  
Contact: Professor Ken-ichi Kasai, Faculty of Pharmaceutical Sciences, Teikyo University, Sagamiko, Tsukui, Kanagawa 199-01, Japan. (Further details published in Vol. 540.)

Sept. 26-27, 1991  
Baden Baden, Germany

**5th Symposium on Handling of Environmental and Biological Samples in Chromatography**  
Contact: Workshop Office, IAEAC, M. Frei-Häusler, Postfach 46, CH-4123 Allschwil 2, Switzerland. Tel.: (004161) 632789 and (004161) 732950. (Further details published in Vol. 513.)

Sept. 29-Oct. 4, 1991  
Sopron, Hungary

**\* 3rd International Conference on Biochemical Separations**  
Contact: Hungarian Biochemical Society, 3rd ICBS, Fö u. 68, MTESZ room 314, P.O. Box 433, Budapest, H-1371 Hungary. (Further details published in Vol. 540.)

Oct. 6-9, 1991  
Denver, CO, U.S.A.

**\* International Ion Chromatography Symposium**  
Contact: Century International Inc., P.O. Box 493, Medfield, MA 02052, U.S.A. Tel.: (508) 359-8777; Fax: (508) 359-8778.

Oct. 6-11, 1991  
Anaheim, CA, U.S.A.

**\* Joint Meeting of the Federation of Analytical Chemistry and Spectroscopy Societies and the Pacific Conference on Chemistry and Spectroscopy**  
Contact: FACSS, P.O. Box 278, Manhattan, KS 66502, U.S.A. Tel.: (301) 846-4797.

Oct. 14-18, 1991  
Budapest, Hungary

**ECASIA 91, 4th European Conference on Applications of Surface and Interface Analysis**  
Contact: ECASIA 91, MTA ATOMKI, Pf. 51, H-4001 Debrecen, Hungary. Tel.: (36) 52-16181; Telex: 72210 (atom h); Fax: (36) 52-16181.

- Oct. 15–16, 1991  
Frederick, MD,  
U.S.A.
- \* Frederick Conference on Capillary Electrophoresis**  
Contact: Margaret L. Fanning, Conference Coordinator, PRI, NCI-FRDC, P.O. Box B, Frederick, MD 21702-1201, U.S.A. Tel.: (301) 846-1089; Fax: (301) 846-5886.
- Oct. 20–23, 1991  
Washington, DC,  
U.S.A.
- 11th International Symposium on High-Performance Liquid Chromatography of Proteins, Peptides and Polynucleotides**  
Contact: Janet E. Cunningham, Barr Enterprises, P.O. Box 279, Walkersville MD 21793, U.S.A. Tel.: (301) 898-3772; Fax: (301) 898-5596. (Further details published in Vol. 513.)
- Oct. 20–24, 1991  
Knoxville, TN,  
U.S.A.
- \* 7th Symposium on Separation Science and Technology for Energy Applications**  
Contact: Dr. J.S. Watson, Oak Ridge National Laboratory, P.O. Box 2008, Oak Ridge, TN 37831-6223, U.S.A. Tel.: (615) 574-6795 or 574-4934. (Further details published in Vol. 540.)
- Oct. 21–24, 1991  
San Miniato (Pisa),  
Italy
- \* Colloquium Chemiometricum Mediterraneum**  
Contact: Dr. L. Lampugnani, Ist. Chimica Analitica Strumentale – C.N.R., Via Risorgimento 35, I-56100 Pisa, Italy. Tel.: (+39 50) 501224; Fax: (+39 50) 587260.
- Nov. 11–15, 1991  
Somerset, NJ, U.S.A.
- \* 30th Annual Eastern Analytical Symposium and Exposition**  
Contact: Program Committee Eastern Analytical Symposium, P.O. Box 633, Montchanin, DE 19710-0633, U.S.A. Tel.: (302) 453-0785; Fax: (302) 738-5275.
- Jan. 6–11, 1992  
San Diego, CA, U.S.A.
- \* 1992 Winter Conference on Plasma Spectrochemistry**  
Contact: Dr. R. Barnes, c/o ICP Information Newsletter, Department of Chemistry, CRC Towers, University of Massachusetts, Amherst, MA 01003-0035, U.S.A. Tel.: (413) 545-2294; Fax: (413) 545-4490; Bitnet: RBARNES@UMASS.
- Feb. 18–21, 1992  
Antwerp, Belgium
- 2nd International Symposium on Hyphenated Techniques in Chromatography**  
Contact: Dr. R. Smits, p.a. BASF Antwerpen N.V., Scheldelaan B-2040 Antwerp, Belgium. Tel.: (32) 5682831; Fax: (323) 5683355; Telex: 31047 basant b. (Further details published in Vol. 508, No. 2.)
- April 6–8, 1992  
Nancy, France
- \* PREP-92, 9th International Symposium on Preparative and Industrial Chromatography**  
Contact: PREP-92 Secretary, E.N.S.I.C.–L.P.C.I., 1 rue Grandville, B.P. 451, F-54001 Nancy Cedex, France. Tel.: (33) 83300276; Fax: (33) 83350811.
- May 5–8, 1992  
Liège, Belgium
- \* 4th International Symposium on Drug Analysis**  
Contact: Dr. J. Crommen, Drug Analysis '92-Liège, University of Liège, Institute of Pharmacy, rue Fusch 5, B-4000 Liège, Belgium. Tel.: (+3241) 237002; Fax: (+3241) 221855.



May 12-14, 1992  
La Grand Motte, France

\* **4th European Meeting of Groupe Français de Bio-Chromatographie**  
Contact: Groupe Français de Bio-Chromatographie, Unité d'Immuno Allergie, Institut Pasteur, 28 rue de Docteur Roux, 75724 Paris Cedex 15, France. Tel.: (1) 45688000, ext. 7143; Fax: (1) 43069835; Telex: 250609 F. (Further details published in Vol. 540.)

May 17-22, 1992  
Kyoto, Japan

**4th International Conference on Fundamentals of Adsorption**  
Contact: Prof. M. Suzuki, Conference Chairman, Institute of Industrial Science, University of Tokyo, 7-22-1 Roppongi, Minatoku, Tokyo 106, Japan. (Further details published in Vol. 508, No. 2.)

June 9-12, 1992  
Dortmund, Germany

\* **22nd Roland W. Frei Memorial Symposium on Environmental Analytical Chemistry and Workshop on Detection in Environmental Analysis**  
Contact: Symposium Office IAEAC, M. Frei-Häusler, P.O. Box 46, CH-4123 Allschwil 2, Switzerland. Tel.: (+41 61) 632789; Fax: (+41 61) 4820805.

Aug. 24-27, 1992  
Jena, Germany

\* **COMPANA '92, 5th Conference on Computer Applications in Analytical Chemistry**  
Contact: COMPANA '92, Friedrich Schiller University Jena, Institute of Inorganic and Analytical Chemistry, Steiger 3, Haus 3, O-6900 Jena, Germany. Tel.: (82) 25467 or (82) 25029.

Sept. 5-11, 1993  
Edinburgh, U.K.

\* **EUROANALYSIS VIII, 8th European Conference on Analytical Chemistry**  
Contact: Miss P.E. Hutchinson, Analytical Division, The Royal Society of Chemistry, Burlington House, Piccadilly, London W1V 0BN, U.K. Tel.: (071) 4378656; Fax: (071) 7341227; Telex: 268001.

---

\* Indicates new or amended entry

Views and opinions expressed in this section do not necessarily reflect those of the Publisher or the Editors. No responsibility is assumed by the Publisher for any injury and/or damage to persons or property as a matter of products liability, negligence or otherwise, or from any use or operation of any methods, products, instructions or ideas contained in the material herein.



## PUBLICATION SCHEDULE FOR 1991

*Journal of Chromatography and Journal of Chromatography, Biomedical Applications*

MONTH	D 1990- F 1991	M	A	M	J	J	
Journal of Chromatography	Vols. 535-539	540/1 + 2 541/1 + 2 542/1	542/2 543/1	543/2 544/1 + 2 545/1	545/2 546/1 + 2 547/1 + 2	548/1 + 2	The publication schedule for further issues will be published later
Cumulative Indexes, Vols. 501-550							
Bibliography Section		560/1			560/2		
Biomedical Applications	Vols. 562, 563	564/1	564/2 565/1 + 2	566/1 566/2	567/1	567/2	

### INFORMATION FOR AUTHORS

(Detailed *Instructions to Authors* were published in Vol. 522, pp. 351-354. A free reprint can be obtained by application to the publisher, Elsevier Science Publishers B.V., P.O. Box 330, 1000 AH Amsterdam, The Netherlands.)

**Types of Contributions.** The following types of papers are published in the *Journal of Chromatography* and the section on *Biomedical Applications*: Regular research papers (Full-length papers), Review articles and Short Communications. Short Communications are usually descriptions of short investigations, or they can report minor technical improvements of previously published procedures; they reflect the same quality of research as Full-length papers, but should preferably not exceed six printed pages. For Review articles, see inside front cover under Submission of Papers.

**Submission.** Every paper must be accompanied by a letter from the senior author, stating that he/she is submitting the paper for publication in the *Journal of Chromatography*.

**Manuscripts.** Manuscripts should be typed in double spacing on consecutively numbered pages of uniform size. The manuscript should be preceded by a sheet of manuscript paper carrying the title of the paper and the name and full postal address of the person to whom the proofs are to be sent. As a rule, papers should be divided into sections, headed by a caption (*e.g.*, Abstract, Introduction, Experimental, Results, Discussion, etc.). All illustrations, photographs, tables, etc., should be on separate sheets.

**Introduction.** Every paper must have a concise introduction mentioning what has been done before on the topic described, and stating clearly what is new in the paper now submitted.

**Abstract.** All articles should have an abstract of 50-100 words which clearly and briefly indicates what is new, different and significant.

**Illustrations.** The figures should be submitted in a form suitable for reproduction, drawn in Indian ink on drawing or tracing paper. Each illustration should have a legend, all the legends being typed (with double spacing) together on a *separate sheet*. If structures are given in the text, the original drawings should be supplied. Coloured illustrations are reproduced at the author's expense, the cost being determined by the number of pages and by the number of colours needed. The written permission of the author and publisher must be obtained for the use of any figure already published. Its source must be indicated in the legend.

**References.** References should be numbered in the order in which they are cited in the text, and listed in numerical sequence on a separate sheet at the end of the article. Please check a recent issue for the layout of the reference list. Abbreviations for the titles of journals should follow the system used by *Chemical Abstracts*. Articles not yet published should be given as "in press" (journal should be specified), "submitted for publication" (journal should be specified), "in preparation" or "personal communication".

**Dispatch.** Before sending the manuscript to the Editor please check that the envelope contains four copies of the paper complete with references, legends and figures. One of the sets of figures must be the originals suitable for direct reproduction. Please also ensure that permission to publish has been obtained from your institute.

**Proofs.** One set of proofs will be sent to the author to be carefully checked for printer's errors. Corrections must be restricted to instances in which the proof is at variance with the manuscript. "Extra corrections" will be inserted at the author's expense.

**Reprints.** Fifty reprints of Full-length papers and Short Communications will be supplied free of charge. Additional reprints can be ordered by the authors. An order form containing price quotations will be sent to the authors together with the proofs of their article.

**Advertisements.** Advertisement rates are available from the publisher on request. The Editors of the journal accept no responsibility for the contents of the advertisements.

# HETEROCYCLES

AN INTERNATIONAL JOURNAL FOR REVIEWS AND COMMUNICATIONS IN HETEROCYCLIC CHEMISTRY

## Editor:

Keiichiro Fukumoto, Japan

## Honorary Editorial Associates:

D.H.R. Barton (USA)

H.C. Brown (USA)

M. Hamana (Japan)

T. Nozoe (Japan)

V. Prelog (Switzerland)

G. Stork (USA)

S. Sugawara (Japan)

K. Takeda (Japan)

Lord Todd (UK)

K. Tsuda (Japan)

## Aims and Scope:

Since its inception in 1973, *Heterocycles* has provided a platform for the rapid exchange of research in the areas of organic, pharmaceutical, analytical, and medicinal chemistry of heterocyclic compounds.

The journal publishes reviews, communications, reports and original papers.

A section of the journal is devoted to the total synthesis of previously documented natural products with heterocyclic ring systems.

## Fast Publication:

Due to the fact that the journal is able to publish articles within two months of receipt of the manuscripts, researchers in this field can obtain up-to-date information on heterocyclic research by reading *Heterocycles* regularly.

## Abstracted/Indexed in:

Chemical Abstracts, Current Contents: Physical, Chemical & Earth Sciences, PASCAL/CNRS

## Subscription Information:

1991: Vol. 32 (12 issues)  
US\$ 778.50 / Dfl. 1440.00  
including postage  
ISSN 0385-5414

*A free sample copy is available on request*



**Elsevier Science Publishers**

P.O. Box 330, 1000 AH, Amsterdam, The Netherlands

P.O. Box 882, Madison Square Station, New York, NY 10159, USA